SSCL-SR-1209

SSCL-SR-1209

Superconducting Super Collider Laboratory

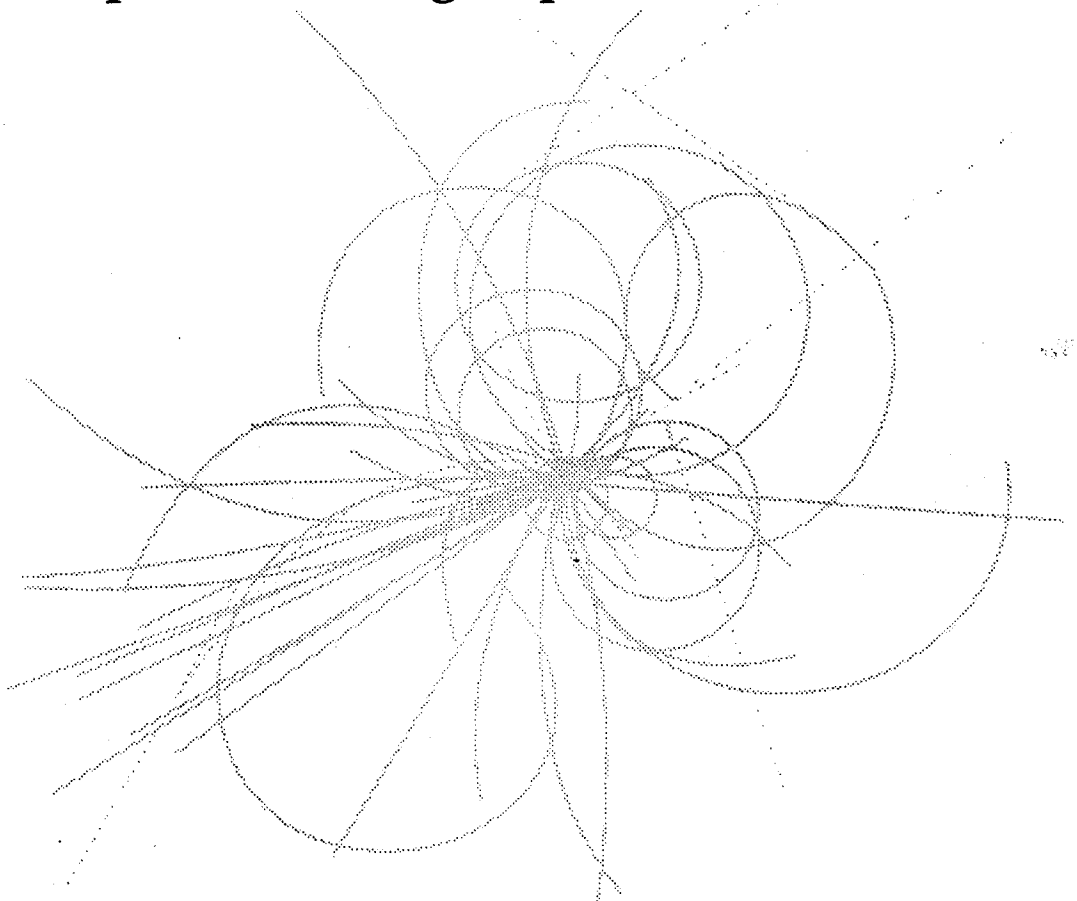

Full Acceptance Detector

J. D. Bjorken, P. N. Burrows,
J. P. Venuti, and A. W. Weidemann

March 1992

SSCL-SR-1209

Full Acceptance Detector

J. D. Bjorken, P. N. Burrows,
J. P. Venuti, and A. W. Weidemann

Superconducting Super Collider Laboratory†
2550 Beckleymeade Ave.
Dallas, TX 75237

March 1992

†Operated by the Universities Research Association, Inc., for the U.S. Department of Energy under Contract No. DE-AC35-89ER40486.

Superconducting Super Collider

Full Acceptance Detector

March 13-14, 1992

Contents

Executive Summary

Agenda

Transparencies

Additional Papers

Appendix

Operated by Universities Research Association, Inc.
Under Contract with the United States Department of Energy

16 March 1992

Executive Summary of F.A.D. Meeting at SSCL
March 13-14, 1992

F.A.D. Organising Committee:
J.D. Bjorken, P.N. Burrows, J.P. Venuti, A.W. Weidemann

1.1 Introduction - Fred Gilman

We were delighted that Fred Gilman was able to open the meeting with welcoming remarks and a brief summary of the status of the SSC project.

1.2 Civil Construction - Tim Toohig

Toohig reported that Robbins has been contracted to bore a 2.7 mile section of tunnel on the W side (this is the 'F.A.D. side'), at a cost of around $18M. The design group is studying the bypass section for IR-1; this is a ± 1km section around the I.P. A tunnel diameter of 17 feet is needed at the beam separation point. This may well have to increase to accommodate service installations (cryogenics *etc.*), but the case for any further increase in size for a detector will have to be made very strongly, within about 6 months. Current plans are for a magnet delivery shaft several hundred metres upstream of the I.P. at IR-1, which could well have to serve as an installation shaft for the detector components; IR-1 is 150 feet below ground.

2. Physics I

2.1 Rapidity Gap Physics - Dieter Zeppenfeld

Zeppenfeld considered the processes:

- $p\,p \rightarrow N\,N\,W^+W^-$
- $q\,q \rightarrow q\,q\,H, \qquad H \rightarrow b\bar{b}$

In the first case, for a central ($|\eta| < 3$) two-photon system, the cross-section is about 0.3 pb. In the second case, in the absence of rapidity gaps rejection of background events at the 99.5% level appears to be needed. Zeppenfeld was pessimistic regarding the observability of the latter mode, even including the gap-plus jet signatures. Bjorken was more optimistic, but another round of calculation is needed.

2.2 Rapidity Gap Physics - J. D. Bjorken

Bjorken gave an outline of the principles of F.A.D. He went on to describe flagship physics topics as presented in seminars to others, especially finding a 1 TeV-mass Higgs using the rapidity gaps plus jets signature. The claim is that this is so easy and clean that even a FAD could do it.

2.3 Event Simulation - Gary Greenbaum

Event signatures of the texture of a rapidity gap plus edge have been carried out using Lepto 5.2 (for proton fragmentation at HERA). They agree with expectations. Some Higgs decays to W-pairs were also shown.

3. Detector Issues

3.1 The Detector - Bjorken

Bjorken outlined the milestones for putting together candidate detector architectures, insisting on bottom-up thinking. They include in sequence, laying out the 100m-1KM region, then the beam-pipe and wall layout, tracking , and finally the magnetic layout (with countless iterations). He also presented ideas (and a central detector model) for an inexpensive (June-July) level-0 detector based on a lego pixel size of 0.7x 0.7 and body-centered cubic symmetry.

3.2 Interaction with Machine Lattice - John Venuti

Venuti discussed machine lattice considerations for a Full Acceptance Detector. He discussed the problems concerning dispersion matching with the main lattice and the solution posed by the SSCL machine lattice group. He emphasized that none of the current plans are firmly established and that we should begin to establish a set of parameters best suited for a F.A.D. and try to get the SSC to implement them. The major issues to be considered in cooperation with the machine lattice group are: the distance from the IP to the first set of focusing quadrupole magnets, the aperture of the magnets, the configuration of the SSC dipole cryostat, and the options for dispersion matching.

2.3 Backgrounds I - Nikolai Mokhov

Mokhov briefly outlined some of the issues involved in considering backgrounds from the accelerator, including beam halo, beam loss and radiation. He has sophisticated codes at his disposal to do the calculations. F.A.D. should decide what levels it can tolerate near the beam axis in the downstream region and let Mokhov decide if the goals are feasible.

3.3 Backgrounds II - Achim Weidemann

Weidemann summarized various sources of background. One of the potentially more serious ones comes from showers started at inner edges of detector elements. As an example, he showed the distribution of particles 15 m downstream generated by 500 GeV photons or electrons incident on the edge of a 30 X_0 lead block, using EGS4.

This should also be studied with hadronic codes.

He also showed lego plots for 1000 events of the Minimum Bias Rockfeller generator.

3.4 Beampipe - Wayne Vernon

Vernon gave a summary of generic problems confronting the design of an F.A.D. beampipe.

4. Physics II

4.1 QCD Physics - Leonid Frankfurt

The subject of hard and semihard diffraction was reviewed by Frankfurt. The accompanying notes are very explicit and readable and you are urged to peruse them. The ideas are relevant to recent data on hard diffraction by Schlein et al., and one can expect clarification of this difficult physics issue in the very near future.

4.2 Inclusive Neutrons - Larry Jones

Jones motivated study of the process p p $\rightarrow$ n + X. From fixed target experiments every fourth proton is expected to give rise to a neutron.

4.3 Forward-Physics Ideas - Bill Walker

Walker presented (1) data supporting a long mfp for quarks in nuclear matter, (2) an appeal for a pi-pi collider, tagging on one-pion exchange, and (3) a search for exotic colorless objects produced as beam fragments in inelastic diffraction events.

4.4 The L.P.M. Effect - Steven Strausz

Strausz described the Landau-Pomeranchuk-Migdal Effect, whereby photon emission by an electron traversing nuclear matter is suppressed at very high energies. Inconclusive measurements exist from cosmic ray experiments, but a demonstration may be possible at SSC. Strausz also made the point that the SSC c.m. energy is equivalent to a PeV proton striking a stationary target, *i.e.* the possibility exists to measure cross-sections which are currently accessible only to cosmic ray experiments. Better understanding of these cross-sections will help cosmic ray physics tremendously.

4.5 Cosmic Ray Physics - Gaurang Yodh

Yodh continued the connection with cosmic rays by outlining some interesting observations made in that field over the past two decades. These could be tantalising glimpses of new physics, or they could be peculiar fluctuations which are as yet not understood.

Yodh also showed results of simulations of minimum bias events by Bob Ellsworth, who was unable to be present. Ellsworth calculates that a detector wall of radius 15 cm at 1 km from the I.P. would receive an average of 1 photon per event of energy above 1-2TeV. A similar study for the number of neutrons is under way.

5. Possible Overlap with b Physics

5.1 The BCD Experiment - George Kalbfleisch

Kalbfleisch briefly presented the case for a b physics detector at SSC, the aim being to get at CP violation. He outlined the BCD detector proposal (E.o.I - 8) which occupies the central region $|\eta| < 5.5$. With a luminosity of 10^{32} the claim is that BCD could reach precision on the unitarity triangle comparable to 10 years of running at a b-factory. For BCD the design of the trigger is seen as a critical path item. Kalbfleisch stated that whilst it is not obvious that BCD could form the central section of the F.A.D. detector without compromising the b physics programme, he is willing to do further study on the idea of integrating the two detectors.

5.2 A Forward Spectrometer for b Physics - Freddy Fridman

Fridman and his group are considering the design of a forward spectrometer with coverage for charged particles in the region $2.5 \leq |\eta| \leq 5$. They hope to arrive at conclusions on the feasibility of the project in time for the SSC b physics symposium in October.

5.3 A Forward Spectrometer for b Physics - Jerry Rosen

Rosen outlined a sophisticated forward spectrometer with price tag to match. He assumes there will be no extracted beam for a fixed target and is considering a gas jet target. He is investigating staging the installation to ease the financial contraints.

5.4 A Collider Mode b Detector - Peter Schlein

Schlein described a two-arm spectrometer for b physics in colliding beam mode. Trials of a Si vertex detector at the CERN $p\bar{p}$ collider were very successful. Current thinking is to operate the detector at LHC.

6. Discussions

The following important issues were raised in the discussions:

- The need for hadronic calorimetry (Albrow).

- Venuti will ask the lattice design group for a luminosity of 10^{32} and a central space of > 100m + 100m and wait for their reaction.

- Should we put together an E.o.I. and ask TNRLC for funding for travel and R.&D. in time for the November 1 deadline? (Strausz, Jones)

- Albrow, Yodh and Goulianos requested up-to-date drawings of the current lattice design around IR-1. Venuti will try to get them.

Next Meeting: April 16-17 in Madison

Appendix I: List of Participants

MICHAEL ALBROW	Fermilab	ALBROW@FNALD
THEODOROS ALEXOPOULOS	U. of Wisconsin	THEOALEX@WISCPSL
JAMES BJORKEN	SLAC	BJORKEN@SLACVM
PHILIP BURROWS	MIT	BURROWS@SLACVM
JOE COYNE	SSCL	COYNEJ@SSCVX1
PER DAHL	SSCL	
ROBERT ELLSWORTH	George Mason U.	
LEONID FRANKFURT	Mich. St. U.	FRANKFURT@MSUNSCL
FREDDY FRIDMAN	SSCL	FRIDMAN@SSCVX1
FRED GILMAN	SSCL	GILMAN@SSCVX1
KONSTANTIN GOULIANOS	Rockefeller	DINO@FNALD
GARY GREENBAUM	UCSD	GARYG@SLACVM
LAWRENCE JONES	U. Michigan	JONES@UMIPHYS
GEORGE KALBFLEISCH	U. Oklahoma	SSCVX1::GRK
RICHARD KOFLER	U. Mass	RKOFLER@SLACVX
S. MANI	U.C. Davis	MANI@UCDHEP.UCDAVIS,EDU
SYDNEY MESHKOV	SSCL	SYD@SSCVX1
NIKOLAI MOKHOV	SSCL	MOKHOV@SSCVX1
FRANK PAIGE	SSCL	
JERRY ROSEN	Northwestern U.	FNAL::JROSEN
PETER SCHLEIN	UCLA	SCHLEIN@UCLAHEP
TANAJI SEN	SSCL	
RAY STEFANSKI	SSCL	STEFANSKI@SSCVX1
STEVEN STRAUSZ	U.Washnigton	STRAUSS@UWAPHAST
TIM TOOHIG	SSCL	TOOHIG@SSCVX1
JOHN VENUTI	Vanderbilt	JPV@SLACVM
WAYNE VERNON	UCSD	VERNON@SLACVX
WILLIAM WALKER	Duke U.	DUKHEP::WALKER
ACHIM WEIDEMANN	U. of Tennessee	ACHIM@SLACVM
ALAN WHITE	ANL	ARW@ANLHEP
GAURANG YODH	U.C. Irvine	YODH@VWSCYG.PS.UCI.EDU
DIETER ZEPPENFELD	U. of Wisconsin	DIETER@WISCPHEN

Appendix II: Future Meetings/Workshops

• April 13 - 15 1992: SSC Physics Symposium, Madison, Wi.
Contact: Linda Dolan, SSCSYMP @ WISCPHEN

• June 21 - 27 1992: 7th International Symposium on Very High Energy Cosmic Ray Interactions, Ann Arbor, Mi.
Contact: USERHHY3 @ UMICHUB

• July 1992: Workshops at Rocky Mountain Detector Center, Boulder, Co.

Session 1: 5 - 11 July 1992: Detector Performance at High Luminosity. (J. Rutherfoord, J. Brau, M. Sites)

Session 2: 12 - 18 July 1992: Charged Particle Tracking for Advanced HEP Experiments. (W. Ford)

Session 3: 19 - 25 July 1992: Performance of Muon Tracking and Triggering in SSC Detectors. (U. Nauenberg)

Session 4: 26 July - Aug. 1 1992: The Structure, Scattering and Multi-particle Production of Hadrons at the SSC. (P. Carruthers)

Contact: Karen Lubatti, Univ. of Arizona, (602) 621 4271.

• (Tentative) September 16-18 1992: Full acceptance physics, Fermilab.
Contact: Alan White, ARW @ ANLHEP

F.A.D. Agenda
March 13-14, 1992

Friday, March 13			Talk
9:00-9:15	Introduction	Fred Gilman	
9:15-10:00	SSC Interface	Tim Toohig	1
10:00-10:15	Break		
10:15-11:15	Rapidity Gaps and Jets	Bjorken/Zeppenfeld	2/3
11:15-12:00	Event Simulation	Gary Greenbaum	4
12:00-2:00	Lunch		
2:00-3:00	Machine Lattice	John Venuti	5
3:00-4:00	Backgrounds	Achim Weideman	6
4:00-5:00	Beampipe & Vacuum	Wayne Vernon	7
5:00-6:00	Discussion		

Friday Evening Social
Host - Joe Coyne

Saturday, March 14			
9:00-10:00	Diffractive Physics	L. Frankfurt/M. Strikman	8
10:00-10:30	Break		
10:30-11:30	Cosmic Ray Physics and the Forward Spectrometer Design	Jones/Walker/ Strausz/Yodh	9/10 11/12
11:30-12:00	Discussion		
12:00-2:00	Lunch		
2:00-4:00	B-Physics at SSC/Compatibility with a Full Acceptance Detector	Fridman/ Kalbfleisch/Rosen	13/14
4:00-5:00	Summary Discussions - Allocation of Work		15

Toohig

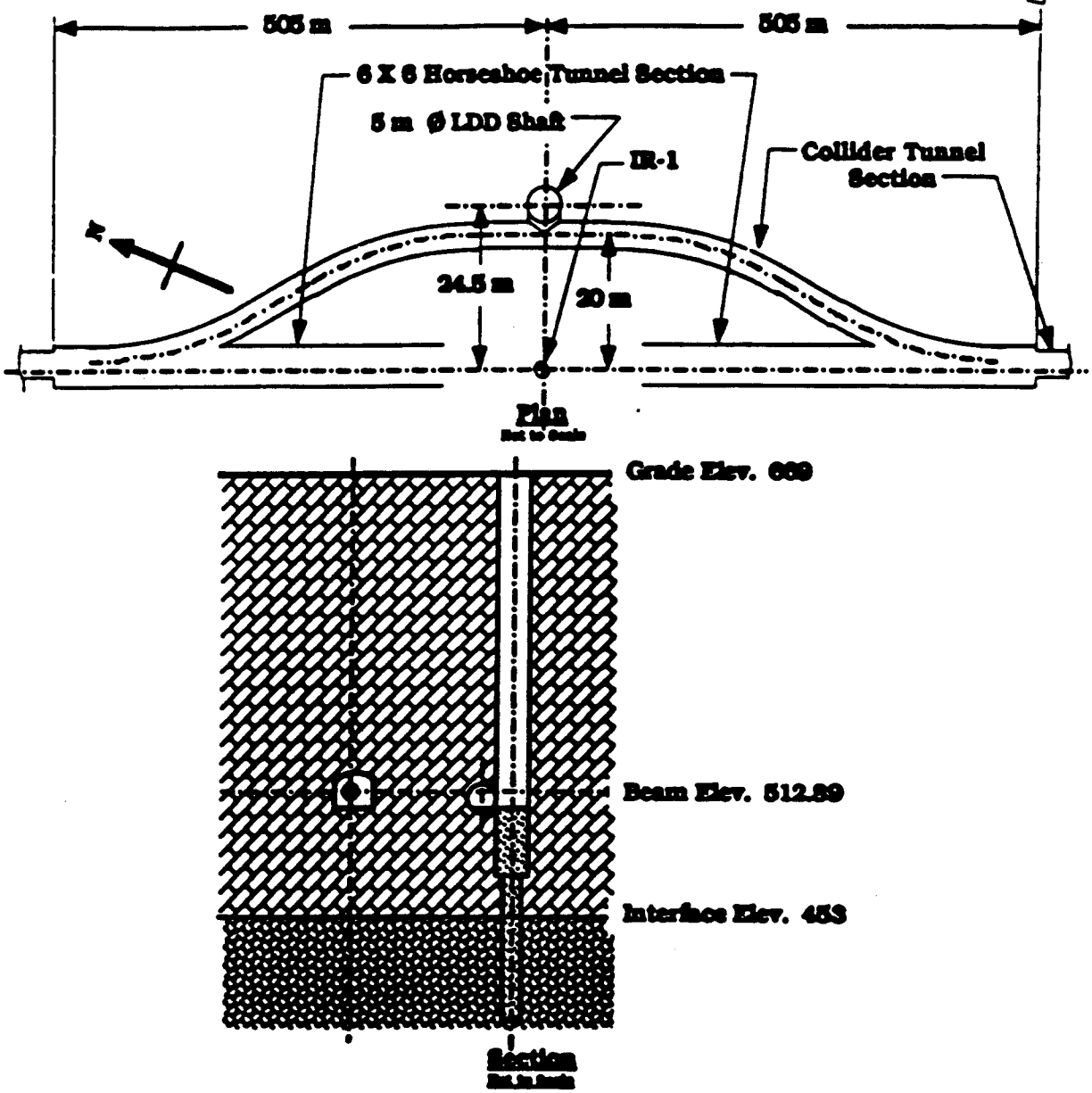

Figure 1.2. Underground Facilities at IR-1 for the Baseline Detector Arrangement

2. CONSIDERATION OF OTHER CANDIDATE EXPERIMENTS.

The following is a list of other known experiments which are candidate for incorporation into the SSC. The propriety of considering each of these in sizing and configuring the generic facility at IR-1 is discussed in the subheadings of this section.

A. SSC-EOI-0001; Krisch; "Inclusive Spin-Spin Effects and Cross Section Near 20TeV."

B. SSC-EOI-0002; Orear; "Low P_t Physics at the SSC."

DRAFT

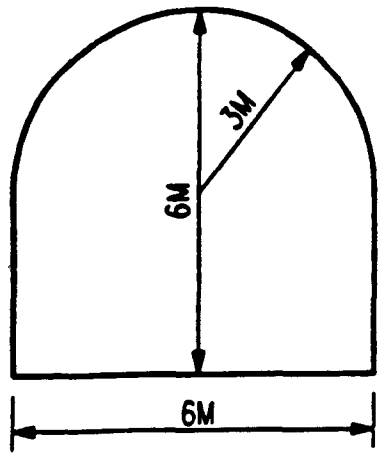

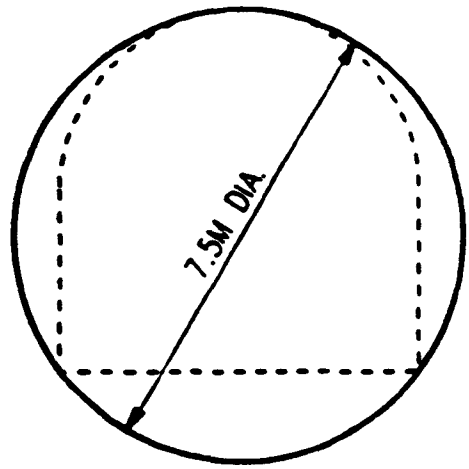

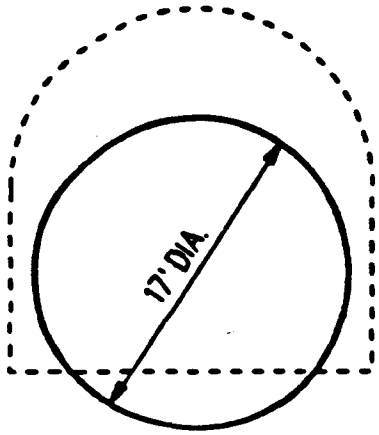

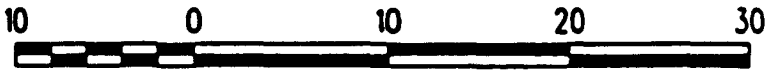

SCALE: 1" = 10'

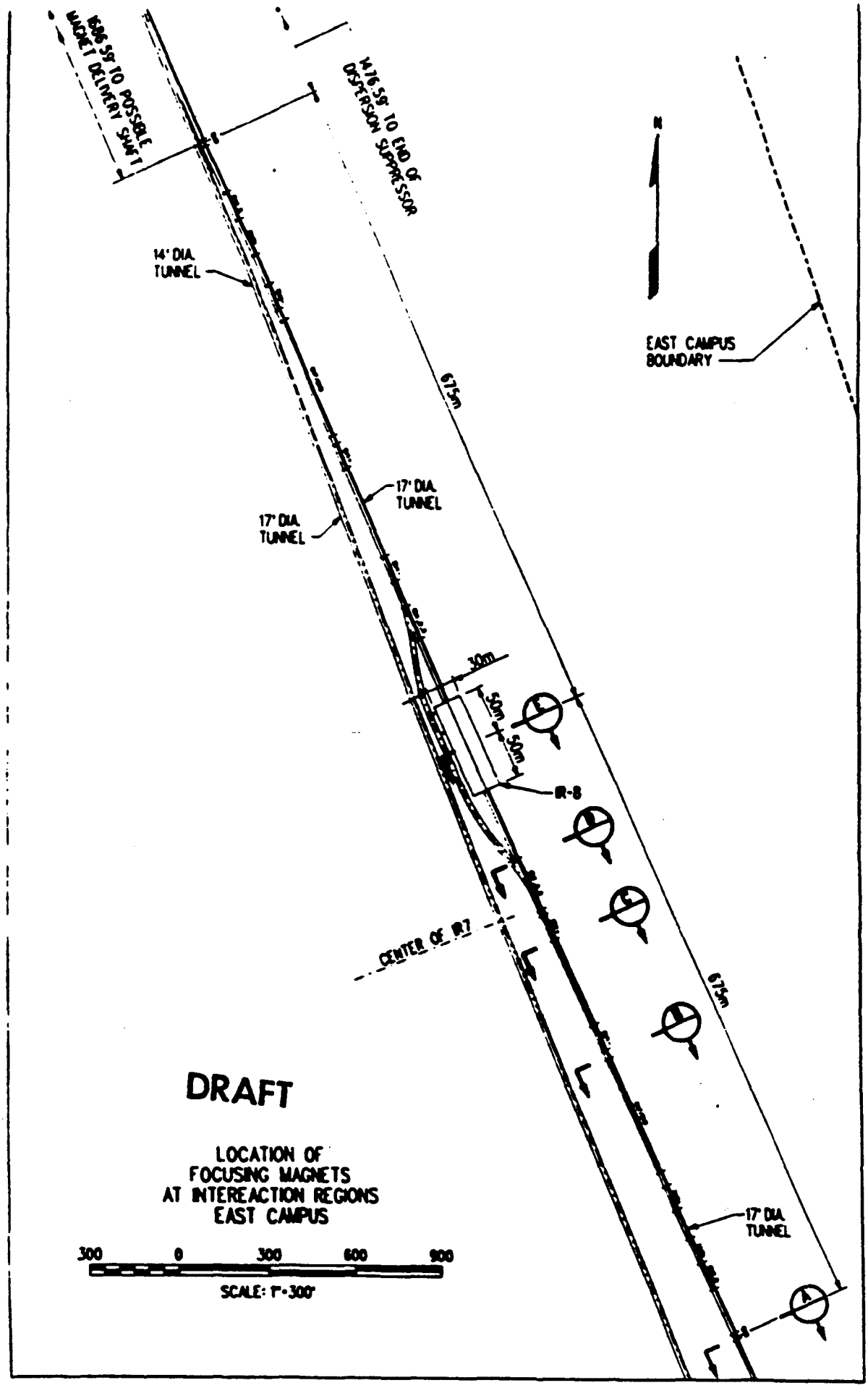
1506 SF TO POSSIBLE MAGNET DELIVERY SHAFT
1476 SF TO END OF DISPERSION SUPPRESSOR
N
14' DIA. TUNNEL
EAST CAMPUS BOUNDARY
675m
17' DIA. TUNNEL
17' DIA. TUNNEL
30m
50m
50m
IR-8
CENTER OF IR7
675m
DRAFT
LOCATION OF FOCUSING MAGNETS AT INTEREACTION REGIONS EAST CAMPUS
300 0 300 600 900
SCALE: 1"=300'
17' DIA. TUNNEL

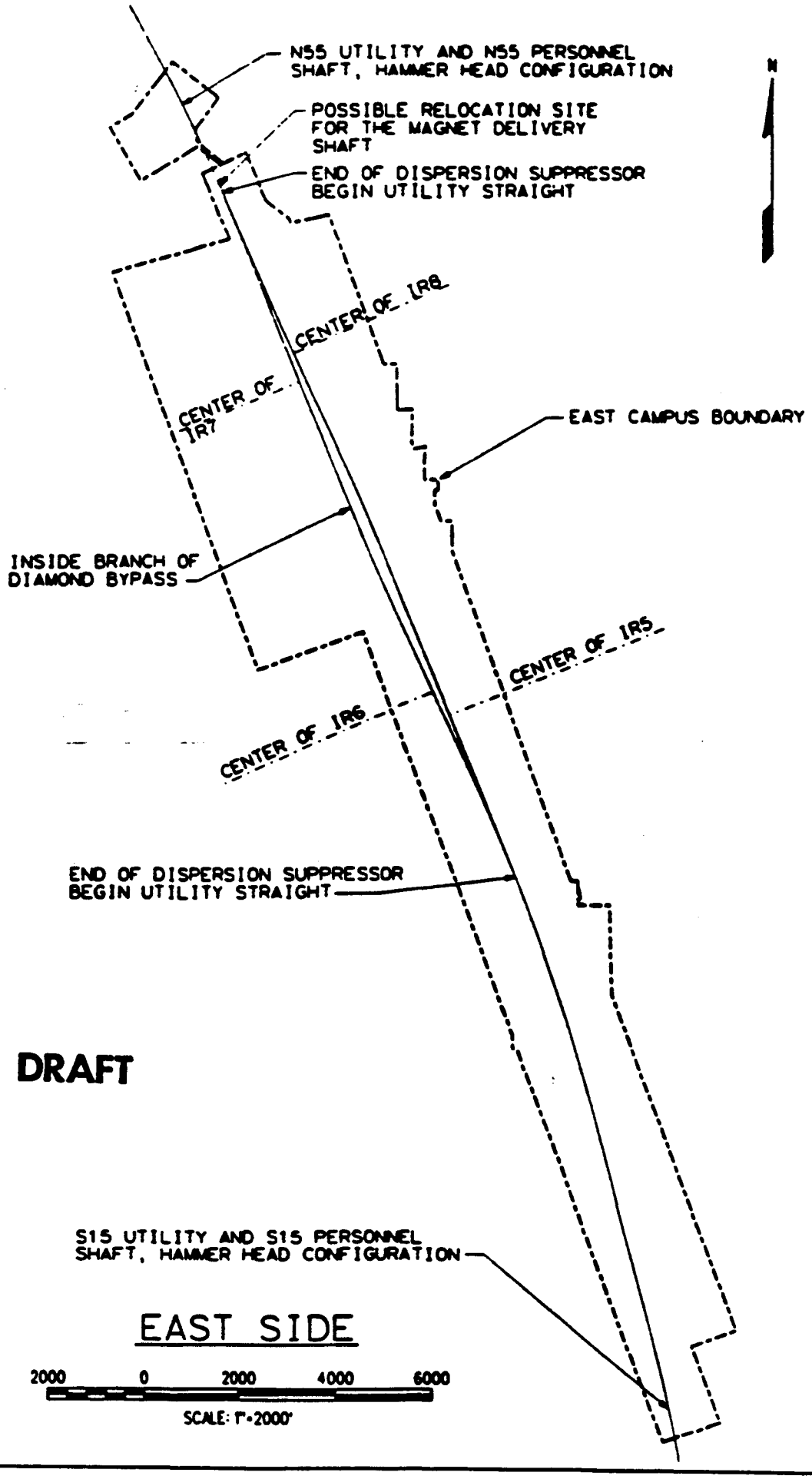
N55 UTILITY AND N55 PERSONNEL SHAFT, HAMMER HEAD CONFIGURATION
POSSIBLE RELOCATION SITE FOR THE MAGNET DELIVERY SHAFT
END OF DISPERSION SUPPRESSOR BEGIN UTILITY STRAIGHT
N
CENTER OF IR8
CENTER OF IR7
EAST CAMPUS BOUNDARY
INSIDE BRANCH OF DIAMOND BYPASS
CENTER OF IR5
CENTER OF IR6
END OF DISPERSION SUPPRESSOR BEGIN UTILITY STRAIGHT
DRAFT
S15 UTILITY AND S15 PERSONNEL SHAFT, HAMMER HEAD CONFIGURATION
EAST SIDE
2000 0 2000 4000 6000
SCALE: 1"=2000'

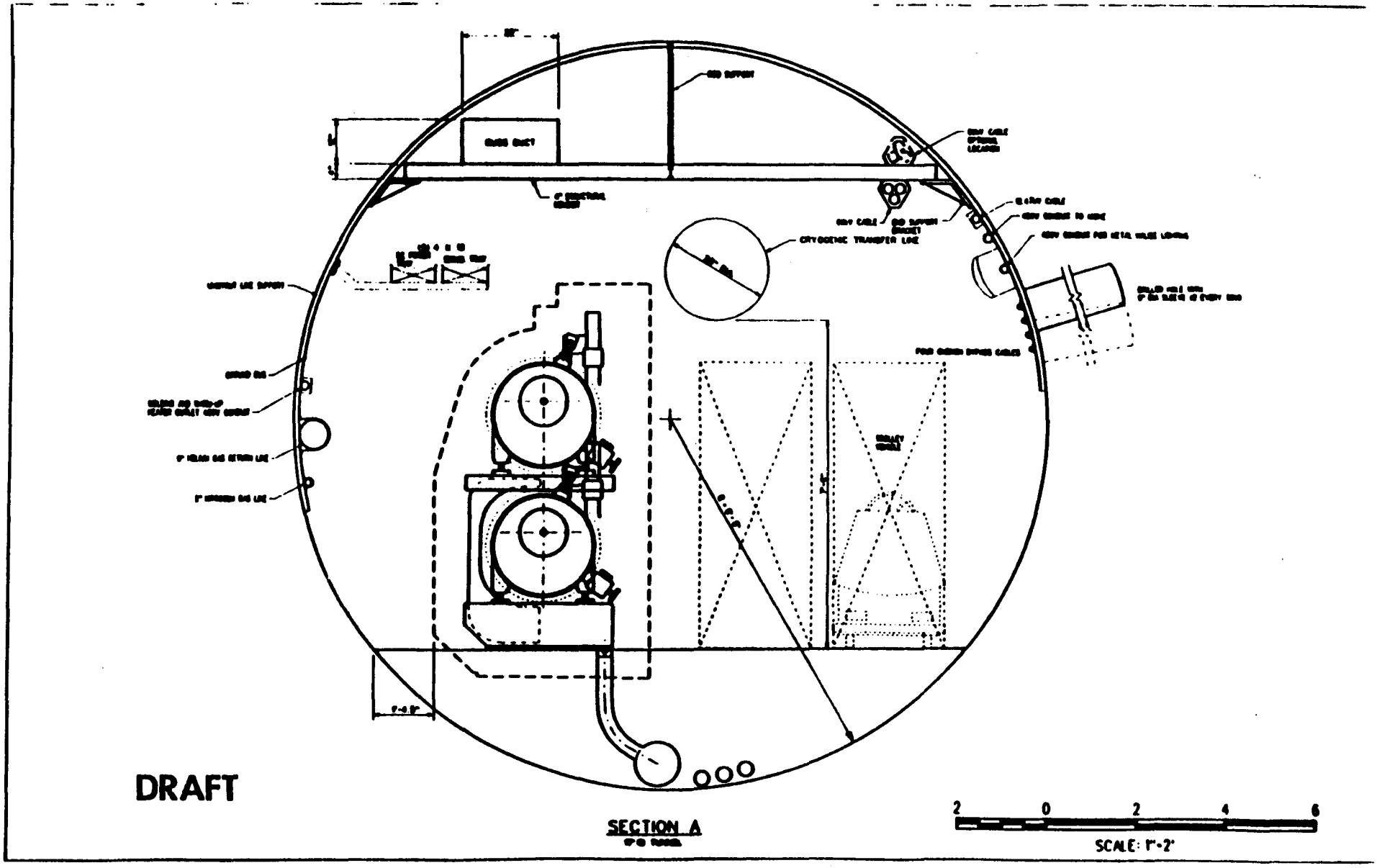
CRYOGENIC TRANSFER LINE
DRAFT
SECTION A
SCALE: 1"=2'
2 0 2 4 6

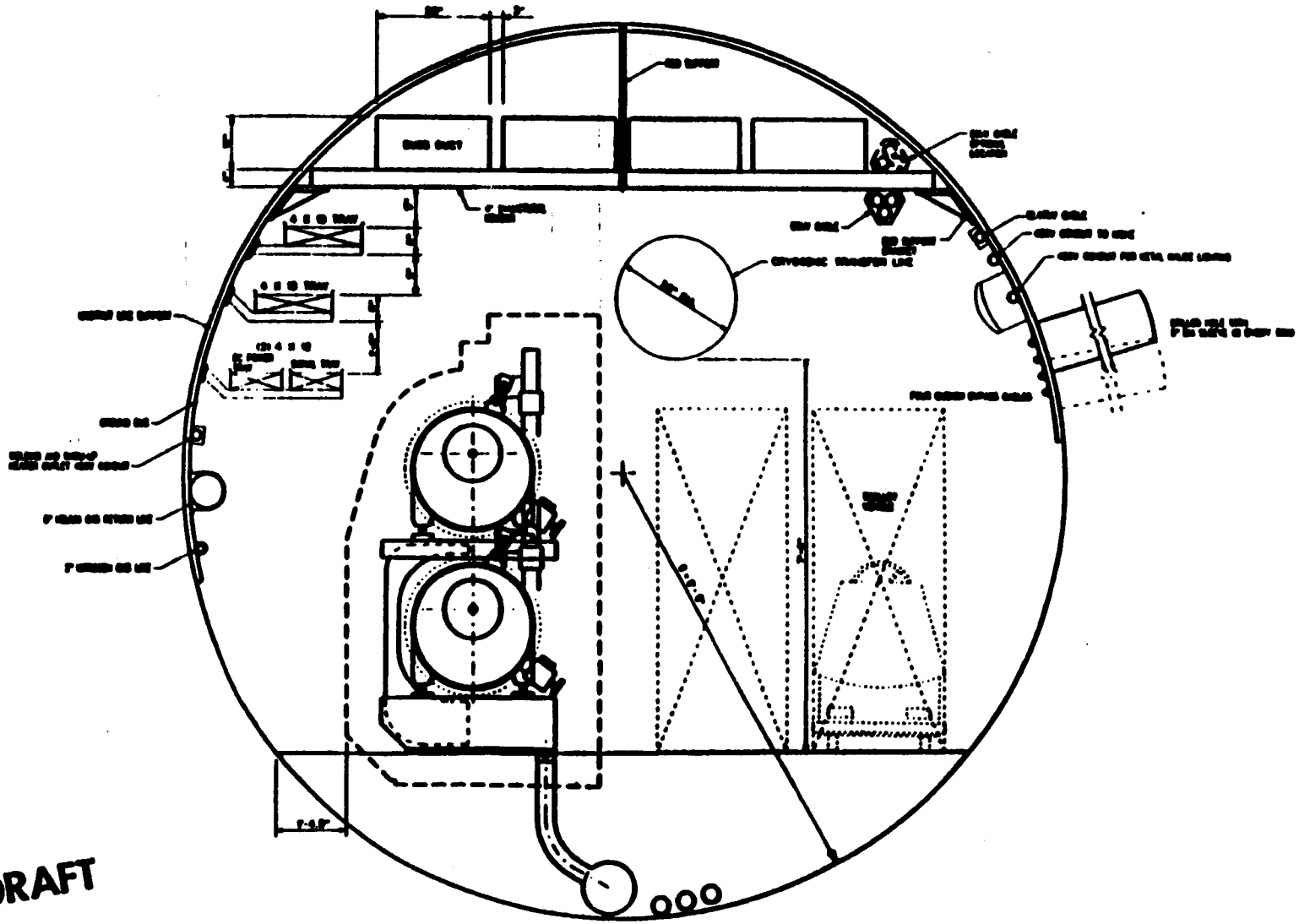

DRAFT

SECTION C

2 0 2 4 6

SCALE: 1"=2'

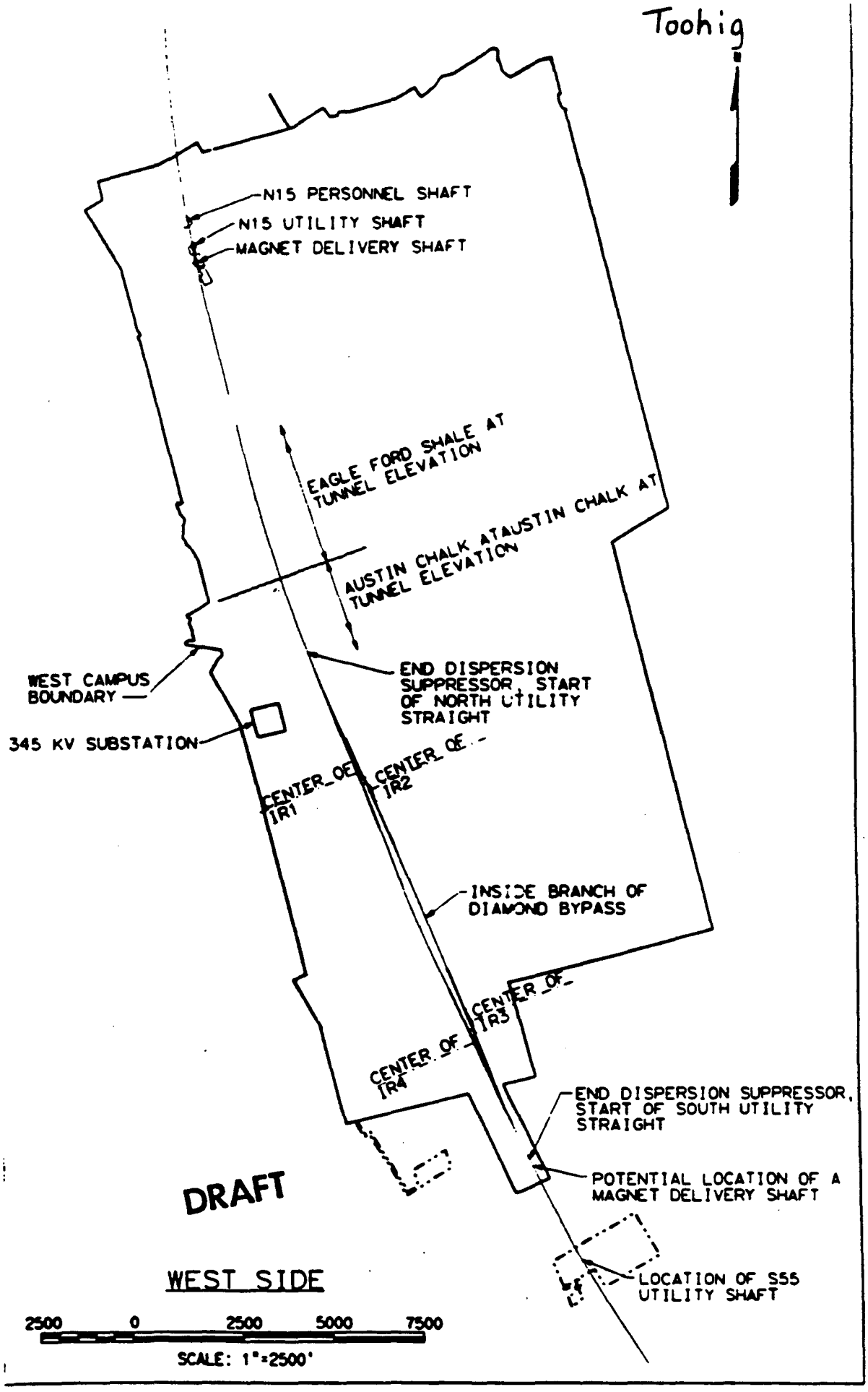
Toohig
N15 PERSONNEL SHAFT
N15 UTILITY SHAFT
MAGNET DELIVERY SHAFT
EAGLE FORD SHALE AT TUNNEL ELEVATION
AUSTIN CHALK AT
AUSTIN CHALK AT TUNNEL ELEVATION
WEST CAMPUS BOUNDARY
END DISPERSION SUPPRESSOR, START OF NORTH UTILITY STRAIGHT
345 KV SUBSTATION
CENTER OF IR1
CENTER OF IR2
INSIDE BRANCH OF DIAMOND BYPASS
CENTER OF IR3
CENTER OF IR4
END DISPERSION SUPPRESSOR, START OF SOUTH UTILITY STRAIGHT
POTENTIAL LOCATION OF A MAGNET DELIVERY SHAFT
DRAFT
WEST SIDE
LOCATION OF S55 UTILITY SHAFT
2500 0 2500 5000 7500
SCALE: 1"=2500'

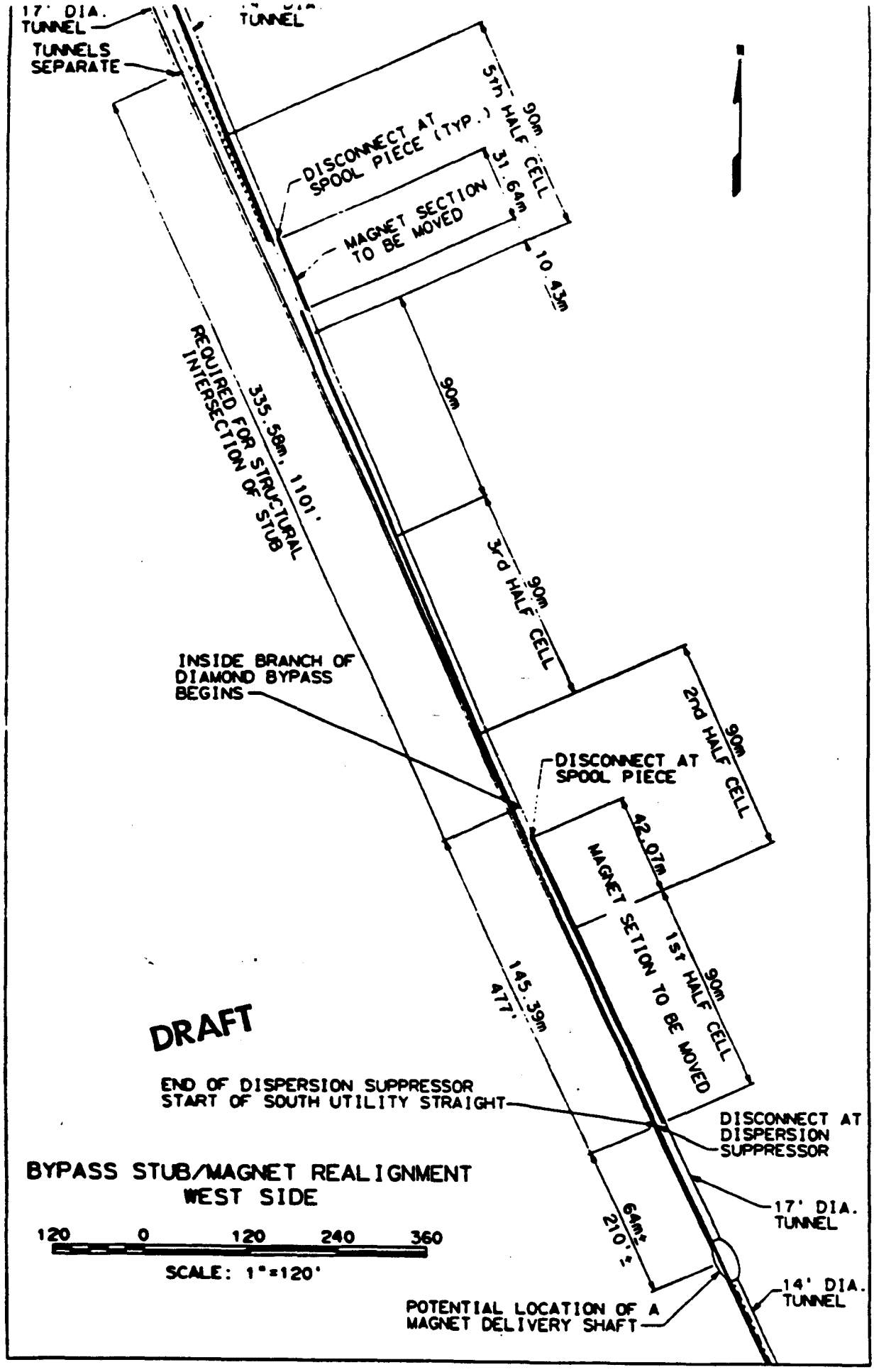
17' DIA. TUNNEL
TUNNELS SEPARATE
TUNNEL
5th HALF CELL
90m
DISCONNECT AT SPOOL PIECE (TYP.)
31.64m
MAGNET SECTION TO BE MOVED
10.43m
REQUIRED FOR STRUCTURAL INTERSECTION OF STUB
335.58m, 1101'
90m
3rd HALF CELL
90m
INSIDE BRANCH OF DIAMOND BYPASS BEGINS
2nd HALF CELL
90m
DISCONNECT AT SPOOL PIECE
42.07m
MAGNET SETION TO BE MOVED
1st HALF CELL
90m
145.39m
477'
DRAFT
END OF DISPERSION SUPPRESSOR
START OF SOUTH UTILITY STRAIGHT
DISCONNECT AT DISPERSION SUPPRESSOR
BYPASS STUB/MAGNET REALIGNMENT
WEST SIDE
17' DIA. TUNNEL
64m*
210'*
120 0 120 240 360
SCALE: 1"=120'
14' DIA. TUNNEL
POTENTIAL LOCATION OF A MAGNET DELIVERY SHAFT

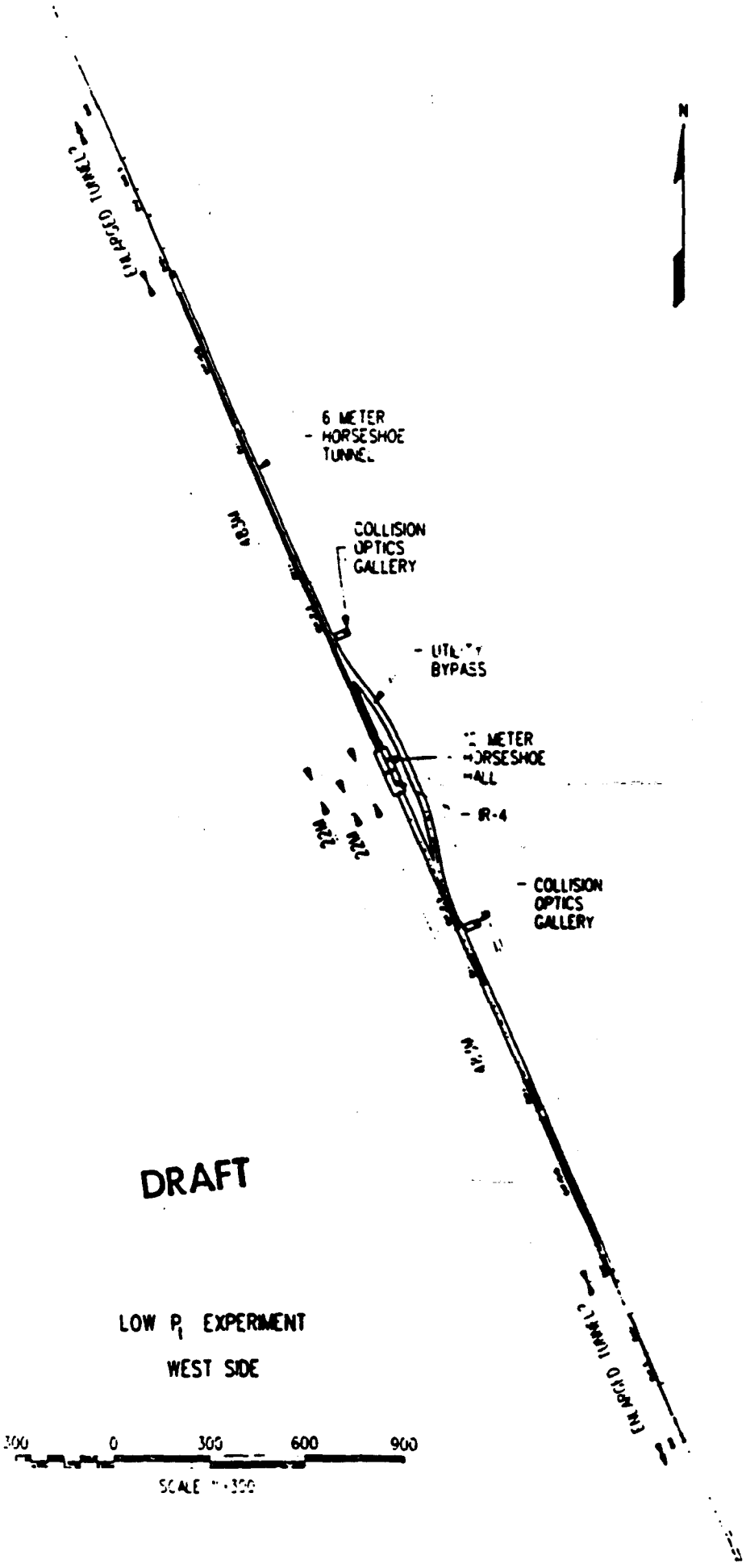
N
6 METER
HORSESHOE
TUNNEL
COLLISION
OPTICS
GALLERY
BYPASS
IR-4
COLLISION
OPTICS
GALLERY
DRAFT
LOW P_t EXPERIMENT
WEST SIDE
300
0
300
600
900

DRAFT

Interaction Region Magnet Layout

Plan View (to scale horizontally)

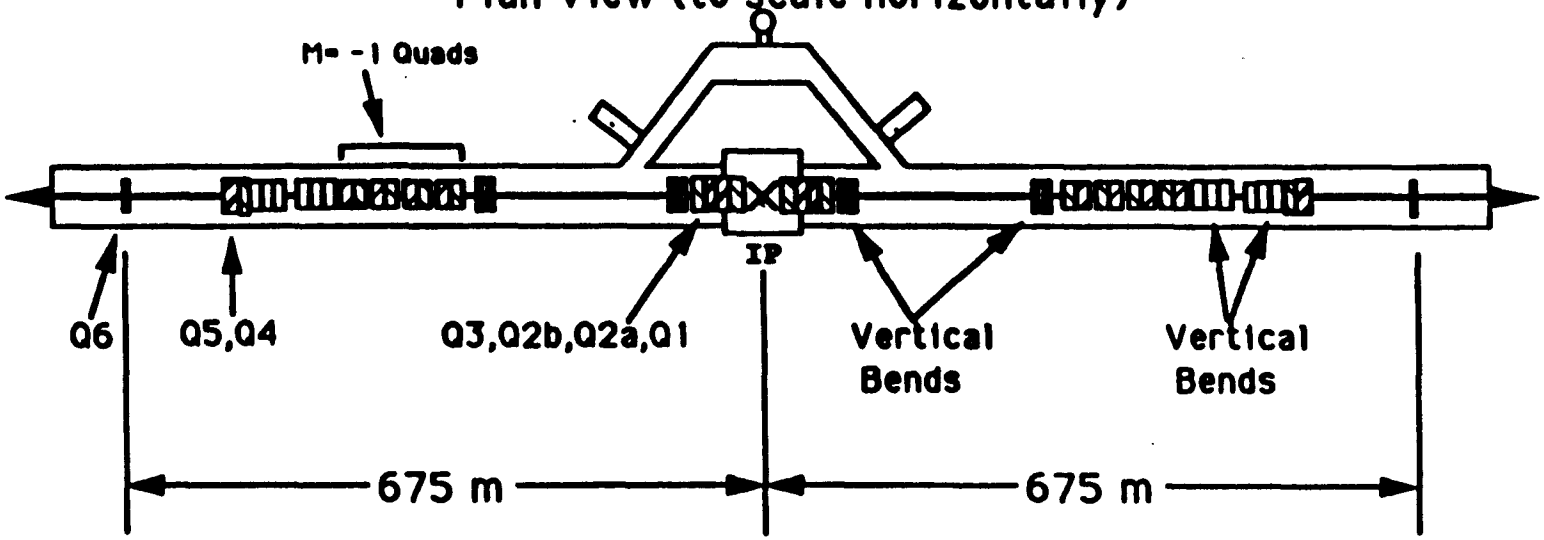

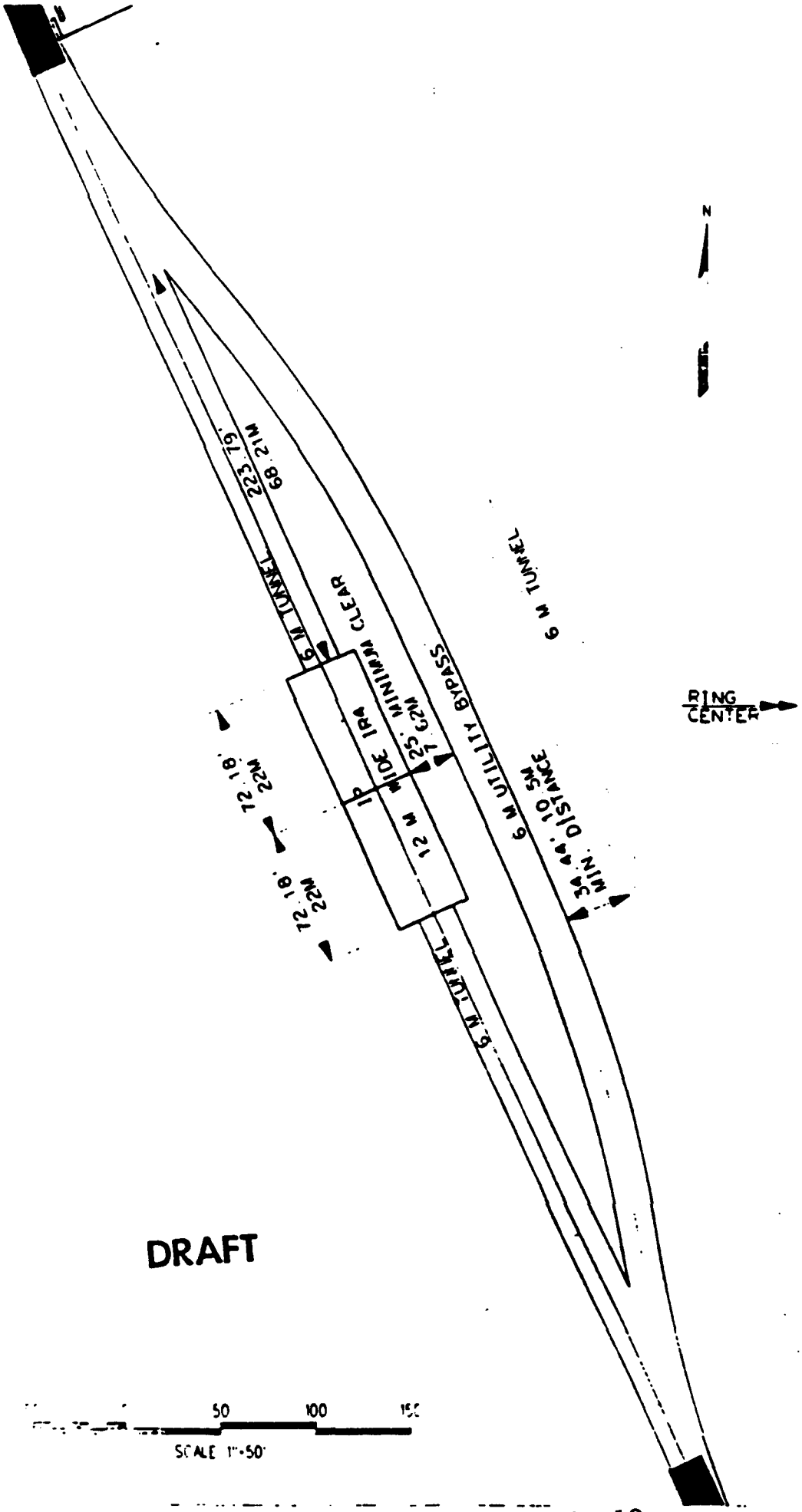
N
RING CENTER
6 M TUNNEL
6 M UTILITY BYPASS
MIN. 34.4 M 10 SM DISTANCE
12 M WIDE IRA
MINIMUM CLEAR
25.62 M
6 M TUNNEL
223.79
68.21M
72.18
22M
72.18
22M
DRAFT
50
100
150
SCALE 1"=50'

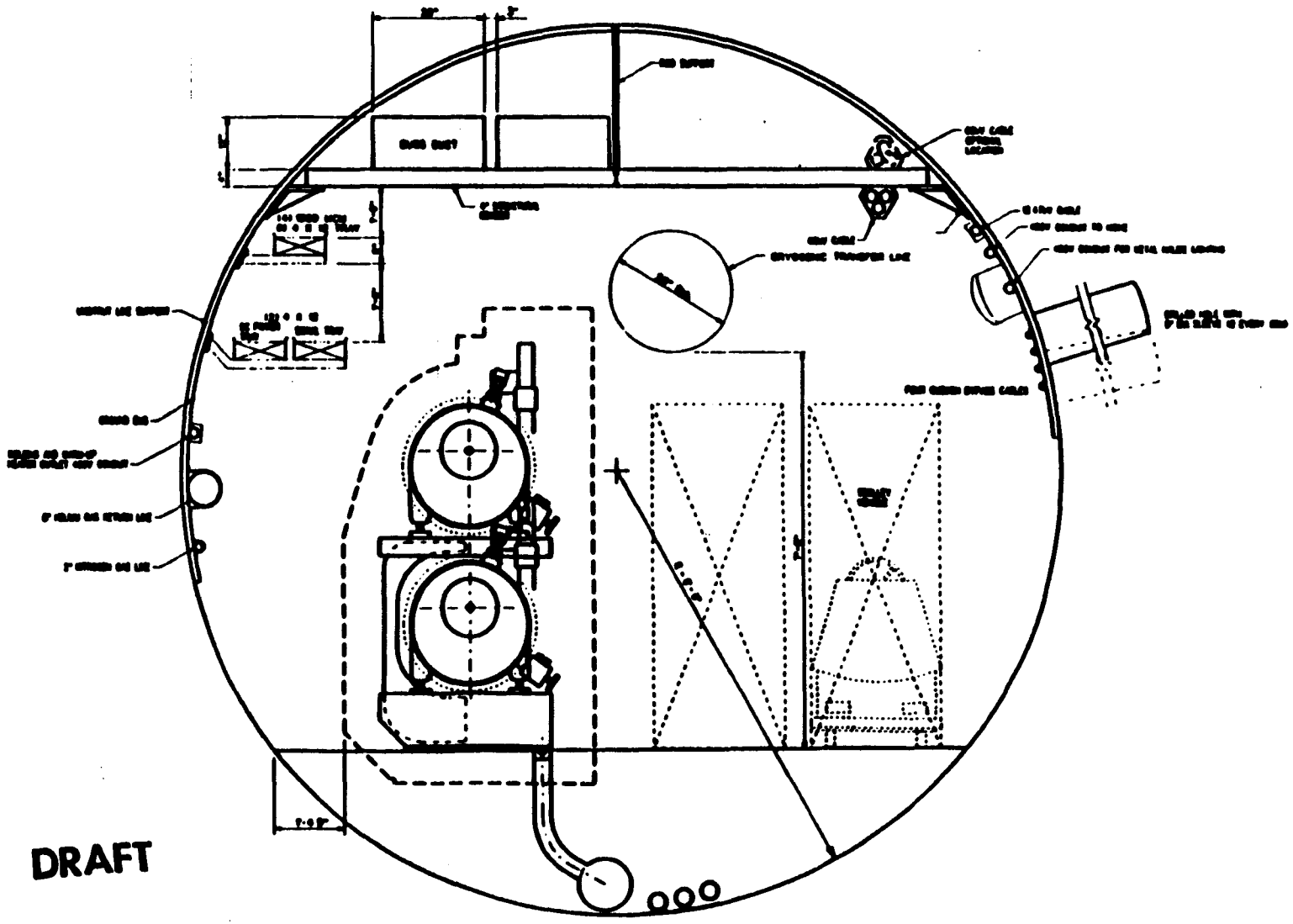
DRAFT
SECTION B
SCALE: 1"=2'

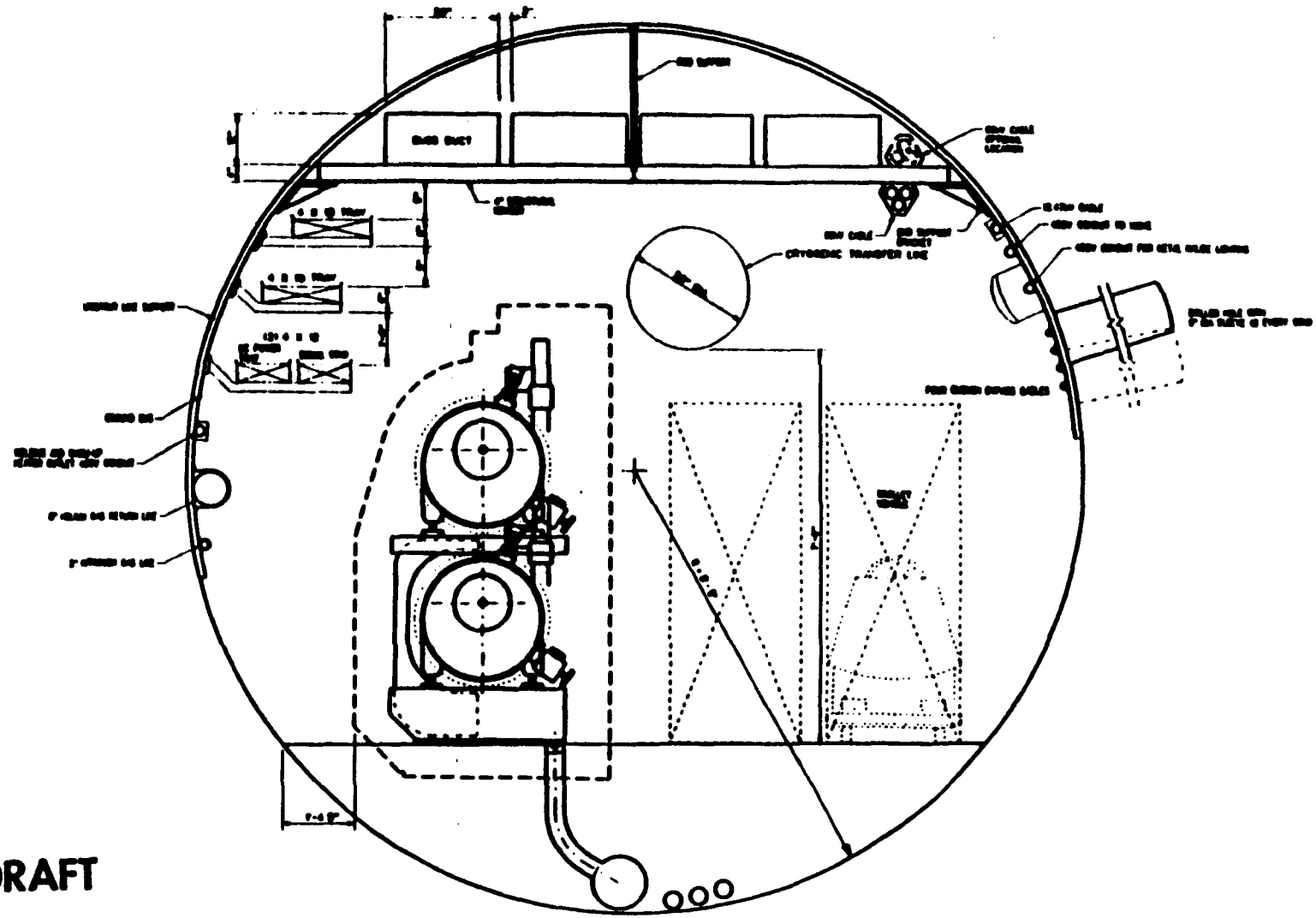

DRAFT

SECTION D

2 0 2 4 6

SCALE 1"=2'

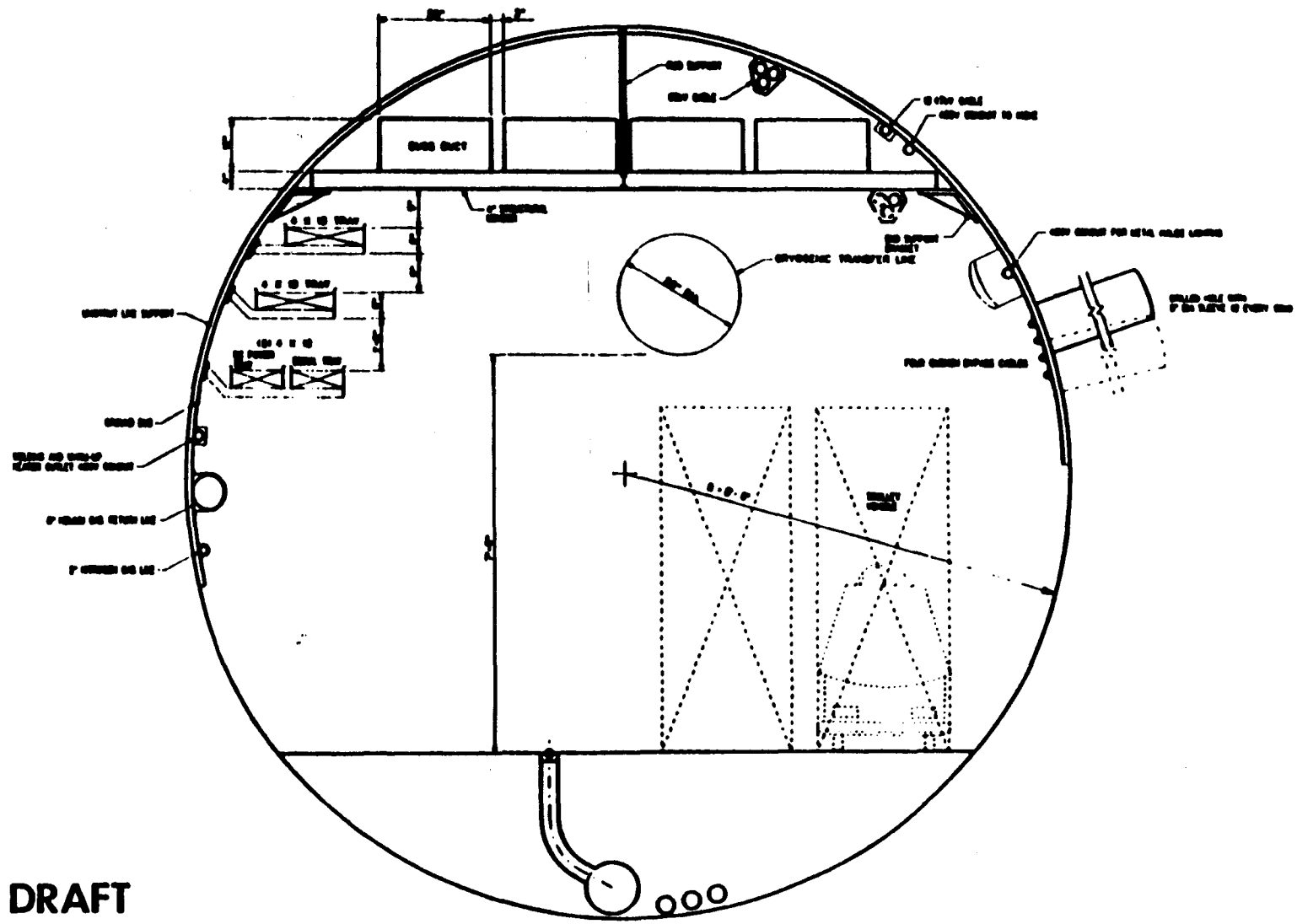

DRAFT

SECTION E

2 0 2 4 6

SCALE: 1"=2'

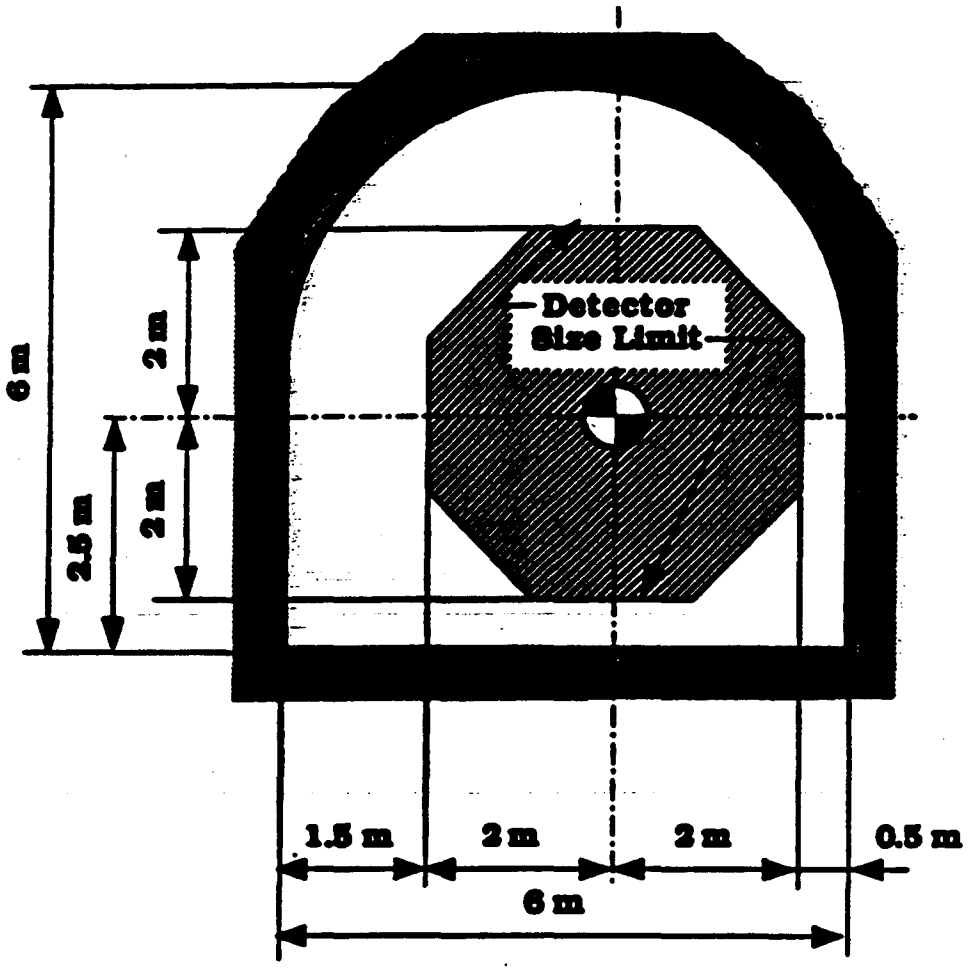

Scale ~ 1 : 125

Section At Ends

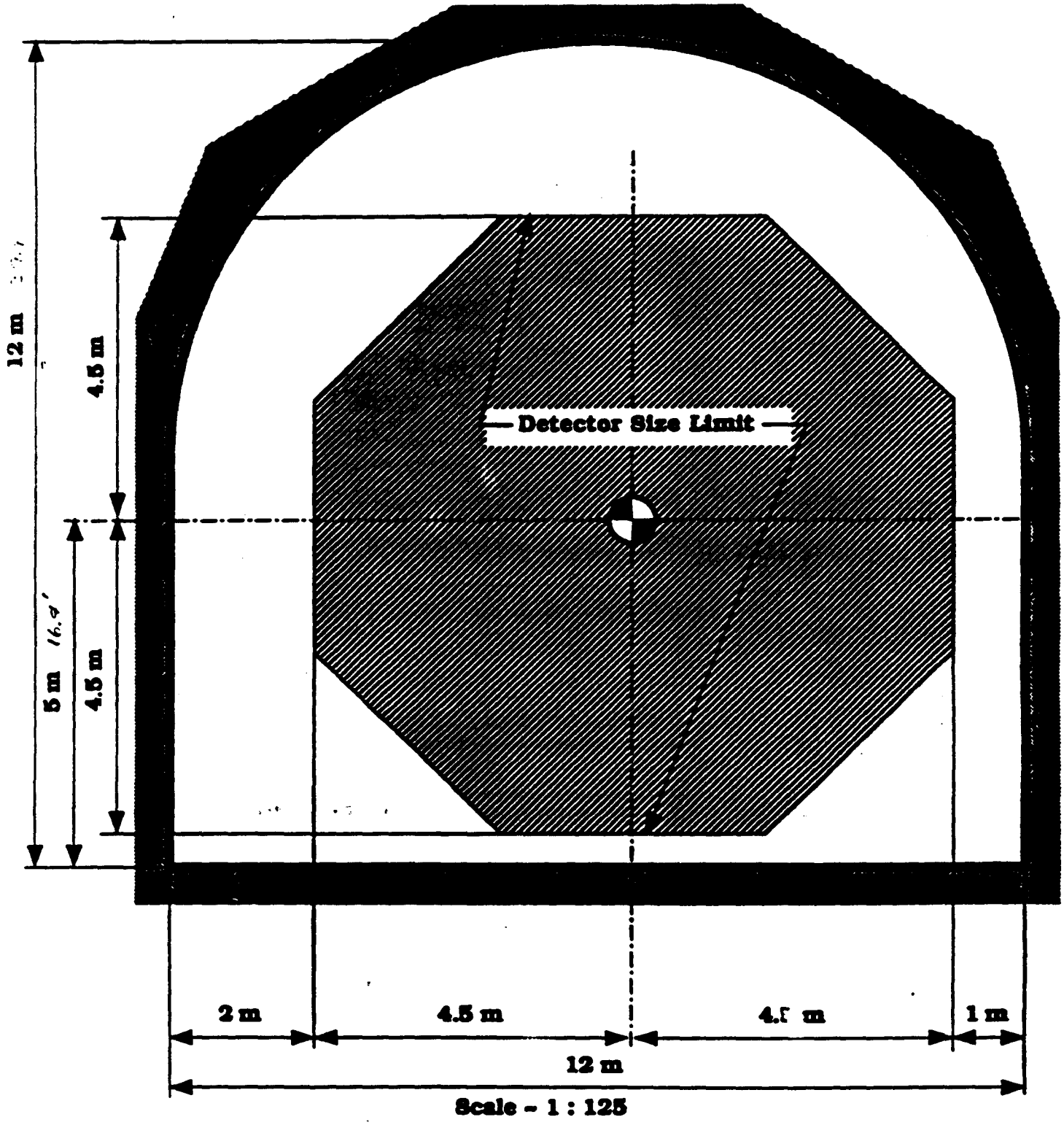

Section At Center

J. Bjorken
Jan '92

F.A.D

A FULL ACCEPTANCE DETECTOR FOR PHYSICS AT THE SSC

OUTLINE

I. What is FAD?
- Philosophy
- History & Status

II. Critical-path items
- Detector architecture
- Backgrounds
- Physics
  - a) Rapidity-gaps + jets
  - b) Leading particle physics & the cosmic-ray connection
  - c) Quark-quark strong force as $s \to \infty$, t large but fixed
  - d) Low-p_t and vacuum structure
  - e) "Conventional" topics

III. Future plans

I. WHAT IS FAD?

"Fun And Discoveries"

Non-negotiable criteria for the FAD:

1. "All" charged particles seen & momenta measured well (if p_t not too large).
2. "All" photons seen & momenta measured well.
3. Physics of rapidity-gaps (diffraction, Pomeron physics, etc.) not compromised.

Examples:

300 MeV π^+ at 90° seen

10 TeV π^0 with $p_t \sim 0.5$ GeV seen ($\theta = 50\,\mu rad$)

Dynamic range in p_ℓ is $\sim 10^5$

$200\,MeV < p_\ell < 20\,TeV$.

Important variables are LEGO

p_t : (typically, 0.5 GeV within factor 2)

φ : azimuthal angle

$\eta = -\log \tan \frac{\theta}{2}$ = (pseudo)rapidity

Important: THINK LEGO

At the SSC

$$-12 \lesssim \eta \lesssim +12$$

η	θ	p_z at $p_t = 0.5$ GeV	Distance from beam axis at $z = 100$ m
0	90°	0	∞
3	100 mrad	5 GeV	10 m
6	5 mrad	100 GeV	50 cm
9	250 μrad	2 TeV	2.5 cm
(11.3)	25 μrad	20 TeV	2.5 mm
12	12.5 μrad	40 TeV	1.25 mm

Physics philosophy:

FAD is a <u>survey instrument</u>

Sensitive to everything
Optimized for (almost) nothing

FAD physics strength is in perception of <u>complex patterns in individual events</u> as a signature of new and/or interesting physics. Examples will come later.

Some examples where FAD's led to breakthroughs:

1. Berkeley Bubble Chamber: Multihadron final states (hadron resonances)

2. Mark I: First 4π detector (it saw jets with it

3. Pisa-Stony Brook at ISR
   30" Chamber at FNAL
   15' BC at FNAL } (ν's)
   Gargamelle } (ν's)

   } Systematics of particle production; basis of all modern Monte-Carlos.

istory & Status:

.991	January	I begin writing SSC "expression of interest".
	April 1	Presentation to SSC Laboratory
	May	E.I-19 (SLAC-PUB-5545) submitted to SSC Laboratory.
	August	SSC & PAC review the E.I: "enlarge the tunnel ±500 m from 3rd collision point."
	Dec 7	FAD Working Group organized at SLAC meeting.
1992		Lots of work to do
1993		Collaboration formed (??)
		Proposal prepared (??)
	~Dec	Proposal submitted to SSC/PAC
		⋮
2000±2??		SSC PHYSICS

Reasons for an FAD now:

Physics:

1. $x > .01$ unexplored
2. Small x ($10^{-7} < x < 10^{-4}$) is interesting
   PQCD goes out of control
3. Rapidity-gap physics has been neglected
4. Many more ...

Technology:

Goal of FAD is to maximize information per event.

New technologies are what really drives scientific advances.

Most rapidly changing HEP technologies are:

1. Data acquisition: speed/bandwidth
2. Data processing & storage
3. Data analysis: pattern recognition (e.g. neural-networks)

80% of FAD cost is in this technology.

I. Critical-Path Items:

1. Detector Architecture
2. Backgrounds
3. Physics

1. Detector Architecture

1. To see all collision products, detector is two 20 GeV fixed-target spectrometers face-to-face (+ central barrel)

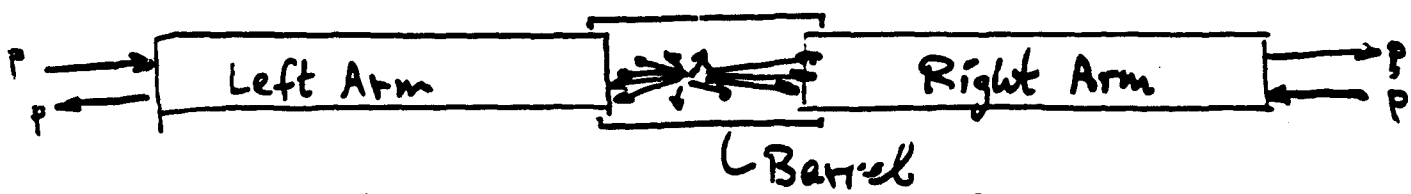

2. Length of arm proportional to beam energy:

$\therefore$ Length = 20 × FNAL ~ 20 × 50m ~ 1 km.

Transverse dimensions are invariant (order mote

3. Beams & beam-pipe go through center of detector

4. Final-focus "low-β" quads embedded within detector arms.

(Tentative) Program for Design Work:

Background studies in parallel with this
Also event generation / physics studies

1. Lay out final-focus architecture & integrate it into SSC lattice design:
   - "Faceplate calorimeter"
   - Endwall calorimeter
   - Leading-particle tracking
2. Photon-detection architecture
   - Placement of upstream calorimeters
   - Beam-pipe design
   - Specifications for calorimeter performance
3. Architecture for charged-hadron detection in absence of magnetic fields.
   - Tracking geometry
   - Pattern recognition
   - Background constraints
4. Magnetic architecture
5. Extras
   - Cerenkov
   - Microvertex
   - Special-purpose subdetectors

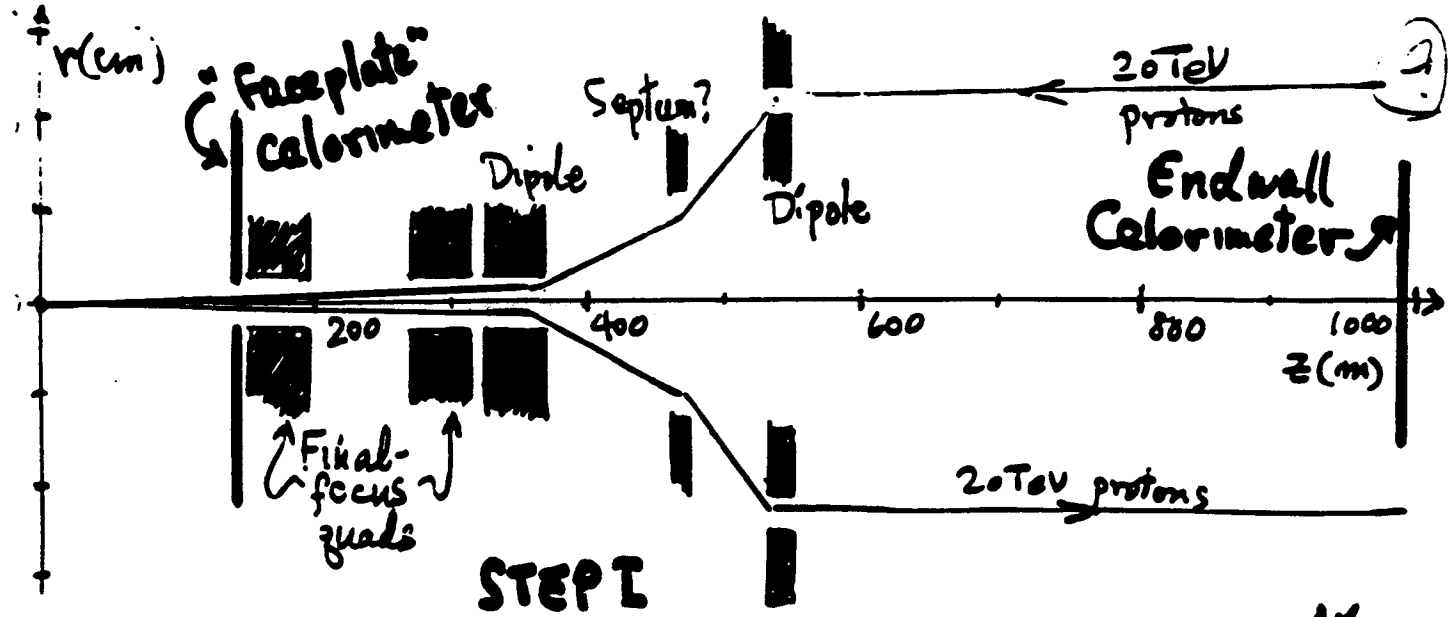

STEP I

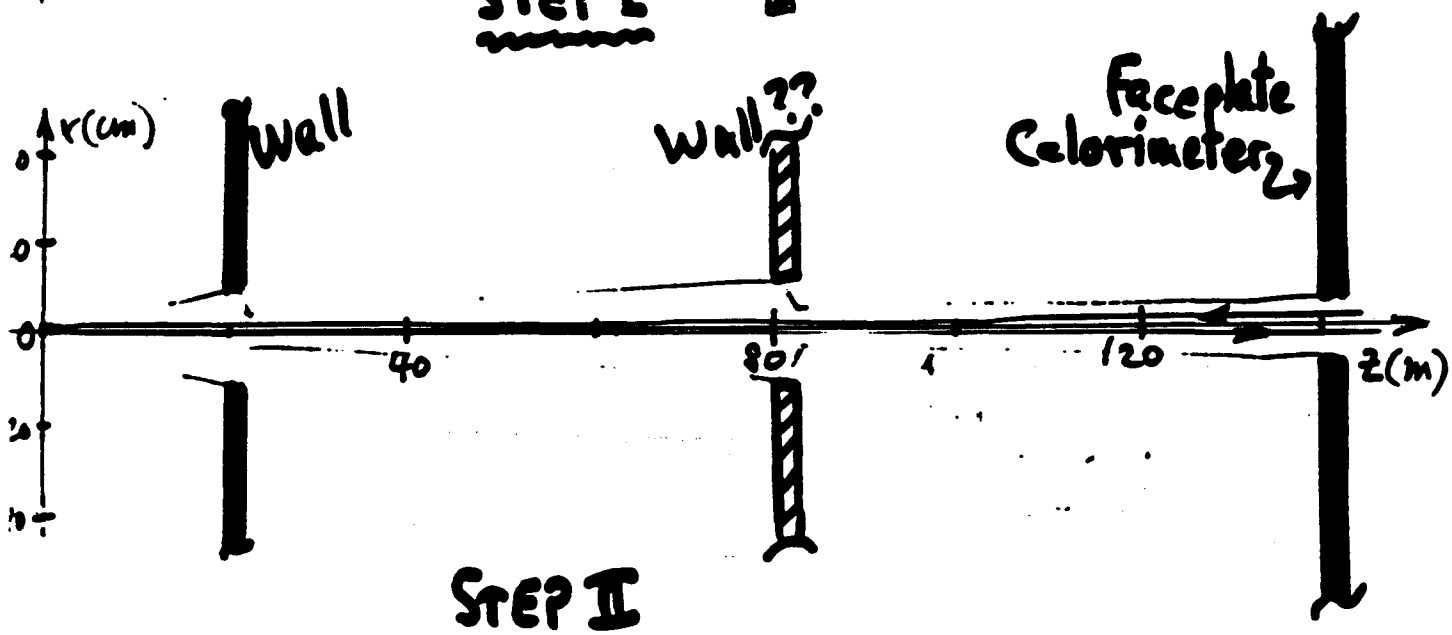

STEP II

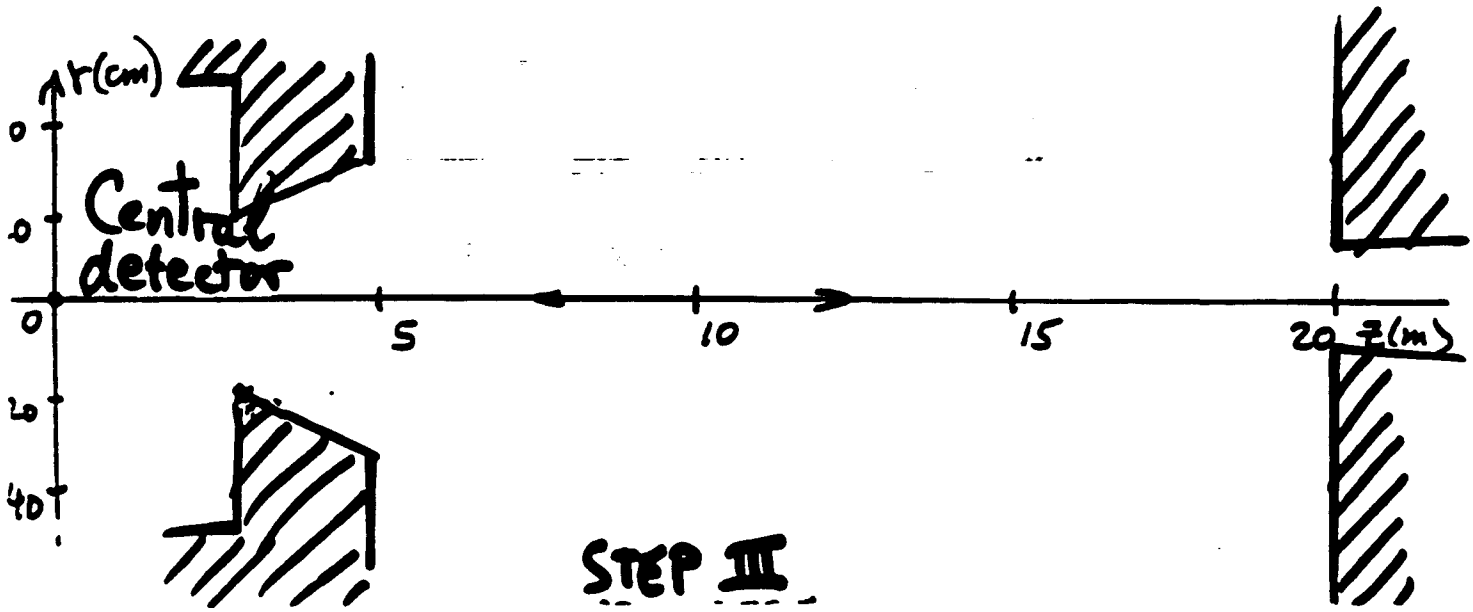

STEP III

2. Backgrounds

Main questions to address:

1. Splash from inner edges of calorimeter apertures:

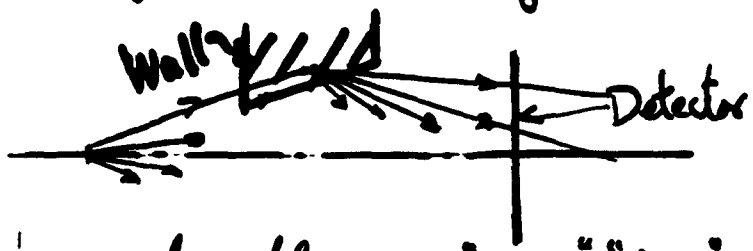

Homework problem: Is "Step I", "Step II", or "Step III" the most difficult case??

2. Grazing collisions with beam pipe

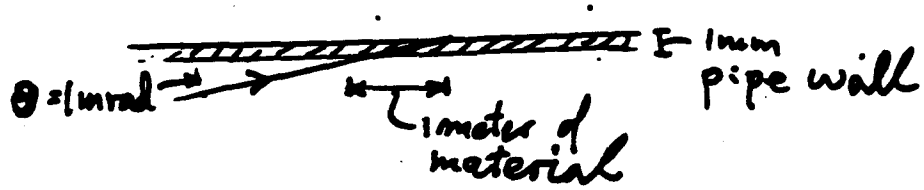

3. Background from beam halo.

Energy-conservation helps here!

Problem easier than

i) fixed target extracted beams

ii) e^+e^- colliders.

Needed: **4. Beam-gas interactions**

Good simulations of transverse shower development near edges. — and theoretical understanding!

3. Physics

The menu is very long.

FAD Working Group will try to select a few "flagship" topics for detailed study.

Candidates include:

1. Rapidity gaps + jets as signature for new-physics searches
2. The cosmic-ray connection: leading-particle physics.
3. Quark-quark interactions as $s \to \infty$ at fixed large t: they get Strong !!
4. Vacuum Structure by observation of low-p_t phenomena (maybe).
5. No doubt, some "conventional" topics:
   - Heavy flavor physics
   - High multiplicity
   - Low multiplicity & "soft" diffraction
   - Multijets & minijets
   - Making a TeV π-π collider (W. Walker)

Rapidity-gaps + jets

Generic minimum-bias event

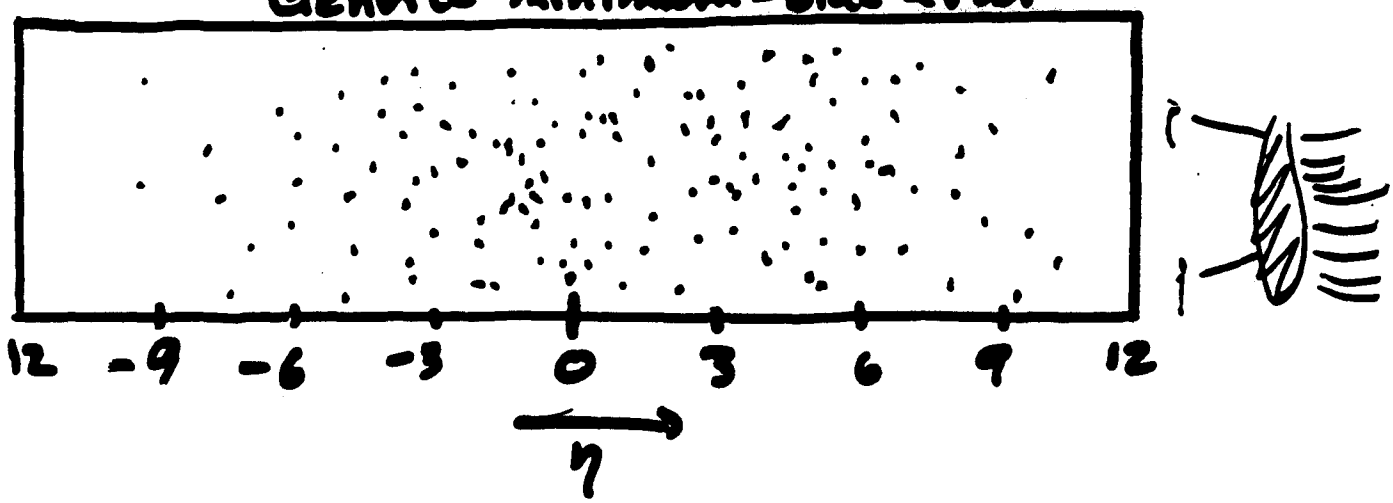

Double inelastic diffraction

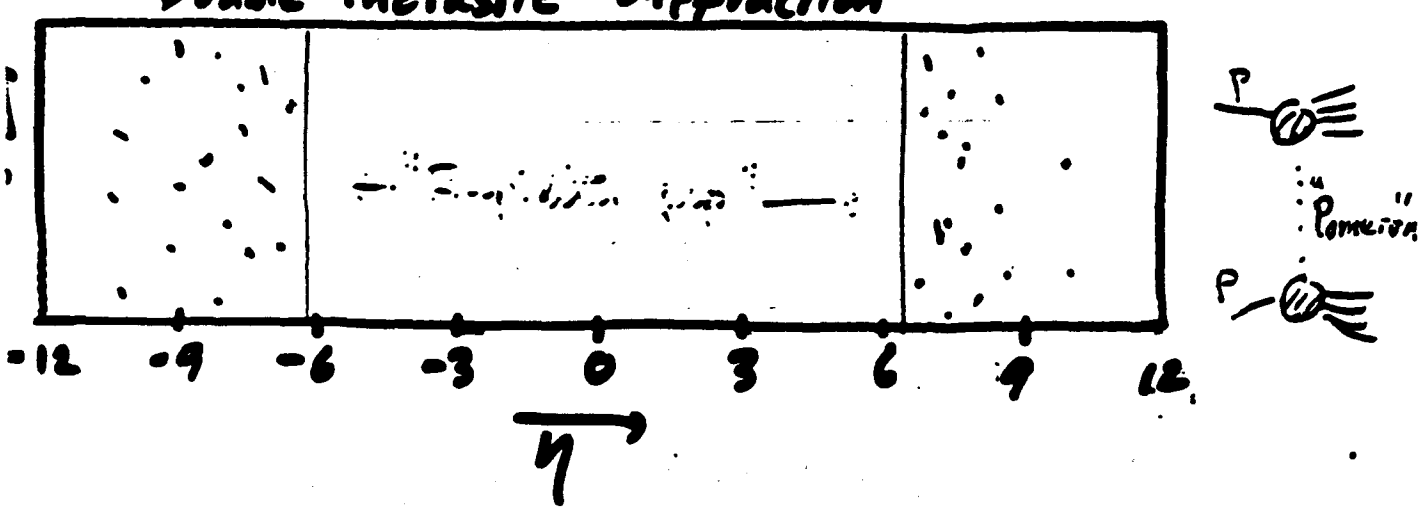

Photon, W, or Z exchange at high Q^2

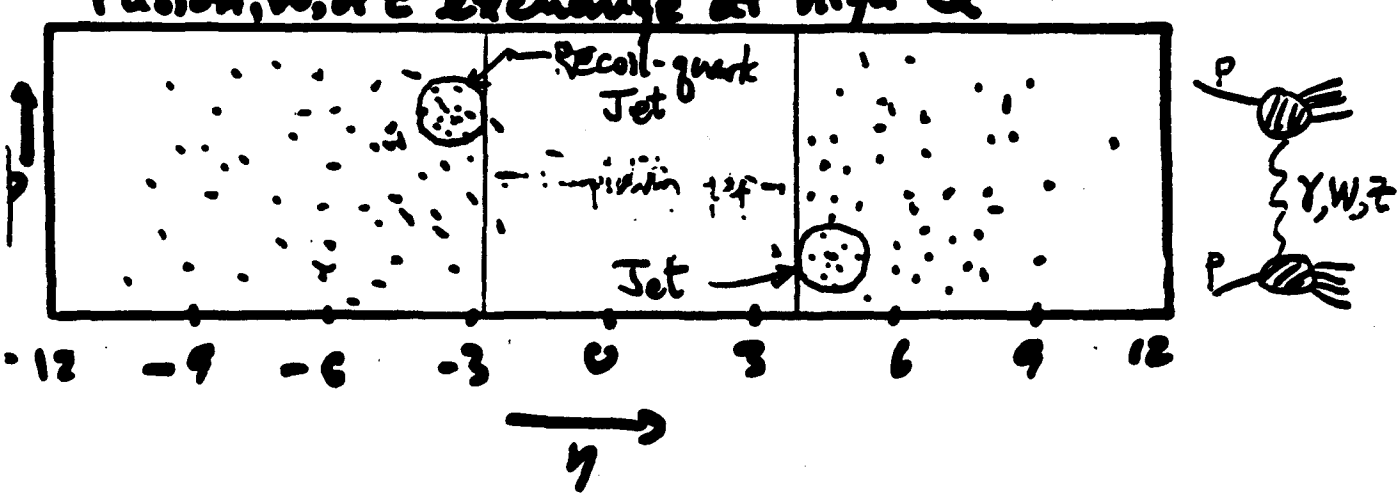

Comments on γ, W, Z-exchange processes:

1. Naive event topology as shown usually does not survive spectator collisions filling in the gap. Estimated survival probability is ~10%, mostly peripheral collisions (impact parameter > 1 f).

2. Define jet as contents in lego plot within radius 0.7 of jet core. Then boundary of gap is tangent to circle, as shown (leakage ≲ 1 particle/edge).

3. It is useful to introduce polar coordinates within circle of radius 0.7 & then remap to rectangular lego coordinates ("extended phase space"). [Idea due to Gustafsson/Lund]

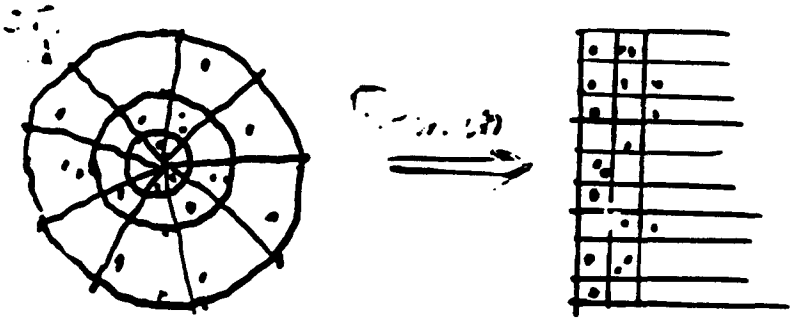

This will be used later.

$\gamma\gamma \to \mu\mu$ at high Q^2 and $\hat{s}$

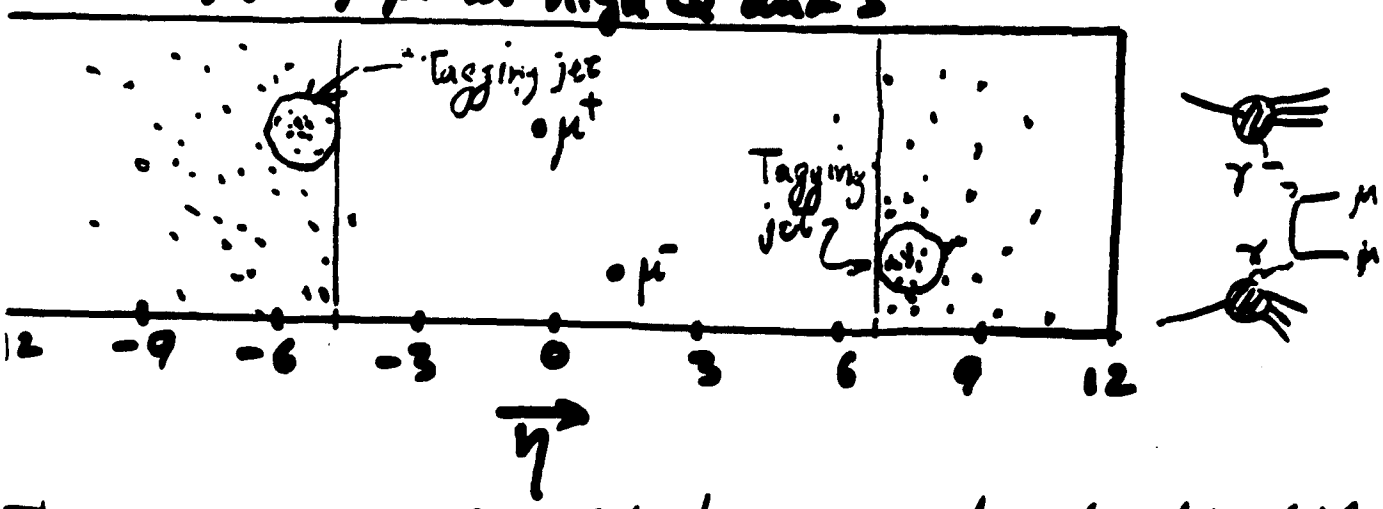

This process good for calibrating survival probability of the gap.

$WW \to b\bar{b}$ or $WW \to H \to b\bar{b}$

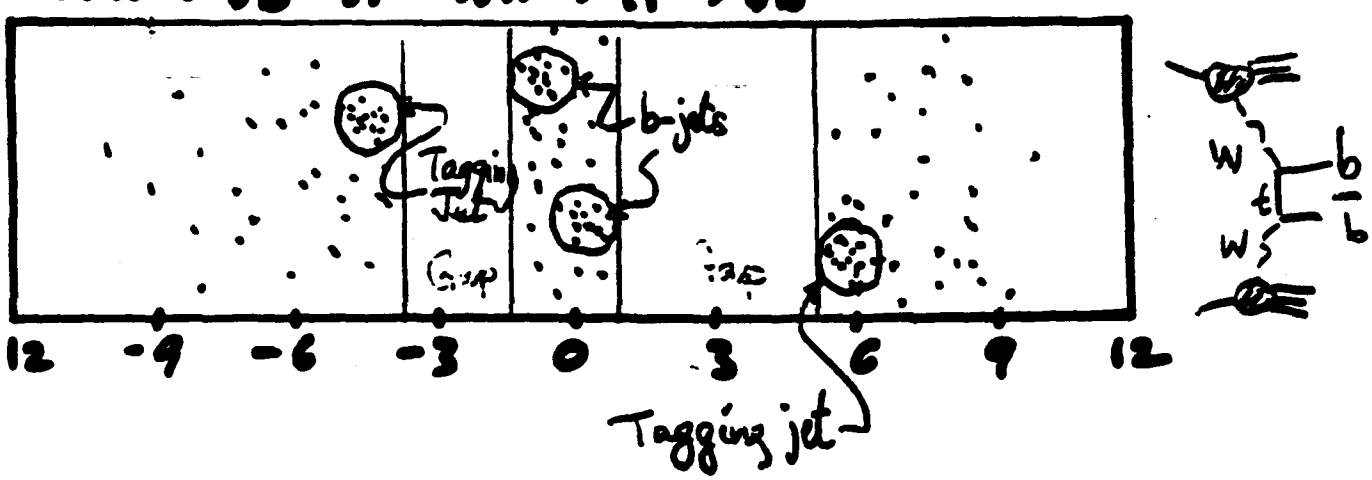

This process <u>may</u> have a strong-interaction background even at high p_t. Subprocess is shown below. If it is big, then $gg \to$ Higgs also has rapidity-gap topology: can't lose!!

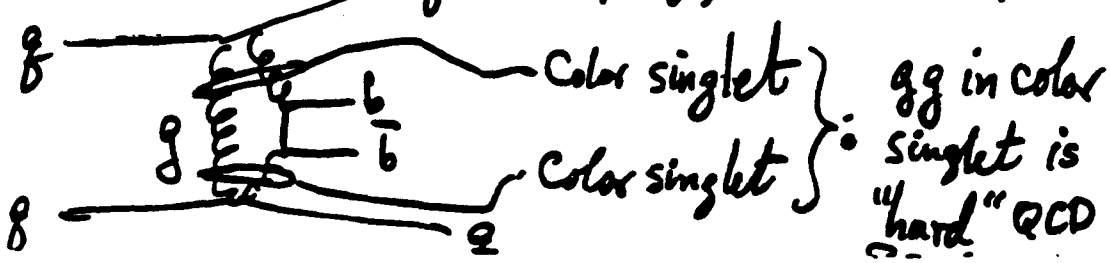

A gold-plated WW event at the TeV mass scale.

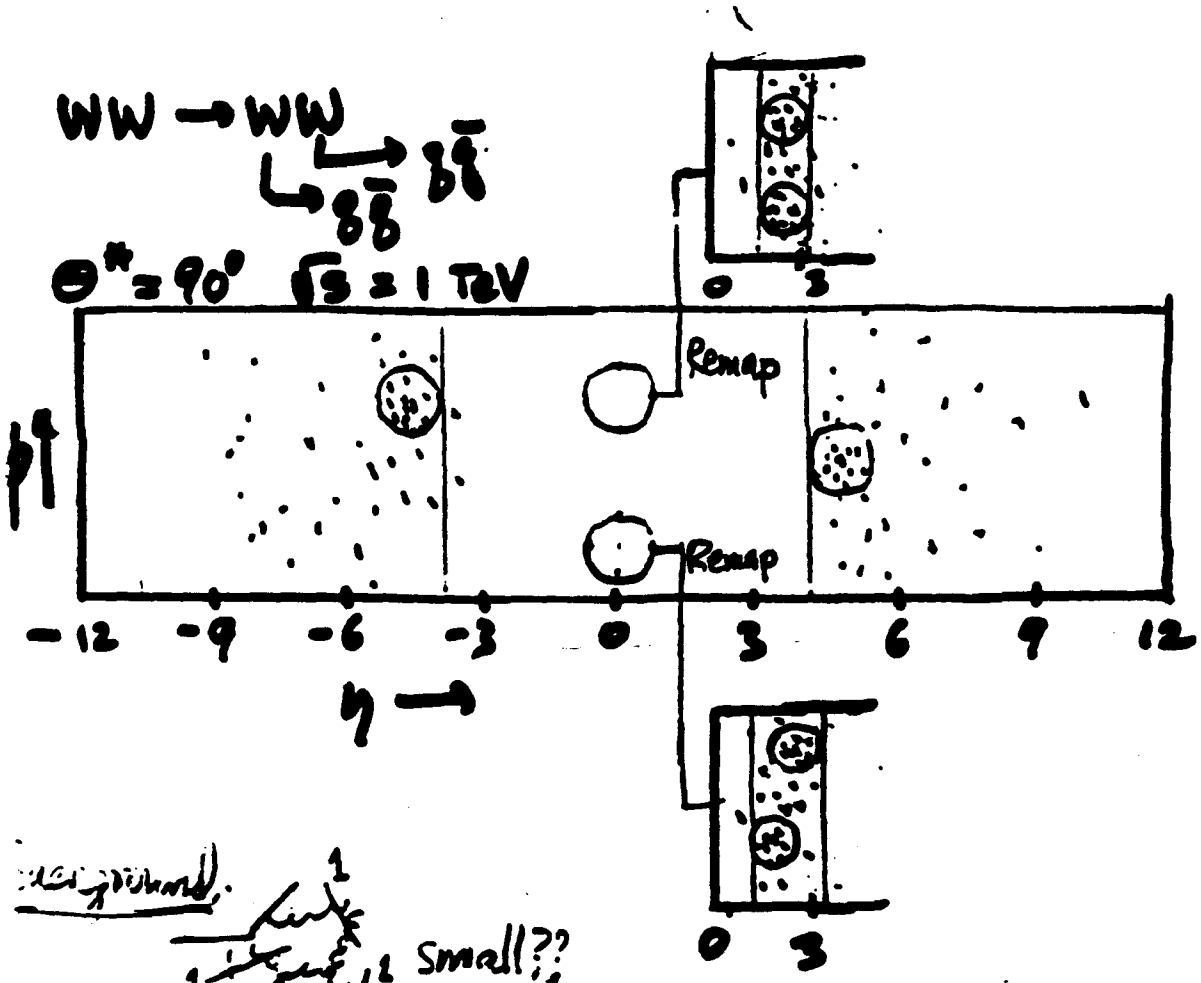

Background

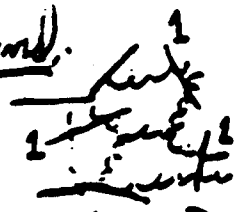

small??

Signature: 1) longitudinal + transverse rapidity gap.
2) dijets within each jet which reconstruct (precisely in principle !!) to m_W.
3) Signature improves as m_{WW} increases.

Rate: Total Higgs yield is 2 pbarn at $m_H = 1$ TeV
With survival-of-gap of 12%; yield ≈ .25 pbarn.
Even the FAD might see a 1TeV Higgs !!!

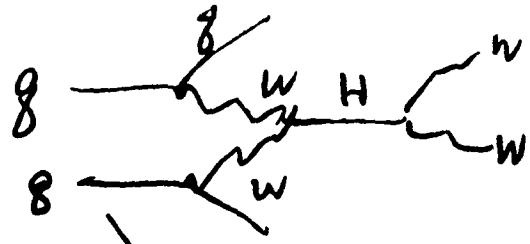

automatically land in the gap region because $\sqrt{s}_{qq}$ is so large.

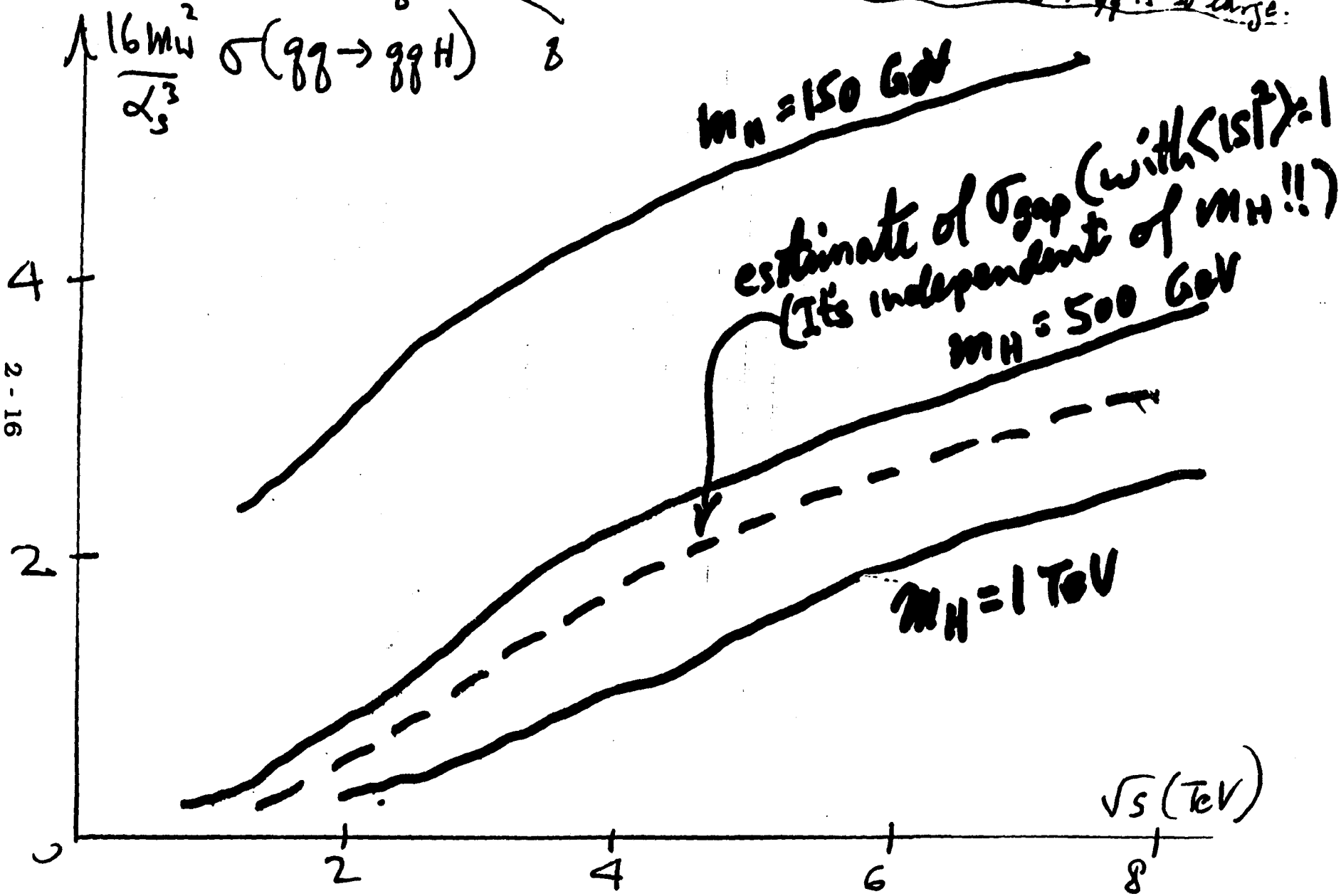

$F(b)$ = qq luminosity as function of impact parameter b

(From Block, Halzen, Margolis)

$|S(b)|^2$ = survival probability of gap: transmission ~~coefficient~~ probability for pp at impact parameter b

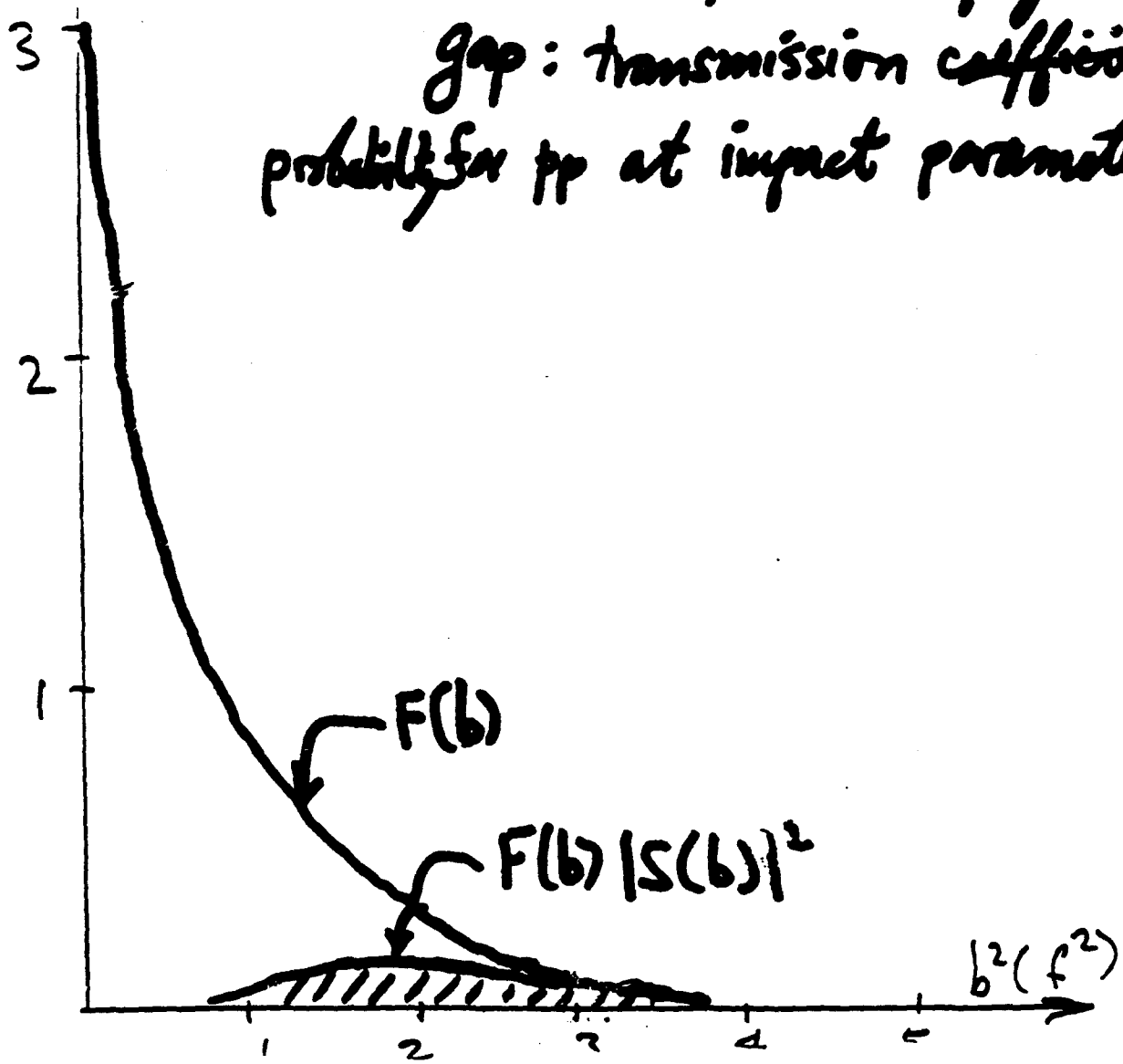

Finding the TeV Higgs:

If the survival of the gap, $\langle |S|^2 \rangle$, is estimated properly, then it's easy even for Stage I FAD $\left(\frac{d\$}{d\eta} = \$1M\right)$.

1 TeV Higgs is the <u>easiest</u> case.

All decay modes available.

WW as well as ZZ can be seen $\left(\frac{WW}{ZZ} = 2\right)$:

Take $\mathcal{L}_{FAD} = 5 \times 10^{31}$ (SSC design, not EOI-19)

$$\frac{\text{FAD Rate}}{\text{"Gold-plated" 4l Rate}} = \left(\frac{WW+ZZ}{ZZ}\right) \cdot \frac{\mathcal{L}_{FAD}}{\mathcal{L}_{SSC}} \cdot \frac{1}{(BR)^2_{ll}} \cdot \langle |S|^2 \rangle \cdot \left(\begin{array}{c}\text{fraction with gaps}\\ \text{wide enough}\end{array}\right)$$

$$3 \cdot \frac{1}{20} \cdot \frac{1}{(.06)^2} \cdot (.05) \cdot 1$$

$$= 2$$

No BACKGROUND UNDER FAD EVENTS (except nonresonant WW)

[Of course, signature not unique to FAD.]

A Stage I FAD that can see the 1 TeV Higgs:

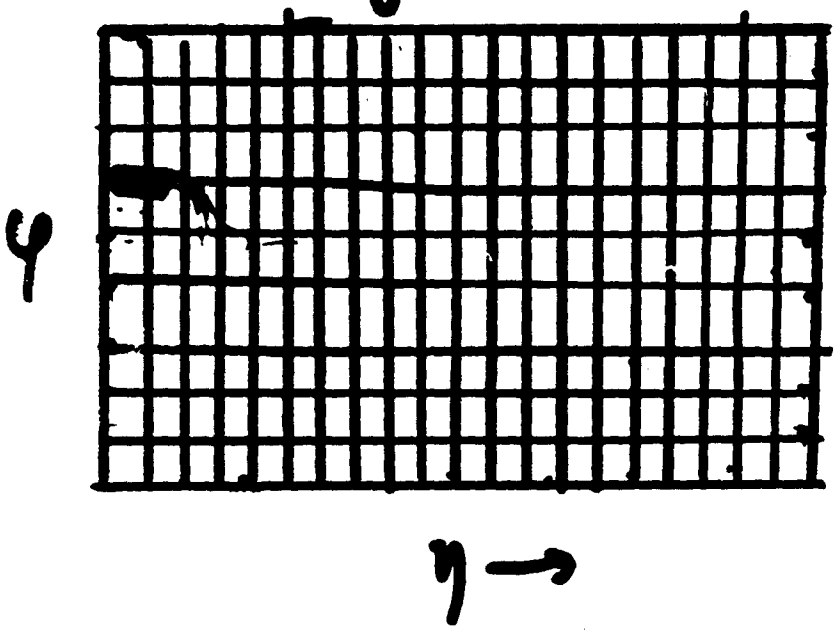

1. Endwalls omitted here (but not in FAD Stage I !!)
2. 9×20 pixels
3. $\Delta\eta \sim \pm 7$

One independent detector/pixel. It reads out the following basic information:

N_{ch} (typically 0 or 1)

E_T (em)

E_T (had)

Muon count (if isolated, i.e. the only charged particle seen).

An example of an architecture for the basic downstream detection plane: $\Delta\eta = 0.7$; all $\Delta\psi$:

$\Delta\varphi = \frac{2\pi}{9} = 0.70$

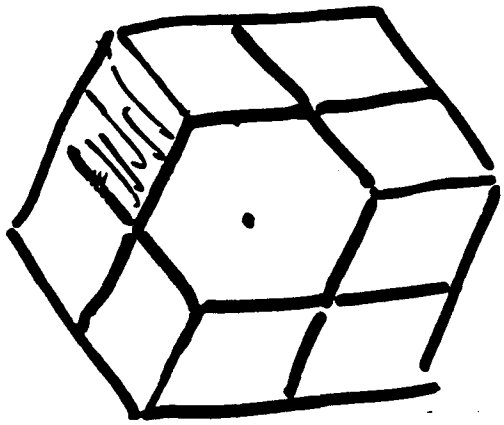

1. All panels are the same shape:
2. Projective geometry.
3. All panels can be read out on the outside edge even after upgrading to strip subdivisions:

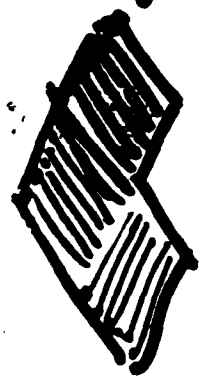

4. Nice extension to the central detector (

5. Panels for central detector are square. (15.6)

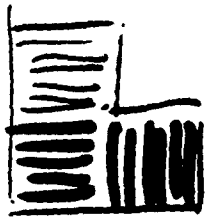

6. They fit together to make a BOX, with beam-axis down the body-diagonal (See model)

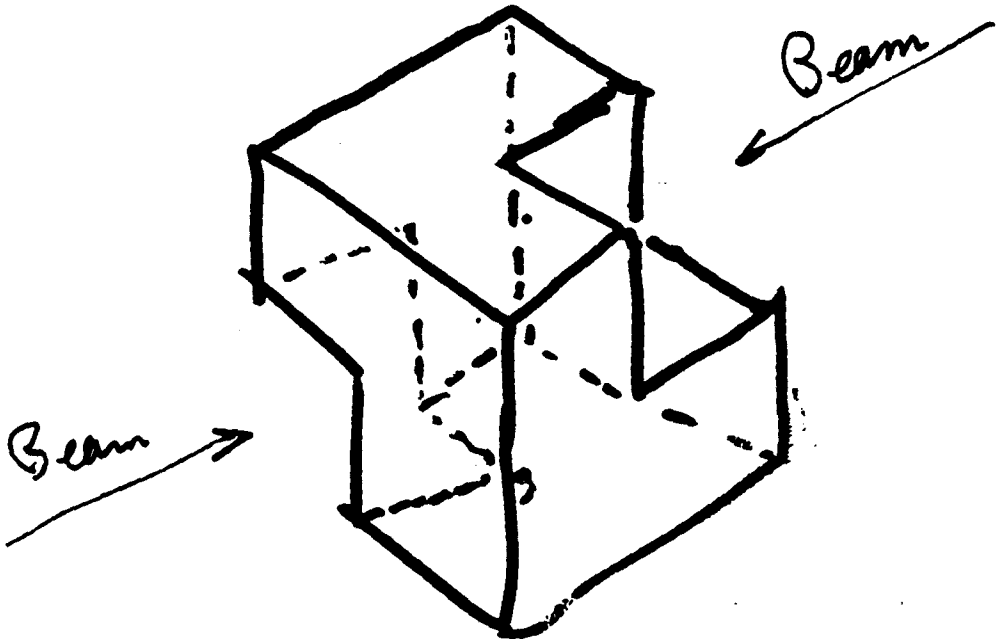

An example of a detector for a lego pixel: (5.7)

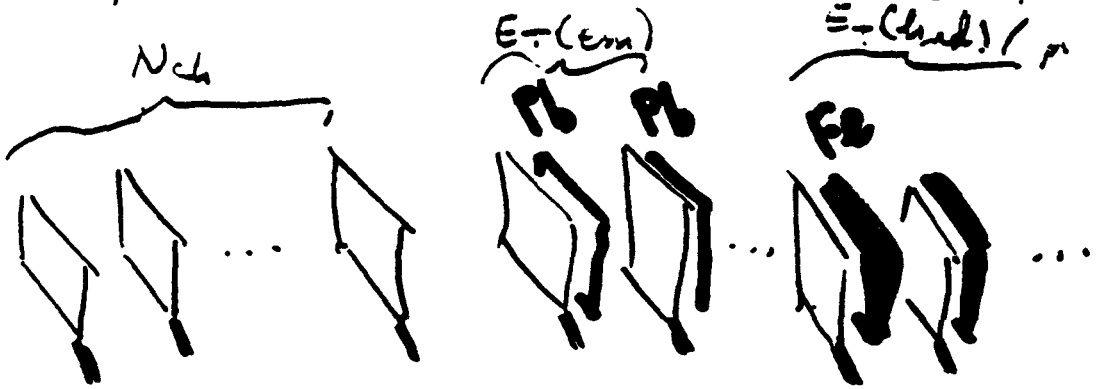

Apologies for the 1950's technology).

30 ± 15 scintillator panels
30 ± 15 PMT
Fe
Pb
Electronics & processor.

$\lesssim$ \$70K ??

14 pixels/$\Delta\eta = 1$

$\lesssim$ \$1M/$\Delta\eta = 1$

This should be good enough for the Higgs signature characterized mainly by lots of zero readings in the central region of the detector.

2. The Cosmic-Ray Connection (F. Halzen presentation; 7 Dec)

Considerable interest in FAD from the cosmic-ray community:

1. Origin of cosmic rays in PeV - EeV range: (10^{15} - 10^{18} eV; extensive air showers):

   a) Origin simply NOT KNOWN.
   Issues involve { early universe / exotic astrophysical objects

   b) To determine primary composition, requires knowledge of interaction properties in atmosphere. <u>Leading particle production</u> is crucial.

   c) Emulsion-chambers, etc. argue against simple scaling up in energy. Also exotic events (Chiron, Centauro) are still unexplained.

2. Cosmic rays have anticipated correctly HEP in recent past:
   Jet structure & strong growth of $\bar{n}$
   Heavy flavors

Quark-quark interactions get strong as $s \to \infty$ with t large and fixed!! (A. Mueller presentation; 7 Dec)

Consider large-t scattering of leading quarks: ($x_F \sim 0.1$); say $t \sim 100 - 10^3\ \mathrm{GeV}^2$.

Naive cross-section:

$$\sigma_{Naive} \equiv \frac{d\sigma}{dt\, dx_1\, dx_2} \sim Q(x_1, t)\, Q(x_2, t)\, \frac{4\pi\alpha_s^2(t)}{t^2}$$

Structure-functions known: no extrapolations!

QCD expectation: keeping x_1, x_2, t fixed and $\hat{s} \to \infty$, σ_{Naive} is wrong!! the real σ grows as a power of $\hat{s}$ ($\sqrt{\hat{s}} = qq$ cms energy $= \sqrt{x_1 x_2 s}$)

Define enhancement factor $f \equiv \dfrac{\sigma}{\sigma_{Naive}}$

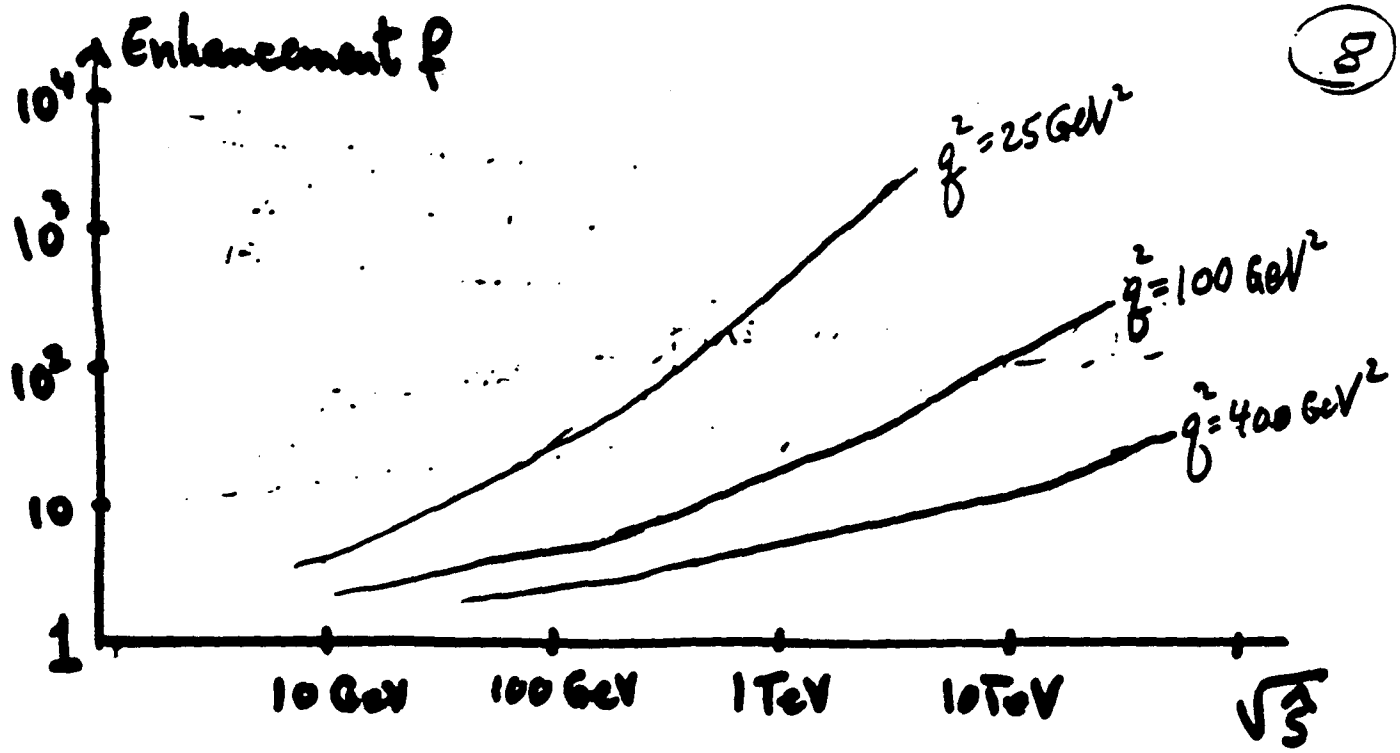

The physics is multiple emission of gluons of $k_t \sim q$. The evolution equation is BFKL, not DGLAP (Altarelli-Parisi).

Mueller-Navelet suggestions for experiments:

1. Measure f (analogue of σ_{tot}) by determining qq scattering vs $\hat{s}$ (2 jets at ends of lego plots)

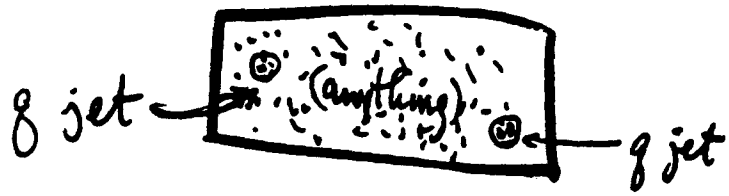

2. Measure analogue of σ_{el} looking at pure coplanar leading jets at ends of lego plot.

Jet-jet angular correlation (in azimuthal angle)

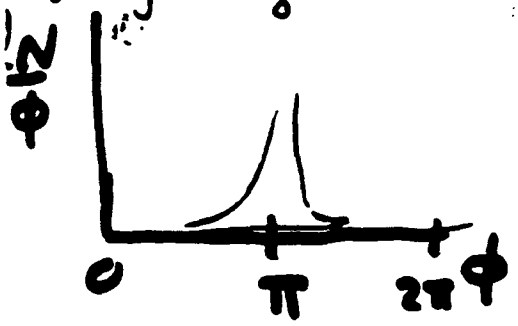

Small $\hat{s}$

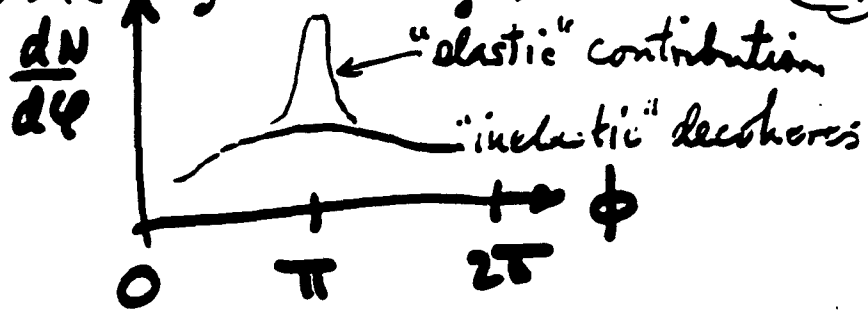

Large $\hat{s}$

As f increases toward unitarity saturation $\sigma_{el}/\sigma_{inel} \to 1$ ("black-disk" limit). Elastic peak is therefore observable.

An alternative strategy: Pay the price of a rapidity gap and the elastic contribution is just double diffraction at high t: it should be <u>enhanced</u>.

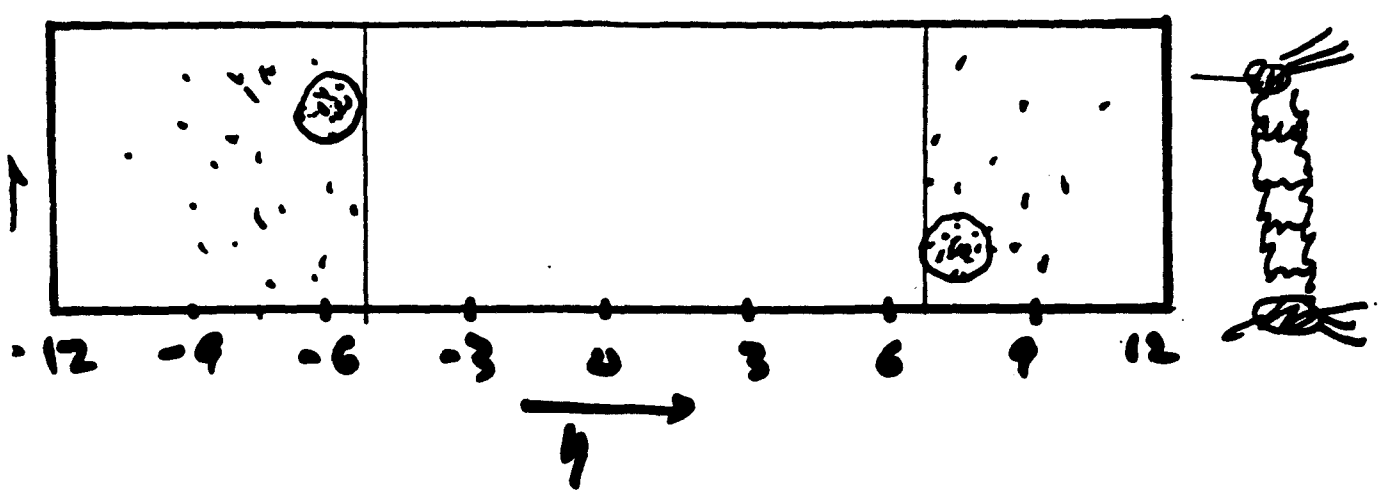

4. Vacuum Structure via Low-p_t Observations with M. Weinstein

(20)

The experiment:

1. Choose non-jetty events with large $\frac{dN}{d\eta}$

2. Look at p_t distribution. It should have anomaly at low p_t:

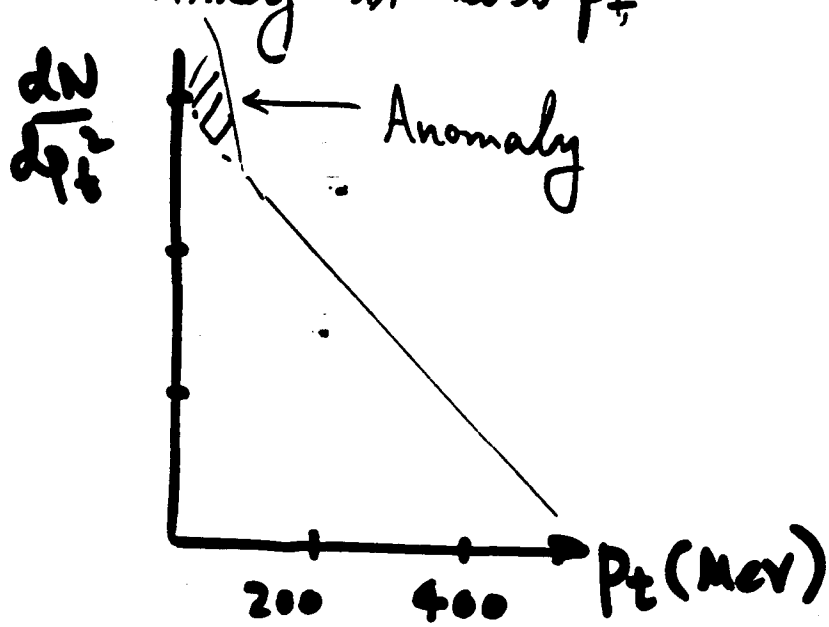

3. Cut on anomaly: keep the low p_t piece.

4. Look at charged/neutral ratio anomaly for individual events:

$$f = \frac{N_{\pi^0}}{(N_{\pi^0} + N_{\pi^+} + N_{\pi^-})}$$

5. Distribution of f should be <u>broader</u> than Poisson statistics, $\sim f^{-1/2}$:

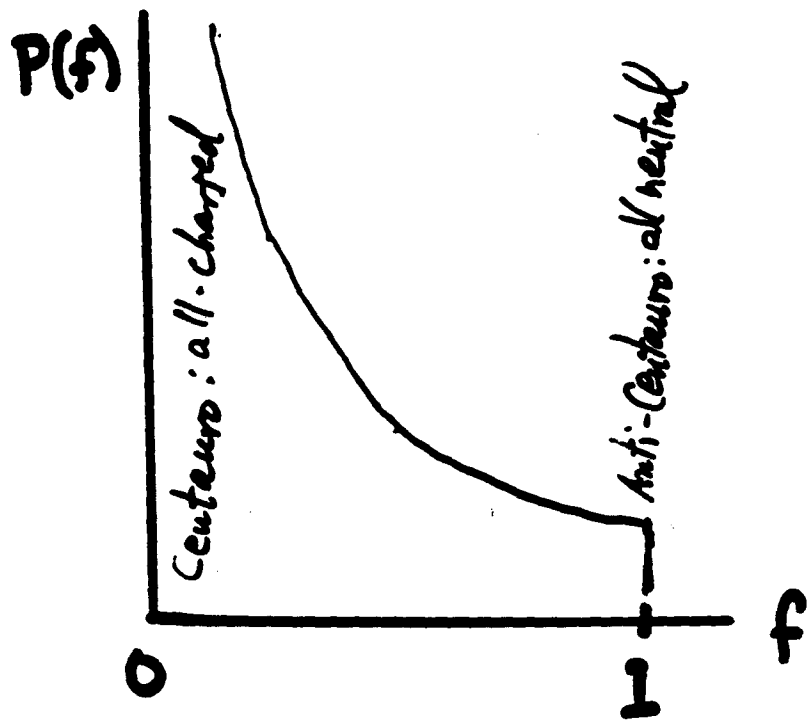

This is Centauro-like behavior.

The physics:

Before |→ ←|

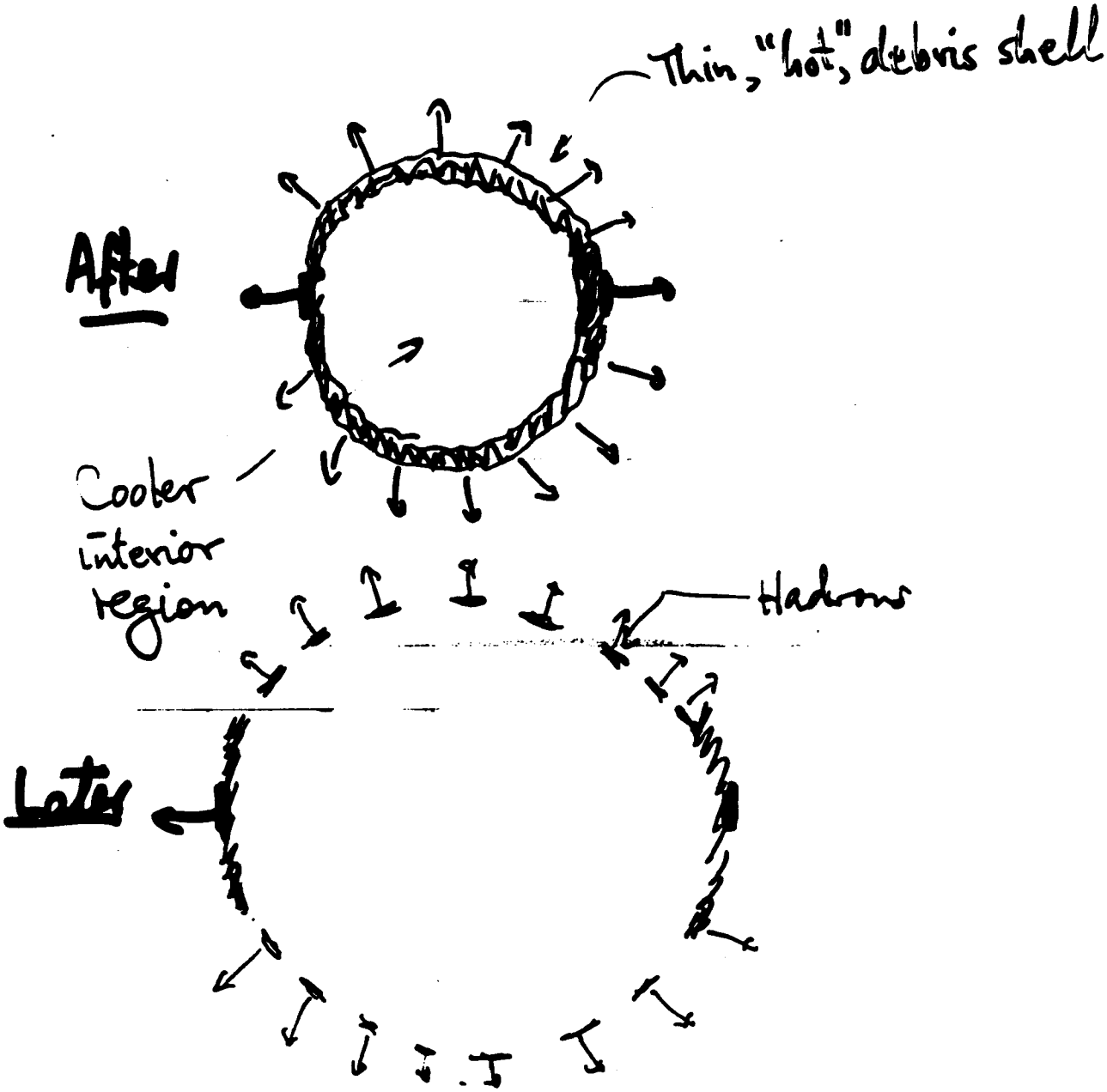

Vacuum disoriented
"tilted" toward π^0

σ
Vacuum oriented in σ direction

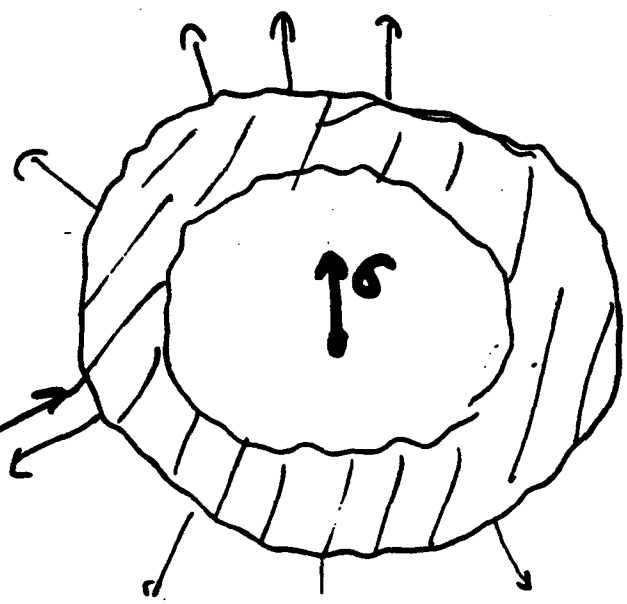

σ

π^0 field radiated away

Data? See Van Hove, Ann Phys 1988 (a3

Advantages of SSC:

1. Large $\frac{dN}{dy}$:

$$\left(\frac{dN}{dy}\right)_{\text{ordinary}} \sim R^2$$

$$\left(\frac{dN}{dy}\right)_{\text{Anomalous}} \sim R^3$$

R: "decoupling radius" ($\gtrsim$ 3-5 f ??)

2. Large η: Easier to see low-p_t γ's & $\pi^\pm$??

Note: Idea is speculative, but
If correct, could teach things about
QCD chiral vacuum:
Spinoff: Technicolor theories.

I. Future Plans for FAD Working Group

(24)

Dec 7 mtng
~35 people showed up at Dec. meeting
Other additional parties very interested.
Experimentalist representation from

Wisconsin	Rockefeller
UC San Diego	U Tennessee
UC Berkeley	Vanderbilt
UC Santa Cruz	MIT
SLAC/SLD	Maryland/George Mason

Additional (experimentalist) interest

SSC Lab	Pisa	Michigan
Seattle	Torino	Duke
Cornell	Pavia	

Considerable theorist interest - and it is growing

However, not clear yet how many will be able to do real work on the FAD.

2. Stage I

In order to be practical, FAD needs to be staged.

An acceptable scenario is Stage I ($\sim\$30 \pm 10$M from SSC) ready at commissioning; full detector in all its splendor finished within 5 years of commissioning.

What is Stage I?

At Dec? meeting, consensus was that Stage I adhere to full-acceptance philosophy. Instrument all η's, but austerely

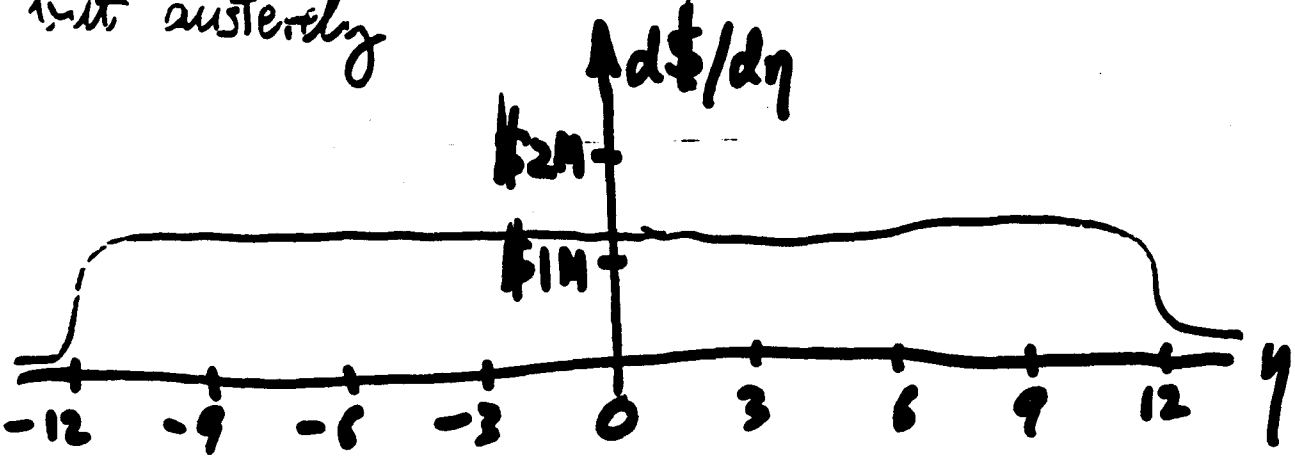

Tentative guideline/conceptual-design constraint is $d\$/d\eta \lesssim \$1$M. Since most of cost is readout, a lot of this might be mitigated by coarsening the coverage.

If local bumps in $d\$/dy$, then preference of Dec 7 participants was $3<|\eta|<7$. or $|\eta|>7$, not $|\eta|<$

3. Subgroups

a) Physics (bj)

b) Backgrounds (A. Wiedemann)

c) SSC interface (J. Venuti)

d) Management (P. Burrows)

4. Landmarks

Several meetings this year where FAD participants hopefully will gather.

March 13-15	FAD at SSC
April 13-15	SSC Symposium / Madison WI
June 21-27	Cosmic Ray Symposium / Ann Arbor MI
July 5-31	SSC Detector Workshops / Boulder CO
Sept or Oct	Workshop at Argonne
" "	SSC B-physics workshop.

We hope to exhibit tangible progress at/during each of these meetings.

During the next half-year, the basic design criteria & alternative architectures for the detector should be developed.

This is a new kind of detector, requiring bottoms-up thinking. The next year promises to be fun, full of thinking about physics & detector-design fundamentals — hopefully not about $$ and politics.

If we succeed, I think anyone involved will remember this experience with the greatest of pleasure. This kind of opportunity does not often occur.

Some notes I have written - available on request.

"Rapidity gaps & jets as a new-physics signature" (draft ms for Phys Rev)

"Think Lego"
(notes for mapping detector properties into η-ϕ space; useful for comparison studies)

"Chiron/Centauro Phenomenology for FAD"

"High Energy Jet Phenomenology for FAD"

"Comments on the Far-Forward Spectrometer"

D. Zeppenfel

Rapidity gaps in electroweak physics

Hassan Chehime, Beatriz Ducati, Concha Gonzalez-Garcia, Francis Halzen, Alan Stange, Tim Stelzer, Adam Duff, D.Z.

- Two photon physics at the SSC

$$pp \longrightarrow pp\, W^+W^-$$

- Forward jet tagging for the intermediate mass Higgs search

$$qq \longrightarrow qq\, H\,,\ H \rightarrow b\bar{b}$$

Two photon physics (Concha G.

(Quasi)elastic 2-photon events give striking signature

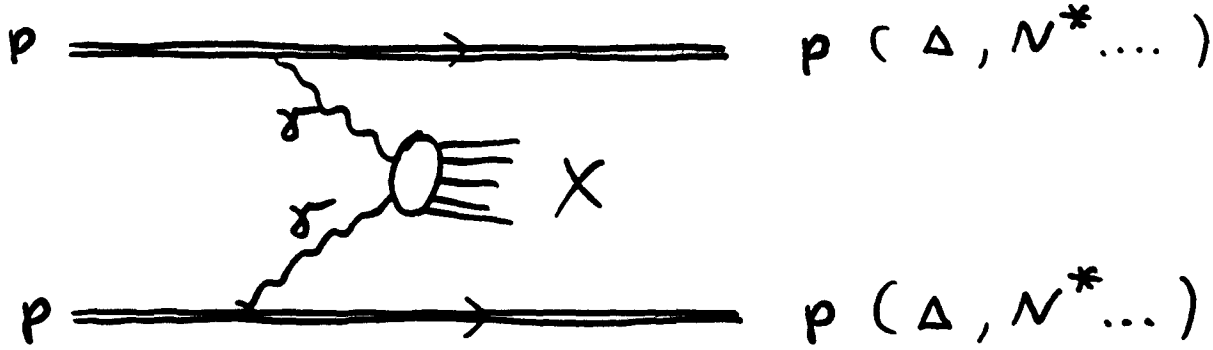

- Produced system X central
- Both protons <u>very</u> forward, ($|\eta_p| \gtrsim 11$) protons at low p_T (σ(100 MeV))

$\Rightarrow$ Huge rapidity gap ($\Delta\eta = 8 \ldots 12$)

- proton energy loss is small (median loss = 200 GeV in W^+W^- production)

$\Rightarrow$ Very hard to see protons

Rapidity of $\gamma\gamma$ system

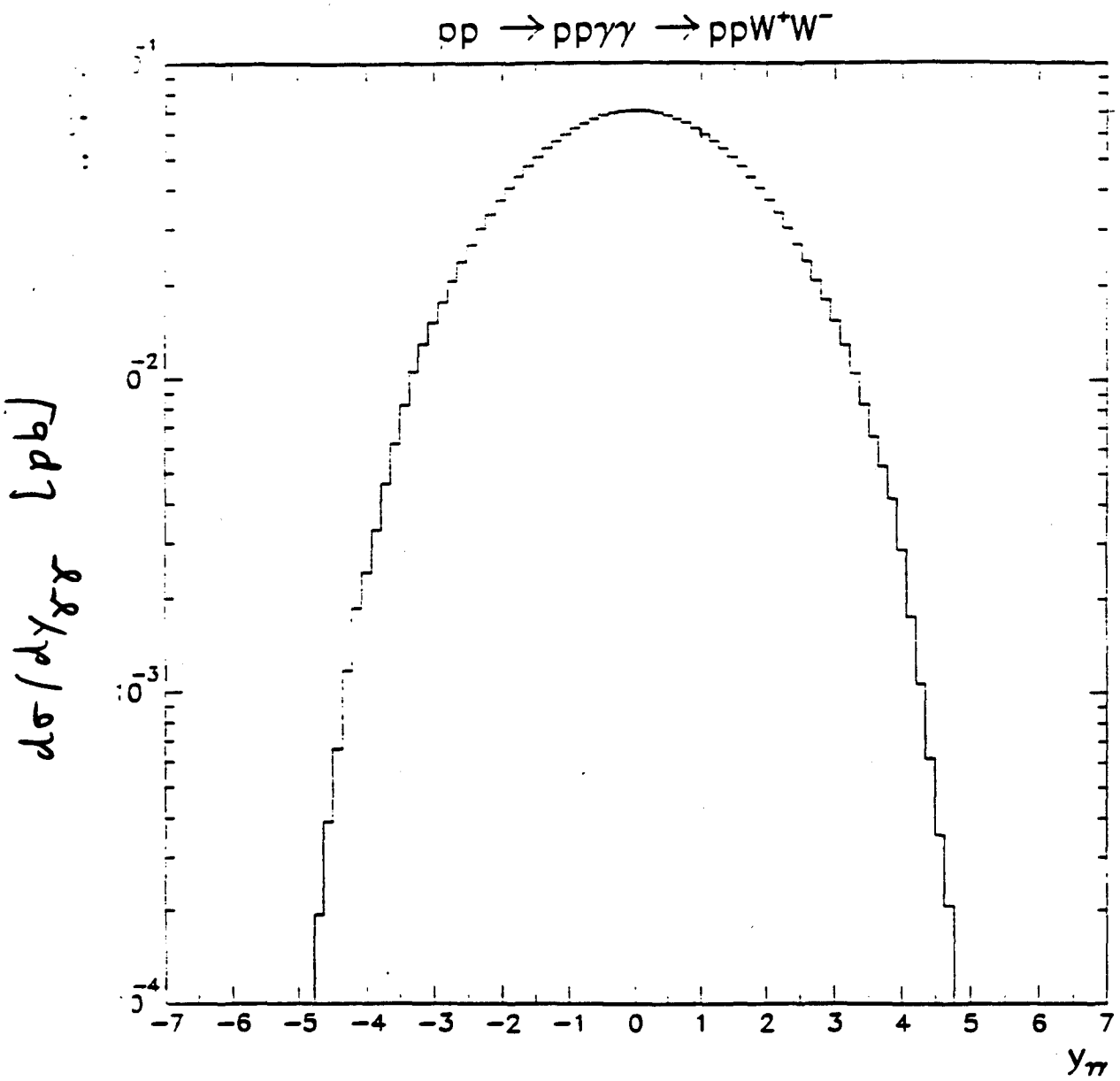

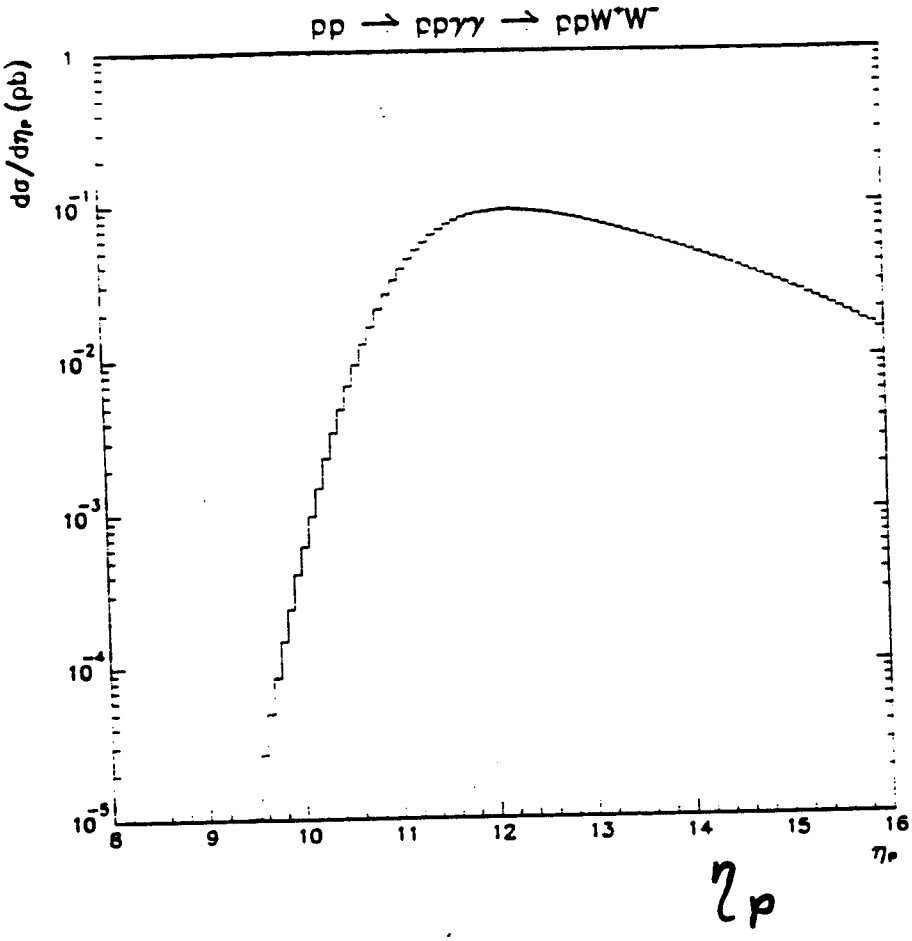

proton pseudo-rapidity

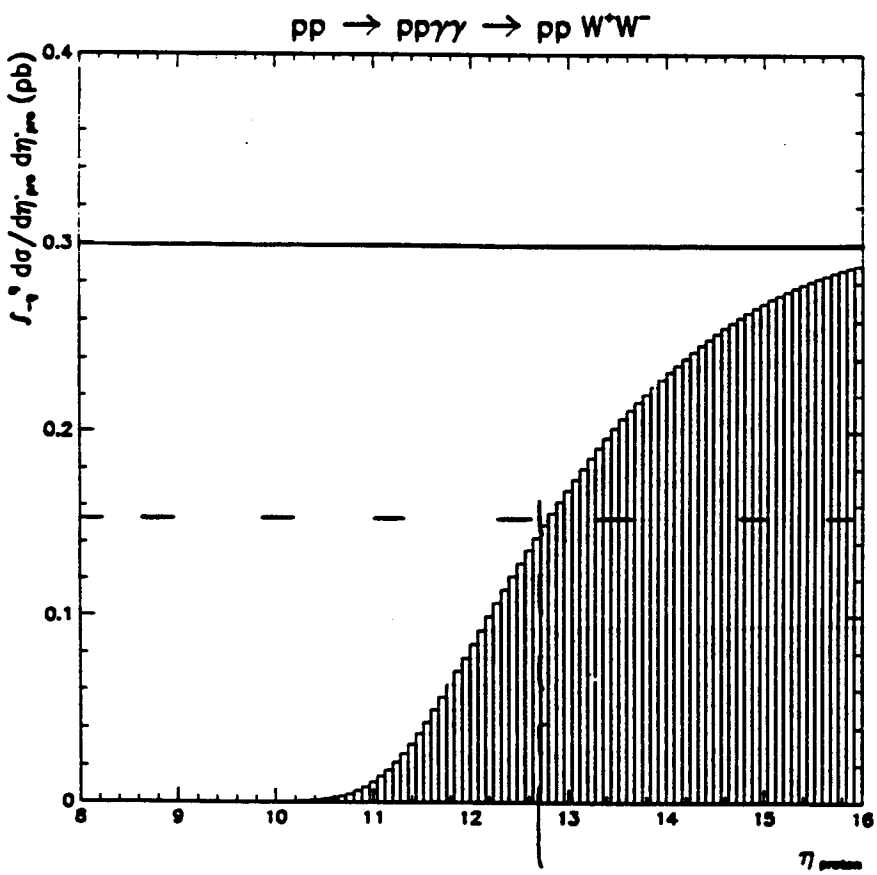

median

12.7

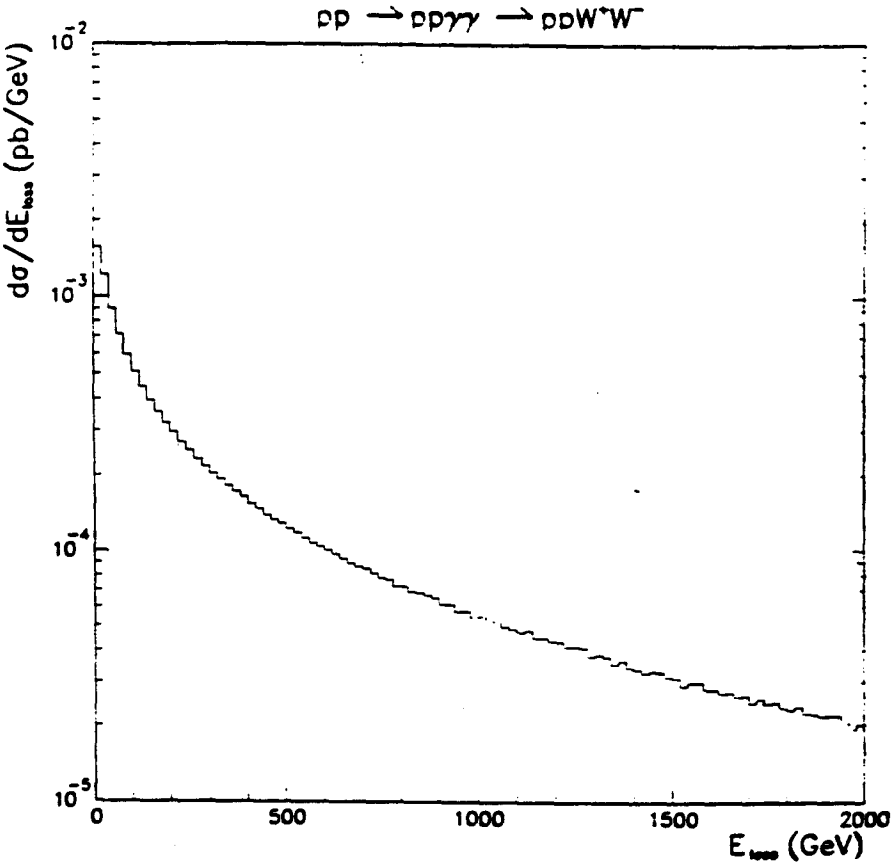

proton energy loss:

many even with larg loss on on side

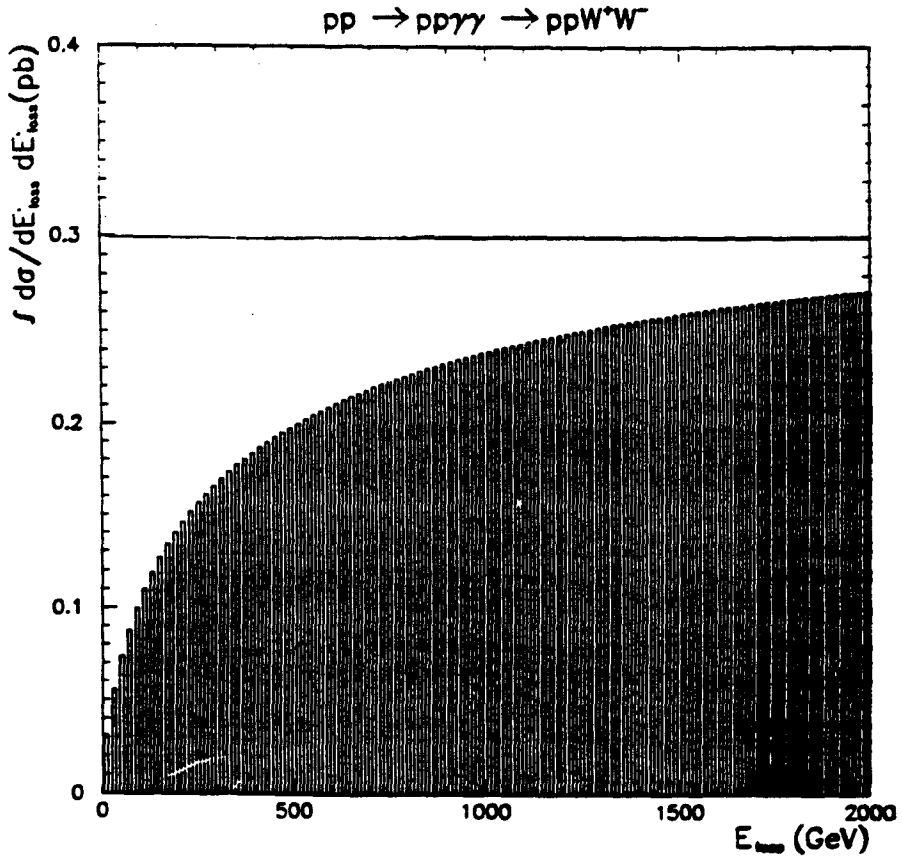

p_T if scattered proton

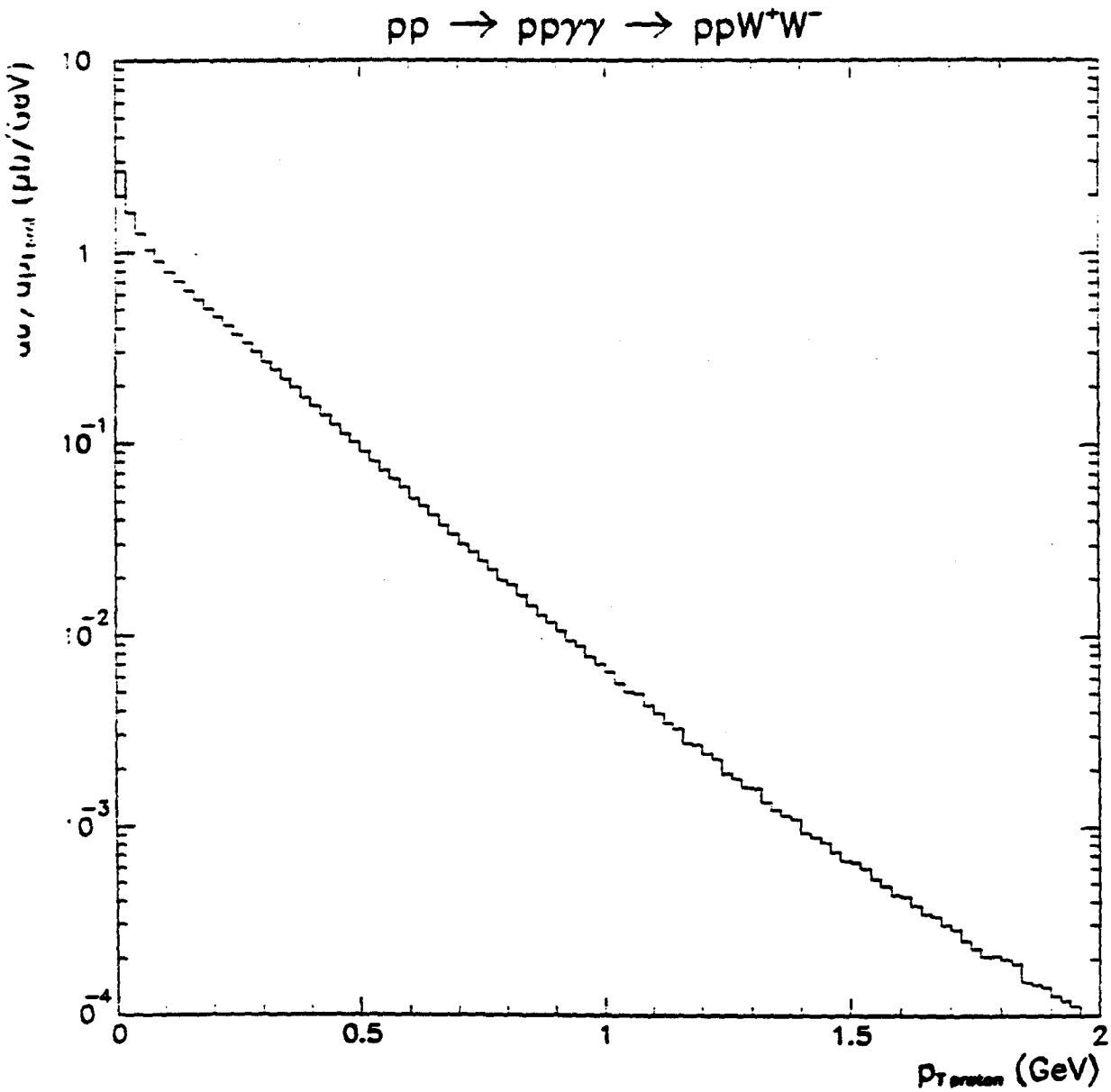

$\Rightarrow$ Need good trigger from produced system X^0!

Special case: $X = W^+W^-$

$\sigma(pp \to pp\, W^+W^-) = 0.3$ pb $*2(?)$ for quasielast

Expect very clean signal for

$W^+W^- \to \ell^\pm \nu\, jj$ (BR = 30% for $\ell = e, \mu$)

- W decay products are fairly centra (60% of $\ell^\pm$ within $|\eta_\ell| < 2$)

- See high p_T lepton ($p_T \sim \frac{m_W}{2}$)

$\Rightarrow$ Expect 10 semileptonic W^+W^- decay in 100 pb^{-1} from elastic production

$*$ ~ 2 quasielastic ($Q^2 \lesssim 4$ Ge

$*$? "not so deep-" inelastic

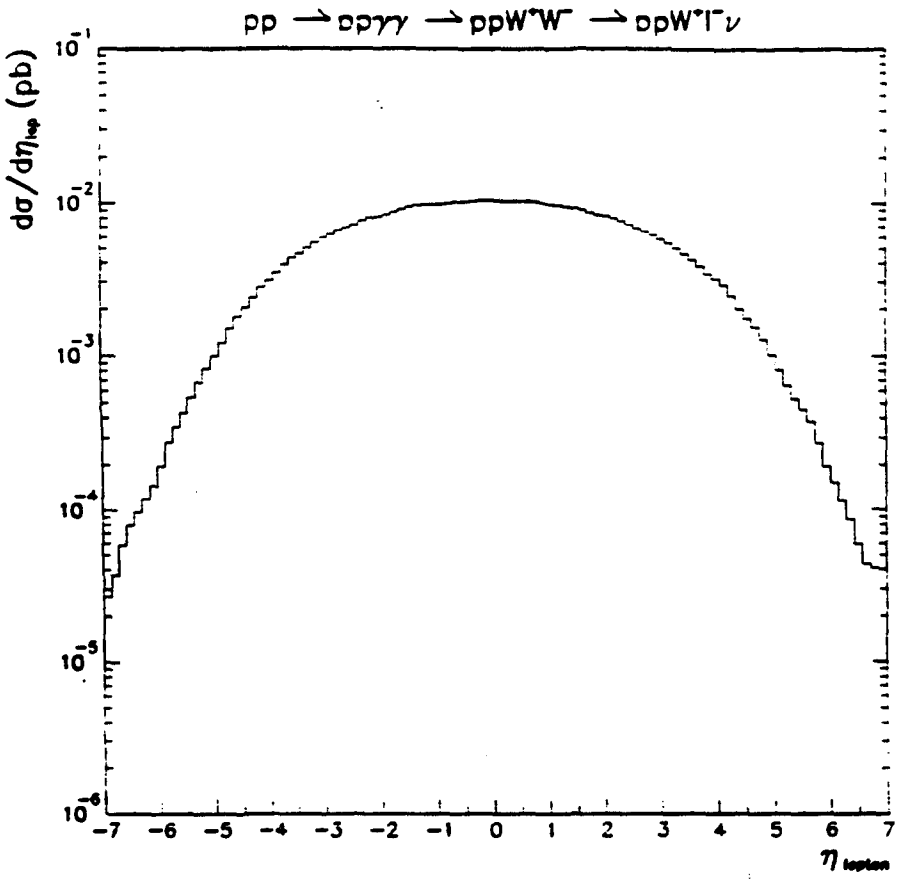

lepton rapidity in $\gamma\gamma \to W^+W^- \to \ell^\pm \nu jj$

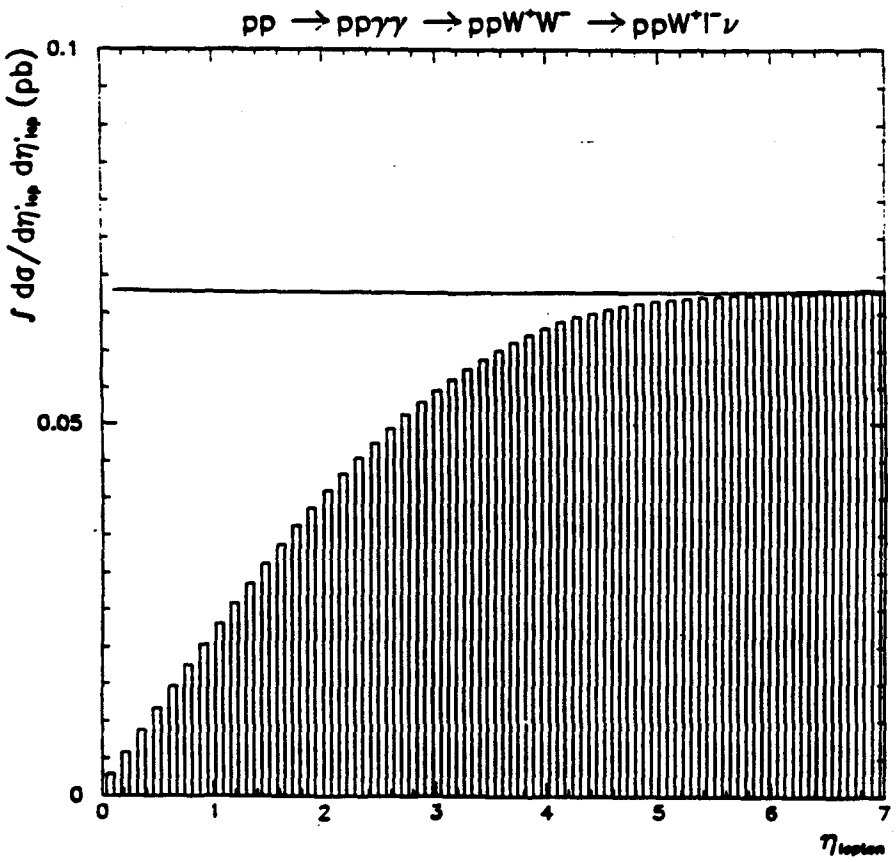

$6.7 \cdot 10^{-2}$ pb

$= \frac{2}{9}$ 0.3 pb

$*2$ for

$W^+W^- \to \ell^\pm \nu$

$\ell^{\pm}$ transverse momentum

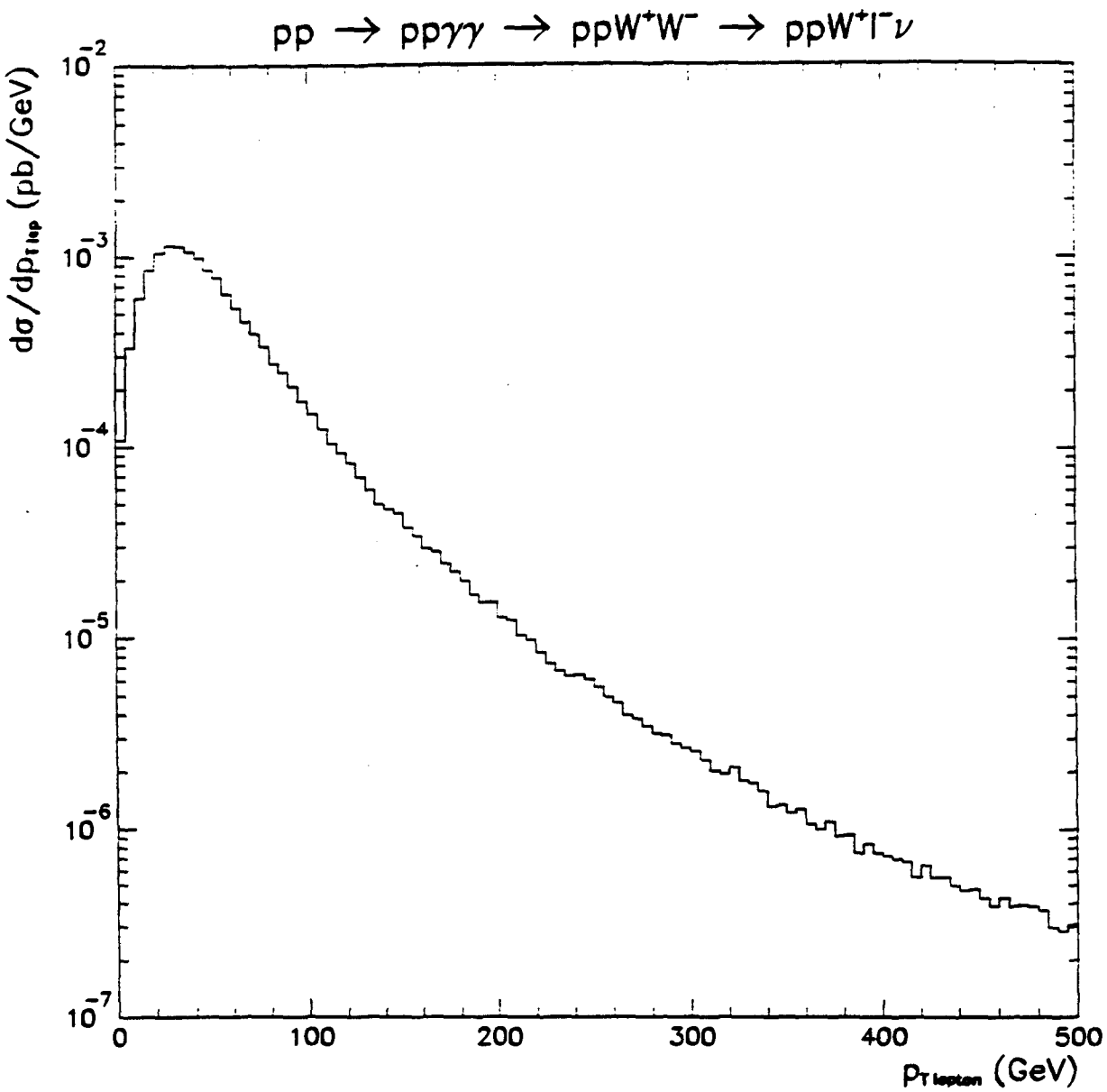

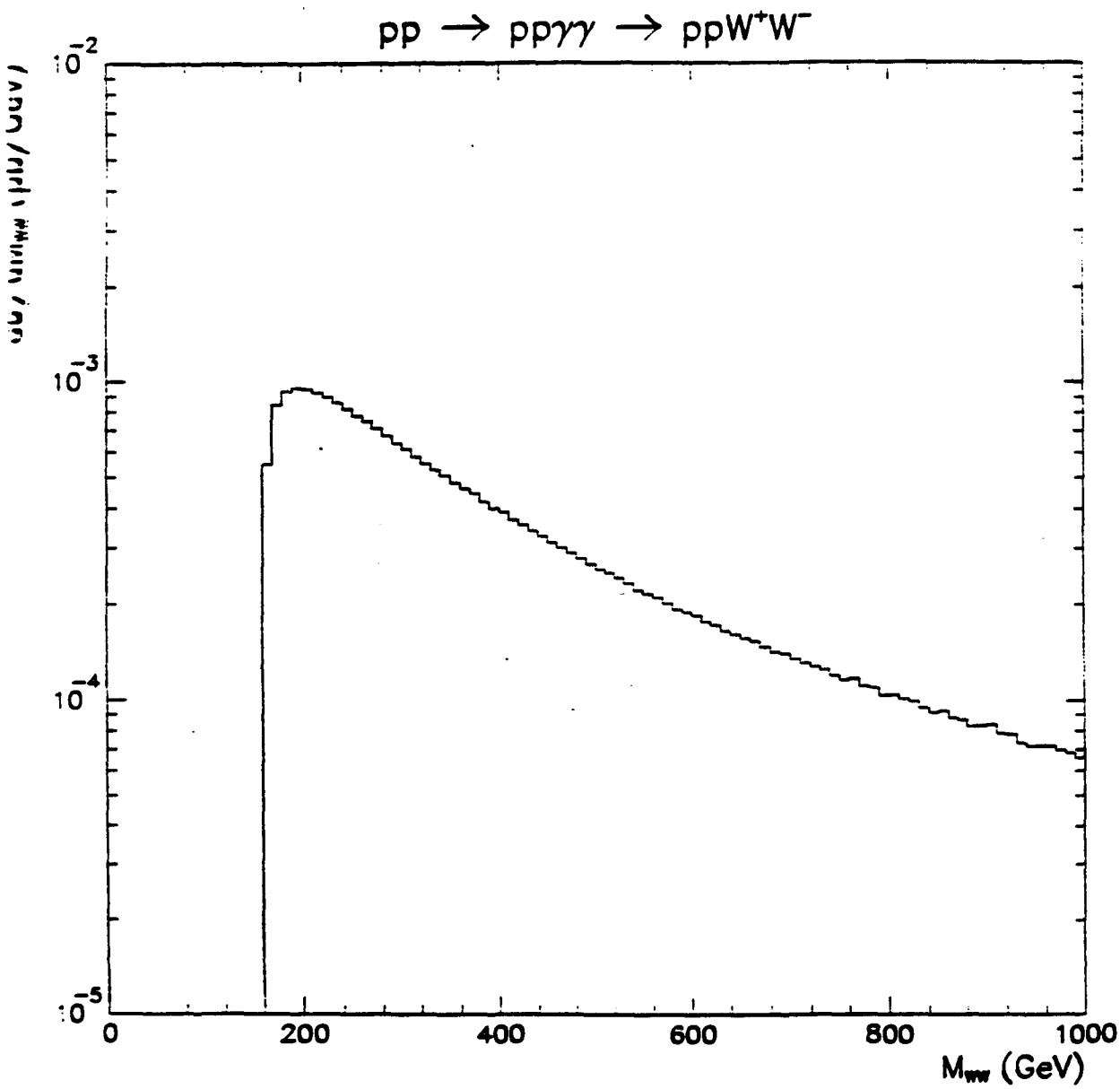
pp → ppγγ → ppW⁺W⁻
10⁻²
10⁻³
10⁻⁴
10⁻⁵
0
200
400
600
800
1000
M_WW (GeV)

Other 2-photon processes

$\sigma(pp \to pp b\bar{b}) \approx 1.3$ pb

Small because of charge supression factor Q^4.

$\sigma(pp \to pp c\bar{c}) \approx 400$ pb

Enhanced by factors

16 : charge

20 : phase space

Problems :

— trigger

— diffractive background for $\gamma\gamma \to$ hadrons

Higgs production via WW/ZZ fusion

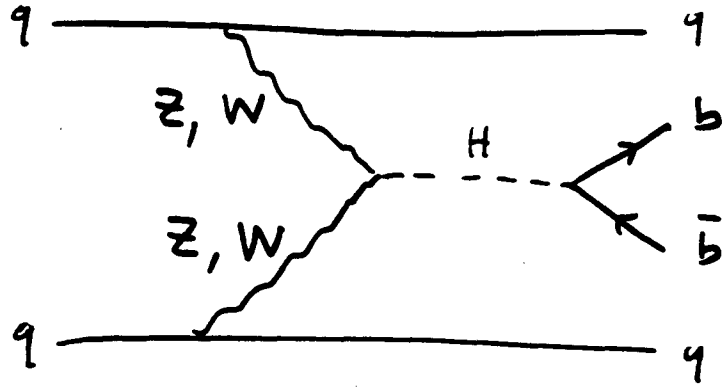

Production cross section varies between 20 pb (m_H = 100 GeV) and ~1 pb (m_H = 1 Te

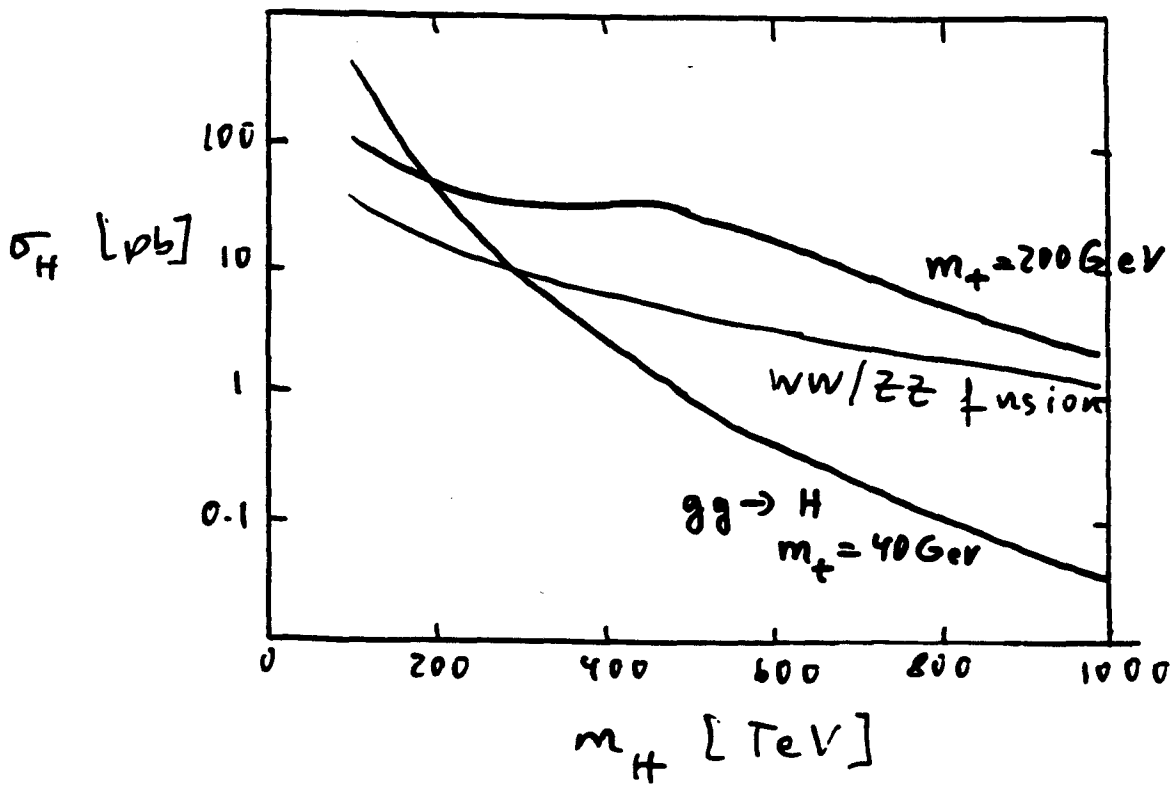

Higgs Hunter Guide [GHK]

Advantage of WW/ZZ fusion vs. gg fusio
tag 2 forward jets to reduce backgr

Note:

$$Br(H \to W^+W^- \to e^-\bar{\nu}\, e^+\nu) = \frac{2}{3}\left(\frac{2}{9}\right)^2 = 3.3\%$$

$$Br(H \to ZZ \to e^+e^-e^+e^-) = \frac{1}{3}(0.066)^2 = 0.15\%$$

$\Rightarrow$ $100\ pb^{-1}$ and $\sigma(qq \to qqH) < 10\ pb$ lear
less than 30 $W^+W^- \to e\bar{\nu}\,\bar{e}\nu$ and
1.5 $ZZ \to 4$ leptons signal events

hopeless: severe backgrounds from $t\bar{t} \to W$

Can be done with high luminosity
interaction region!

Event characteristics for intermediate mas
Higgs ($m_H = 100$ GeV) [H. Chehime]

- no rapidity gap! One spectator jet central, one forward
  Reason: $Q_W^2 \approx \frac{m_W^2}{4}$ is same orde
  of magnitude as mass of produced system.

- produced Higgs is central

- transverse momenta:
  spectator jets: $p_{Tj\,min} \approx 30$ Gel
  b-jets: $p_{Tb\,min} \approx 40$ Gel

- Higgs is produced with substanti
  p_T

$$p_{TH} \approx 70 \text{ GeV}$$

|η|_min. spectator

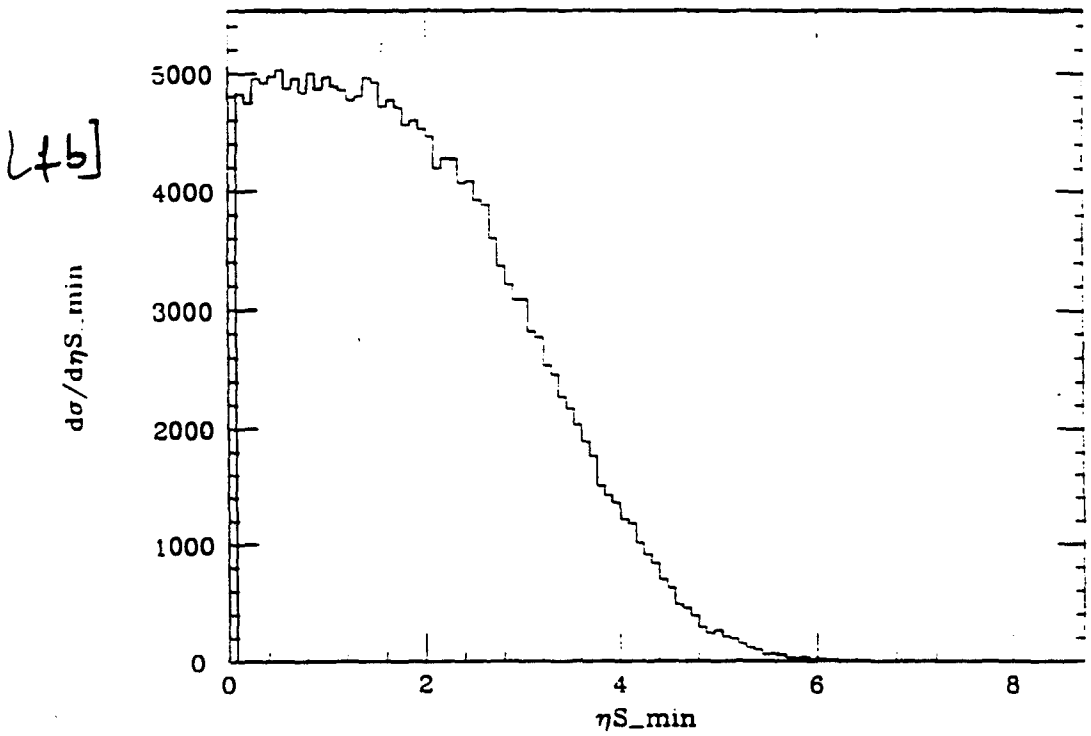

$m_H = 100$ GeV

|η|_max. spectator

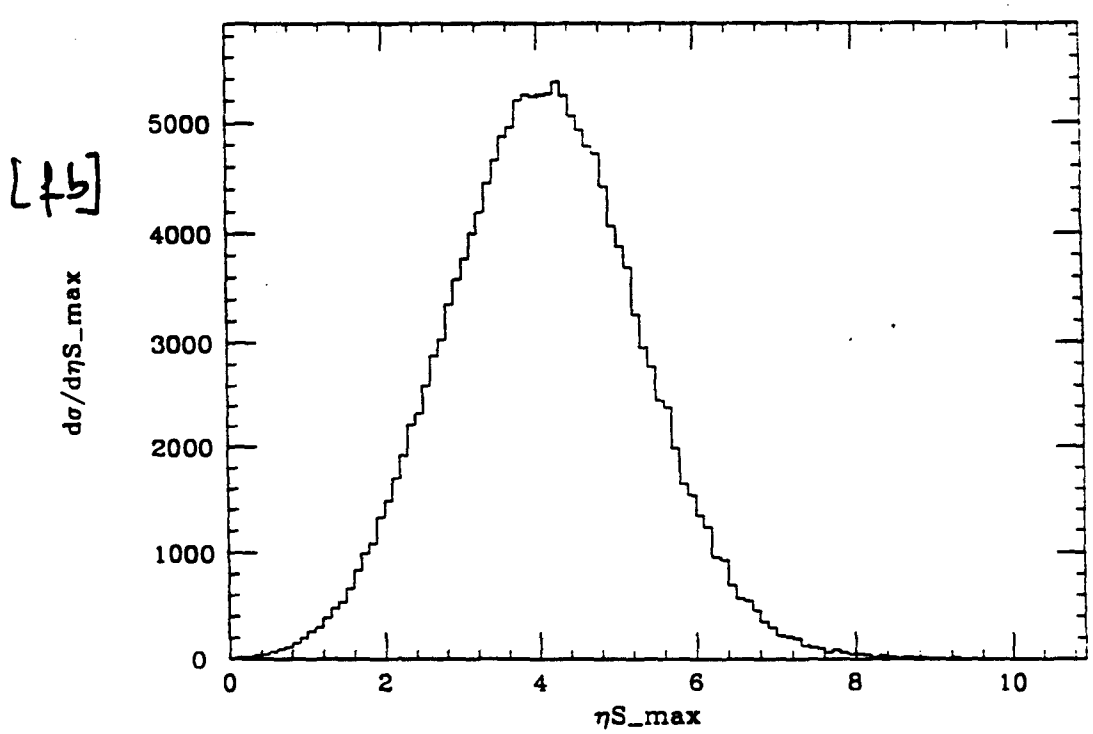

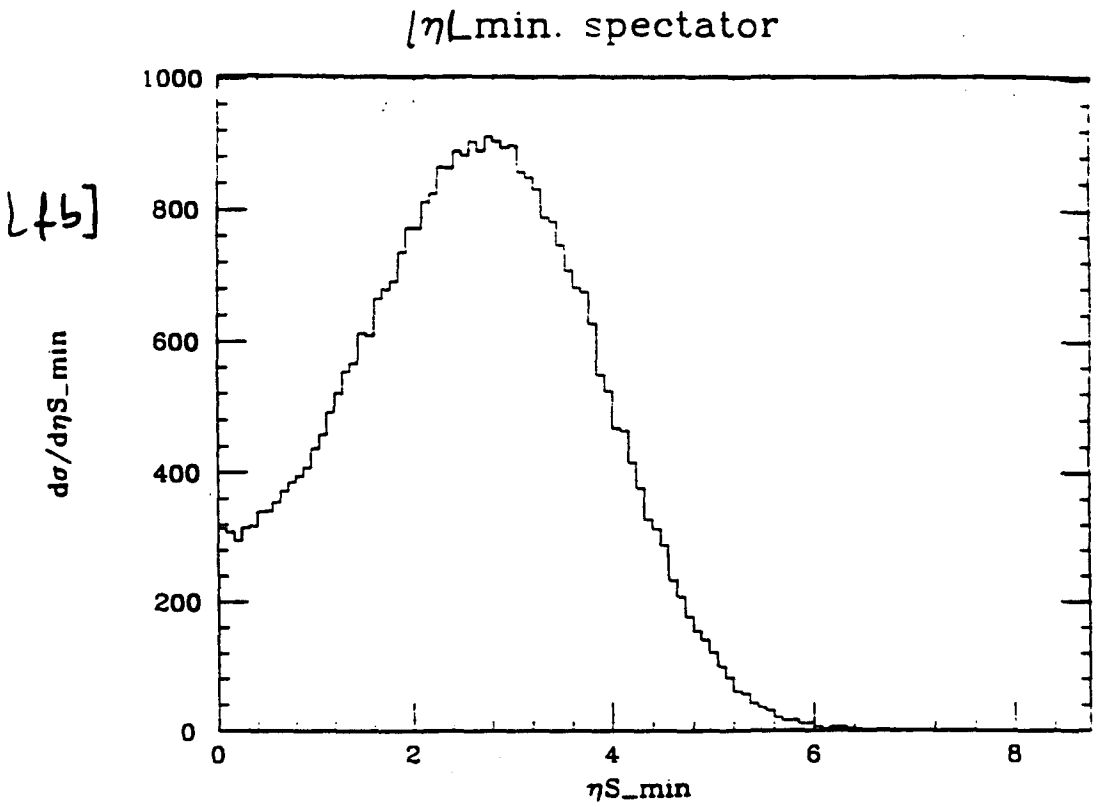
|η|min. spectator
[fb]
dσ/dηS_min
ηS_min
0
200
400
600
800
1000
0
2
4
6
8

$m_H = 600$ GeV

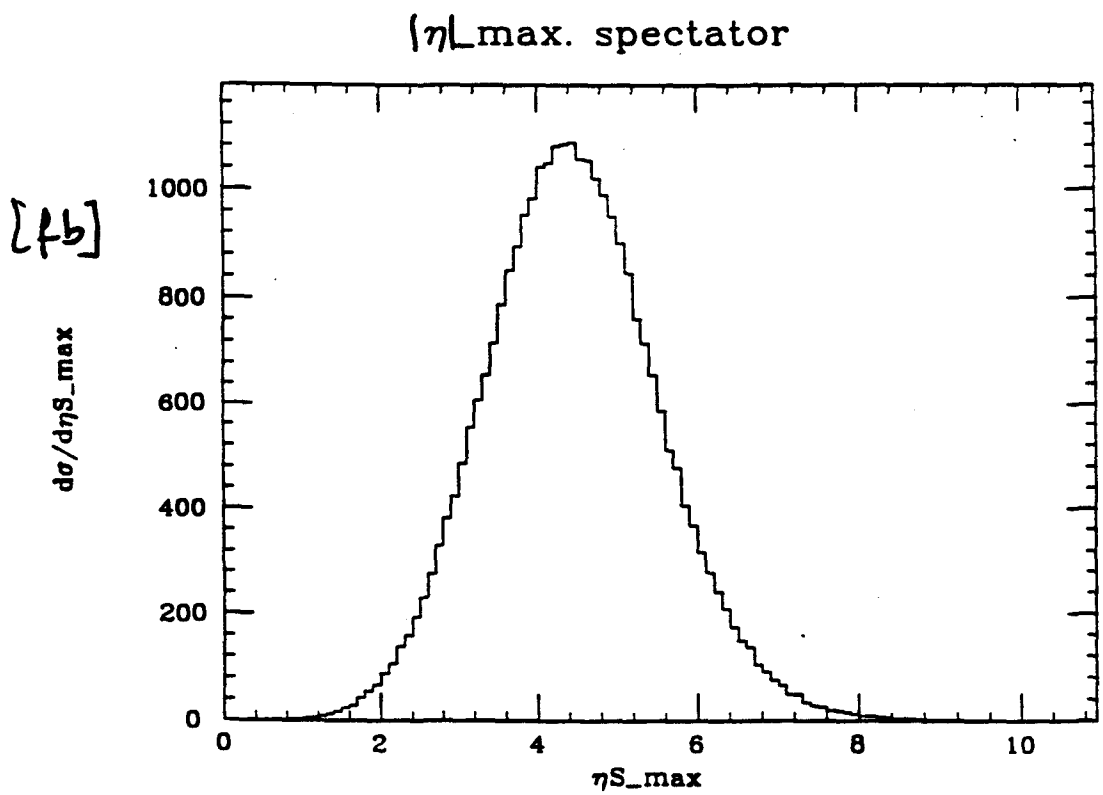
|η|max. spectator
[fb]
dσ/dηS_max
ηS_max
0
200
400
600
800
1000
0
2
4
6
8
10

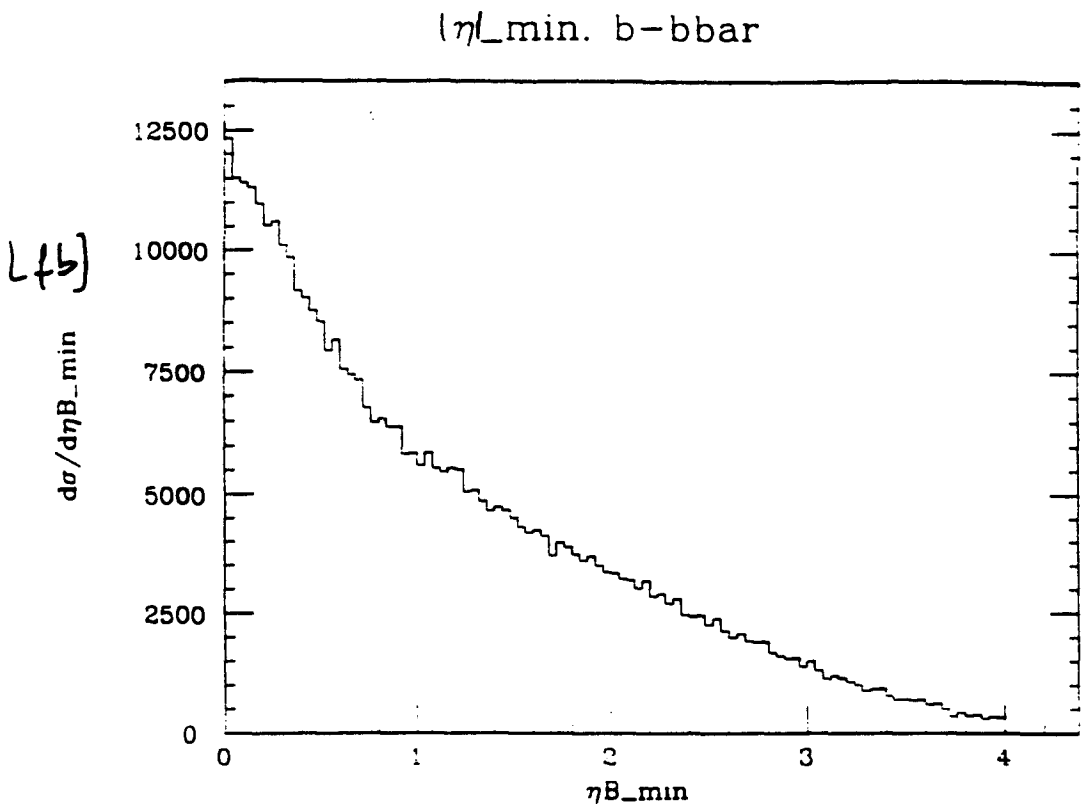
|η|_min. b−bbar
[fb]
dσ/dηB_min
12500
10000
7500
5000
2500
0
0
1
2
3
4
ηB_min

$m_H = 100$ GeV

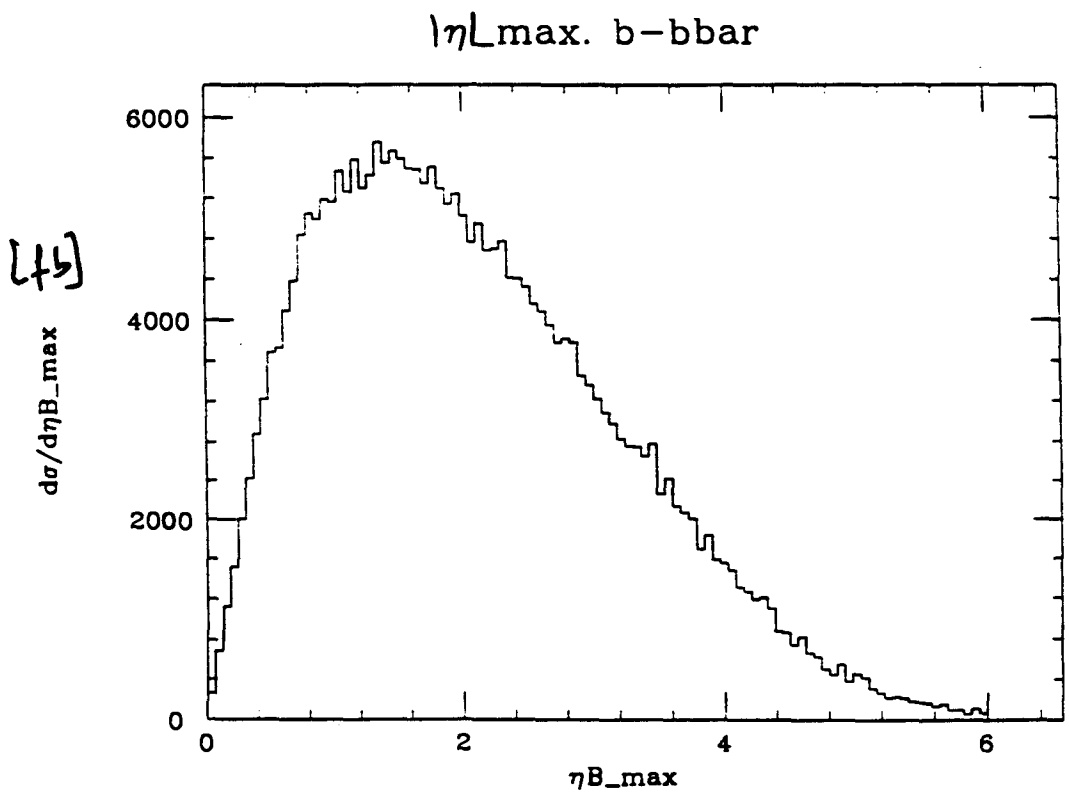
|η|max. b−bbar
[fb]
dσ/dηB_max
6000
4000
2000
0
0
2
4
6
ηB_max

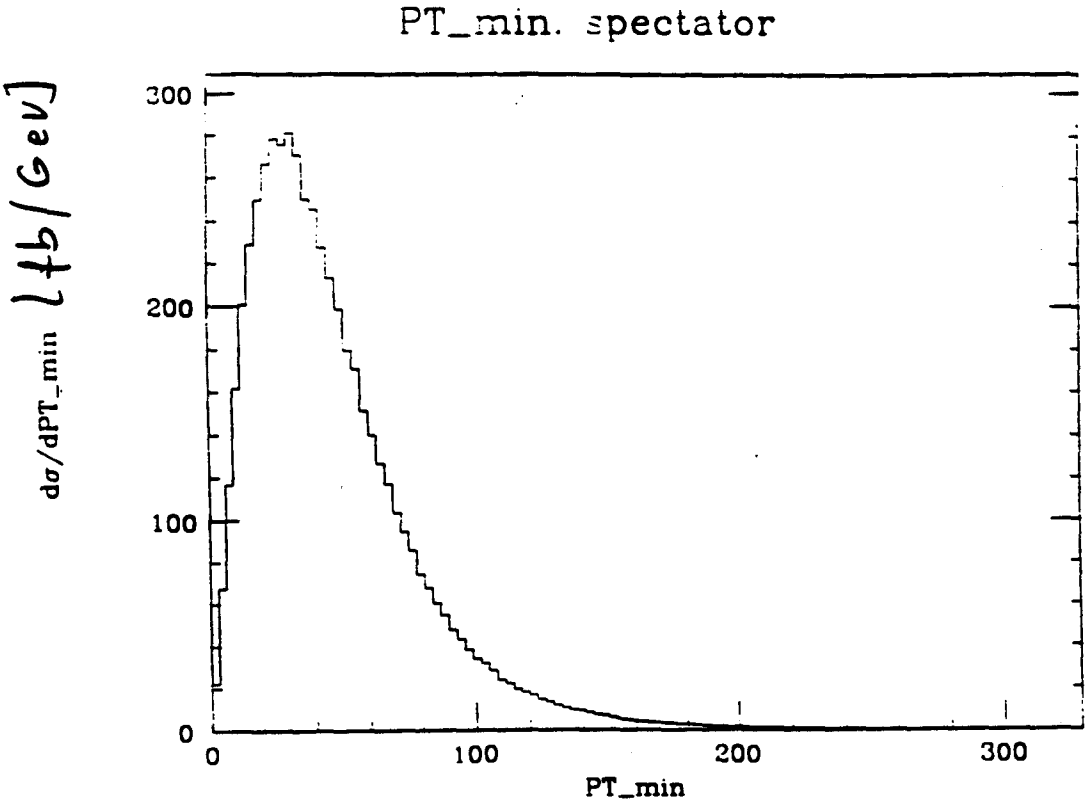
PT_min. spectator
dσ/dPT_min [fb/GeV]
300
200
100
0
0
100
200
300
PT_min

$m_H = 100$ GeV

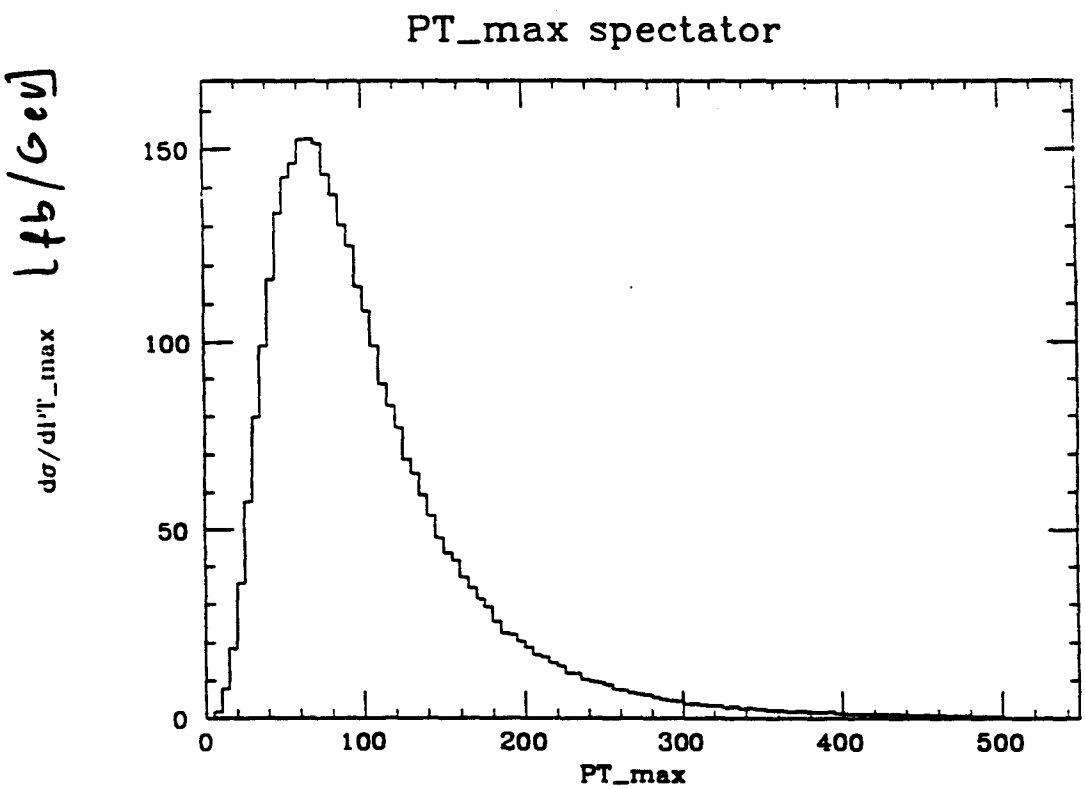
PT_max spectator
dσ/dPT_max [fb/GeV]
150
100
50
0
0
100
200
300
400
500
PT_max

PT_min. b-bbar

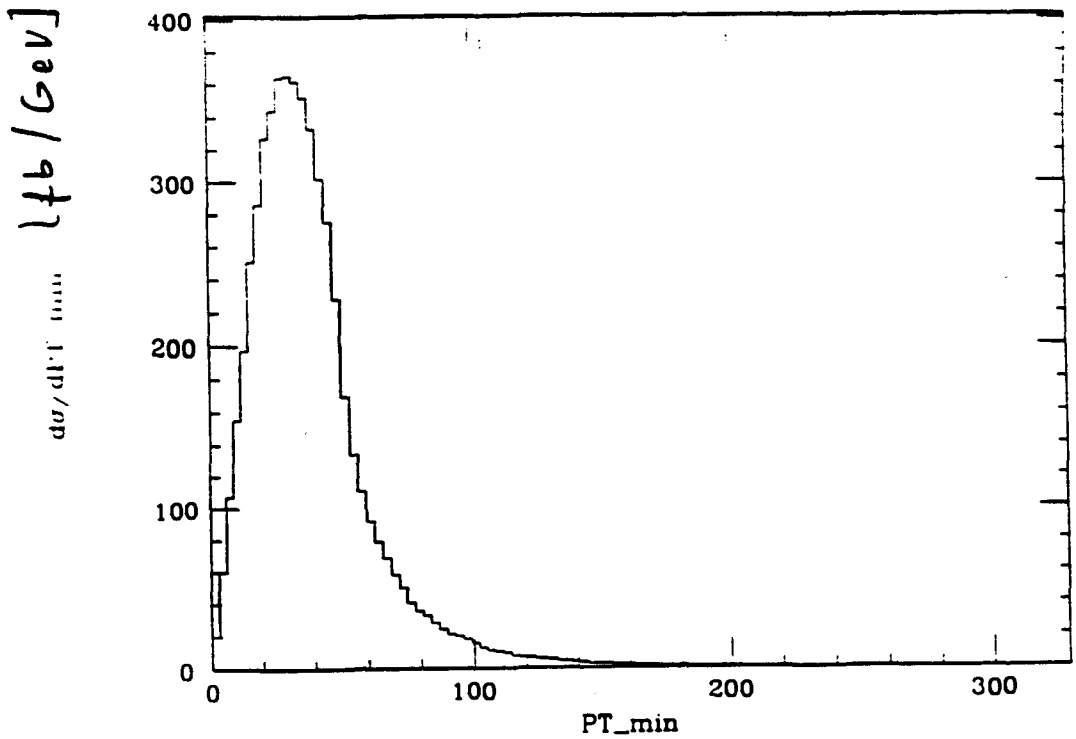

$m_H = 100$ GeV

PT_max b-bbar

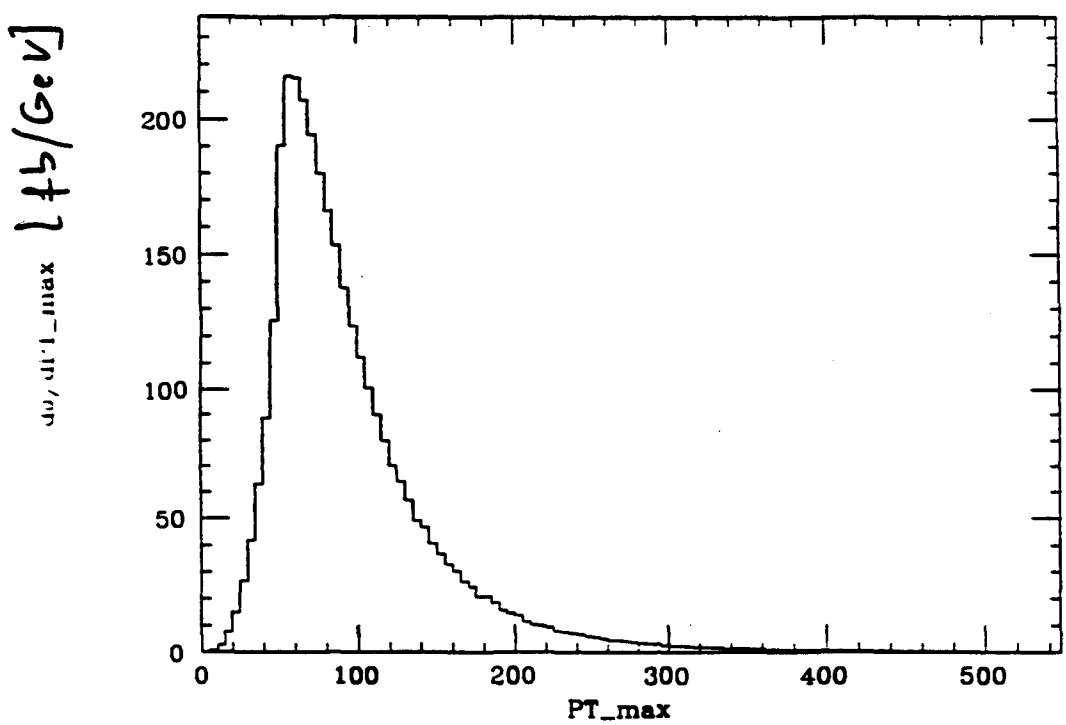

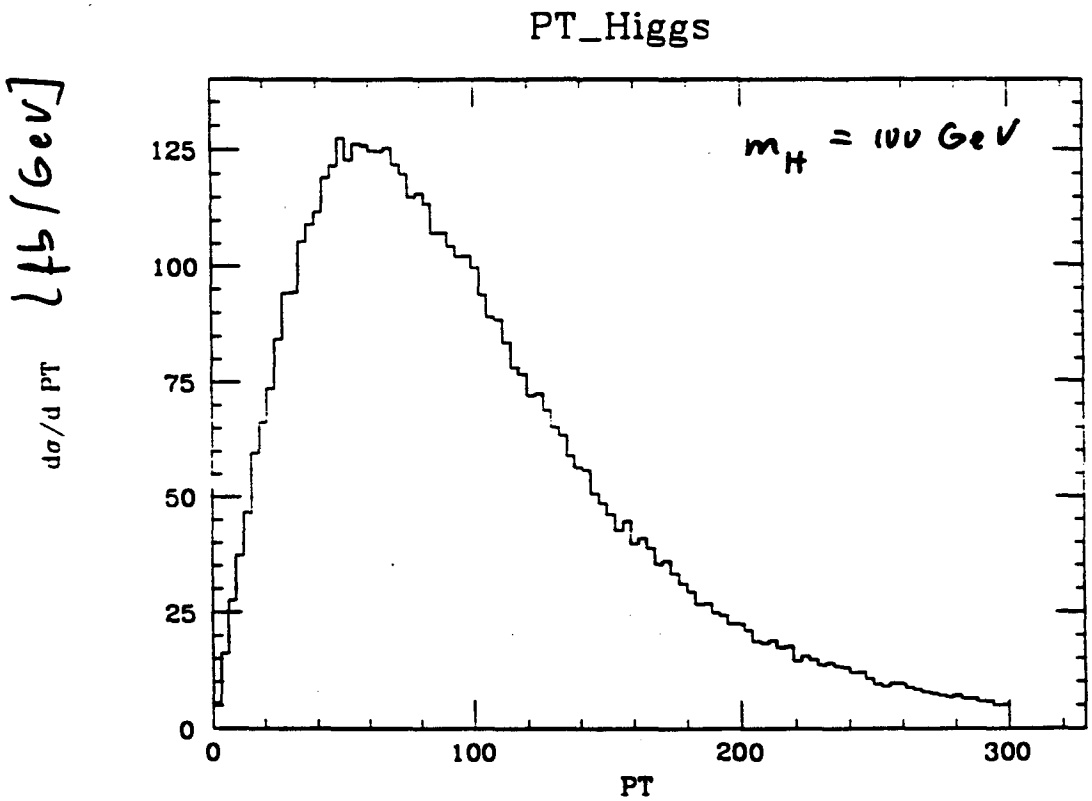
PT_Higgs
m_H = 100 GeV
dσ/d PT [fb/GeV]
125
100
75
50
25
0
0
100
200
300
PT

Event characteristics motivate search in the following phase space region of $b\bar{b}$ + 2 jet events

b cuts:

$|\eta_b| < 2$ microvertex detector

$p_{Tb} > 30$ GeV

spectator jet cuts:

$|\eta_j|_{min} < 3$

$2.5 < |\eta_j|_{max} < 5.5$

$p_{Tj}/_{min} > 20$ GeV

$p_{Tj}/_{max} > 40$ GeV

$\sigma \cdot B(H \to b\bar{b})/_{cu} = 2pb$

$b\bar{b}$ system = H :

$p_{TH} > 50$ GeV ; $m_{b\bar{b}} \in [95, 105]$ GeV

jet separation (b's and spectator)

$R_{jj} > 1$

<u>Backgrounds</u> : Production of $b\bar{b}$ pairs with additional jets

$$\sigma(b\bar{b})\Big/_{b\text{-cuts}} = 47\ nb$$

background from misidentified quarks/gluo

$$\sigma(jj)\Big/_{b\text{-cuts}} = 7.5\ \mu b = 150\ \sigma(b\bar{b})\Big/_{b\text{-}}$$

$\Rightarrow$ need non-b rejection to better than 99.5 %

A) QCD radiation in $gg \to b\bar{b}$ [A. Stange]

included in calculation are $q\bar{q}\,b\bar{b}\,gg$ amplitudes only

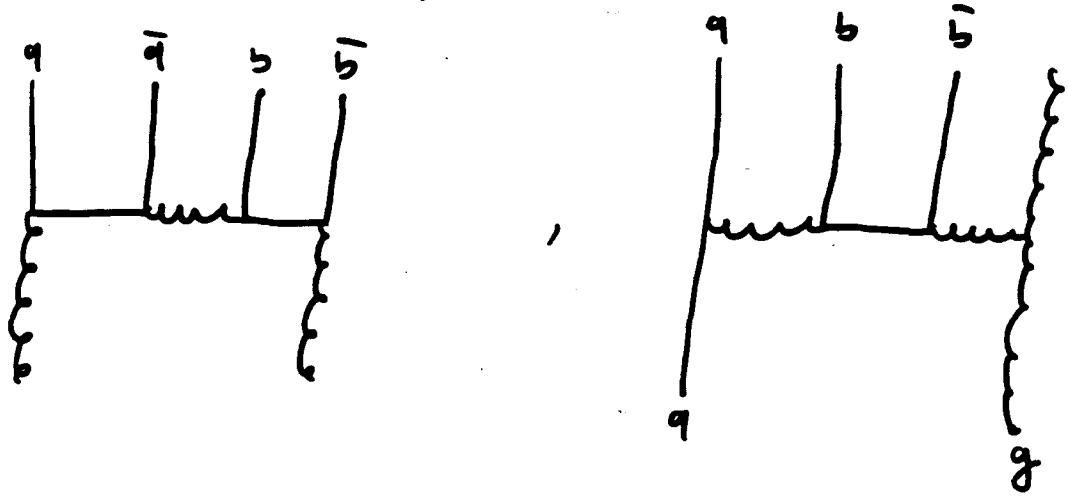

missing still: $gg \to gg\, b\bar{b}$

$\to \quad \sigma_{QCD}(b\bar{b}jj)/_{cuts} > 350\ pb * ?$ for missi channel

Note: Calculation involves region where tre level cross section receives large radiative corrections

$\Rightarrow$ result should be considered order of magnitude estimate

B) Double parton scattering (DPS)

[B. Ducati, T. Stelzer]

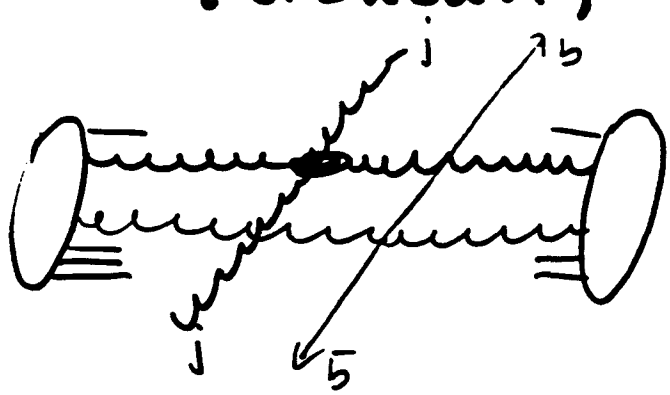

Simple model [Hulzen]

$$\sigma_{DPS} = \frac{\sigma(b\bar{b})\,\sigma(jj)}{\pi R^2} = \frac{\sigma(b\bar{b})\,\sigma(jj)}{16\ mb}$$

With $\sigma_{jj}/_{\text{spec. cuts}} = 70\,\mu b$ one gets

$$\sigma_{DPS}(b\bar{b}jj)/_{\text{cuts}} \approx 200\ pb$$

Note: DPS calculation has

- two pairs of back-to-back jets
- $p_{TH} = 0$

$\Rightarrow$ eliminate DPS background by $p_{TH} > 50\,\text{GeV}$ requirement and/or azimuthal angle between b and $\bar{b}$ or between two spectator jets

Real DPS background is

$$(gg \to g\,b\bar{b}) \otimes (gg \to j(j))$$

where one of the final state jets is misidentified

Not analyzed yet.

Result for $H \to b\bar{b}$ ($m_H = 100$ GeV)

Signal: 2 pb, peak in $b\bar{b}$ invaria mass distribution

Background: ~500 pb in 10 GeV bin around m_H

With 10 GeV mass resolution (very optimist

$$\frac{S}{\sqrt{B}} = \frac{200}{\sqrt{50\,000}} = 0.9\,\sigma$$

Intermediate mass Higgs search at FAD appears hopeless unless some other characteristic difference can be found between WW/ZZ fusion and the QCD background processes.

Charge multiplicities? [Kane et al.]

FAD

Event Simulation

Using Lepto 5.2 and Jetset 6.3

by

Gary S. Greenbaum (UCSD)

March 13, 1992

Hera Event

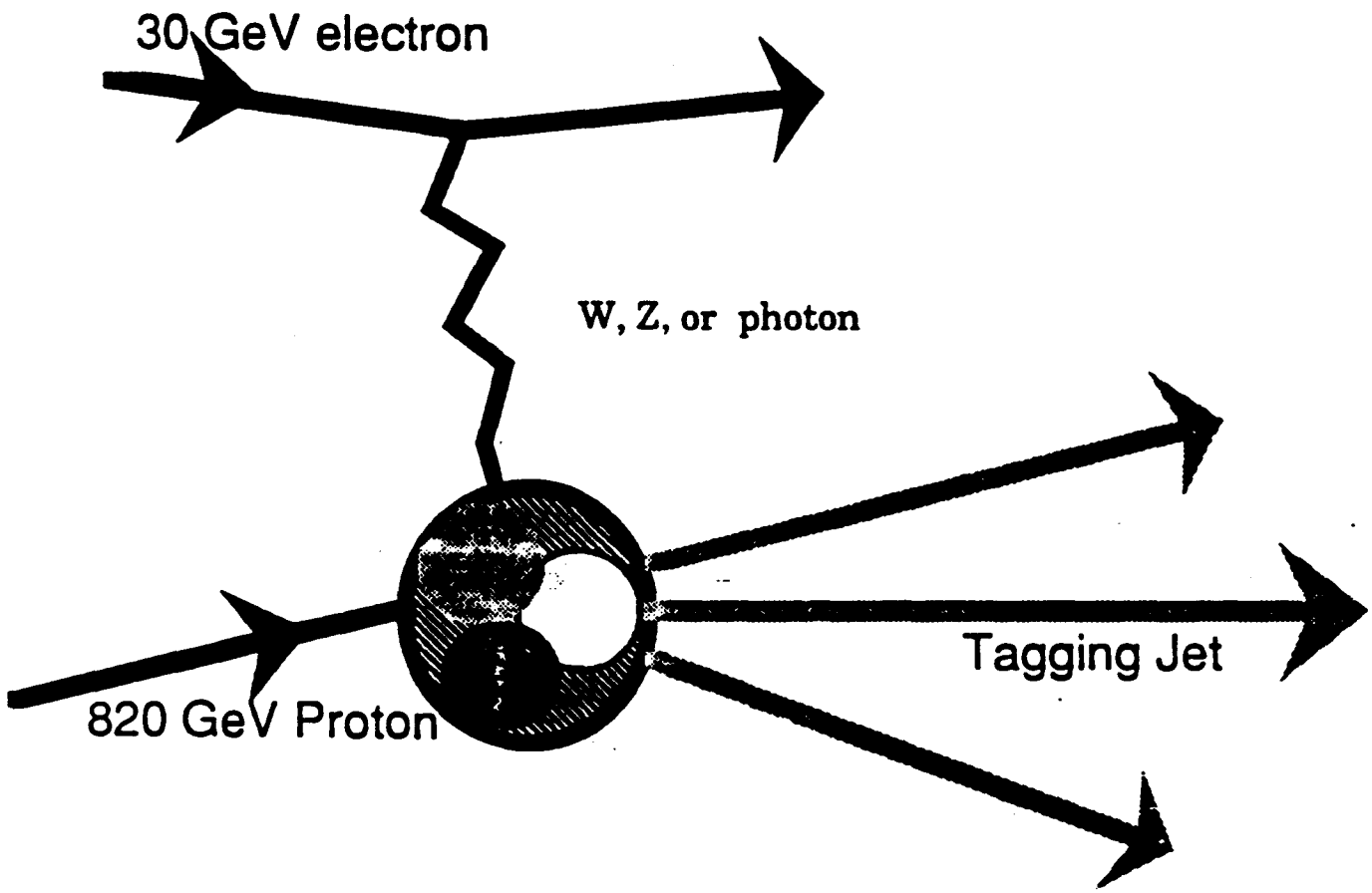

Fad Event

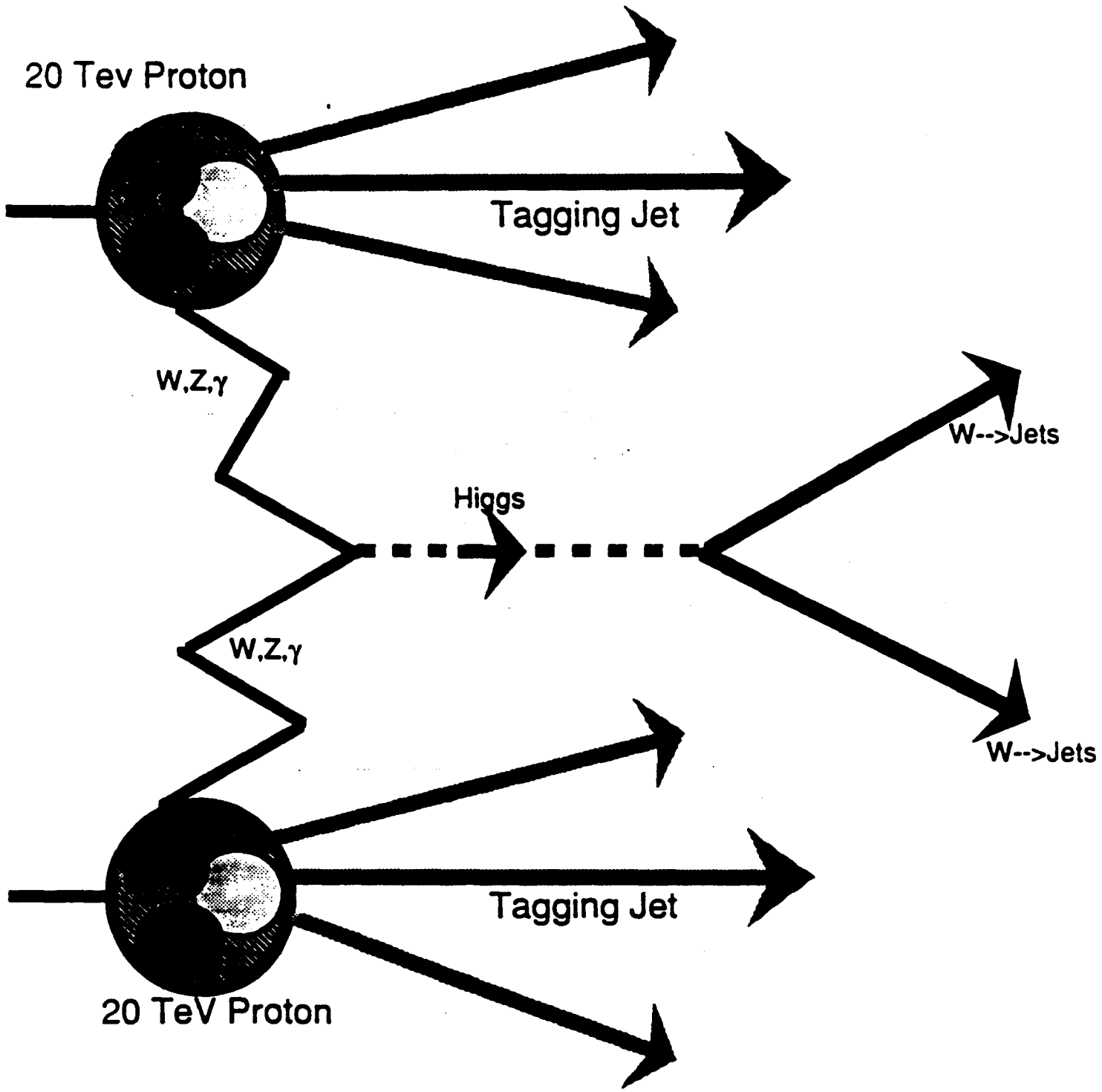
20 Tev Proton
Tagging Jet
W,Z,γ
W-->Jets
Higgs
W,Z,γ
W-->Jets
Tagging Jet
20 TeV Proton

The Vocabulary of LEGO
A Review:

Phase Space:

ϕ: azimuthal angle relative to collision axis
P_t: magnitude of momentum transverse to collision axis
η: psuedo-rapidity=-ln (tanθ/2)

Why Lego: (See BJ's SLAC-PUB 5593)

1. Final state particles are distributed uniformly in η and ϕ and sharply center about $<P_t>$. (Extended lego plot needed for QCD jets.)

2. Convenient longitudinal Lorentz boost properities; facilitates transformation to fix target frame.

3. Area Element=$d\eta d\phi$ is proportional to phase-space area=$P_t dP_t d\phi d\eta$

Vocabulary:

1. Jet: all particles within a circle of radius .7 in a lego plot and whose total P_t exceeds some threshold.

2. Rapidity Gap: regions of η in which no particles are found. Characteristic of diffractive physics processes.

3. Tagging Jet: a jet located at edge of rapidity gap. Represents the hadronized initial-state quarks that emitted virtual interacting particle (e.g. W,Z,Pomeron,etc.) P_{t-q}

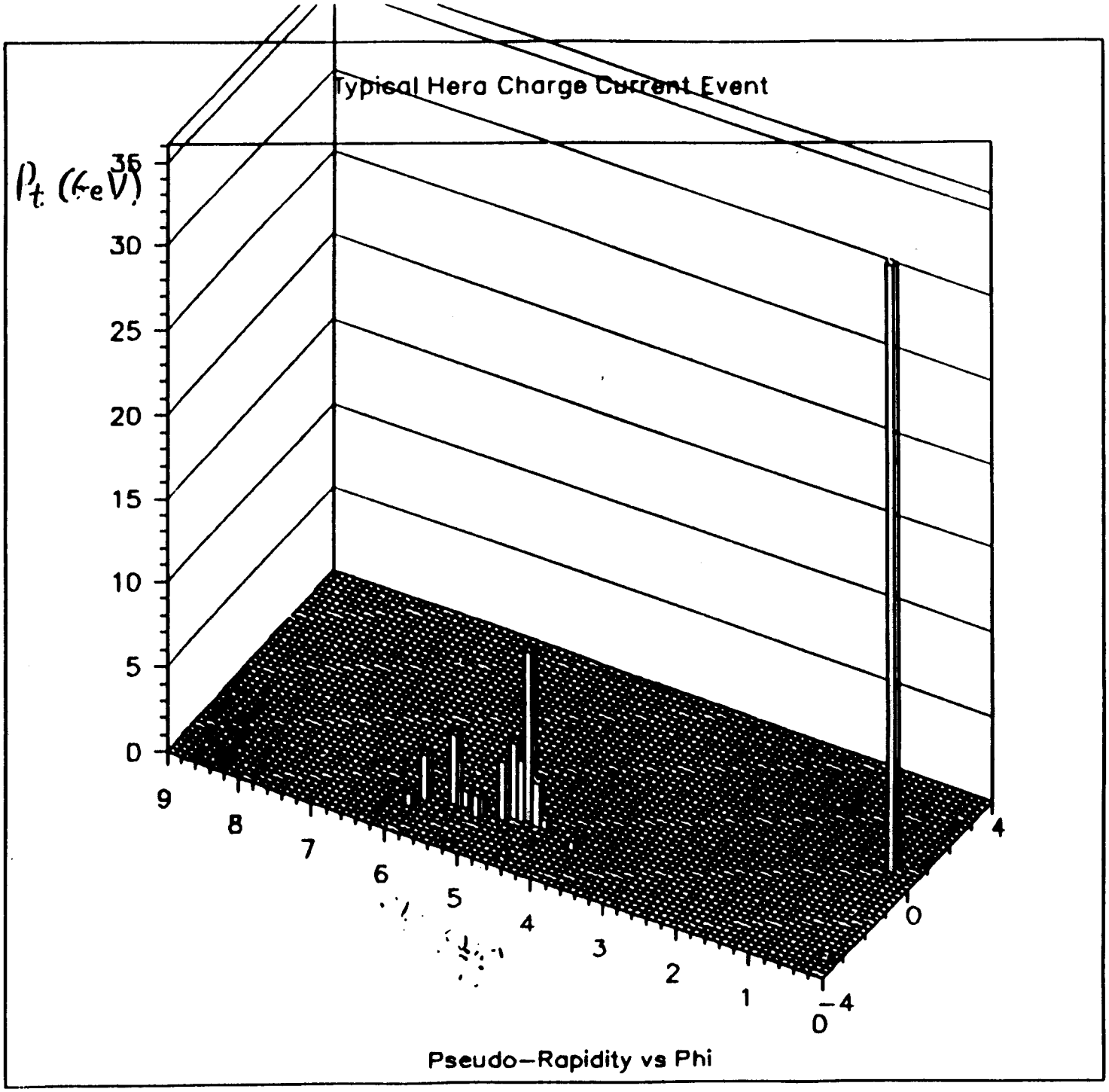
Typical Hera Charge Current Event
P_t (GeV)
35
30
25
20
15
10
5
0
9
8
7
6
5
4
3
2
1
0
−4
0
4
Pseudo−Rapidity vs Phi

TYPICAL HERA CHARGE CURRENT EVENT

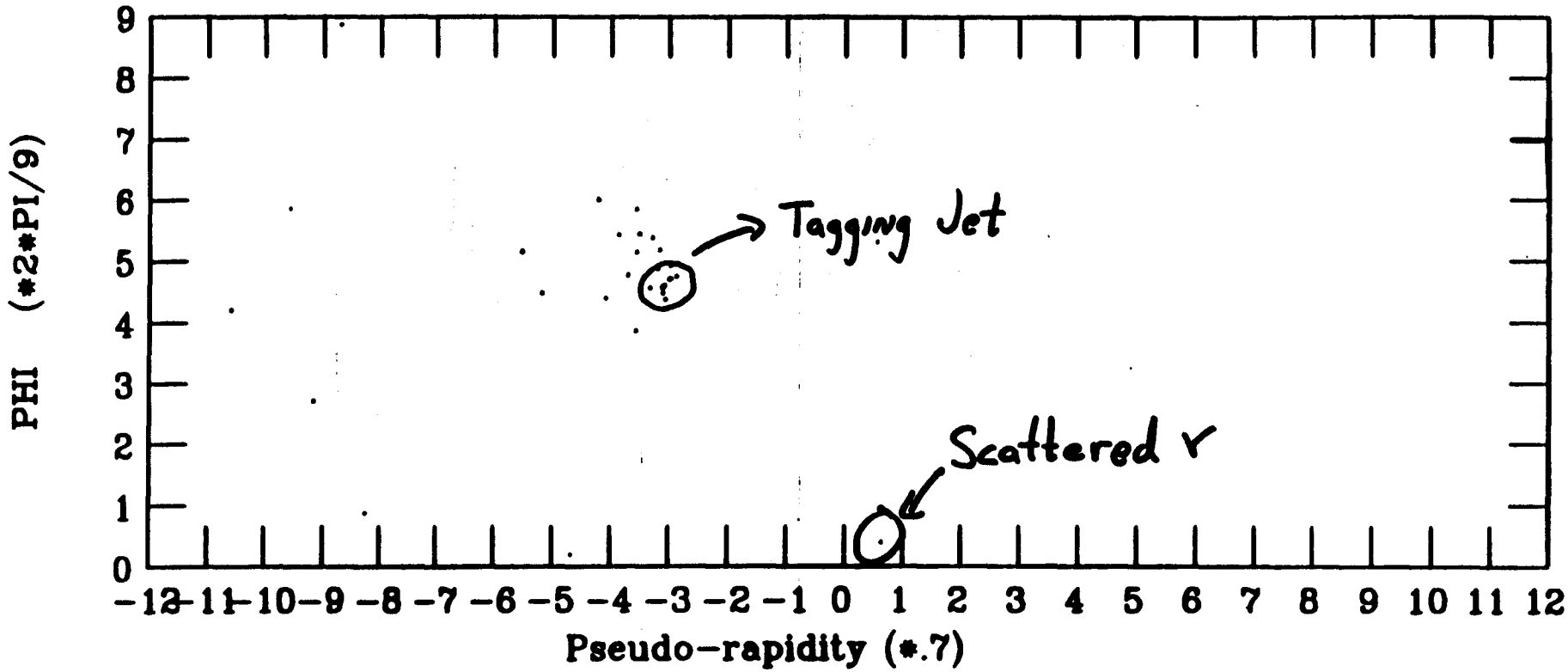

Event number: 1
Number of tracks: 28
Number of jets: 1

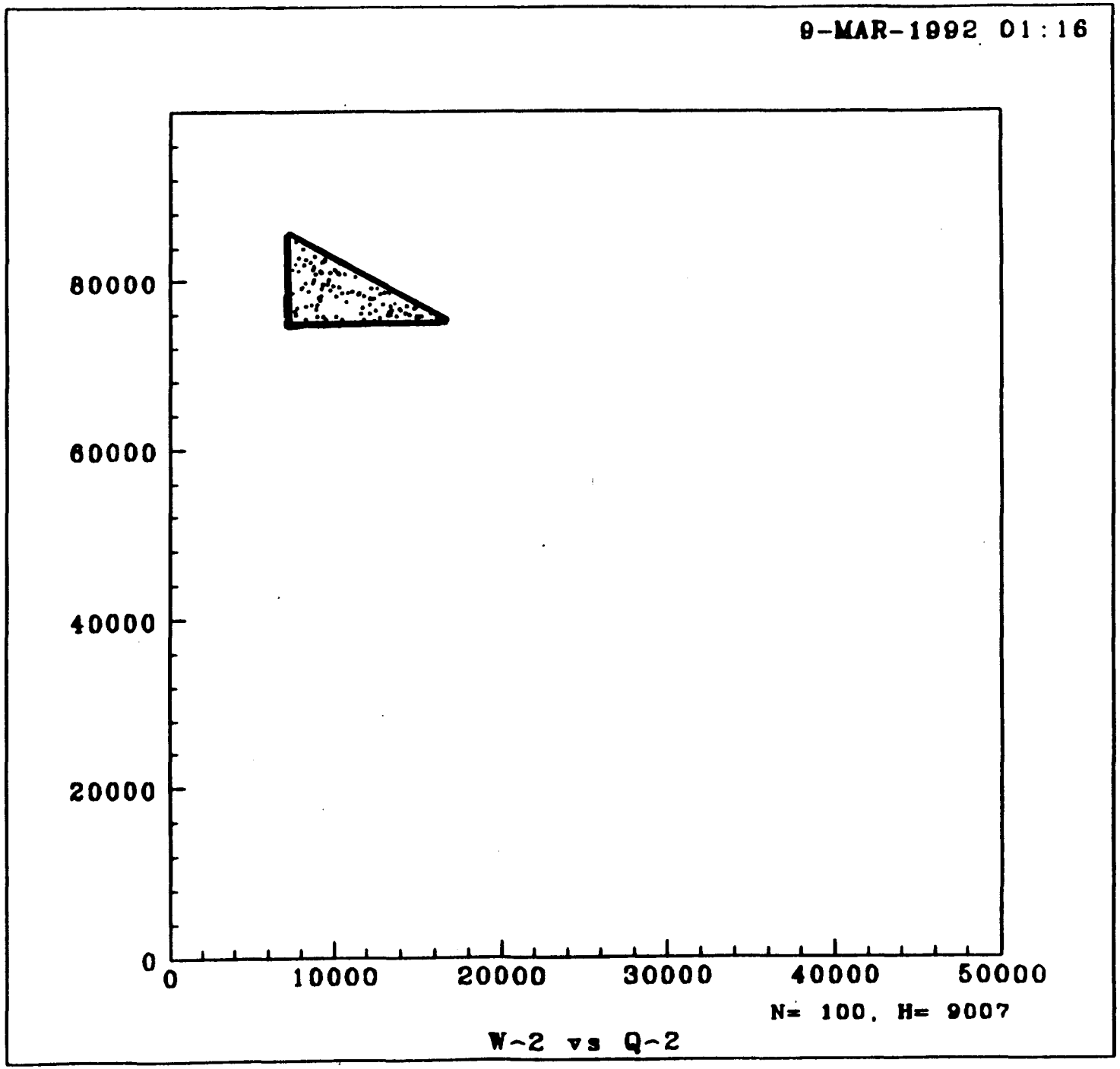
9-MAR-1992 01:16
80000
60000
40000
20000
0
0
10000
20000
30000
40000
50000
N= 100, H= 9007
W~2 vs Q~2

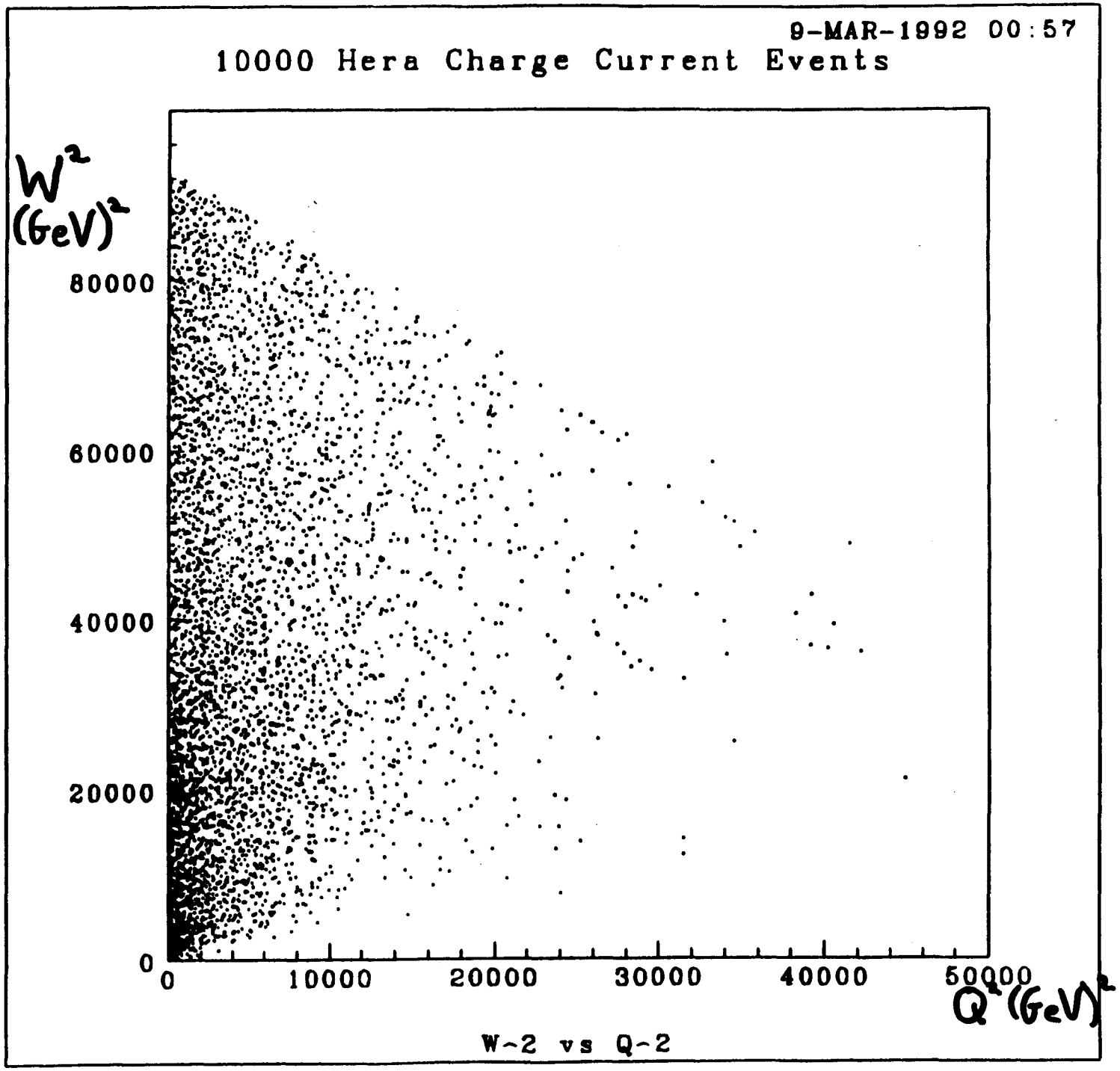
9-MAR-1992 00:57
10000 Hera Charge Current Events
W^2 (GeV)^2
80000
60000
40000
20000
0
0
10000
20000
30000
40000
50000
Q^2 (GeV)^2
W~2 vs Q~2

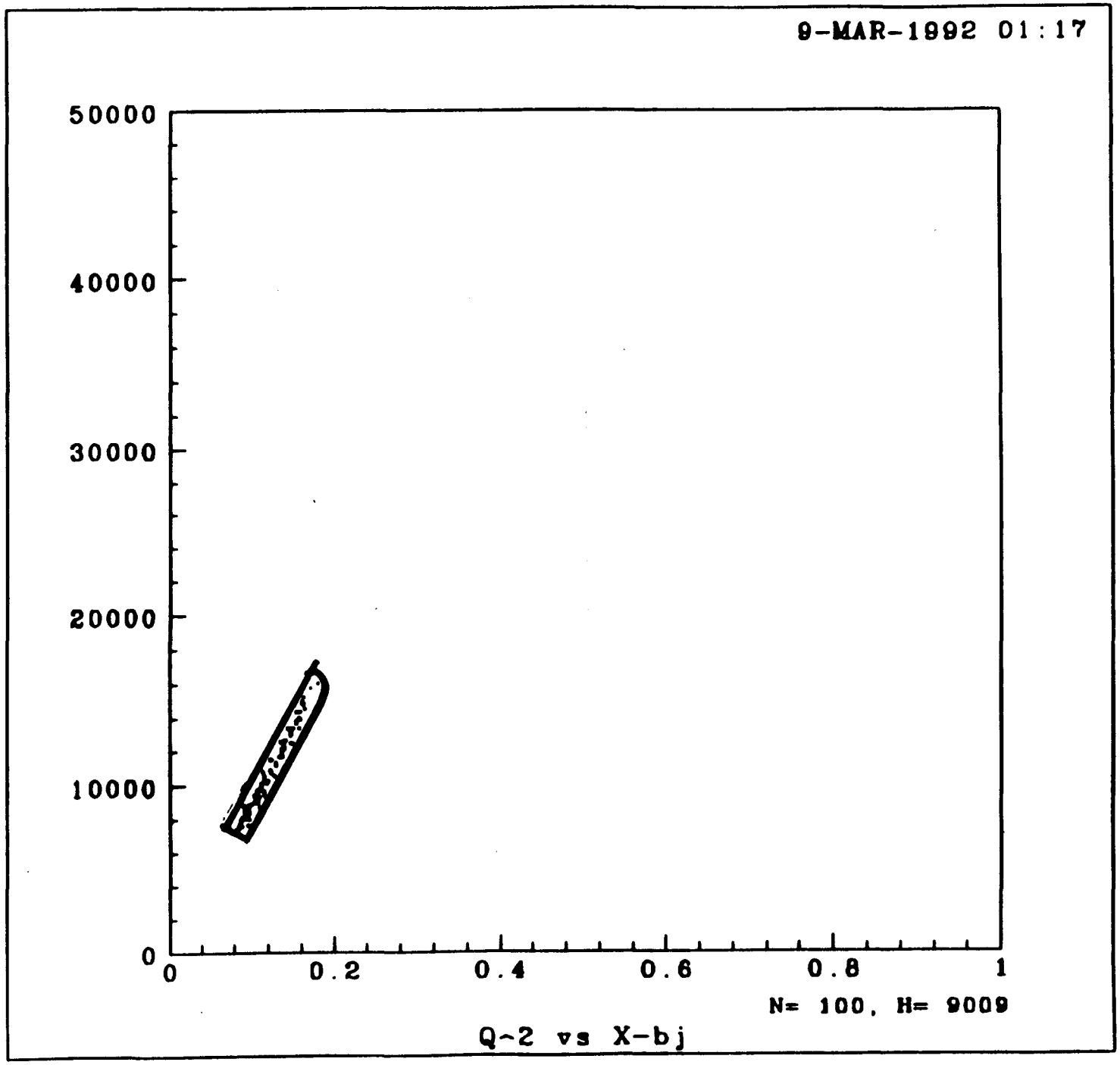
9-MAR-1992 01:17
50000
40000
30000
20000
10000
0
0
0.2
0.4
0.6
0.8
1
N= 100, H= 9009
Q~2 vs X-bj

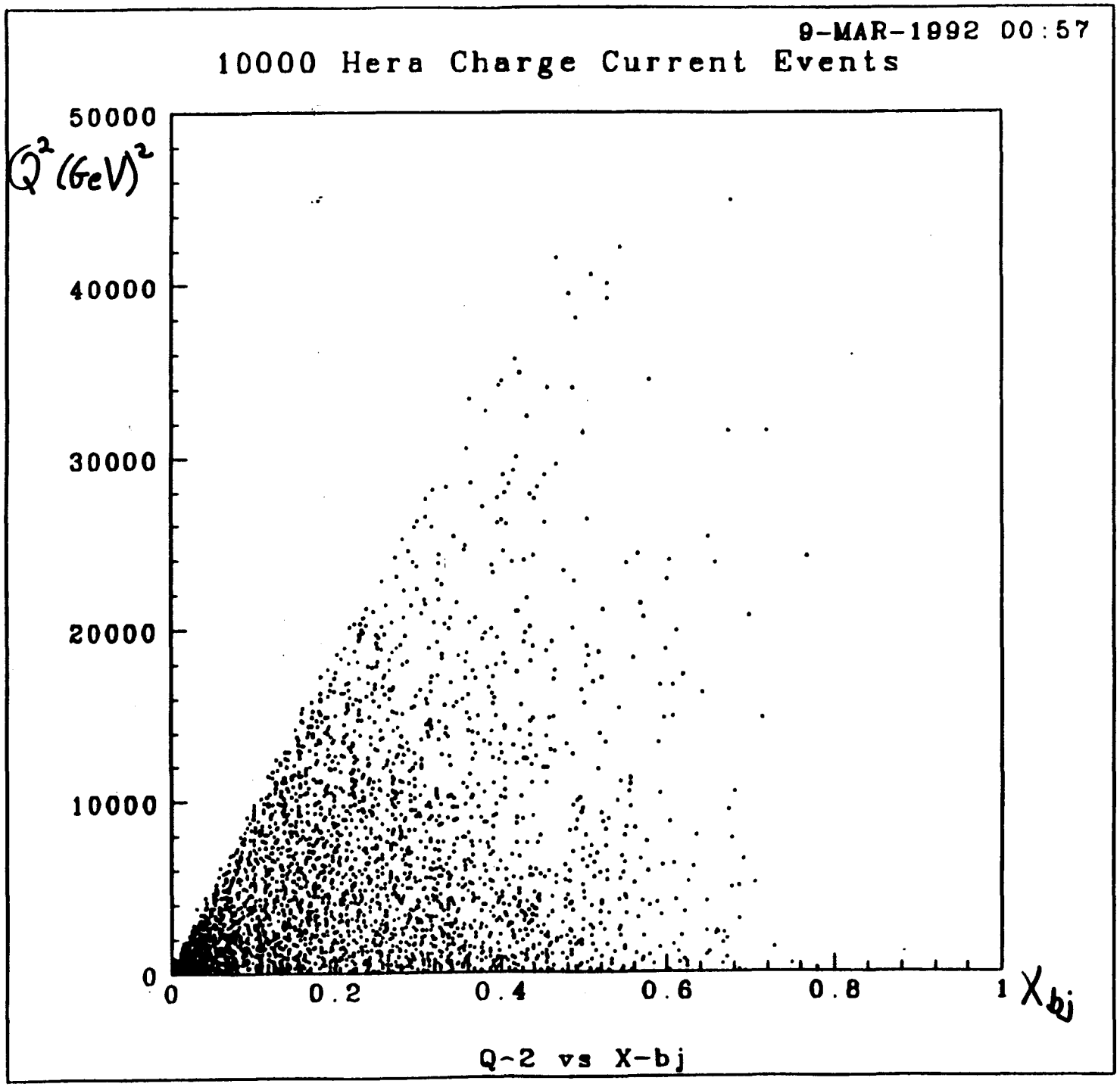
9-MAR-1992 00:57
10000 Hera Charge Current Events
50000
40000
30000
20000
10000
0
Q^2 (GeV)^2
0
0.2
0.4
0.6
0.8
1
X_{bj}
Q-2 vs X-bj

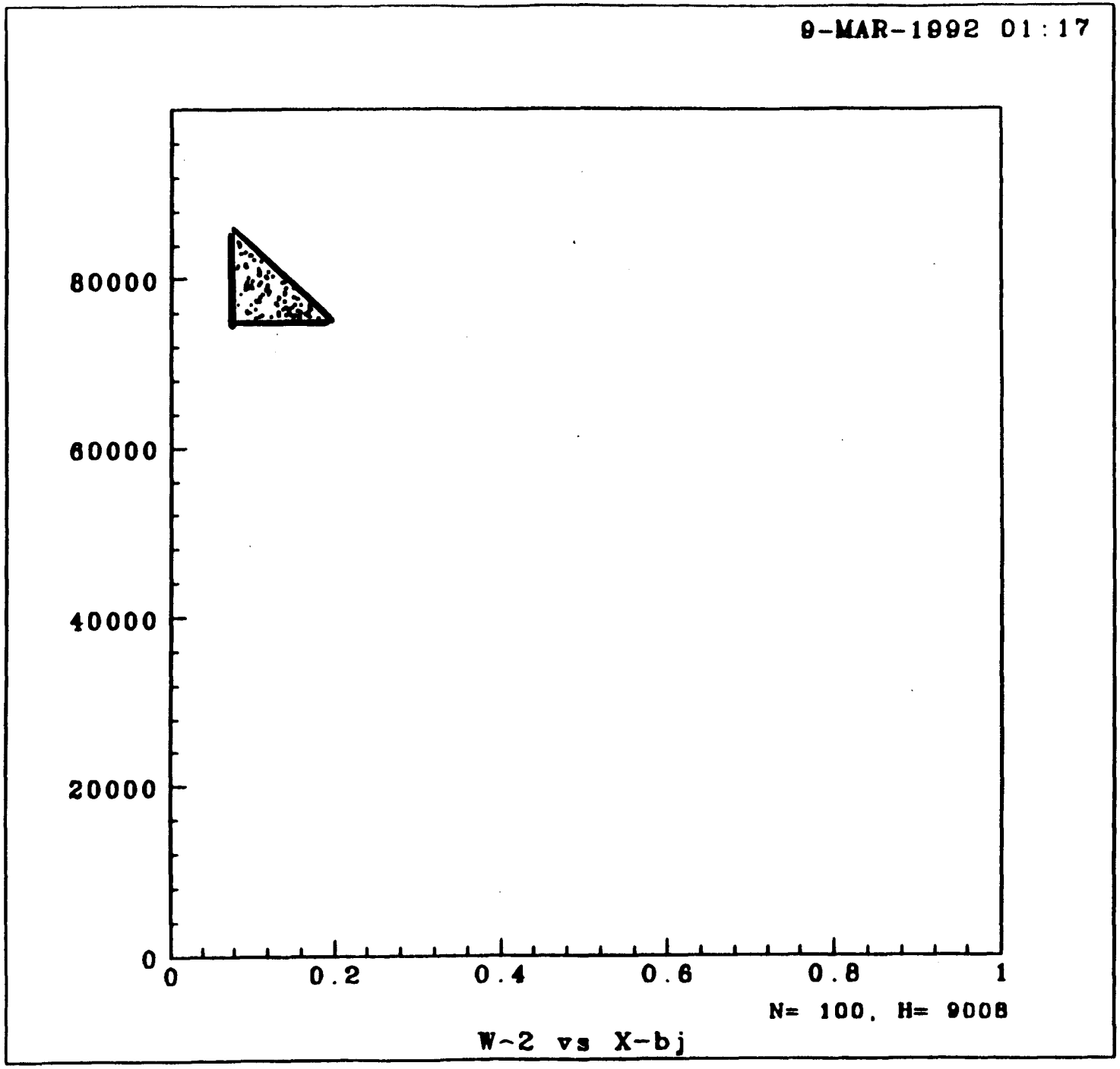
9-MAR-1992 01:17
80000
60000
40000
20000
0
0
0.2
0.4
0.6
0.8
1
N= 100, H= 9008
W~2 vs X-bj

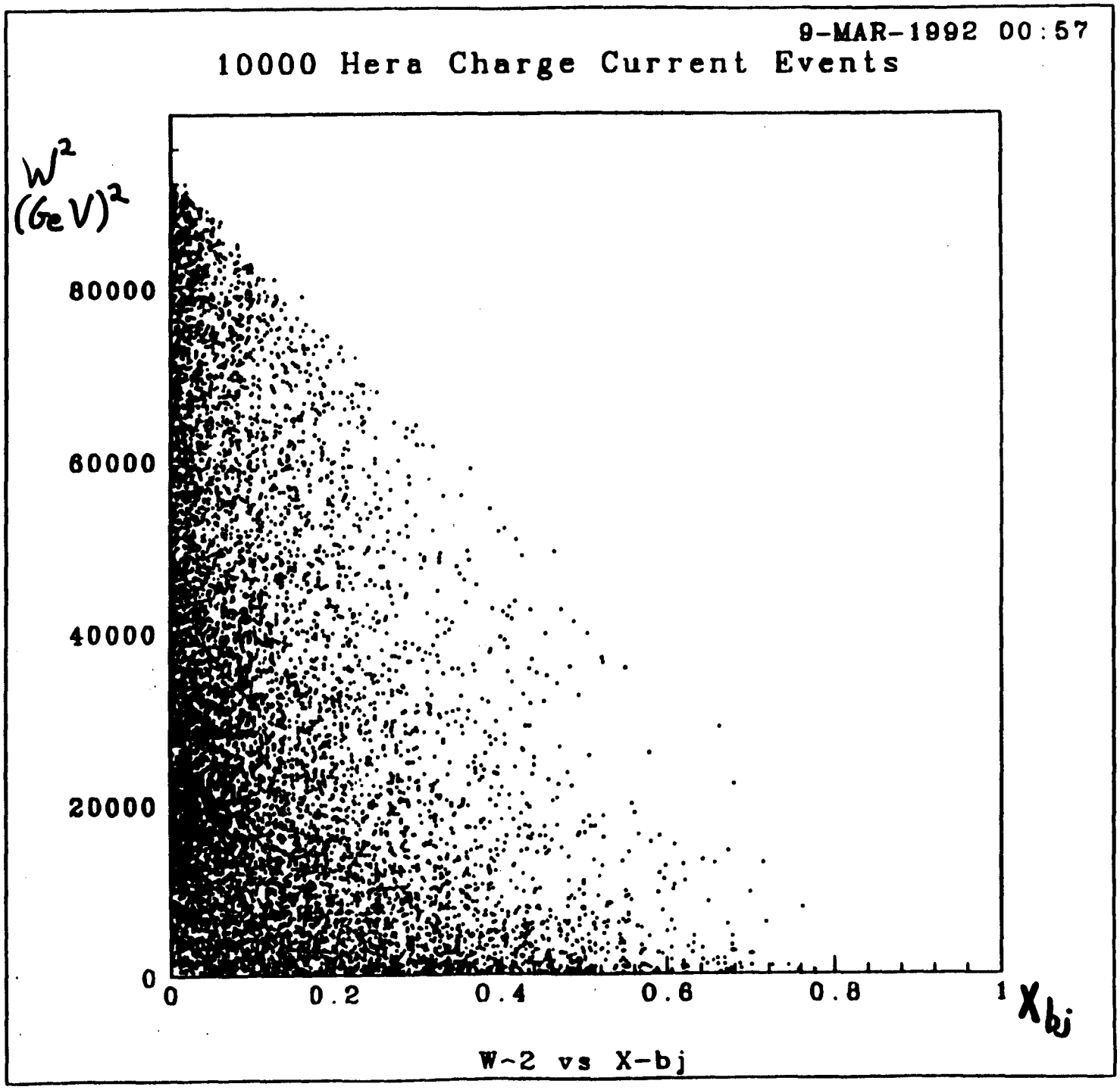
9-MAR-1992 00:57
10000 Hera Charge Current Events
W^2
$(GeV)^2$
80000
60000
40000
20000
0
0
0.2
0.4
0.6
0.8
1
X_{bj}
W~2 vs X-bj

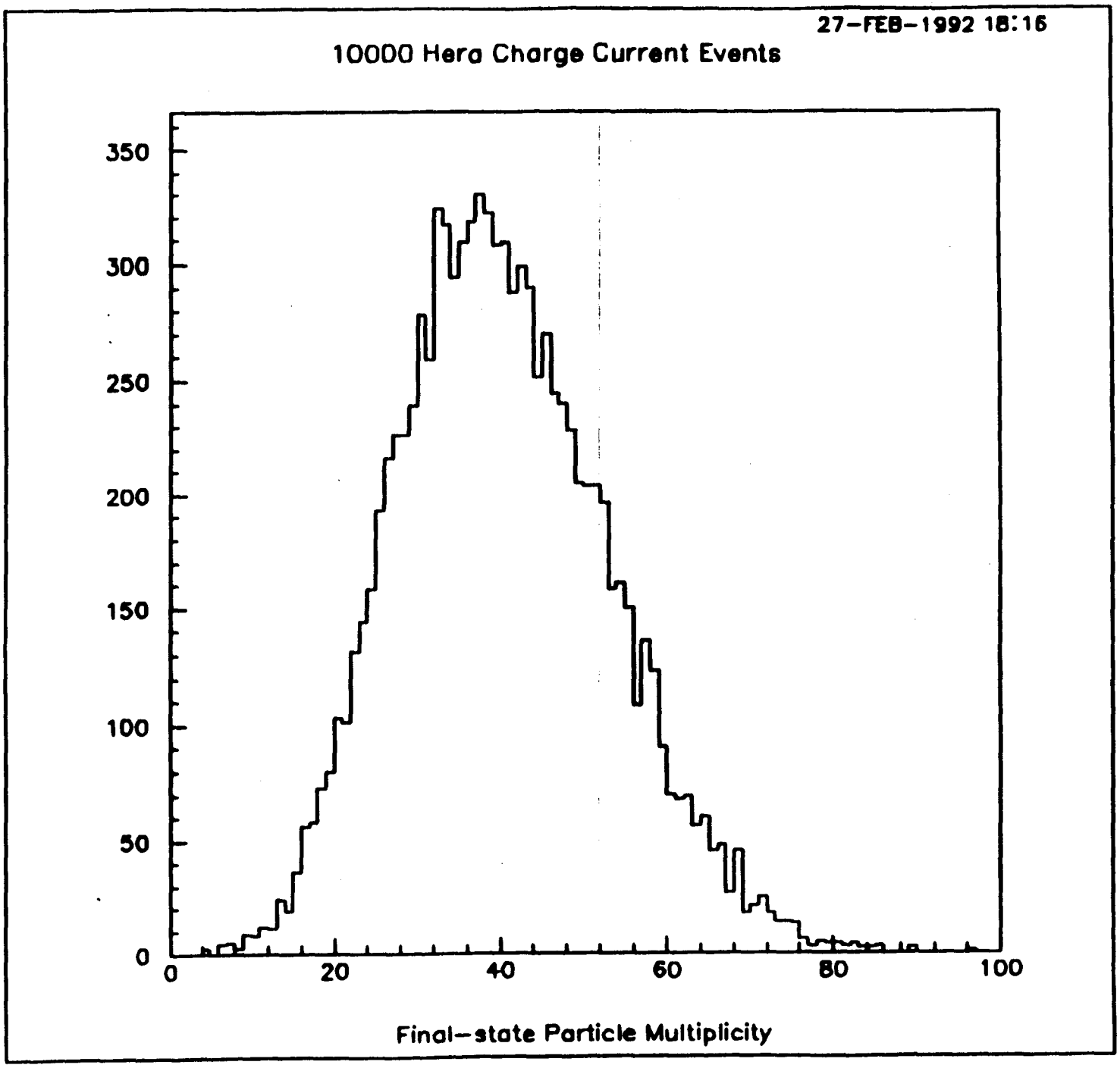
27-FEB-1992 18:16
10000 Hera Charge Current Events
350
300
250
200
150
100
50
0
0
20
40
60
80
100
Final-state Particle Multiplicity

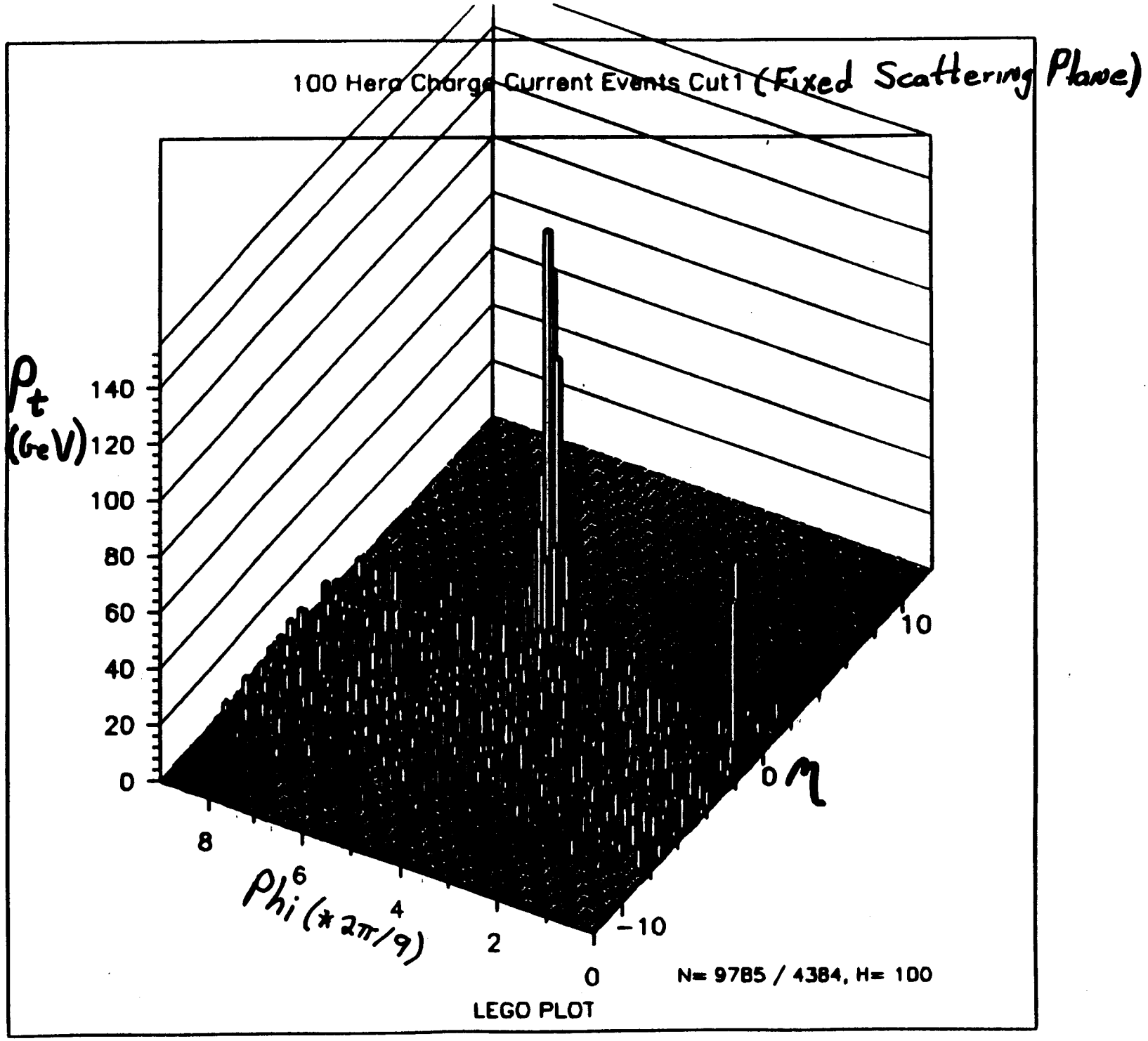
100 Hera Charge Current Events Cut1 (Fixed Scattering Plane)
P_t (GeV)
140
120
100
80
60
40
20
0
8
6
4
2
0
Phi (* 2π/9)
10
0
−10
η
N= 9785 / 4384, H= 100
LEGO PLOT

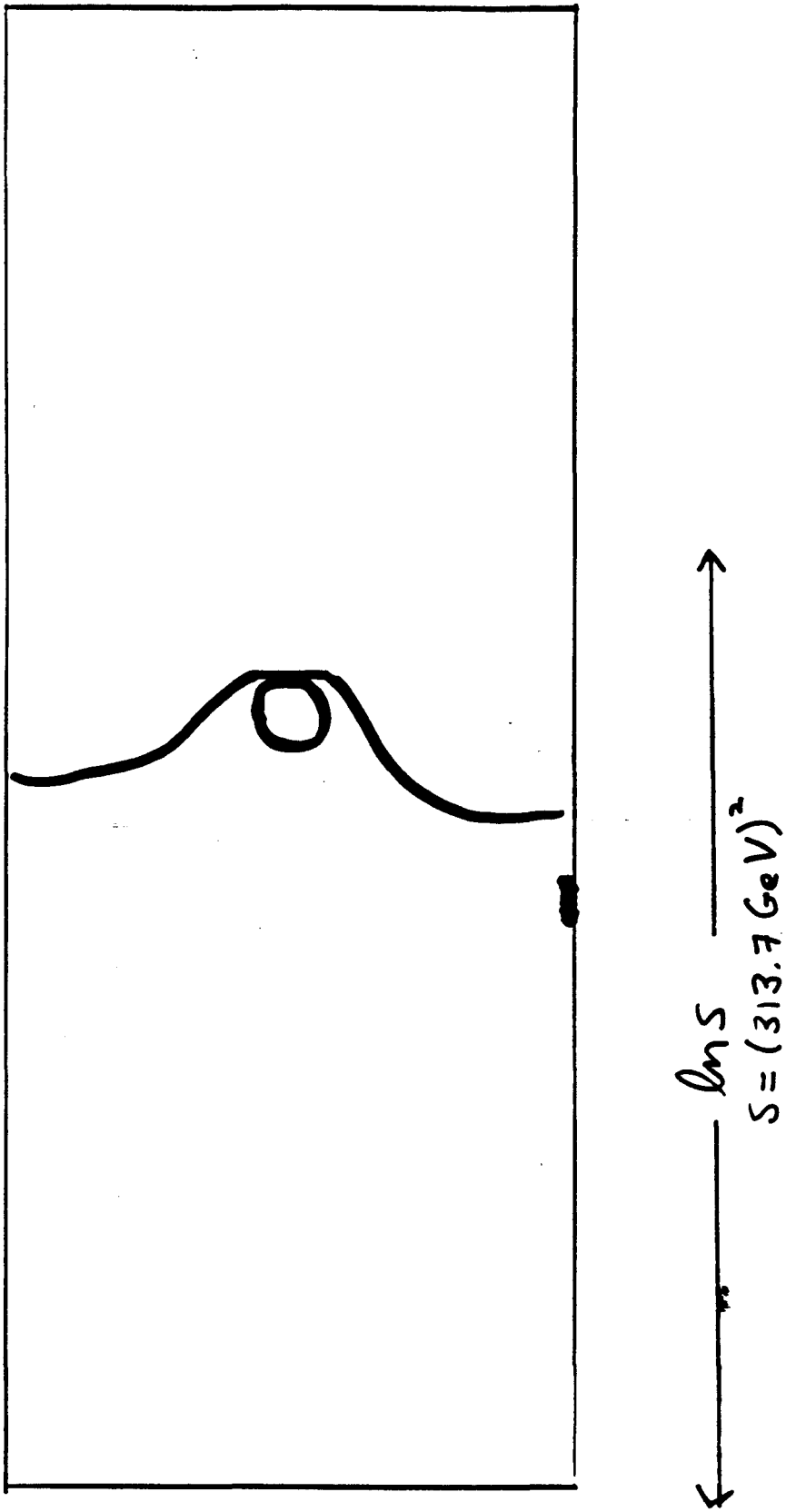
ln S
S = (313.7 GeV)²

100 HERA CHARGE CURRENT EVENTS CUT#1 *

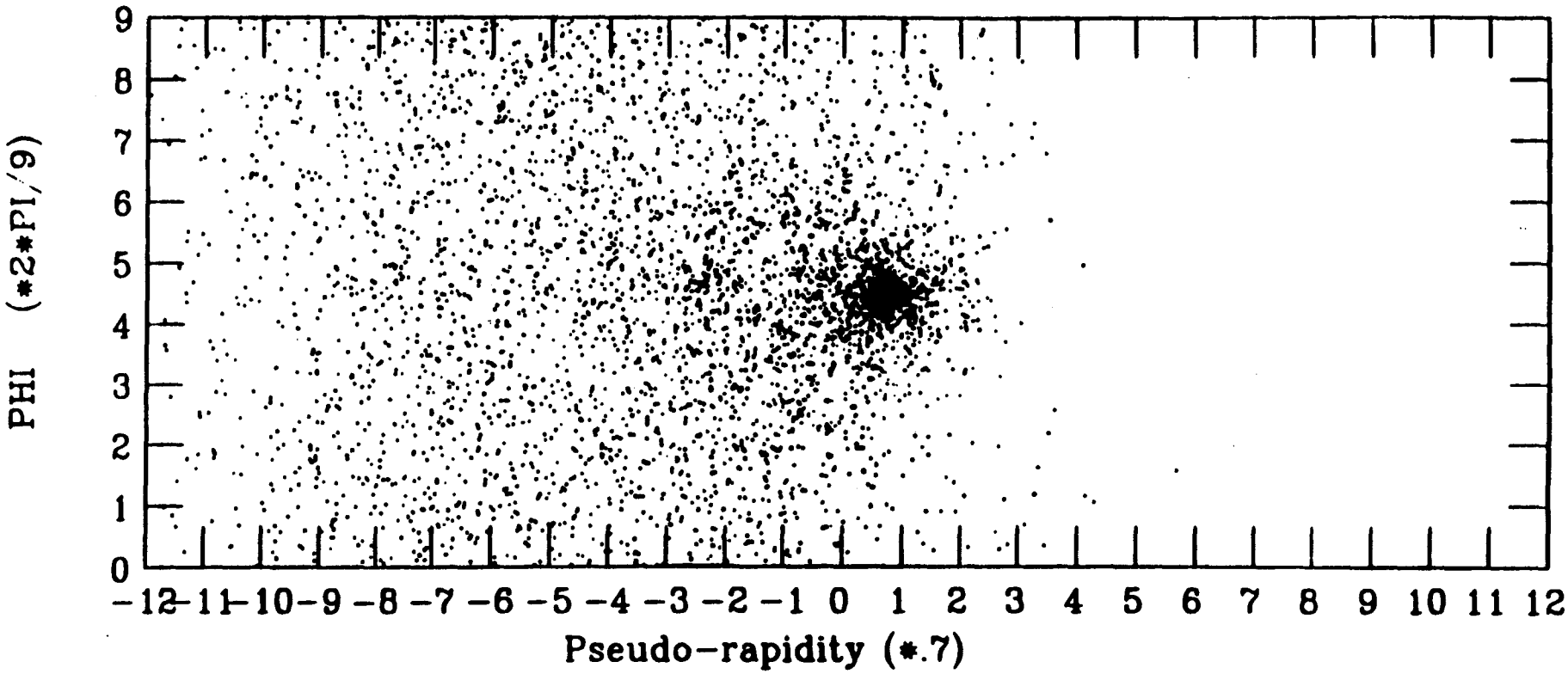

Number of events: 100
Number of tracks: 4384

* fixed scattering Plane.

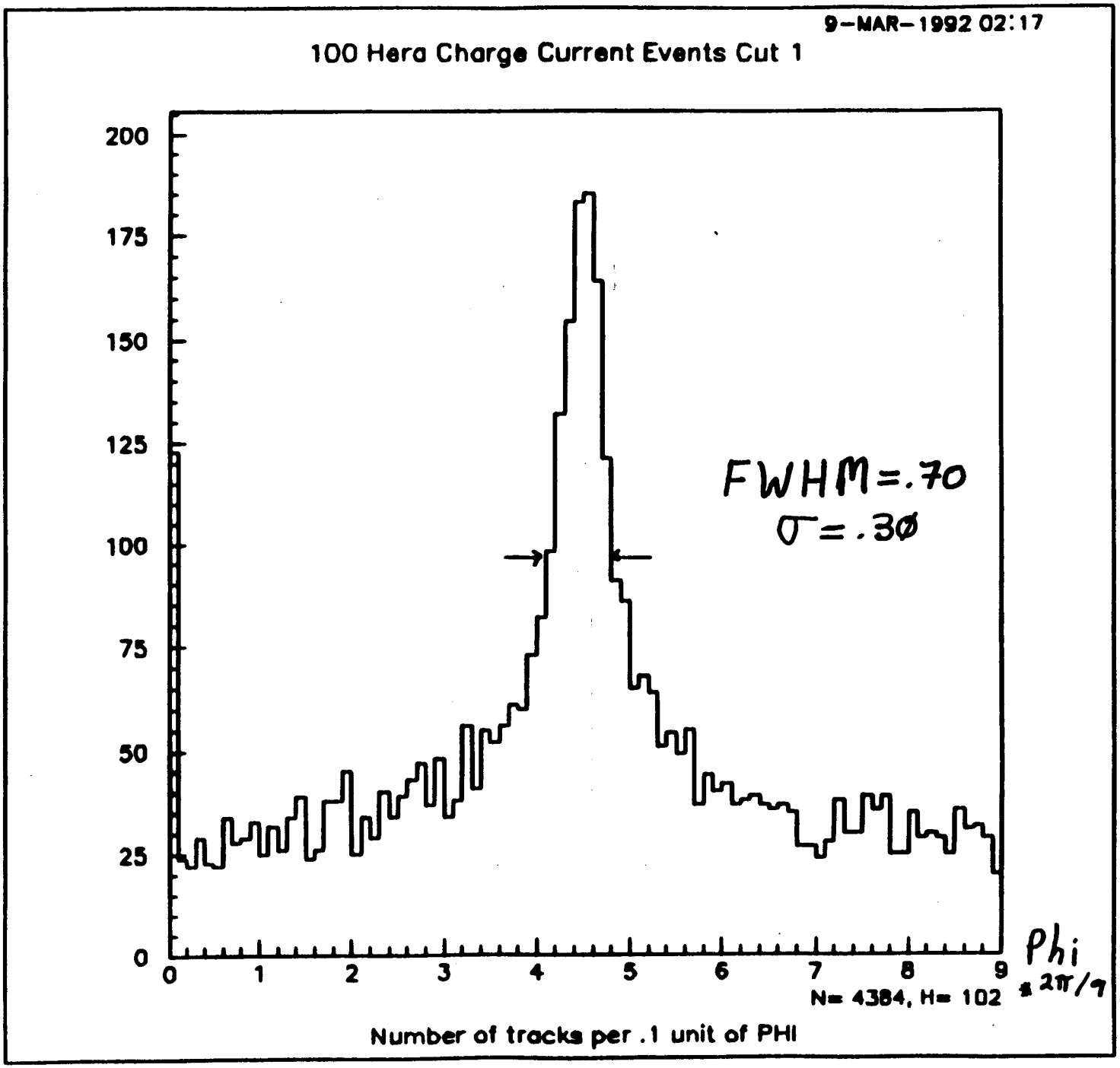
9-MAR-1992 02:17
100 Hera Charge Current Events Cut 1
200
175
150
125
100
75
50
25
0
0
1
2
3
4
5
6
7
8
9
FWHM=.70
σ=.30
Phi
$2π/9
N= 4384, H= 102
Number of tracks per .1 unit of PHI

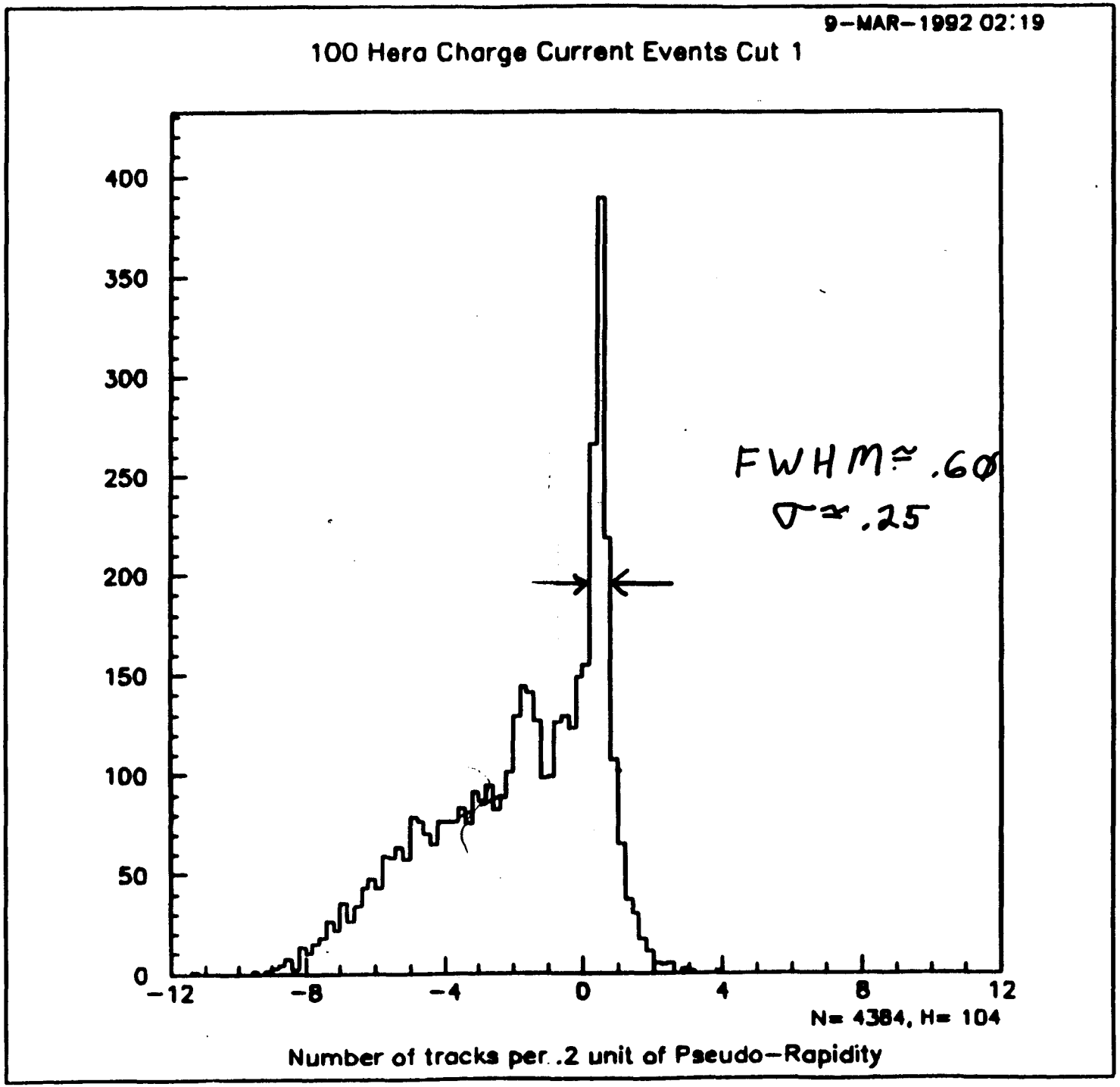
9-MAR-1992 02:19
100 Hera Charge Current Events Cut 1
400
350
300
250
200
150
100
50
0
-12
-8
-4
0
4
8
12
N= 4384, H= 104
Number of tracks per .2 unit of Pseudo-Rapidity
FWHM ≈ .60
σ ≈ .25

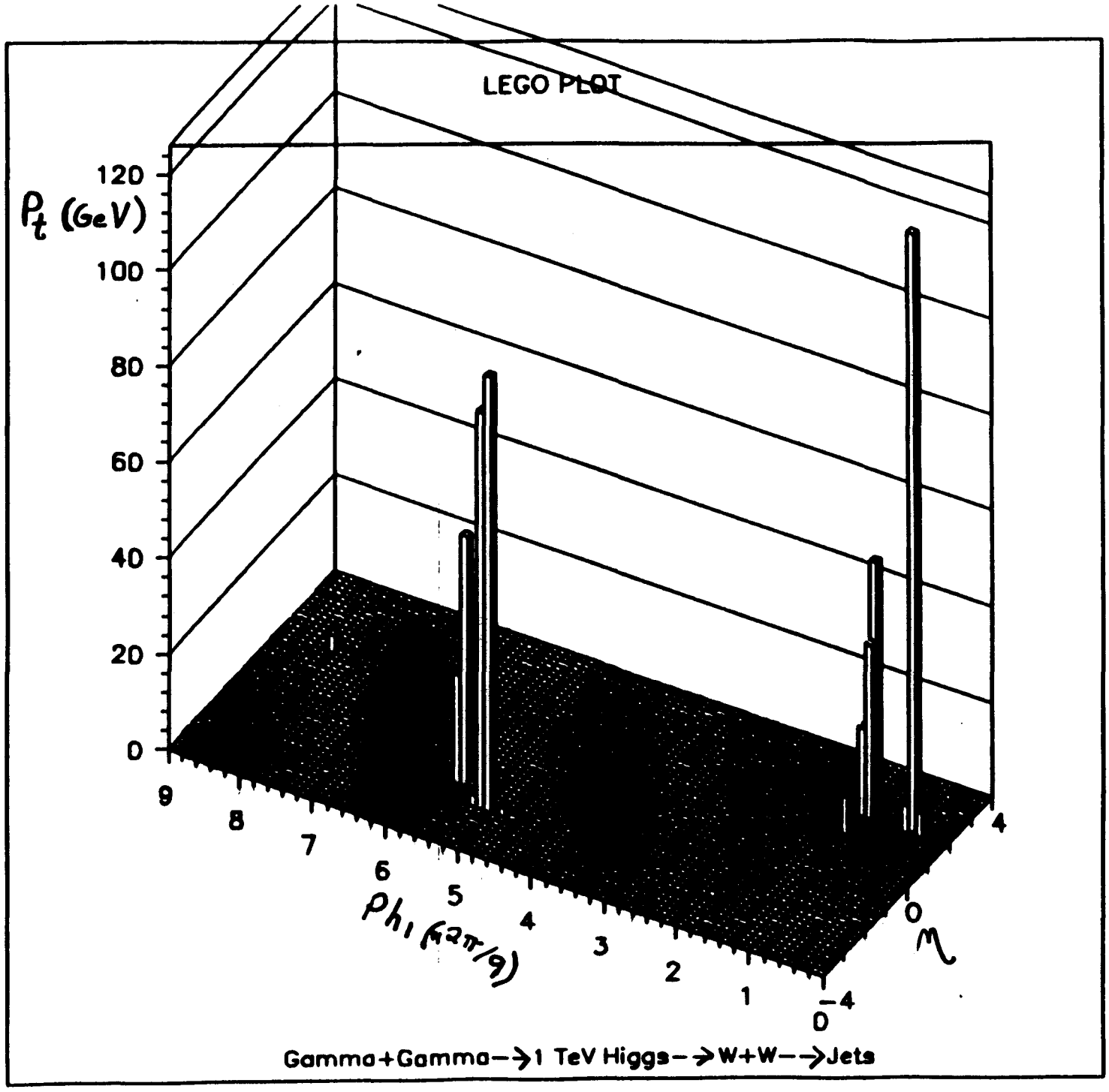
LEGO PLOT
P_t (GeV)
120
100
80
60
40
20
0
9
8
7
6
5
4
3
2
1
0
Phi (*2π/9)
-4
0
4
Eta
Gamma+Gamma-->1 TeV Higgs-->W+W-->Jets

$\gamma+\gamma$-->1 TeV Higgs-->W+W-->Jets

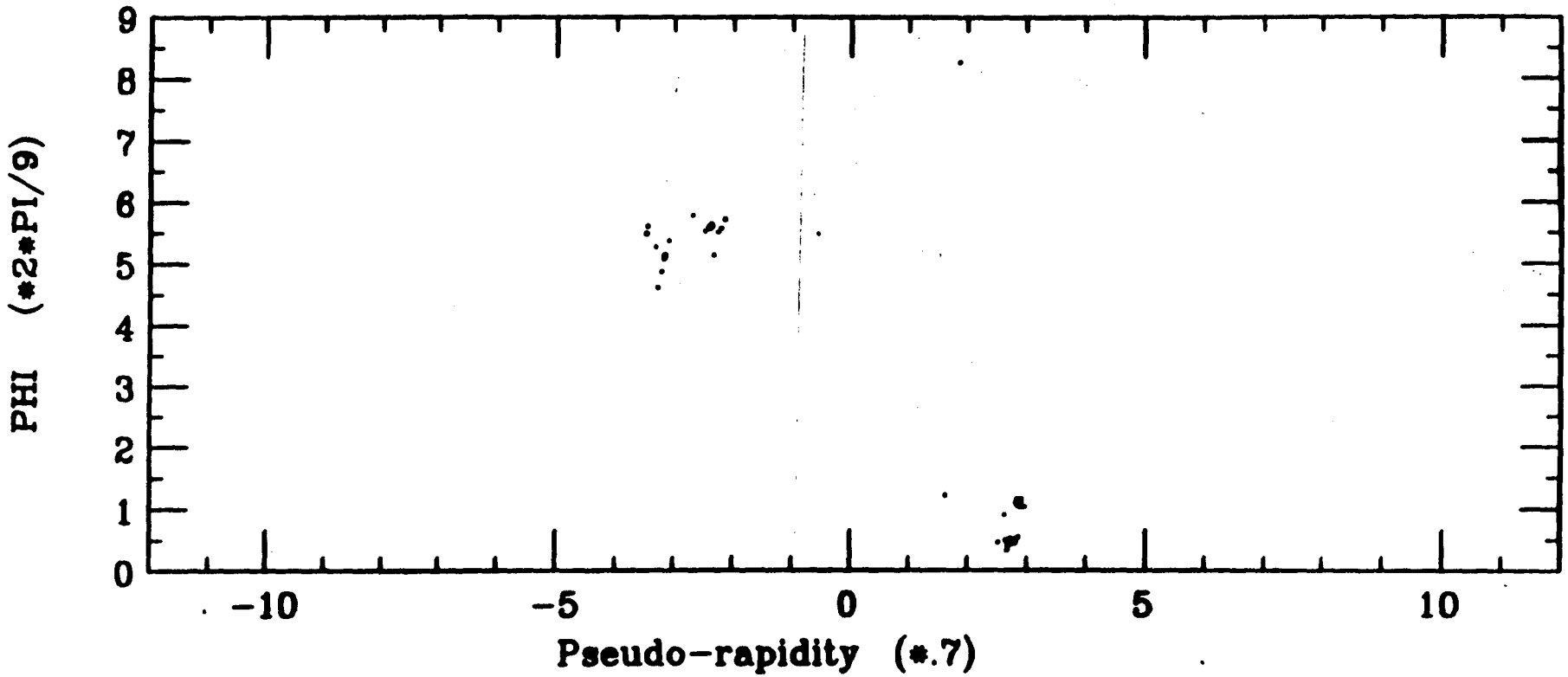

Event number: 4
Input File Name: SPACE:HIGGS_WW.DAT1
Number of tracks: 64

$\gamma+\gamma$-->1 TeV Higgs -->W+W-->Jets *

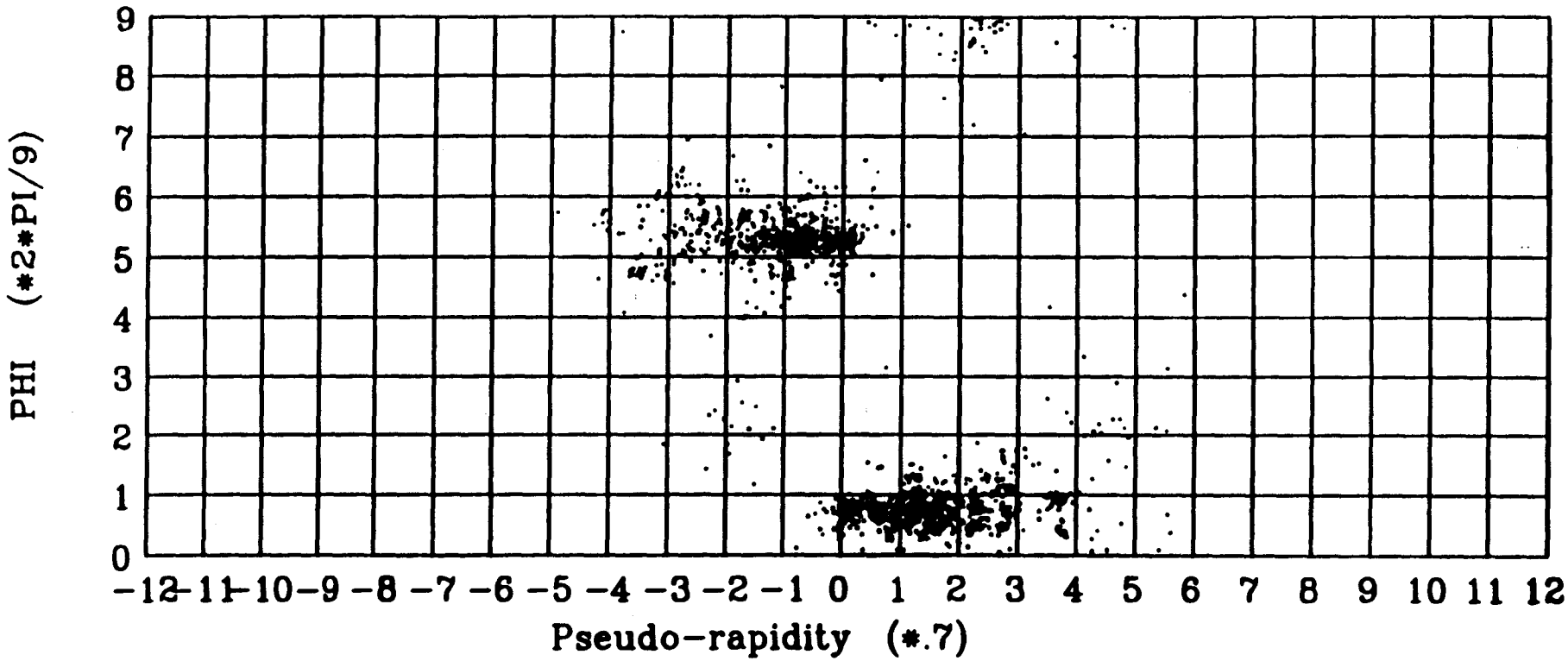

NUMBER OF EVENTS: 50

Number of tracks: 2502

* Fixed Scattering Plane

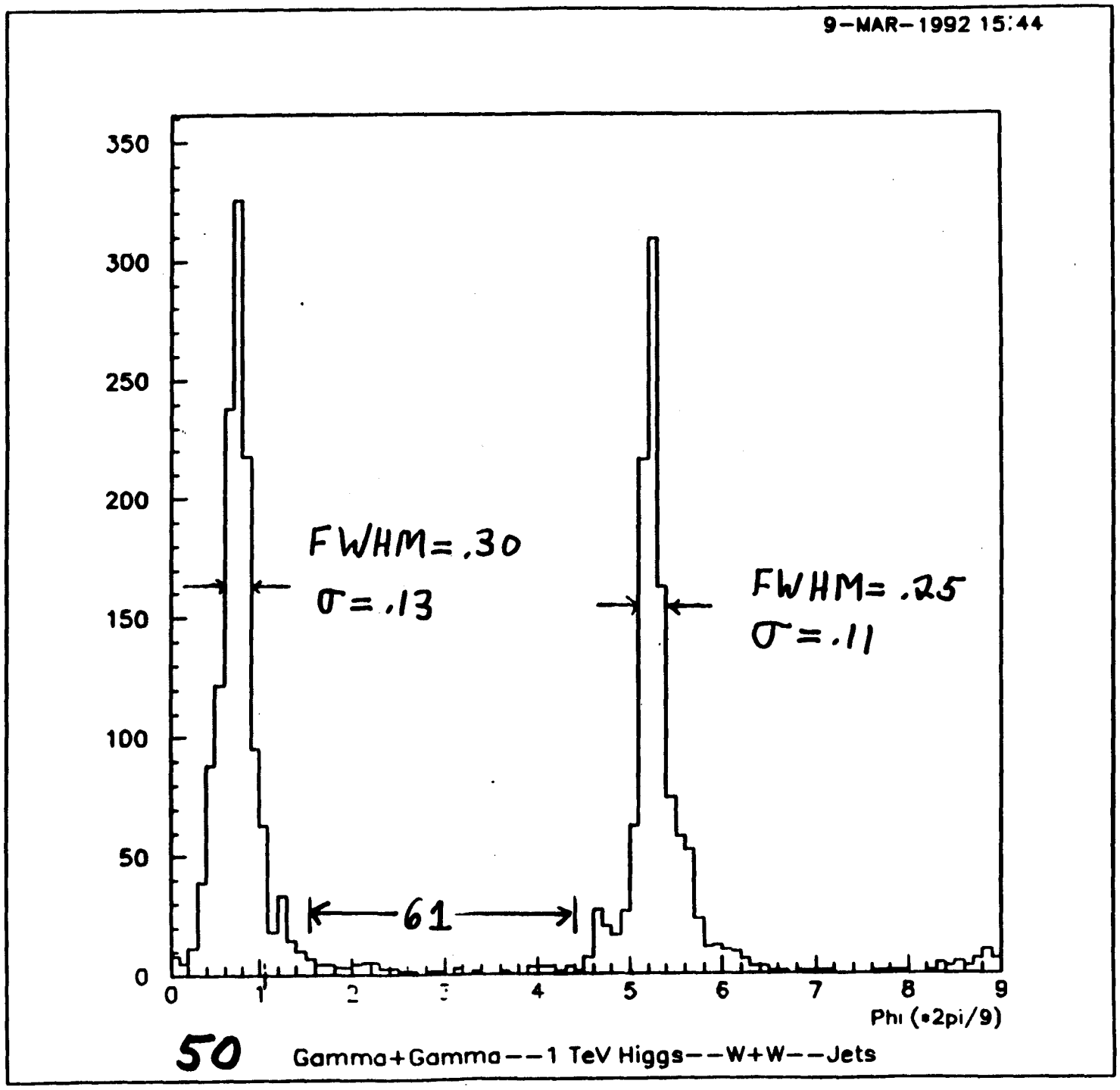
9-MAR-1992 15:44
350
300
250
200
150
100
50
0
0
1
2
3
4
5
6
7
8
9
Phi (*2pi/9)
FWHM=.30
σ=.13
FWHM=.25
σ=.11
61
50
Gamma+Gamma--1 TeV Higgs--W+W--Jets

Future Work

1. Use pattern recognition and/or traditional jet finding algorithms to locate jets in lego plot.

2. Investigate internal jet structure in an extended lego plot (i.e. Jets within Jets)

3. Statistically analyze leakage of particles into rapidity gaps and detailed shape of rapidity edge.

4. . . .

FAD Higgs Event

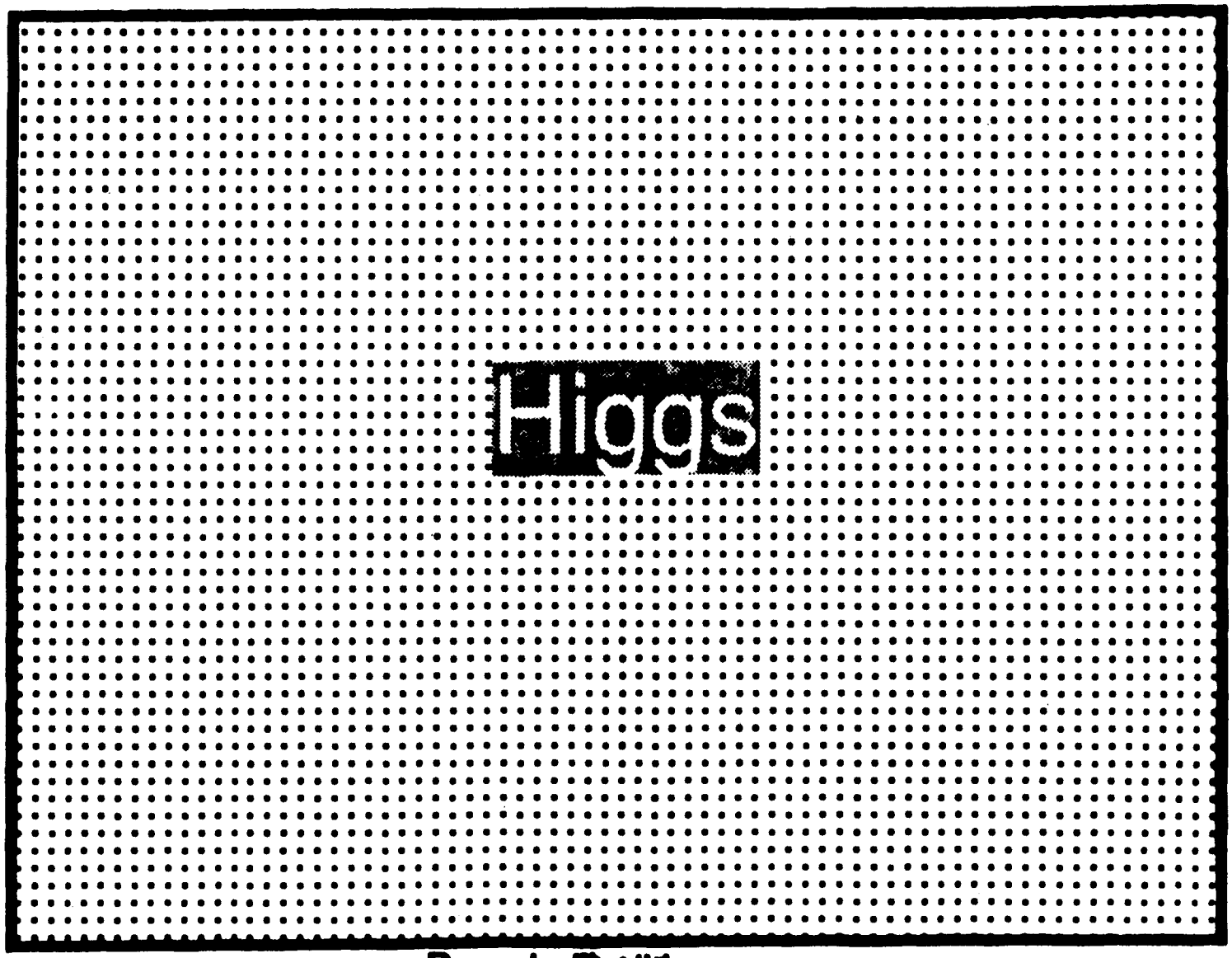

Psuedo [redacted]
Rapidity

Phi

Machine Lattice Considerations for a Full Acceptance Detector at the SSC.

F.H.D. Meeting
13 March 92
John Venturi

What are the Key Issues?

- Dispersion Matching
- Where does the first Calorimeter wall go?
- What is the diameter of the Quads?
- What is the highest luminosity achievable?

KEY PARAMETERS:

β^*, QUAD STRENGTH, DISTANCE BETWEEN QUADS, FREE SPACE BEFORE QUADS.

GOALS FOR THIS STUDY

* ESTABLISH A WORKING RELATIONSHIP WITH SSC LATTICE DESIGN GROUP (D. Johnson et.al.)

* KNOW (AND UNDERSTAND) MACHIN LATTICE CONSTRAINTS ON F.A.D.

* DEVELOPE a 0th ORDER MECHANISM TO CALCULATE β-functions RELAVANT TO F.A.D ARCHITECTURE.

LUMINOSITY AS A FUNCTION OF β^*

$$\mathcal{L} = \frac{f\, N_{MAX}\, \Delta\nu_0\, \gamma}{2\, r_e\, \beta^*}$$

. M. Sands S-P 121,

γ : FOR A GIVEN ENERGY

N_{MAX} : beam Current

f : $= c/2\pi R$ (R radius of ring)

$\Delta\nu_0$: Beam-Beam Interaction parameter

r_e : Classical Electron radius

$\Downarrow$

β^* is THE ONLY Free parameter!

WHAT WAS in EoI - 19

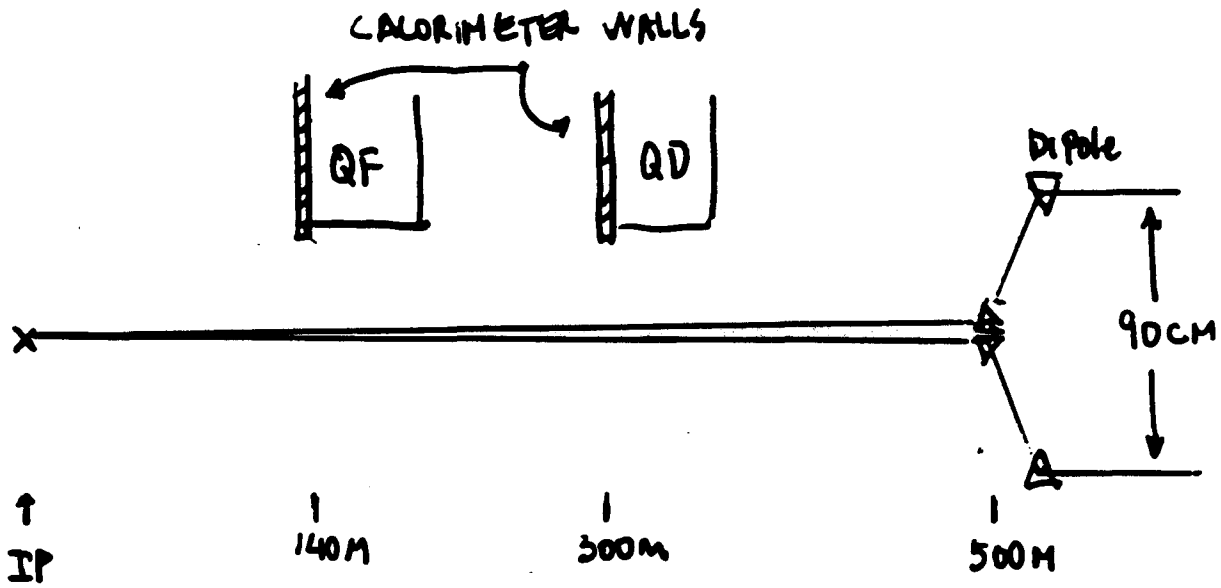

* DISPERSION MATCHING PROBLEMS (?)

SSC Low-β IR

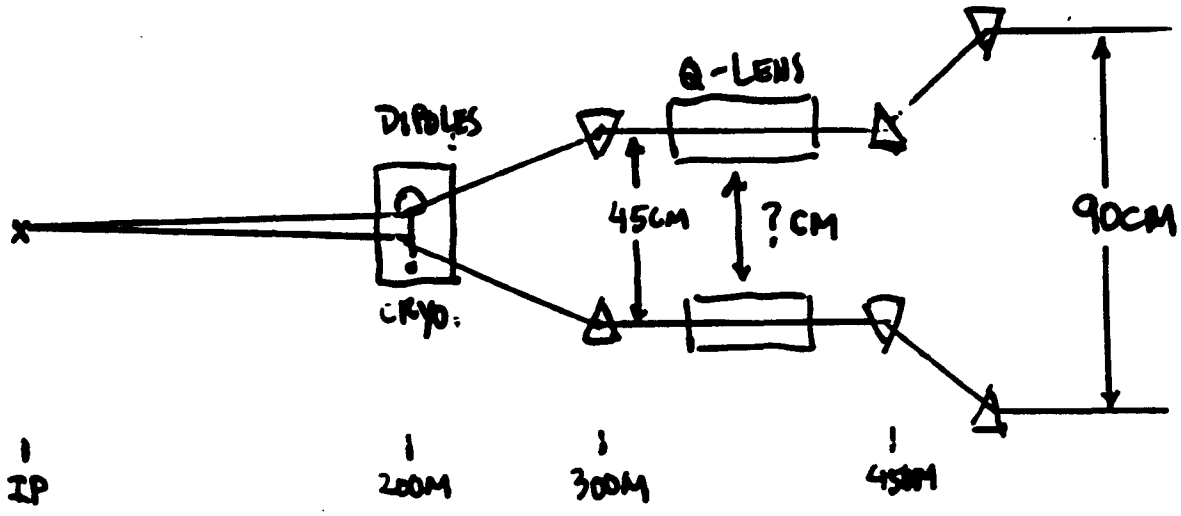

SIMPLE MODEL FOR CALCULATING LATTICE β-function

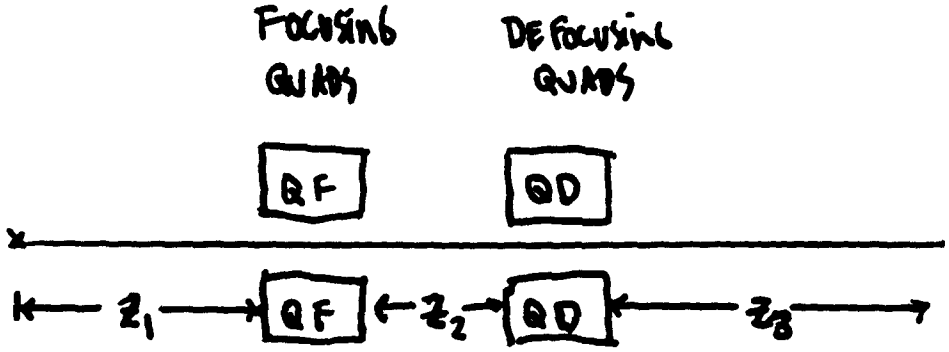

* ASSUME: $\overbrace{\beta^*, \text{ QUAD STRENGTH}, z_2, \text{ and } z_3}^{\text{INPUT PARAMETERS}}$

  ⇒ VARY z_1 ⇒ DET. β-function

* ASSUME NEW SET OF INPUT PARAMETERS (ie change β^*)

  ⇒ VARY z_1 ⇒ DET. β-function

⋮

MORE ASSUMPTIONS

* NOMINAL Gradient : 0.15 T/cm

* LENGTH OF QUAD : 50 Meters

* FOCAL Length :

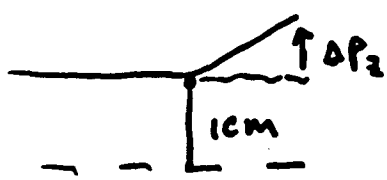

THE $\Delta P_\perp$ "KICK" :

$$(0.15\ T/cm)(1\ cm)(50\ m)(300\ MeV/T\text{-}m) = 2.25\ GeV \sim 2\ GeV$$

$$\Rightarrow \quad \frac{\Delta P_z}{P} \simeq 10^{-4}$$

$$\frac{1}{f} = \frac{\Delta P_z}{P} \cong \frac{1}{100\,m} \quad \text{or} \quad \underline{f \sim 100\,m}$$

Also : $\frac{1}{f} \sim \frac{eG\ell}{P}$

THEORY: ALTERNATE GRADIENT FOCUSING

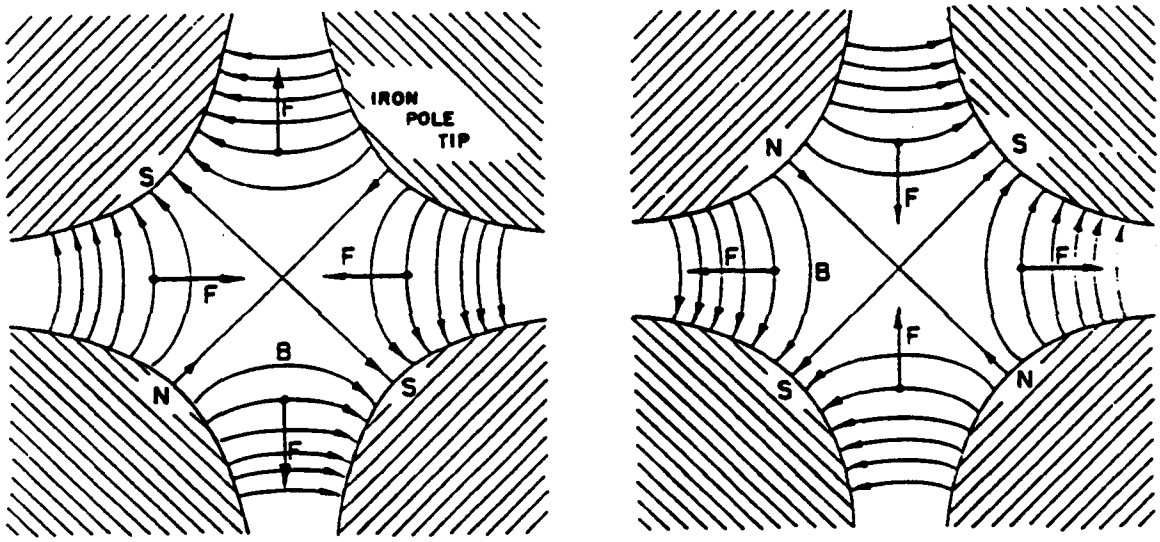

horizontal focusing, vertical focusing

* OVERALL FOCUSING DEPENDS ON FIELD STRENGTH AND DISTANCE BETWEEN QUADRAPILE MAGNETS.

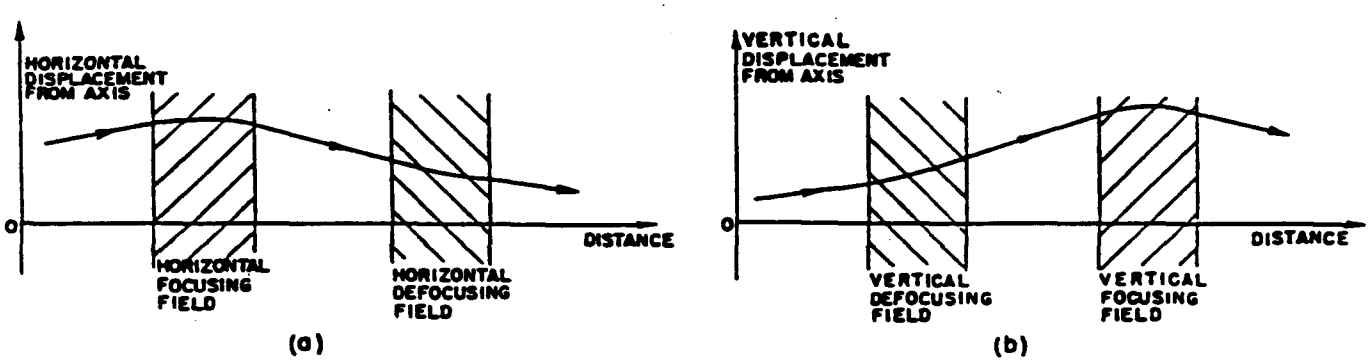

* FOR OVER-ALL FOCUSING:

f (FOCAL LENGTH) $\sim$ L (SPACING)

HOW DOES $\beta_{x,y}$ VARY VS. z_1 (ie position of 1st QF)?

$\beta^* = 10M$, $G_F = G_D = 0.15$ T/cm , $z_2 = 135$ M

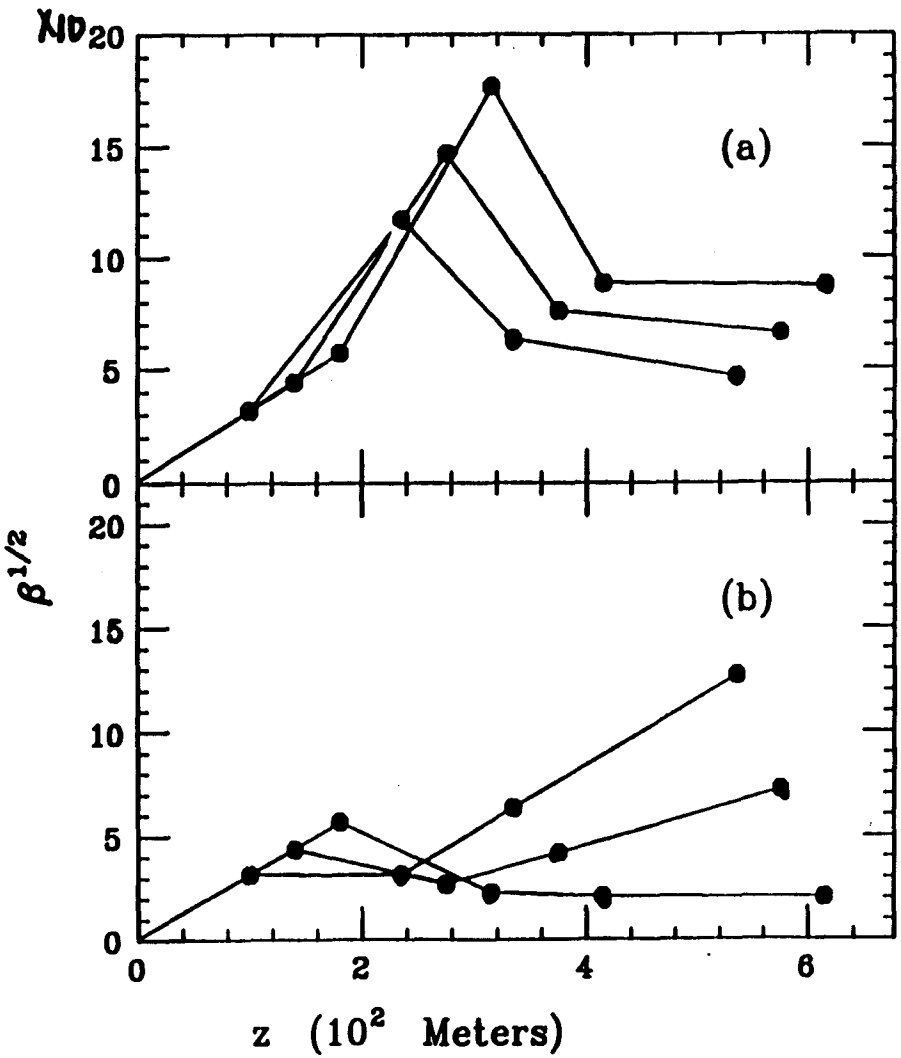

a) $\sqrt{\beta_x}$

- $z_1 = 180$ M
- $z_1 = 140$ M
- $z_1 = 100$ M

b) $\sqrt{\beta_y}$

$\beta^* = 25\,M$

$G_1 = G_2 = 0.15\ T/CM$

$z_2 = 100\,M$

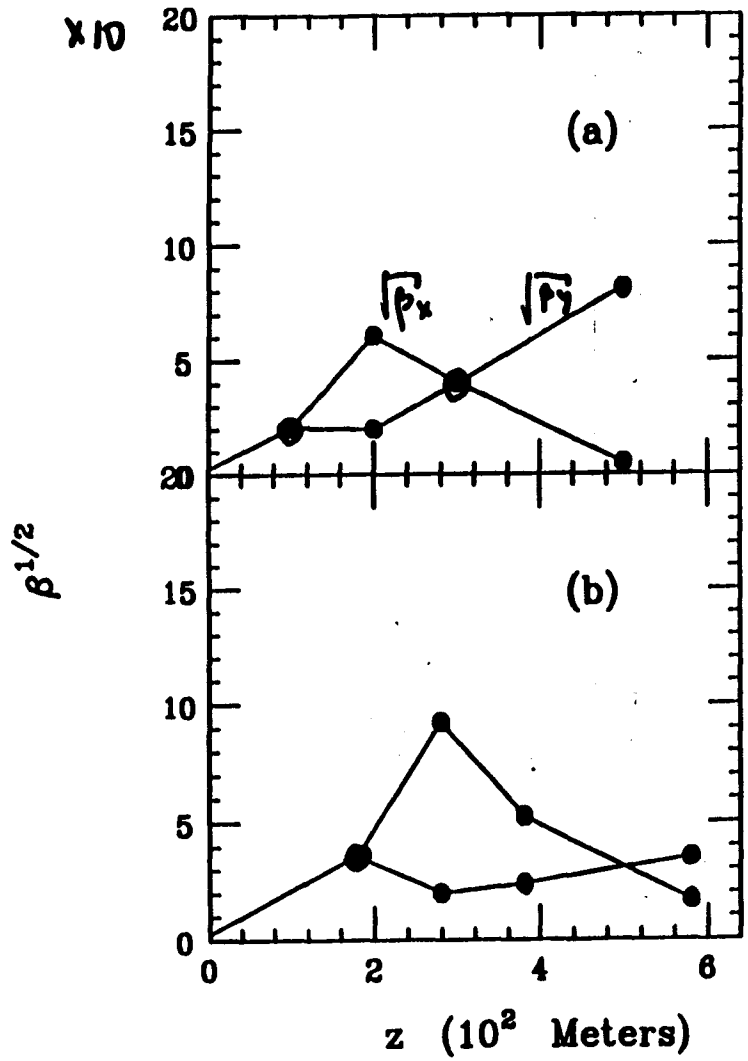

$\beta^* = 25\,M$

$G_1 = G_2 = 0.15\ T/CM$

$z_2 = 135\,M$

$z_1 = 100\,M$

$z_1 = 180\,M$

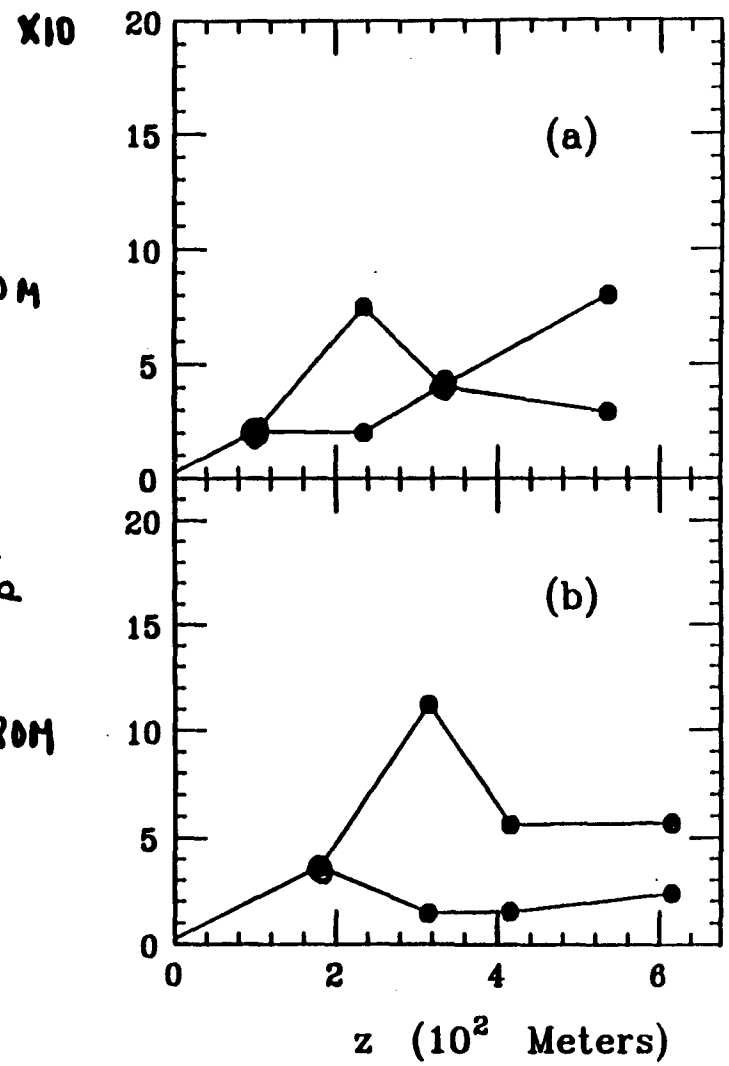

$\beta^* = 10$ M

$G_1 = G_2 = 0.15$ T/cM

$z_2 = 100$ M

$\beta^* = 10$ M

$G_1 = G_2 = 0.15$ T/cM

$z_2 = 135$ M

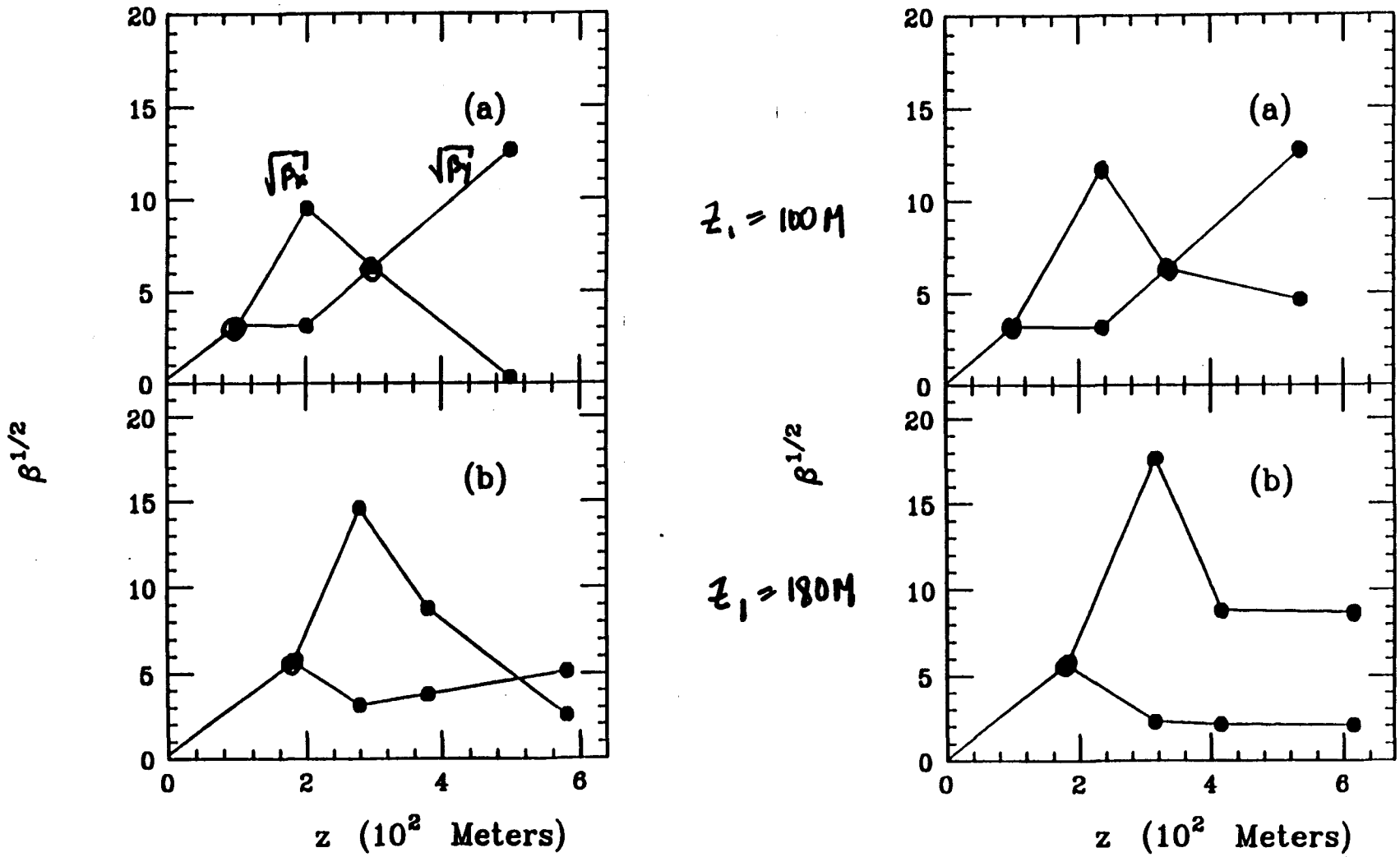

$\beta^* = 10\,M$

$G_1 = G_2 = 0.17\,T/cM$

$z_2 = 135\,M$

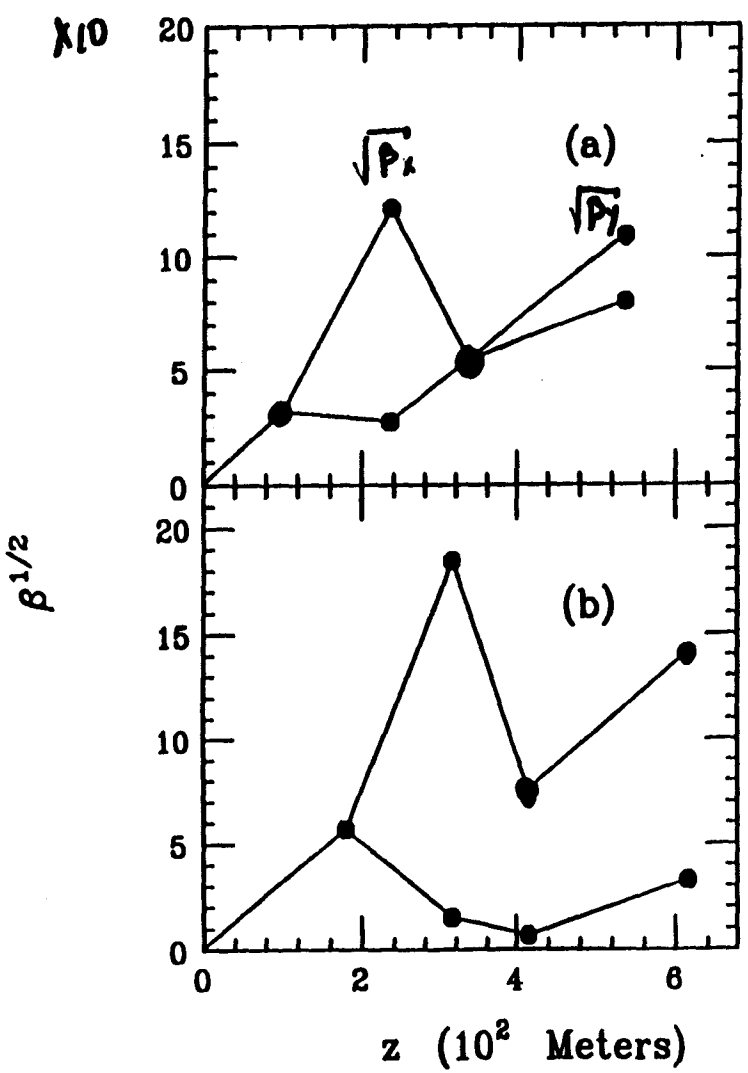

$\beta^* = 25\,M$

$G_1 = G_2 = 0.17\,T/cM$

$z_2 = 135\,M$

$z_1 = 100\,M$

$z_1 = 180\,M$

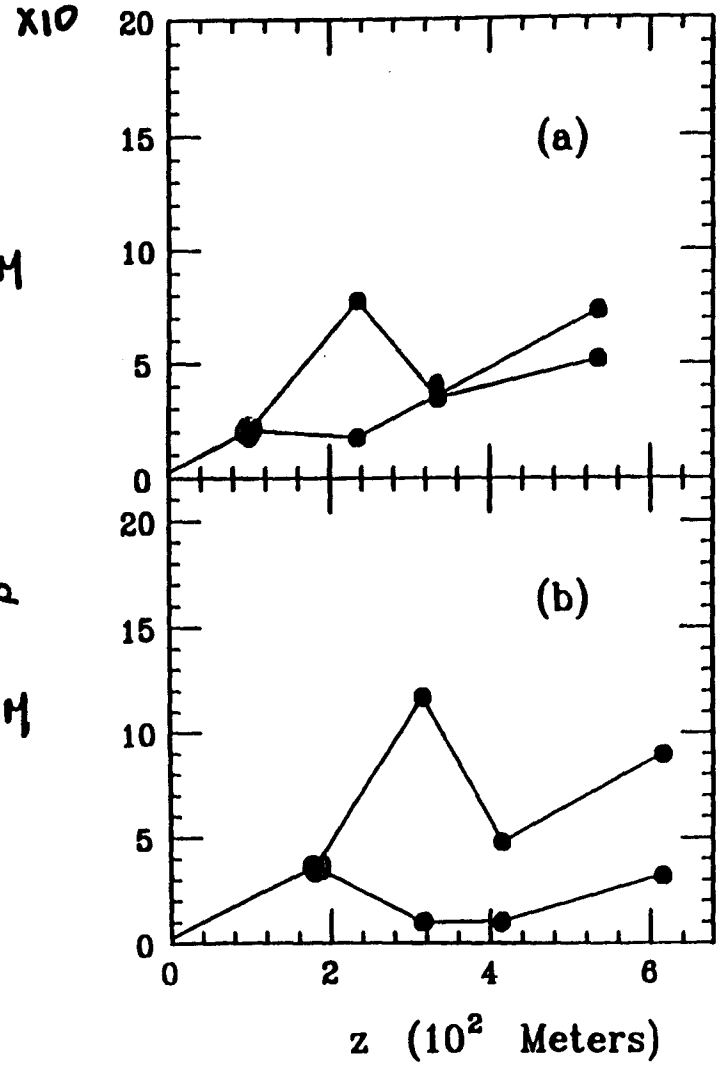

$\beta^* = 10\,M$

$G^F = G^D = 0.17\ T/CM$

$z_2 = 135\,M$

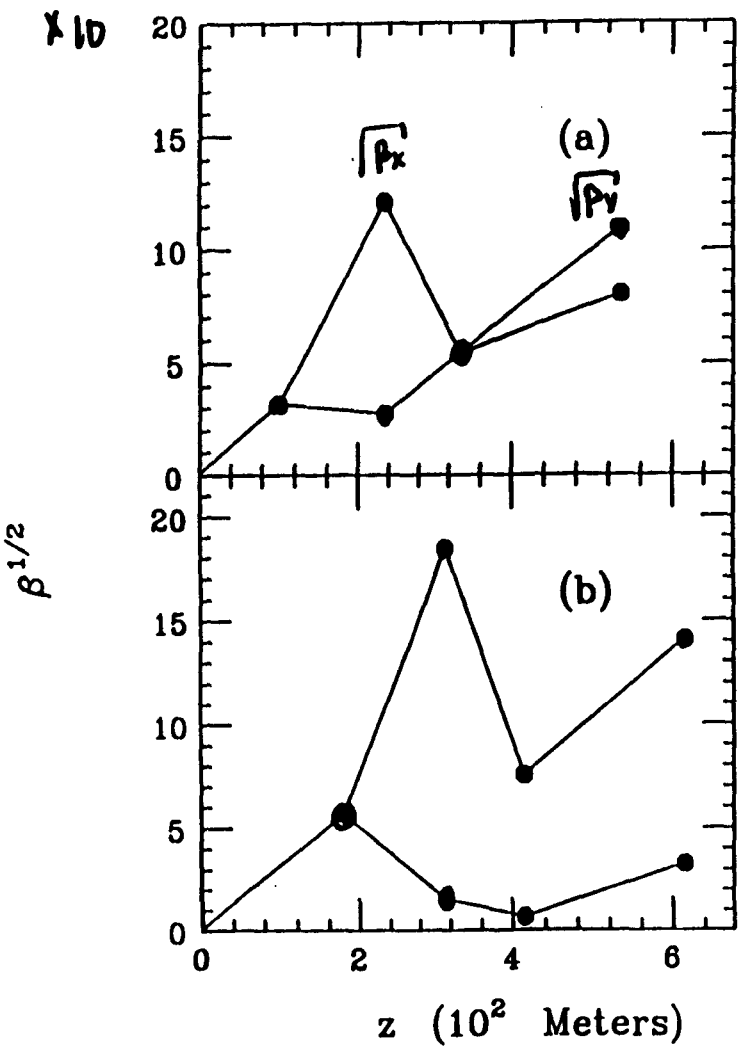

$\beta^* = 10\,M$

$G^F = 0.17\ T/CM,\ G^D = 0.15\ T/CM$

$z_2 = 135\,M$

$z_1 = 100\,M$

$z_2 = 100\,M$

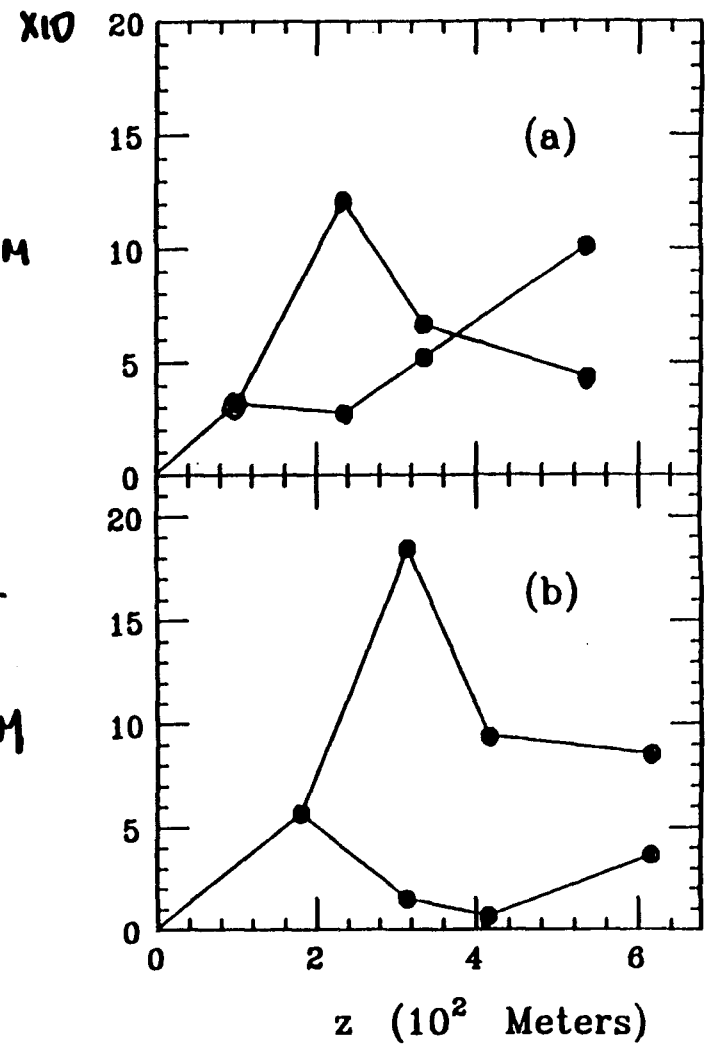

$\beta^* = 5\,M$

$G_1 = G_2 = 0.20\,T/CM$

$Z_2 = 135$

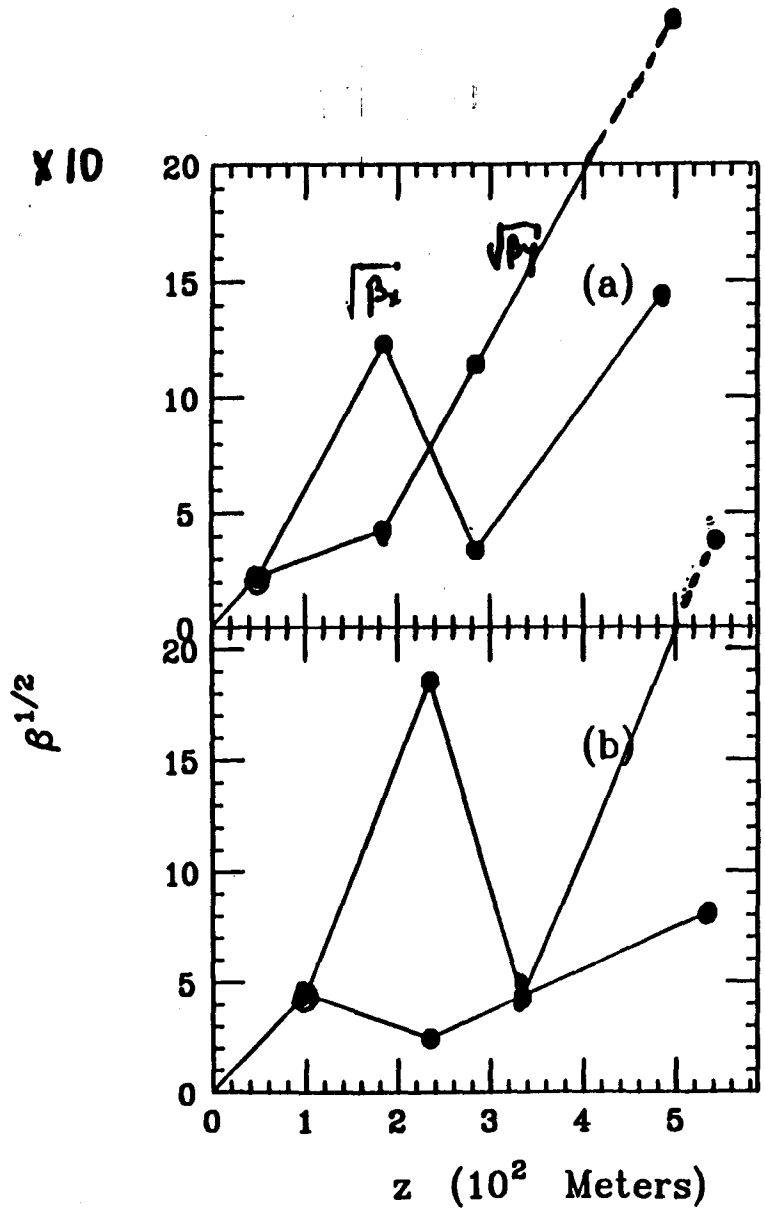

$Z_1 = 50\,M$

$Z_1 = 100\,M$

CONCLUSIONS AND QUESTIONS

* CAN A FAD "FIT" INTO THE SSC? — YES!!

  BUT: NEED TO KNOW DETECTOR LAYOUT!

  NEED TO KNOW PHYSICS SIGNATURES!

* PLACEMENT OF 1ST QUADS. $\lesssim$ 100 meters (I'd like to know if 50 meters is possible!)

* MAXIMUM LUMINOSITY:

  $\mathcal{L}_{max} \simeq 10^{32}$ NOT RULED OUT (DAVE JOHNSON)

. . . AND NOW THE QUESTIONS

* is η- MATCHING ONLY OPTION ?

* DO WE HAVE TO LIVE WITH :

a)

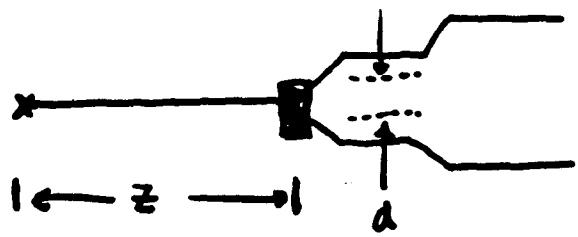

OR CAN WE GO WITH :

b)

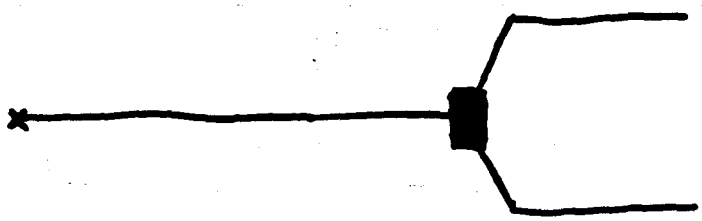

?

* IF a) : • WHAT DOES DIPOLE CRYOSTAT LOOK LIKE ?
  - DOES 1ST BEND HAVE TO BE OR 200 M ?
  - HOW BIG IS d ?

  IF b) • WHAT DOES DIPOLE CRYOSTAT LOOK LIKE ?

F.A.D. Meeting

13 March 1992

Backgrounds

Achim W. Weidemann

---

3 types:

- Machine & Beam-related
- From Interactions at I.P. & Detector-related
- (As above, from I.P.) to physics process studied not mentioned here

Machine & Beam related:

1) Beam gas
2) pp (other I.A. Points)
3) RF noise
4) tails from scrapers
5) power ripples / instabilities
6) low β quads

.... ~ 10^8 p/s Halo

1) Synchrotron Radiation

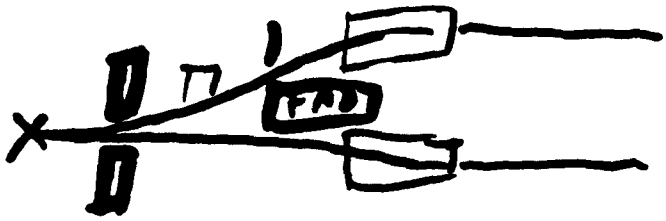

except here, low-energy photons → ignore

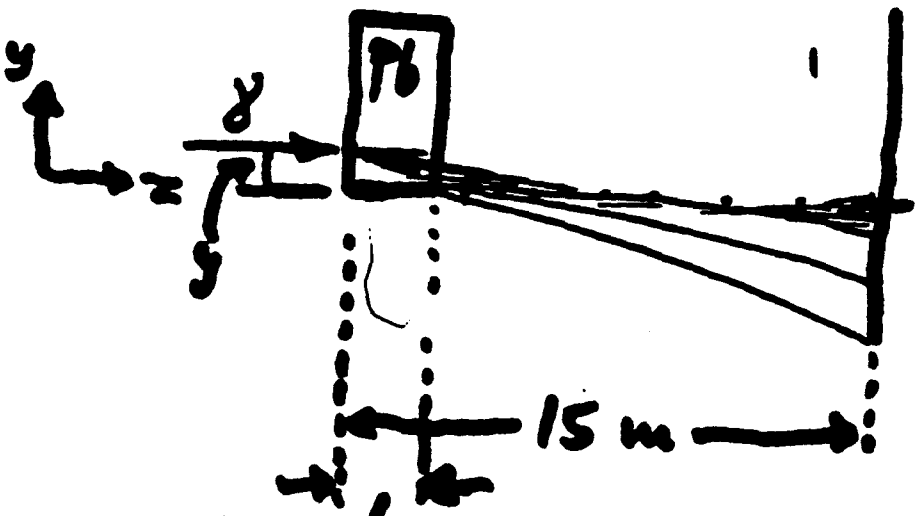

$30 X_0 = 16.852$ cm Pb

500 GeV γ (e^-) in, score Energy as fcn. of y (dist. from edge

EGS4 y =	.1 mm	.2 mm	.5 mm	1 mm	
Av. E/event	14. GeV	3.6	.36	.06	GeV
Av. E/part.	1.5 GeV	1.4	1.4	1.6	GeV
# part/evt	9.5	2.6	.26	.04	#
y ave (e^-)	−19.4 cm	−23.8	−33.	−36.	cm

(Added 3/14/92: Cutoff Energy for above = 1 GeV. much more energy particles seen for smaller cutoff.)

diffractive rate ~ 1/4 ~80% have right phase

..... 10 – 1% have $\theta < 9\mu r$

⇝ background of $10^5 - 10^6$ /sec.

(Possible to decrease by scrapers)

We need to tell acc. physicists tolerable bg. level from this source.

2) pp elastic scattering · beam-beam interaction increases emittance ...

Beam gas losses

10^{14} p /beam with an expected (beam gas) lifetime of $< 10^6$ sec

$\rightsquigarrow$ $\sim 10^8$ (-10^9) interactions/sec in arcs. ($10^8 \cdot 20$ TeV/sec $= 320$ W)

About same order of magnitude as # interactions/sec $\sim 10^8$ in $\mathcal{L} = 10^{33}$ cm^{-2}s interaction region

Original argument: only ± 1 km from FAD relevant $\rightsquigarrow$ $\frac{2}{87}$ th of that rate $\rightsquigarrow$ negligible

Rae Stiening pointed out importance of 1-turn halo:

pp elastic in arc:

If $\theta_{CM} = .1$ rad $\frac{\delta E}{E} \approx .005$

$\rightsquigarrow$ $\theta_{LAB} \approx 490\,\mu r$ .... will disappear from beam

diffractive .... $p_\perp \approx 200$ MeV/c

$\theta \approx 9\,\mu r$

$$X = \theta \cdot \sqrt{305 \cdot \beta_{max}^{in\ quad}} = \underline{\underline{1.5\ cm}}$$

$\beta_{max} \sim 10^4$ m

ID=XYE

ALL

#CALLS= 25 18 0 / 98 2982 0 / 17 14 0 (-UX-/UY IN

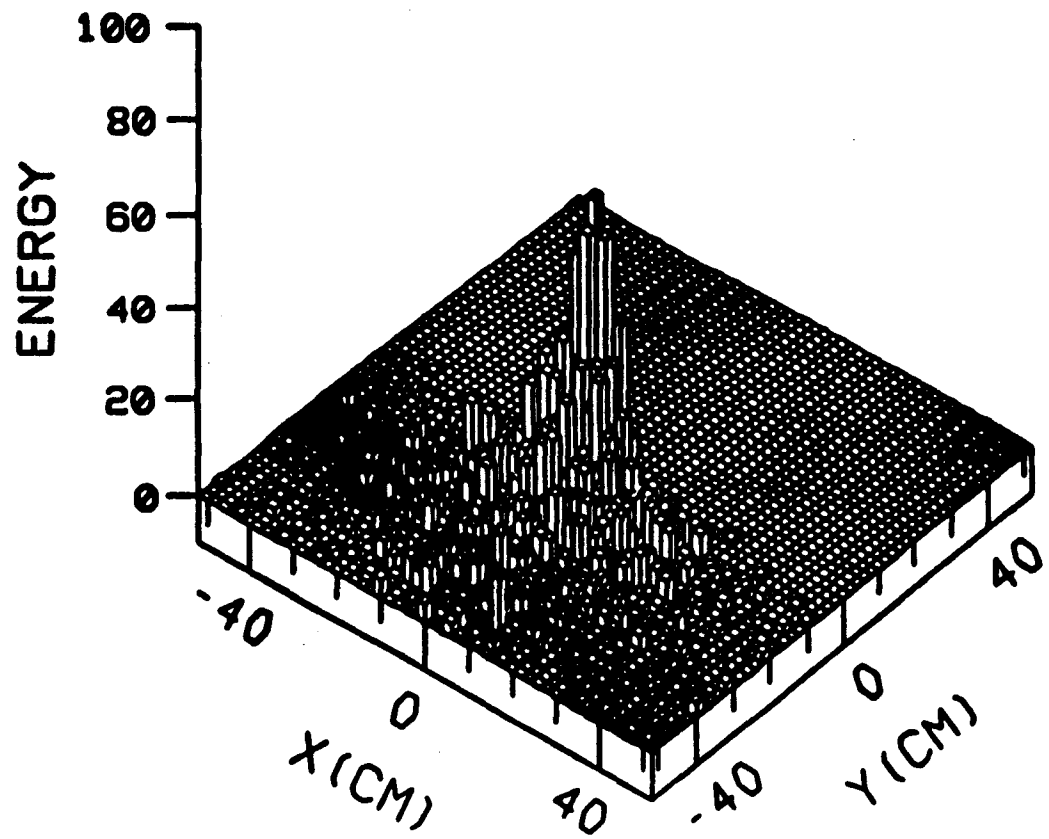

0.1 mm

HANDYPAK YOF01M01 8MAR92

ALL

ID=XYE

#CALLS= 16 12 0 / 64 645 0 / 20 13 0 (-UX-/UY IN (

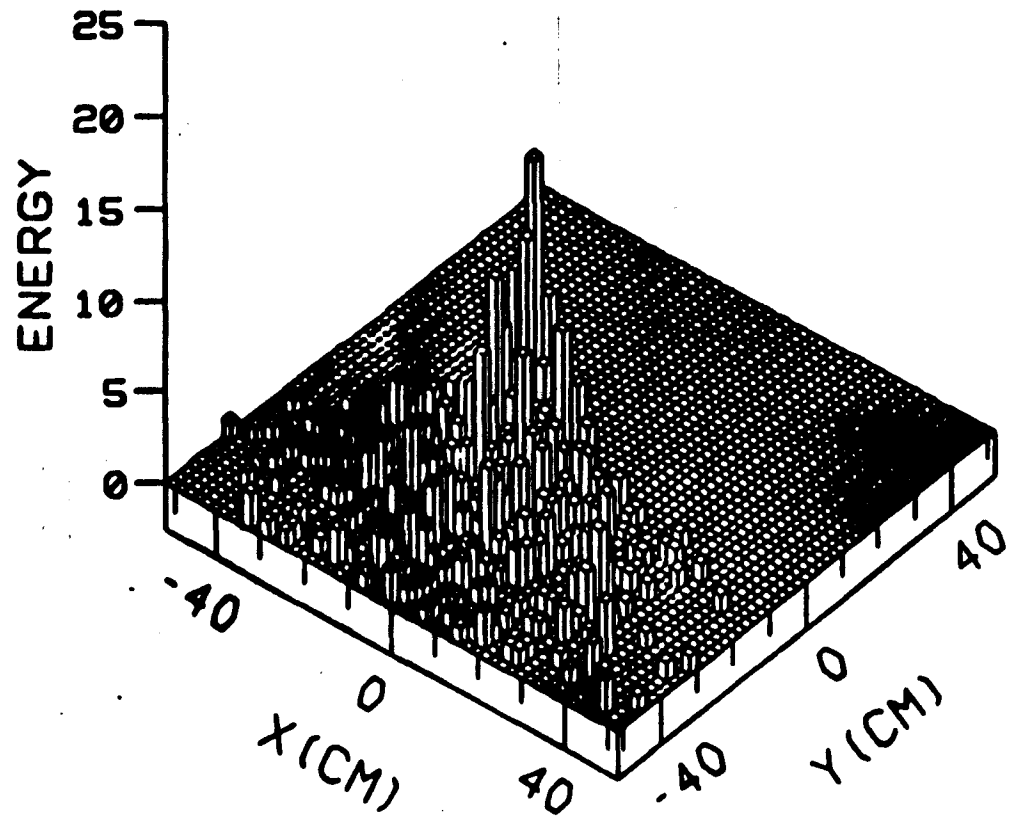

.2 mm

ID=XYE ALL

#CALLS= 5 2 0 / 22 45 0 / 7 0 0 (-UX-/UY IN OY/-OX

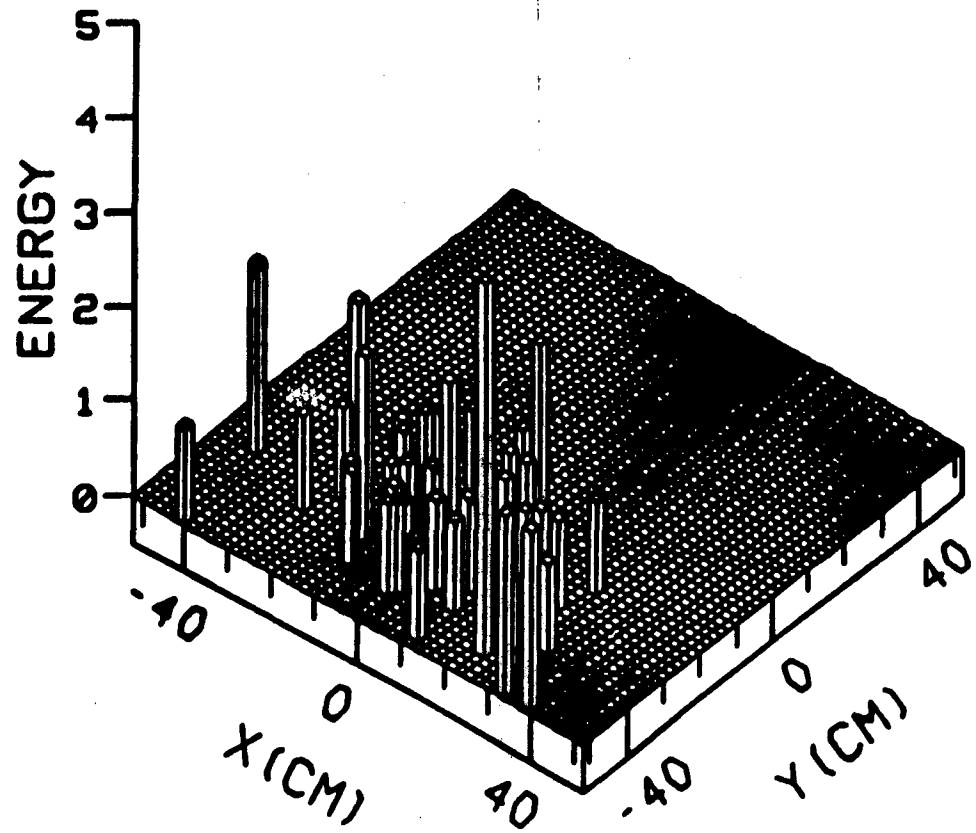

.5mm

ALL

ID=XYE

#CALLS= 6 0 0 / 12 14 0 / 5 0 0 (-UX-/UY IN OY/-OX

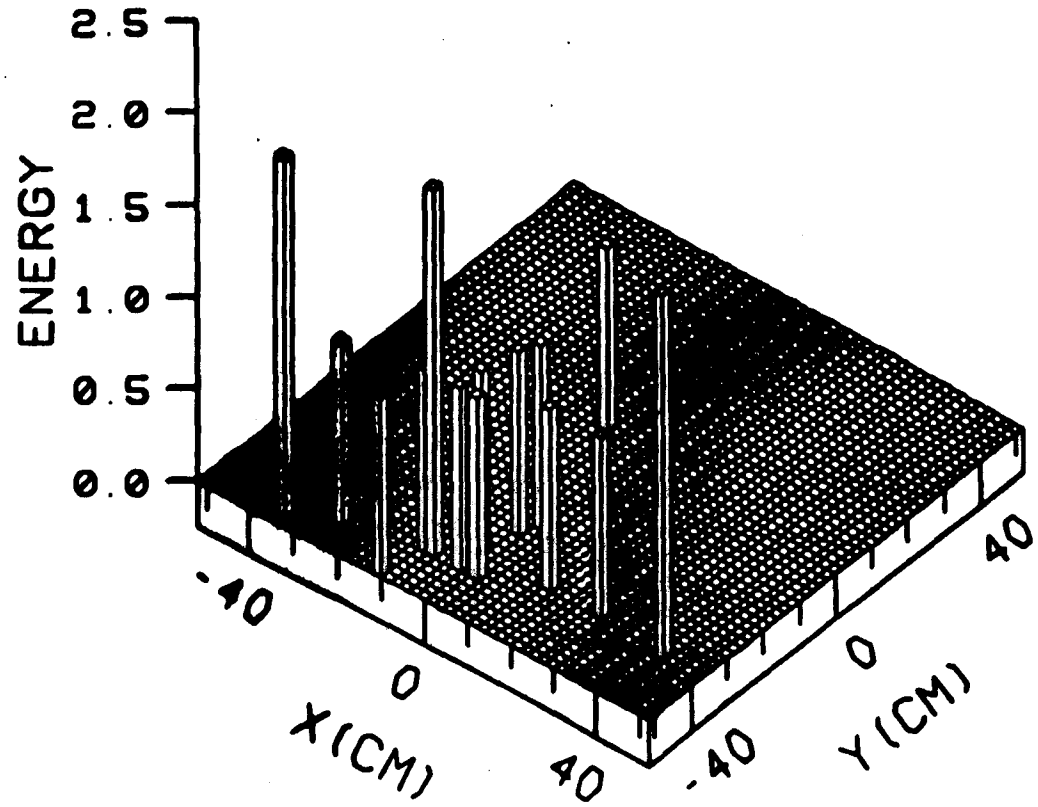

1mm

Should do such study
with protons + appropriate
hadronic transport code.

Laurie Waters of Los Alamos
volunteered to do so with
LAHET (Local version of HETC)

Dr. Mokhov suggested
MARS12 (& STRUCT & ELSIM
& DTUJET ...)

Min bias Event Generators

- Min Bias Rockefeller MC (Gino)
  (1000 $p\bar{p}$ event file on SLACVM / SLACUX)
  $\sqrt{s} = 40$ TeV

- BANG 92A (R. Ellsworth)

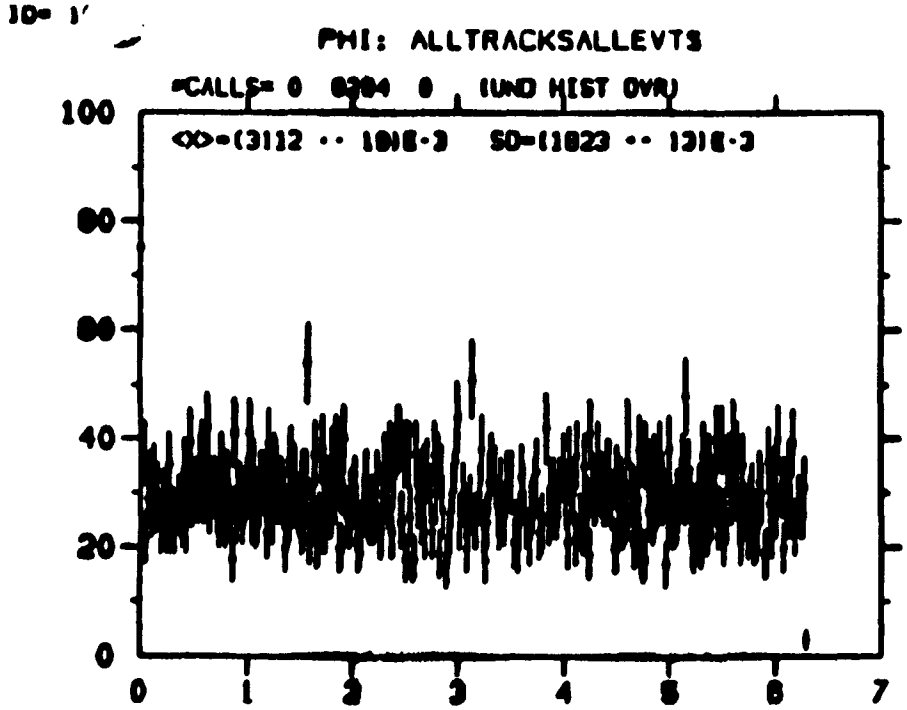
ID= 1
PHI: ALLTRACKSALLEVTS
#CALLS= 0 0204 0 (UND HIST OVR)
<X>=(3112 -- 1018-3 SD=(1823 -- 1318-3
100
80
60
40
20
0
0 1 2 3 4 5 6 7

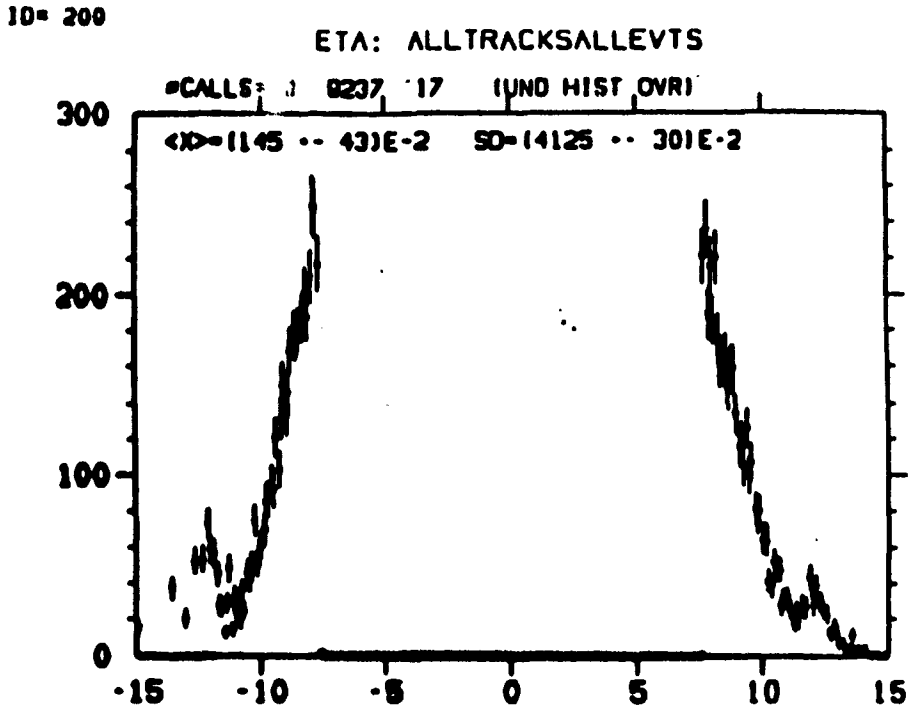
ID= 200
ETA: ALLTRACKSALLEVTS
#CALLS= 0237 17 (UND HIST OVR)
<X>=(145 -- 431E-2 SD=(4125 -- 301E-2
300
200
100
0
-15 -10 -5 0 5 10 15

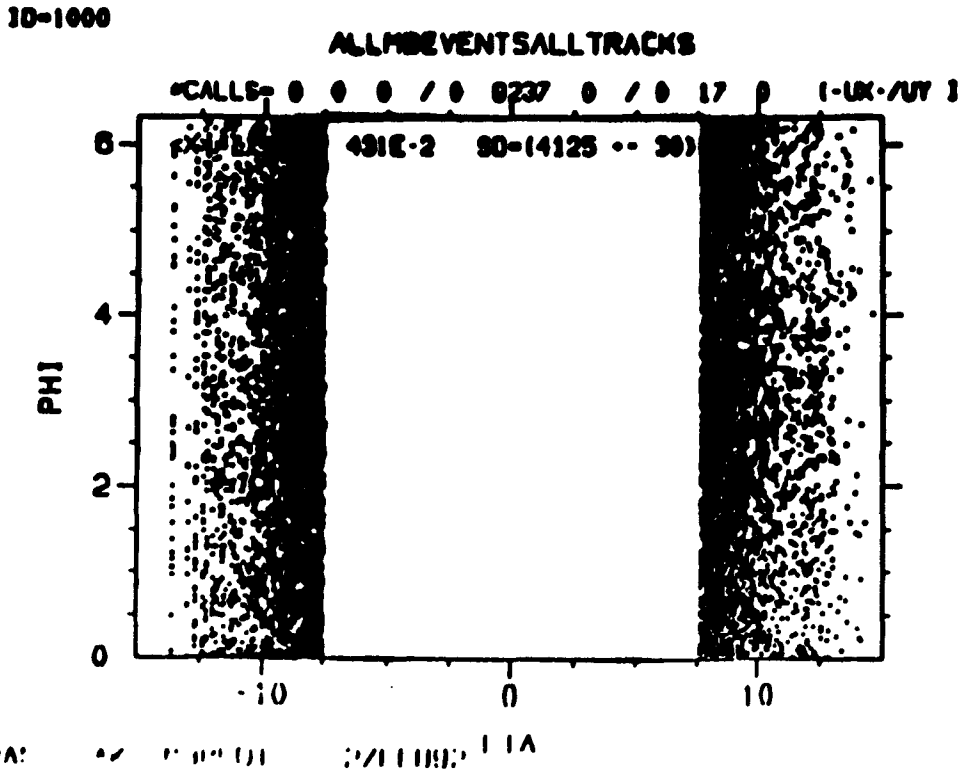
ID=1000
ALLMBEVENTSALLTRACKS
#CALLS= 0 0 0 / 0 0237 0 / 0 17 0 (-UX-/UY)
431E-2 SD=(4125 -- 30)
PHI
6
4
2
0
-10 0 10
ETA

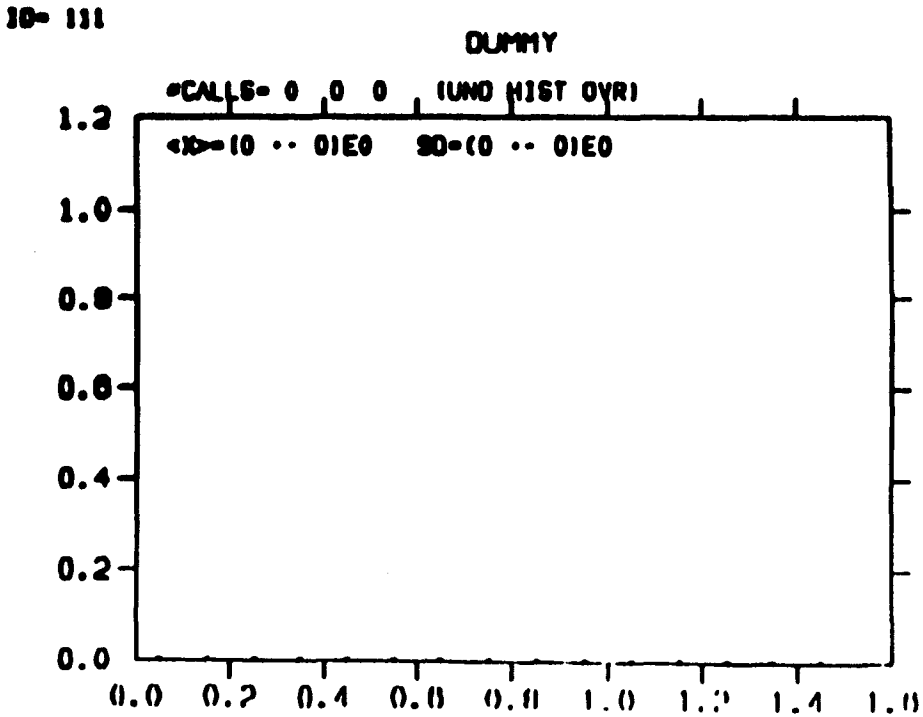
ID= 111
DUMMY
#CALLS= 0 0 0 (UND HIST OVR)
<X>=(0 -- 01E0 SD=(0 -- 01E0
1.2
1.0
0.8
0.6
0.4
0.2
0.0
0.0 0.2 0.4 0.6 0.8 1.0 1.2 1.4 1.6

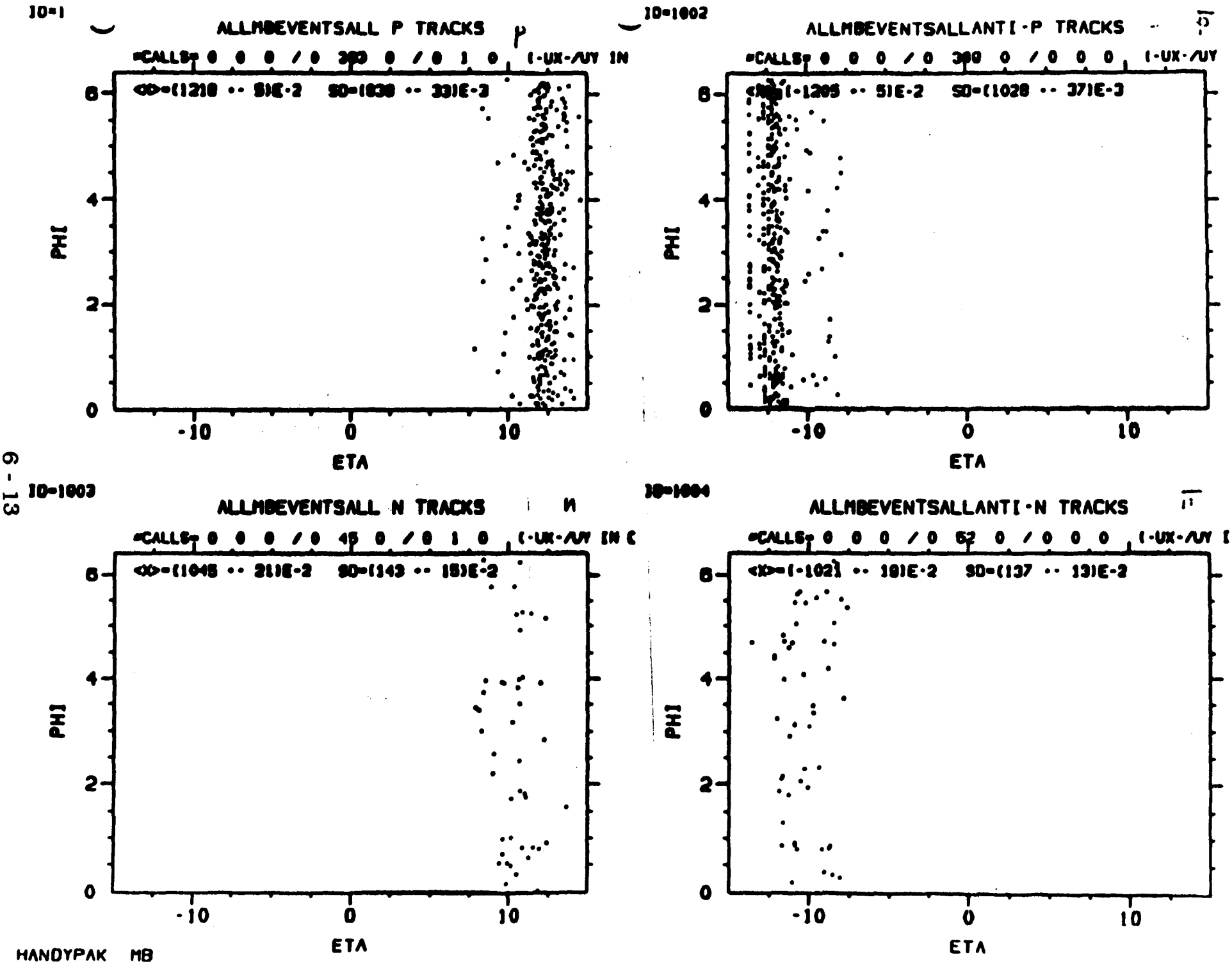
ID=1
ALLMBEVENTSALL P TRACKS
ID=1002
ALLMBEVENTSALLANTI-P TRACKS
ID=1003
ALLMBEVENTSALL N TRACKS
ID=1004
ALLMBEVENTSALLANTI-N TRACKS
PHI
ETA
HANDYPAK MB

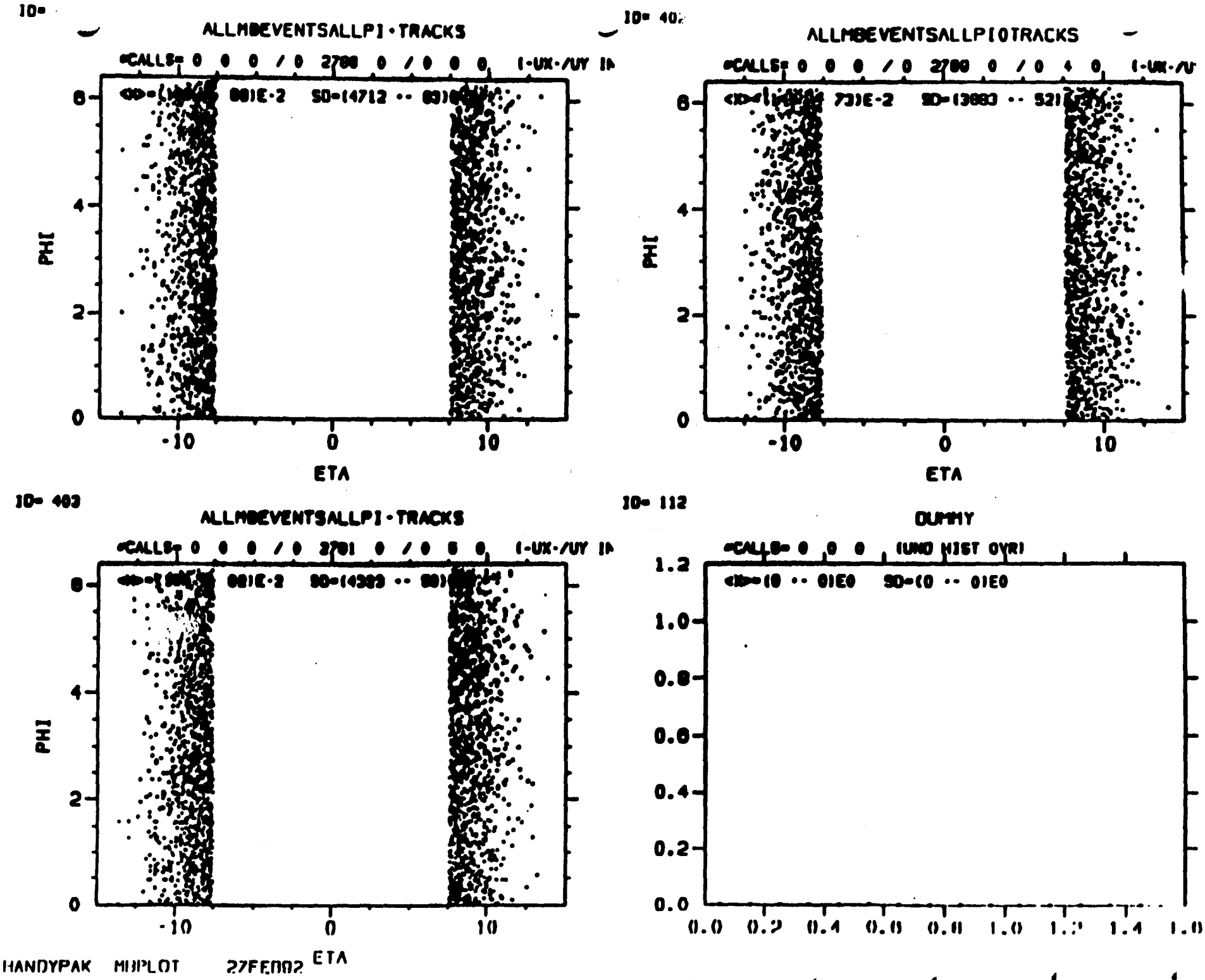
ID= 402
ALLMBEVENTSALLPI·TRACKS
ID= 402
ALLMBEVENTSALLPI0TRACKS
ID= 403
ALLMBEVENTSALLPI·TRACKS
ID= 112
DUMMY
PHI
ETA
HANDYPAK MBPLOT 27FEB82

Inter–gamma dist at Wall

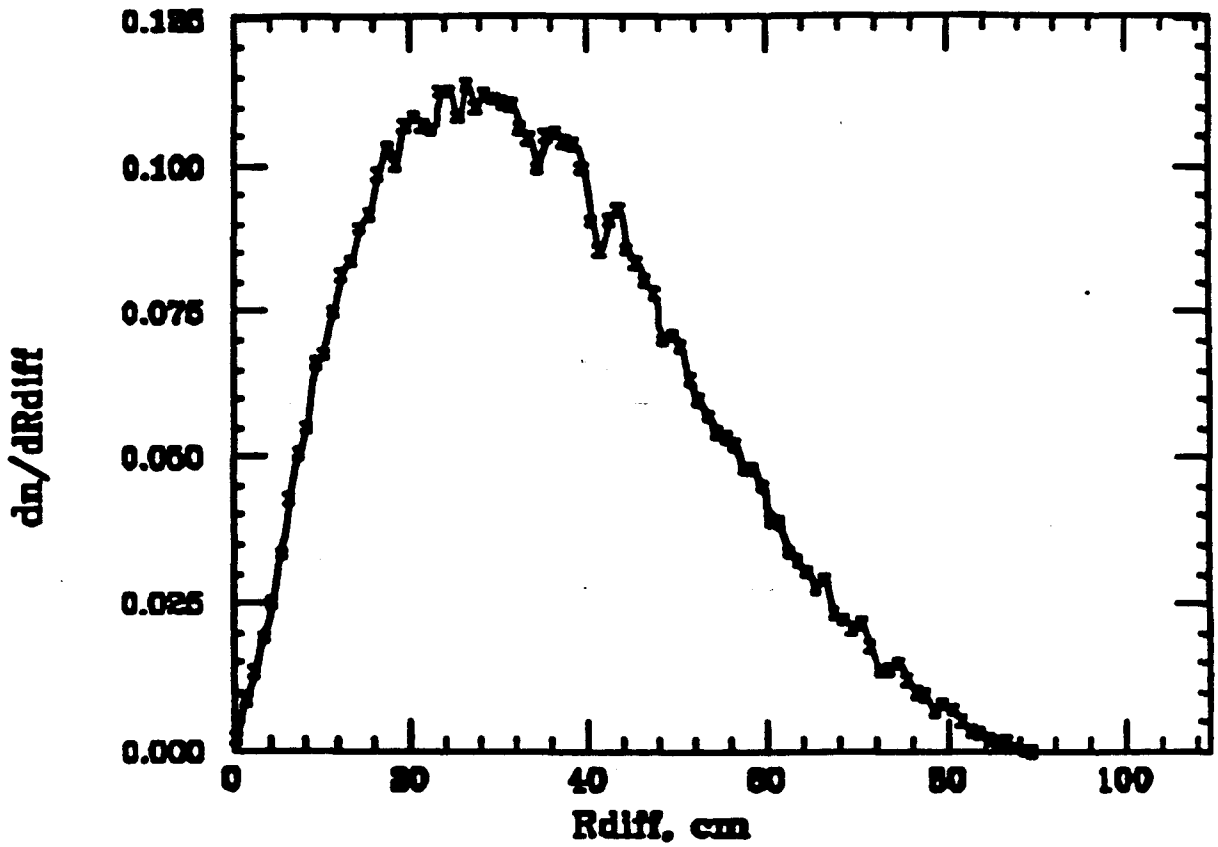

2.76 γs hit /event
1.73 TeV ave Eγ

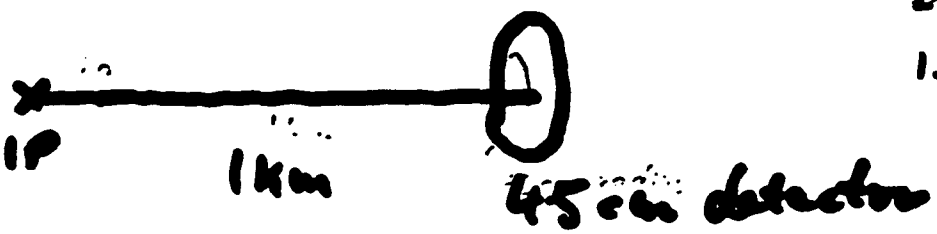

Fig 1 x*dn/dx pizeros

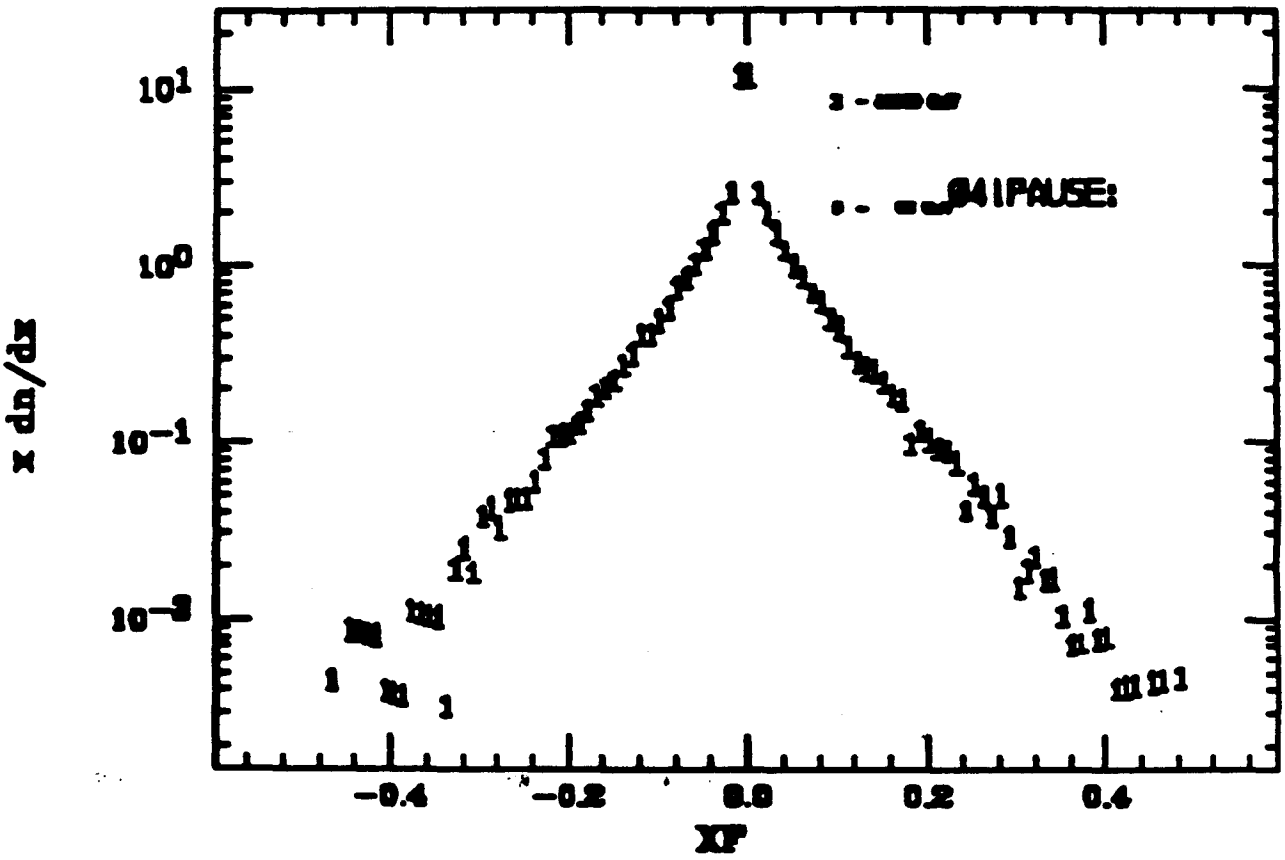

FIG 2 XF gammas

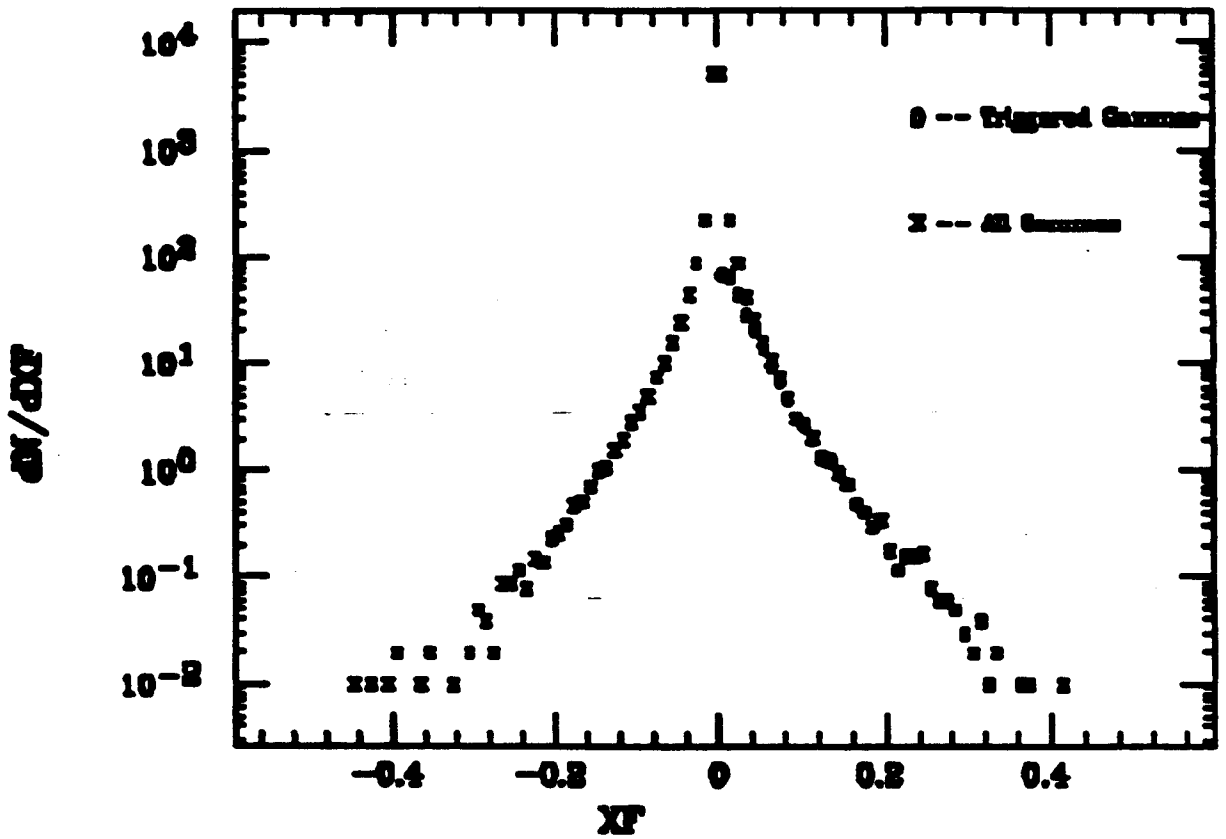

x*dn/dx ALL, TRIG GAMMAS ETA>9.5

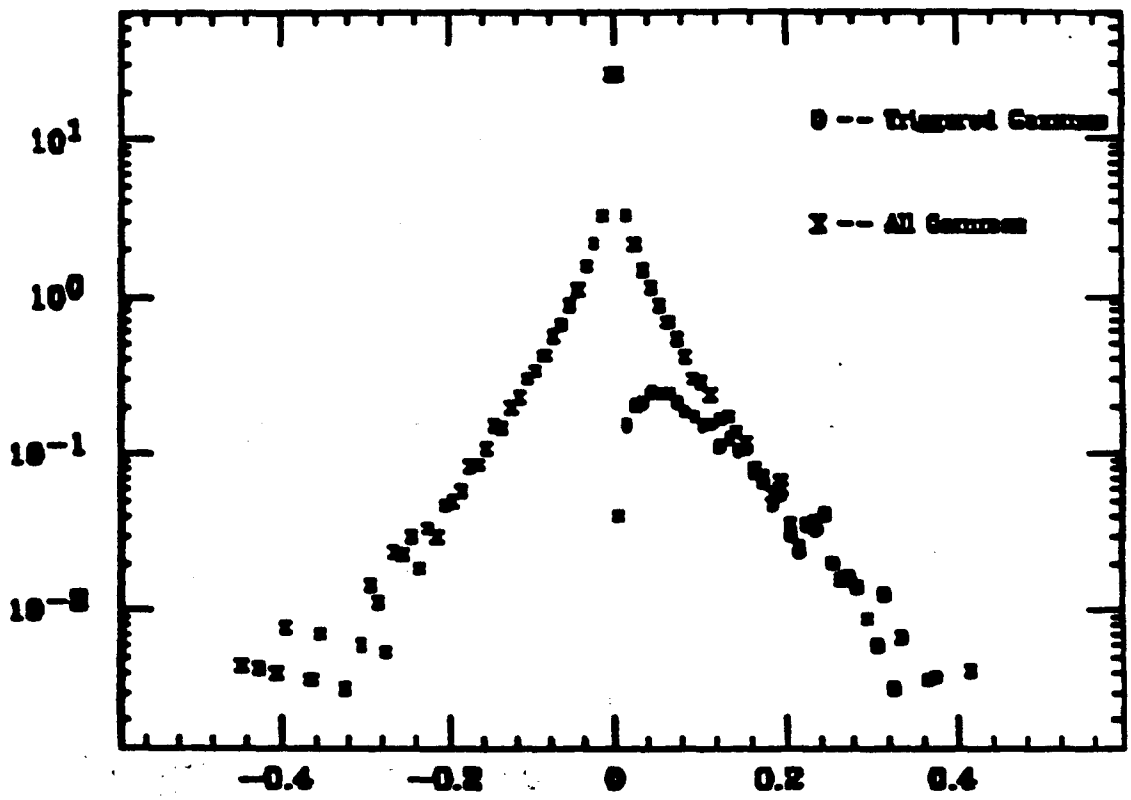

WAYNE VERNON

3/13/92
W. Vernon

Generic Problems for the FAD Beam Pipe

- What is the vacuum in the pipe?
  ⇒ pick the beam-gas interaction rate which is tolerable

- what is the typical pipe diameter:
  ⇒ must meet detector design needs <u>and</u> vacuum conductance requirements.
  [If pipe becomes too large, wall thickness increases]

- How to pick pipe shape (r vs z)?
  ⇒ must control "particle crossing angle"

- what is the state of simulations?
  1) 20 TeV P on gas nuclei ...
     how many secondaries get to detector?
  2) what is the "baseline" 20×20 TeV noise?

The Vacuum —

Start with a "default" pressure

$P_0 = 1n(\text{mbar}) = 1\ \text{pbar} = 10^{-12}\ \text{Atmos.}$

$(\doteq 0.7\ n\ \text{torr})$

Then, $P_0 \Rightarrow \simeq 5 \times 10^7\ N_2$ nuclei/cm^3;

Also pick $\sigma_{interaction} = 0.4$ barn/Nuc,

and assume that there are 1.3×10^{14} protons in the ring $\Rightarrow 4.44 \times 10^{17}$ P/sec

gives ~ 900 int/sec/m

(SSCL 306, page 4, has 1000)

Bottom line: 0.9 MHz interaction rate from each km of pipe — (how much gets in to detectors?)

Note: Collision rate from $\mathcal{L} = 10^{32}$ IR $\Rightarrow$ 5.5 MHz ··· but, much higher multiplicity (and larger angles?)

Pipe Diameter:

See N. Mistri AIP 153 Vol 2

Vacuum "Conductance", C

$\Rightarrow \Delta P = \frac{\Delta q}{C}$ for gas load, Δq

$C = \frac{4\pi}{3} R^3 \frac{\bar{v}^2}{l}$ or $C_0 \doteq 1000$ l/sec for $R = 10$cm, $l = 1$m

for a cylinder

A periodic pumping system:

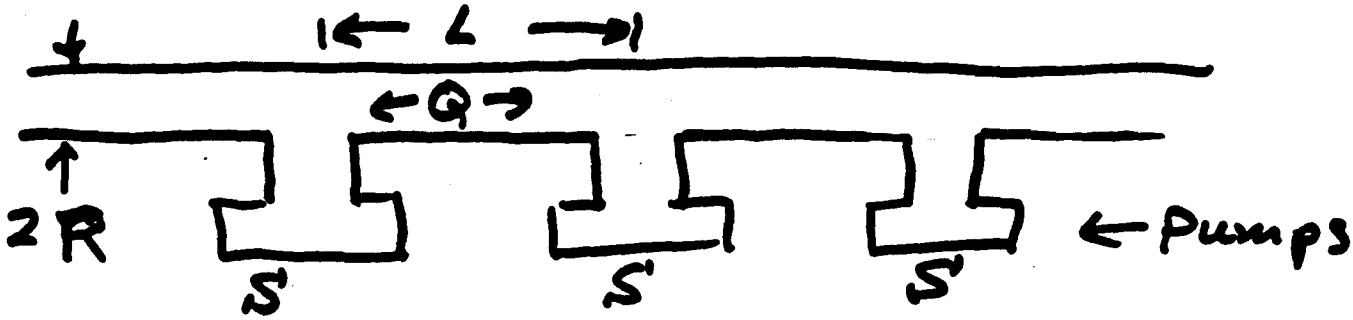

yields a mean pressure

$\langle P \rangle = Q\left(1/S + \frac{1}{12C}\right)$ for $C = \frac{C_0}{l}$

$L = 10$ m $\qquad Q = qL$

$S = 500$ l/sec $\Rightarrow \langle P \rangle = 10^{-7}\left(\frac{1}{500} + \frac{1}{300}\right)$

$R = 5$ cm

$= .5$ pbar ~ ok

when gas load is 3×10^{-12} mbar·l/sec/cm

$\Rightarrow q = 10^{-8}$ mbar·l/sec/m

10cm dia ~ ok

Pipe Shape — Adjust for reasonable particle angle thru wall

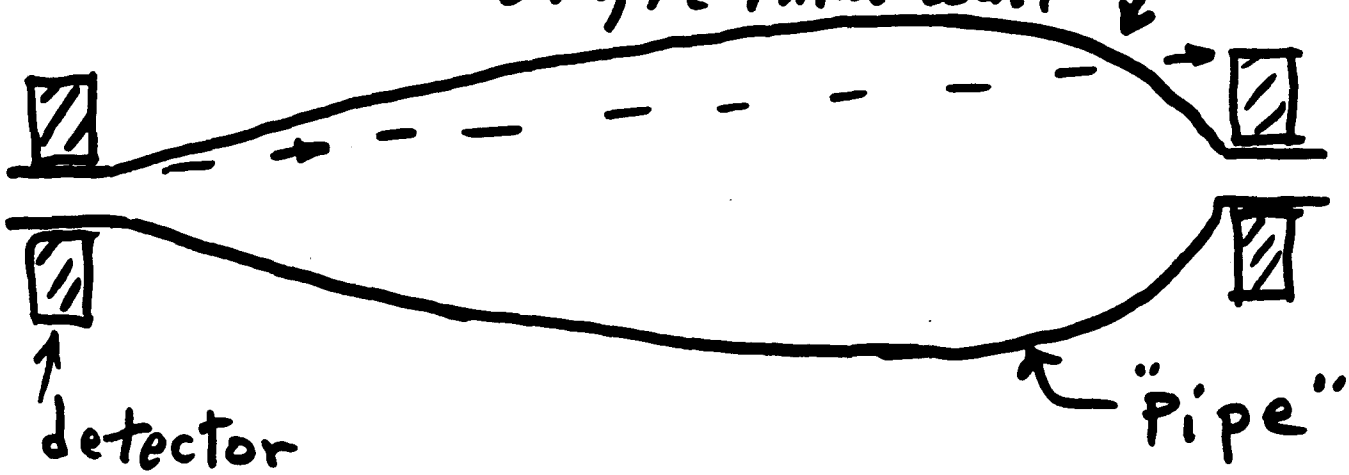

As radius grows, mechanical stability problems will mean that wall must become thicker.

However, density can be reduced, both by use of composites and low density ceramics and by "zig-zag": (or bellows type)

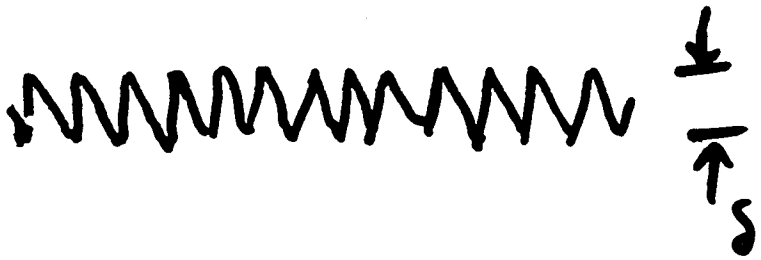

δ is then the key dimension for wall stability —

Make a "thick wall"
for the pipe
but keep mass low –
Important to keep
secondary interaction
from making more noise

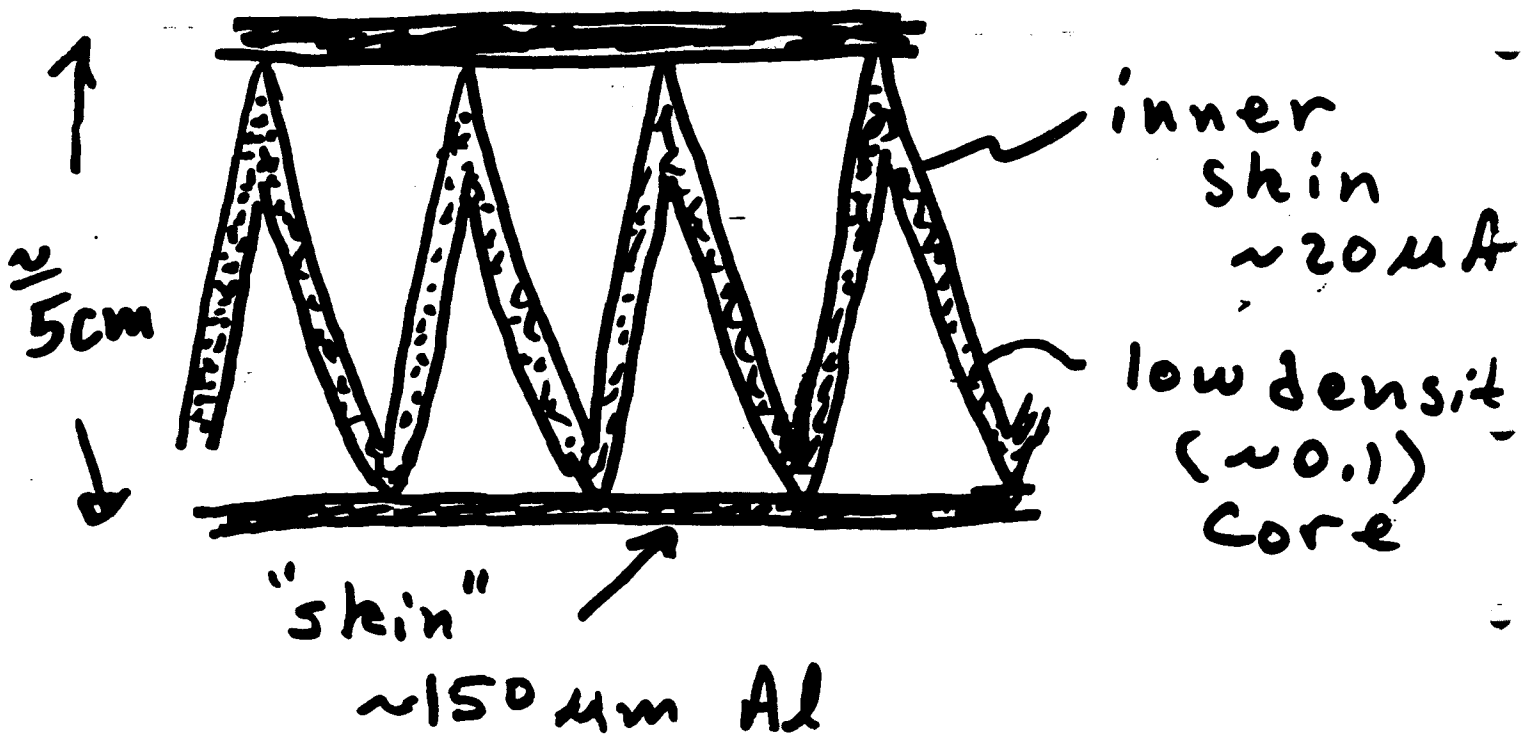

Total ⊥ thickness ~ 400 μm
Al
eq.

Hard diffraction processes at SSC

L. Frankfurt and M. Strikman

Content

1. Why diffraction processes are interesting
2. Lessons from fixed target energy range
3. New type of hard processes - single hard diffraction process.
4. Jet production in hard diffraction.
5. Double hard diffraction.
6. Correlation experiments.
7. Conclusions.

2.

Investigation of hard processes found that QCD is the underlining theory of strong interactions, confirmed asymptotic freedom in QCD:

$$\alpha_s(K^2) = \frac{\alpha_0}{1 + \alpha_0 b \ln\left(\frac{K^2}{\Lambda^2}\right)} \Rightarrow \frac{1}{b \ln \frac{K^2}{\Lambda^2}} \Rightarrow 0$$

Next step is to investigate processes in the regime when $\alpha_s \ll 1$ but $z \sim \frac{1}{2m_N x}$ are large

The interaction is not small when longitudenal distances are large $\sim 1/2m_N$

At SSC two new phenomena:

1. Increase of cross sections of hard processes with energy.
2. Specific role of color screening phenomenon.

-5.

Few words on pQCD at high energies

1. Spin of gluon is 1. So cross sections of processes mediated by gluon exchange does not decrease with energy:

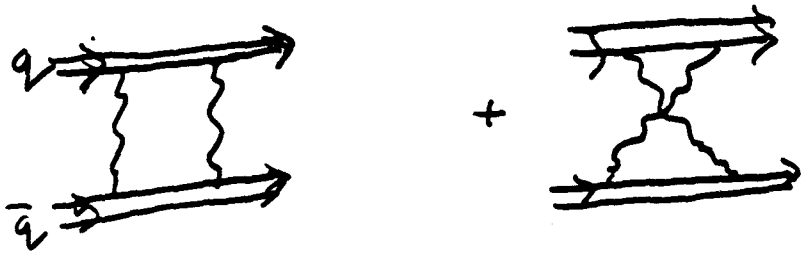

$$\sigma \simeq \frac{\alpha_s^2}{s_0} \qquad \text{for } s = (p_q + p_{\bar{q}})^2 \to \infty$$

2. Cross sections fastly increases with energy.

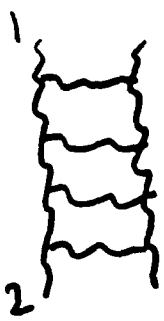

$$s = (p_1 + p_2)^2 \to \infty$$

$$\sigma \sim \frac{\alpha_s^2}{s_0} \left(\frac{s}{s_0}\right)^{\omega_0} = \frac{\alpha_s^2}{s_0} e^{\omega_0 \Delta y}$$

$$\omega_0 = \frac{12\alpha_s}{\pi} \ln 2$$ (Lipatov

$$\Delta y = y_1 - y_2$$

This formulae has been obtained in the approximation:

$$\frac{\alpha_s}{\pi} \ln \frac{s}{s_0} \sim 1 \qquad \text{but } \alpha_s \ll 1$$

Practically it is sufficient to have 4-5 rung to obtain this fast increase with energy. Minimal condition of applicability of formulae:

$$\Delta y > (4 \div 5) \frac{1}{\omega_0} \simeq 8-10$$

Thus this physics may reveal itself at SSC.

1 Cross sections of hard processes may achieve value considerably larger than that given by Born diagram

$$\sigma \sim \alpha_s^2 \left(\frac{s}{s_0}\right)^{\omega_0} \left\{1 - \alpha_s^2 \left(\frac{s}{s_0}\right)^{\omega_0} \dots \right\}$$

It is not understood now how this fast increase of σ will be stopped. May be useful for the investigation of „B" quark physics...

2. In difference from parton model – soft physics long range correlations in the rapidity space does not decrease with Δy:

$$\frac{\dfrac{d\sigma^{a+b\to 1+2+X}}{dy_1\,dy_2}}{\dfrac{d\sigma^{a+b\to 1+X}}{dy_1}\;\dfrac{d\sigma^{a+b\to 2+X}}{dy_2}}$$

increases with Δy as $e^{2\Delta y\,\omega_0}$

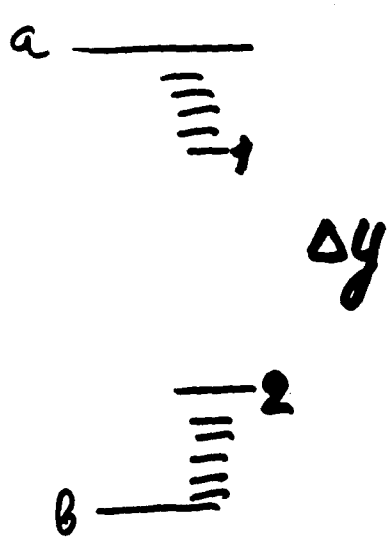

To observe and exercise this physics it is necessary to find hard processes where bQCD is applicable. A. Mueller describe at previous FAD meeting several options.

I will consider here physics of hard diffractive processes

$p + p \to X + p$

$\Delta y \gg 1$

$|t| > 1$ GeV

$\cdot$ (4 GeV^2

$p + p \to X_1 + X_2$

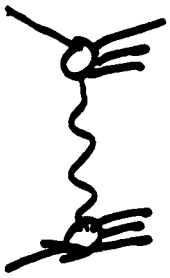

$\Delta y \gg 1$

$|t| > 1$ GeV

By product this process can help to unravel role of color screening phenomenon which is of great interest for me

Six reasons for the hard diffraction:

1. SSC energy range gives practical possibility to investigate hard processes at larger Δy, investigate rare gluons in a nucleon. Limit from step cruises, from enhancement of gluon distribution in nuclei.
2. Cross section of hard processes fastly increases with increase of Δy.
3. Hard diffraction probes QCD in a new way. Unexplored field where pQCD predicts specific phenomena. In difference from structure function limit, masked by evolution of distributions with Q^2.
4. Gives practical possibility to measure gluon distribution in a proton at different x_{Bj}.
5. Effective probe of different size color configurations in a proton.
6. May be effectively explored for „B" physics, for the search of new particles

To explain specific of hard physics I firstly remind you theory of soft diffraction

Few words on soft diffraction processes

sessions: from 1 TeV² energy range.

1. The parton model (Feynman)

i). Short range correlations in rapidity space

$$E_a E_b \frac{d^6\sigma^{N+N\to a+b+X}}{d^3p_a\, d^3p_b}\,\sigma_{NN} \Big/ E_a \frac{d^3\sigma^{N+N\to a+X}}{d^3p_a}\; E_b \frac{d^3\sigma^{N+N}}{d^3p_b}$$

$$= 1 + f$$

$$f \ll 1 \qquad \text{for } |y_a - y_b| \gtrsim 2$$

ii). Lead to „pomeron" - not necessarily a regge trajectory

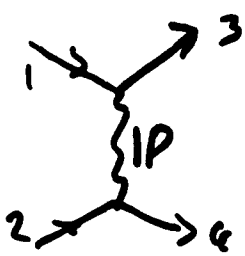

$$\frac{d\sigma^{el}}{dt} = G^2_{NN\mathbb{P}}(t)\; e^{2\{\alpha(t)-1\}\ln\frac{s}{s_0}} \cdot \frac{g_{pp}}{s^2}$$

$$t = (p_1 - p_3)^2, \quad s = (p_1 + p_2)^2$$

Experiment and constituent quark models:

$$G_{NN\mathbb{P}}(t) \simeq G_{Ep}(t)$$

$$\alpha(0) \simeq 1 + \varepsilon \qquad \varepsilon \simeq 0.08\ (?)$$

3) iii) Single diffraction.

$p+p \to p+X$

Kinematics

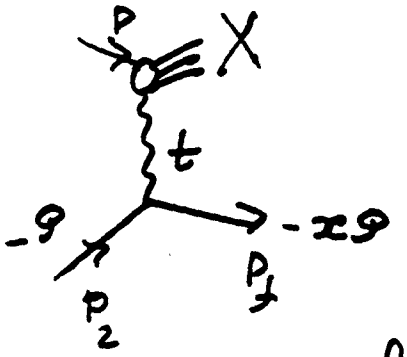

$$\frac{M_X^2}{s} = 1 - x \ll 1$$

$$\Delta y = y_X - y_p = \ln \frac{s}{M_X \sqrt{m^2 + p_T^2}} >$$

Sum of inelastic states can be descr as triple reggeon limit: (Gribov, Mueller, Kancheli)

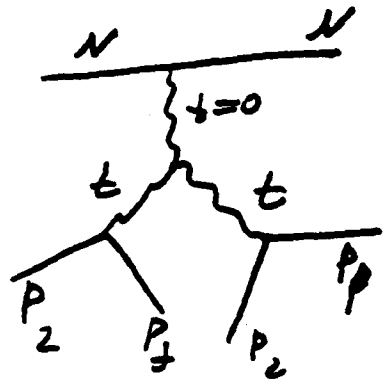

$$\frac{d\sigma^{p+p\to X+p}}{dt\, dM_X^2} = \frac{g^2 \beta_{NN}}{8\pi} G_{3P}(t) \left(\frac{s}{M_X^2}\right)^{2\alpha(t)} \frac{\left(\frac{M_X^2}{s_0}\right)^{\alpha_0}}{s^2} G^2_{IPNN}(t)$$

$G_{3P}(t)$ is rather slow function of t as compared to the elastic form factor of a proton since there is no kinematical restriction on particles production.

Specific of soft diffraction – dependence of M_X^2 distribution on t. Disappears for hard diffrac at large t.

Double soft diffraction

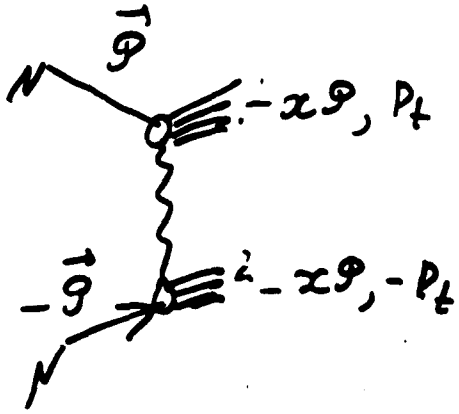

$$\Delta y = y_1 - y_2 = \ln \frac{s\, x^2}{M_1 M_2}$$

$$\frac{d\sigma^{p+p \to X_1 + X_2}}{dt\, dM_1^2\, dM_2^2} = \frac{g^2_{qNN}}{8\pi}\, C^2_{3IP}(t) \left(\frac{M_1^2}{s_0}\right)^{\alpha(0)} \left(\frac{M_2^2}{s_0}\right)^{\alpha}$$

$$\left(\frac{s \cdot s_0}{M_1^2 M_2^2}\right)^{2\alpha(t)} \quad \frac{1}{s^2 s_0}$$

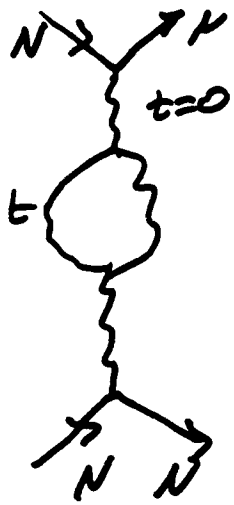

<u>Conclusion</u> double diffraction corresponds to rather slow dependence on t - concentrated at small impact parameters.

for the size of color screening, transverse size of a hadron.

A hadron has space structure

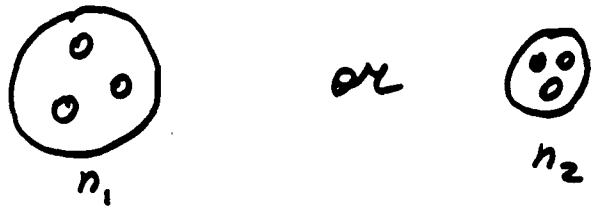

Energetic projectile spend a time

$$t \simeq \frac{1}{E_n - E_p} \simeq \frac{2\mathcal{P}}{M_n^2 - m_N^2} \gg \tau_{col} \sim \frac{1}{\mu}$$

Calculation should be done at fixed transverse size of configuration $|n\rangle$ and averaging with the wave function of a hadron.

$$\langle \sigma \rangle = \int \psi^2(r_t^2)\, dr_t^2\, \sigma(r_t^2) \equiv \int \sigma\, P(\sigma)\, d\sigma$$

$$\sigma(r_t^2) \simeq \frac{r_t^2}{\langle r_0^2 \rangle}\, \sigma_0$$

There are plenty evidences for

$\sigma(r_t^2) \simeq r_t^2/\langle r_{NN}^2\rangle \, \sigma_{NN}$

1. In pQCD - screening of color. F. Low
2. In quark models - result of compositness of hadrons. Experimentally F.S.

$\sigma_{pp}/\langle r_{pp}^2\rangle \simeq \sigma_{\pi p}/\langle r_\pi^2\rangle \simeq \sigma_{Kp}/\langle r_K^2\rangle \ldots$

3. Equivalent to Bjorken scaling in $\sigma_{\gamma^* N}$ at small x_{Bj}.

Inelastic diffraction exists just because σ depends on $r_\perp^2$:

$$\omega = \frac{d\sigma^{pp\to X+p}}{dt} \Big/ \frac{d\sigma^{el}}{dt}\Big|_{t=0} = \frac{\langle\sigma^2\rangle}{\langle\sigma\rangle^2} - 1 \quad \text{(Pumplin, Miettinen)}$$

$$\langle\sigma^2\rangle = \int P(\sigma)\sigma^2 \, d\sigma$$

The same value of ω follows from analysis of inelastic shadowing correction to σ_{pD}^{tot}.

$\langle\sigma^3\rangle/\langle\sigma\rangle^3 \simeq (1+\omega)^2$ - follows from the analysis of inelastic diffraction $p+D\to X+D$

13. <u>Conclusions</u>

1. $P(\sigma)$ is wide but not $\sigma \sim \{\sigma - \langle\sigma\rangle\}$

2. Configurations in the wave function of a nucleon having small interaction cross section with the hadron target has noticeable probability

$$P\left\{\sigma < \frac{\langle\sigma\rangle}{4}\right\} \sim 10\%$$

fixes lowest boundary for the probability of gap survival in the inel processes since for these configurations shadowing is small.

3. For pion projectile $\frac{\langle\sigma^2\rangle}{\langle\sigma\rangle^2} - 1 \simeq 0.5$ – follows from the analysis of inel. shadowing in $\sigma_{\pi D}$. Another evidence for the constituent quark model?

4/1

Collider energies - new features

1. Long range correlations in the rapidity space becomes visible

$$E_b E_a \frac{d\sigma^{p+p\to a+b+X}}{d^3p_a \; d^3p_b} \Big/ E_a \frac{d^3\sigma^{p+p\to a+X}}{d^3p_a} \; E_b \frac{d^3\sigma^{p+p\to b+X}}{d^3p_b}$$

does not tends to constant at $y_a - y_b > 2$.

Parton model (one multiperipheral ladder of partons) is insufficient - more complicated soft interactions

P.L B186 (198 7) 287

2. $$\frac{d\sigma^{p+p\to X+p}}{dt} \Big/ \left.\frac{d\sigma^{pp}_{el}}{dt}\right|_{t=0} \simeq 0.19$$

at $\sqrt{s} = 546$ GeV instead of ~ 0.3 at ISR.

Decrease with energy of this ratio is the hint for the blackening of the interaction at small impact parameters

-142.

Increase with energy of partial waves in pp scattering with small impact parameters

Eicanal diagrams - Conishi.

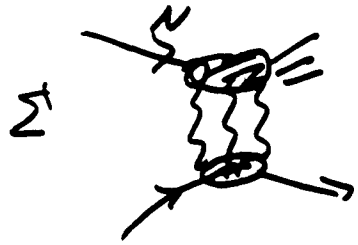

Predictions

1. Some decrease with energy dispersion of $\sigma(r_t^2)$ at small r_t^2 – at small impact parameters

2. Slowing down the dependence of $\frac{d\sigma}{dt\, dM_X^2}$ on t.

3. Complicated parton structure of effective pomeron. – seems to be in contradiction with current data on the parton structure of pomeron

<u>Question</u> how to select processes where $\sigma(r_t^2)$ is small, how to enhance the role of perturbative QCD regime.

15.

Hint from constituent quark model

Electromagnetic form factor of meson.

$$F(q) = \int e^{iqr/2}\, \psi^2(r) \frac{d^3r}{4\pi} = \int \frac{\sin qr/2}{\frac{qr}{2}} \psi^2(r) r^2 dr =$$

$$\simeq \frac{16}{q^4} \quad \psi(r=0) \quad \psi'(r=0)$$

<u>Conclusion</u>: increase q^2 select small size configurations in a hadron where color screening dampen nonperturbative QCD effects

Analysis of realistic quark models of a nucleon, skirmion model shows that small size configurations begin to dominate in the electromagnetic form factors of a nucleon at $|t| \gtrsim 1\ GeV^2$.

Thus increase of $\frac{1}{2}$ tends to make process more close to the perturbative regime.

o. Hard diffraction.

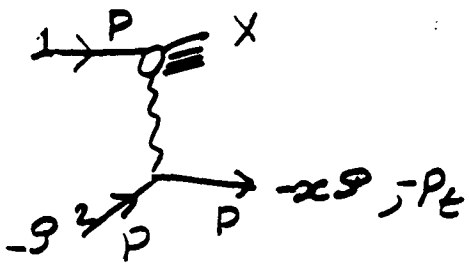

Kinematics:

$s = (p_1+p_2)^2 \gg M_X^2$

$M_X^2/s = 1-x$

$|t| > 1\ \mathrm{GeV}^2$

$t \approx -P_t^2$

$|t|/s \ll 1$

In the lowest order of pQCD this process is described by diagram

F.S. (1988)

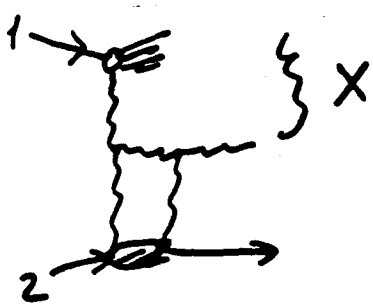

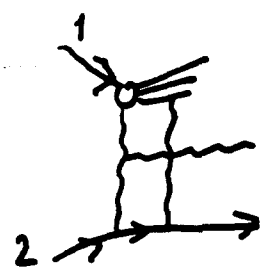

is small.

This diagram dominates since

a). Cross section should not decrease with s – dictate necessity of gluon exchanges in t channel.

b). System X should be white or final state interaction would lead to multiparticle state cf. $e^+e^- \to$ hadrons $\to$ two gluon exchange.

c). Necessary condition of applicability of pQCD is that virtuality of a gluon $\sim |t/4|$ should be large:

$$\left|\frac{t}{4}\right| \gg \lambda^2_{QCD}.$$

Conventional wisdom (from deep inelastic pro

$$\left|\frac{t}{4}\right| > 1\ GeV^2$$ - may be earlier

d). Gap in rapidity between system X and proton is large at SSC energies:

$$y_X - y_p \simeq \ln \frac{2\vartheta x}{M_X} - \ln \frac{\sqrt{m_N^2 + p_t^2}}{2\vartheta x} \simeq$$

$$\simeq \ln \frac{s\, x^2}{M_X \sqrt{m^2 + p_t^2}} \simeq 10.8 \qquad \text{for } x \simeq 0.9$$

Since gap is large it is necessary to account for several rungs in the ladder.

3.

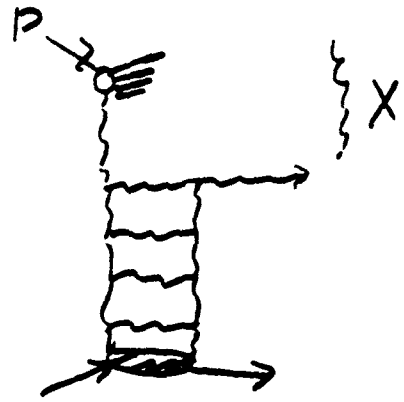

These diagrams dominate in the light-cone gauge.

[illegible]

[illegible] 1314 (1979)

$$\frac{d\sigma}{dt\,dX}^{pp \to X+p} = \frac{\pi \alpha_s^2(t)}{|t|} \cdot G_{IP\,NN}(t)\; f\left\{\alpha_s(t) \ln\frac{s}{t}, t\right\}$$

$$\left(\frac{s}{M_X^2}\right)^2 G_N\left\{\frac{|t|}{M_X^2 - t - m_N^2}, t\right\}$$

1. Here $\alpha_s(t)$ is running coupling constant.
2. $G_{IP\,NN}(t)$ is the form factor for the interaction of two gluons with a nucleon. At present its dependence on t can be calculated at large t only in pQCD

$G_{IP\,NN}(t) = \Sigma$ 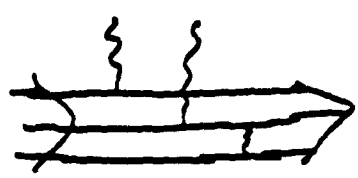

19.

3. f is the contribution of ladder diagrams divided by the contribution of lowest order diagram of pQCD. In the lowest order of pQCD $f=1$.

4. At large s

$$f \simeq \left(\frac{s}{-t}\right)^{\frac{12\alpha_s(t)\ln 2}{\pi}} \frac{1}{\left[\alpha_s(t)\ln\left(\frac{s}{-t}\right)\right]^{3/2}}$$

Thus cross section should fastly increase with s

5. $G_N(y,t)$ is gluon structure function of a nucleon.

Measurement of dependence of cross section on M_X^2 at fixed t measures gluon structure function of proton at any

$$y = \frac{|t|}{M_X^2 - t - m^2}$$

6. Characteristic feature of pQCD is weak dependence of x distribution on t at $|t/M_X^2| \ll 1$

Parton distribution in the perturbative pomeron.

Ingelman and P. Schlein have raised interesting question on the parton structure of pomeron.

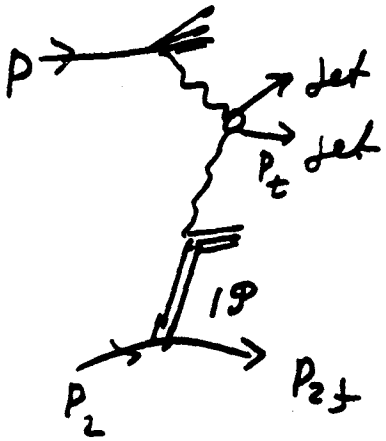

x_p is the fraction of momentum of pomeron carried by hard constituents

It is difficult to formulate mathematically this question at small $t = (P_2 - P_{2f})^2$ where structure of pomeron is not understood.

In old fashioned multiperipheral approach where IP is constructed from the exchanges by usual mesons

$$x_{IP}\, G_{IP}(x_{IP}, P_t^2) \sim (1-x)^{5 \pm 4}$$

1.

$\mathbb{P} =$ 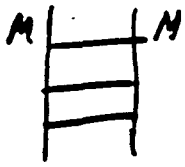

$(1-x)^3$ is due to evolved with p_t structure function of meson. Additional $\sim(1-x)^2$ is from second meson.

Experiment prefers

$$x_p\, G_p(x_p, t) \sim x_p(1-x_p)$$

at $0.6 < |t| < 2\ \mathrm{GeV}^2$ P. Schlein et al.

If eiconal diagrams would domenate in this region of t one should expect more steep than in one ladder decrease of G_p with x_p since more hadrons would share momentum of pomeron.

At large t ($|t| > 4\,GeV^2$?) parton structure of pomeron can be visualized in the form of dominance of certain Feynman diagrams.

In the lowest order of pQCD domina diagrams are

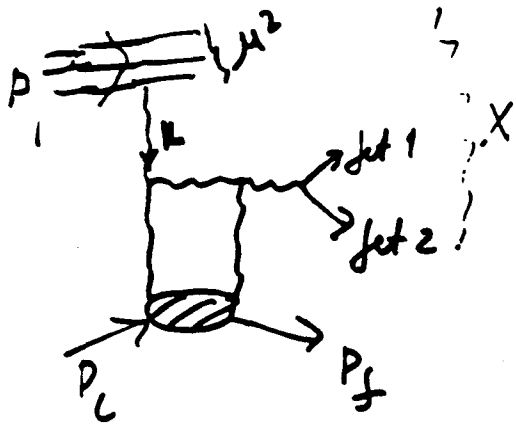

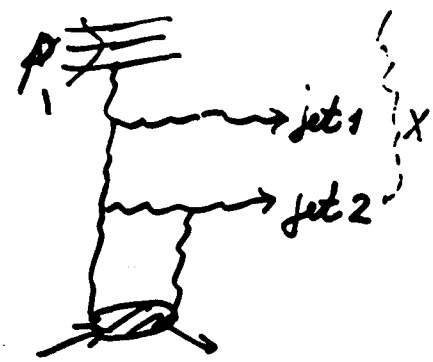

$M^2 \equiv (p_{jet1} + p_{jet}$

$t = (P_i - P_f)^2$

$$\frac{\frac{d\sigma^{diff}}{dM^2\, d^2P_t}}{\sigma^{diff}} = \alpha_s \cdot \varphi\{M^2, P_t^2\}$$

Hard diffraction with production of jets forms α_s fraction of total cross section of diffraction but not $\sim \alpha_s$ as for usual hard processes

Basic properties.

1. Diffractive production of jets by perturbative pomeron has no convolution form.

2. Distribution of jets over x_p is concentrated at $x_p = 1$ in the considered diagrams

$$K = \alpha q + \beta p_1 + K_t$$

$$(p_1 - k)^2 \sim \mu^2 \qquad \alpha \simeq \frac{\mu^2}{M_X^2} \ll 1$$

3. Bremstrahlung of gluons will soften distribution over x_p.

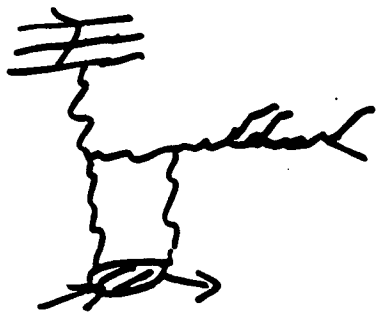

$$\sim G_g(x_p, p_t^2)$$

Here $G_g(x_p, p_t^2)$ is structure function of gluon.

4. If rapidity gap is sufficiently large one should account for several rungs of gluons

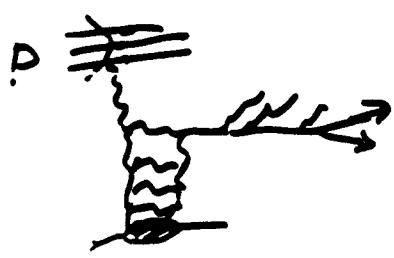

Their number is controlled by Δy.

-3_2

Signatures of perturbative pomeron.

1. Gluon exchanges has only 1 chirality

As a result

a). chirality is conserved in diffraction processes

In processes of diffractive production of resonances

$$p+p \to X + N^*(J=3/2)$$

Transition $\frac{1}{2} \to 3/2$ is suppressed.

b) diffractive production of baryon resonances with opposite space parity is suppressed also.

2. Diffractive production of Drell-Yan pairs, direct photons is suppressed at large x_p as compared to high P_t phenomena

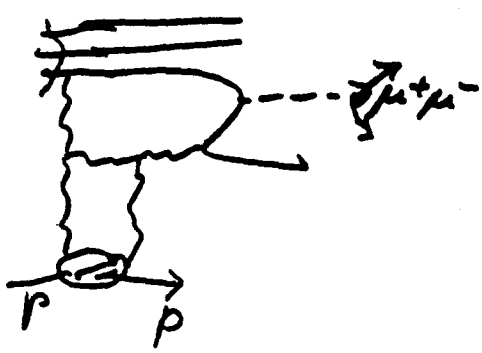

$\sim \alpha^2 \alpha_s$ but not α^2 as in the normal hard processes

Above consideration can be generalized to hard double diffractive processes:

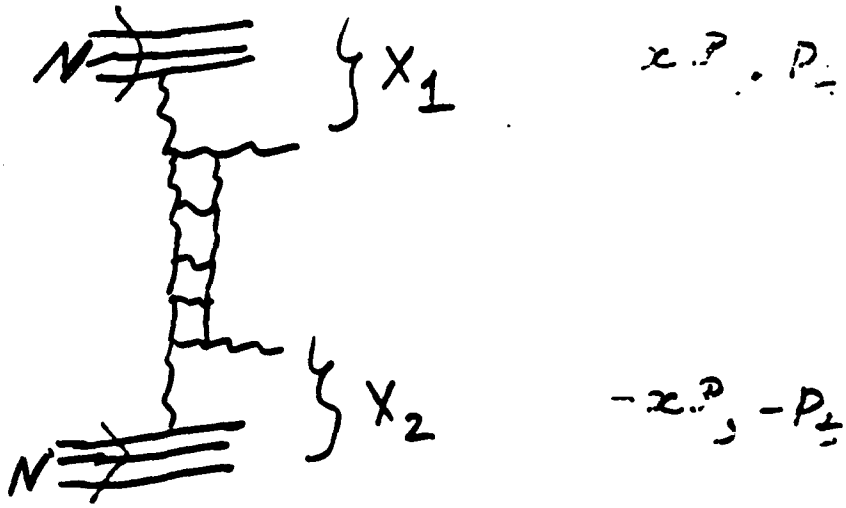

We consider kinematics

$$\Delta y = y_{X_1} - y_{X_2} \simeq \ln\left(\frac{s\, x^2}{\sqrt{M_1^2+P_t^2}\ \sqrt{M_2^2+P_t^2}}\right)$$

At SSC energy range and $M_1 = M_2 = 100\,\mathrm{GeV}$ and $|t| > 4\,\mathrm{GeV}^2$

$$\Delta y \simeq 12$$

We restrict ourselves by ladder diagrams to guarantee that states X_1 and X_2 are white to keep gap in rapidity between X_1 and X_2.

For double diffraction argument with α_t is inapplicable - so question on gap survival exists.

-5.

Correlation experiments.

We discussed above that there are different space-size configurations in the hadron. The question arises how this property reveal itself in the distributions of partons.

Old question:

Why quark counting rules work in the domain of nonperturbative QCD.

Investigation of ct phenomena hints that selection of parton with large x enhances the role of small space size configurations in the hadron. ($|3q\rangle$ configuration should have small size to avoid decay of p into bare quarks)

5.

If so selection of parton with large x would suppress the probability of wee partons with small transverse momentum and would increase the probability of wee partons with large transverse momentum. The investigation of this physics is possible at SSC, at Tevatron.

Generic experiment would be measuring hard collision which accompany $W, Z, \mu^+\mu^-$ pair production

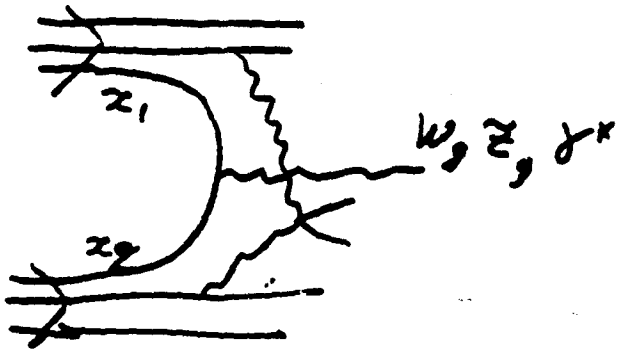

Accompanying process may be any hard process - production of jets, $b(\bar{b})$ particles production, etc.

Preferable kinematics to suppress background would be asymmetric kinematics

$x_1 >> x_2$, $x_2' >> x_1'$

$$R = \frac{\dfrac{d\sigma^{p+p \to e\bar{e} + \text{dijet} + X}}{dM^2_{e\bar{e}}\; dx_{e\bar{e}}\; dM^2_{\text{pair jet}}\; d^2p_{t\,\text{jet}}}}{\dfrac{d\sigma^{pp \to e\bar{e}+X}}{dM^2_{e\bar{e}}\; dx_{e\bar{e}}} \quad \dfrac{d\sigma^{pp \to \text{dijet}+X}}{dM^2_{\text{dijet}}\; d^2p_{t\,\text{jet}}}}$$

i). If there is no correlation between wee and hard partons R would be independent on x_2, x_1'

ii). If increase of x_2 enhances contribution of small size configurations in the projectile nucleon R should decrease with increase of x_2.

Conclusions.

1. There is good case to improve considerably our understanding of QCD in the new kinematical domain, to investigate physics relevant for the transition between pQCD and nonperturbative QCD phenomena.
2. Role of compositeness of proton - color screening phenomenon may be investigated. Important for the construction of physics of superdense hadron matter.
3. May be explored for searching for new physics - new particles, b quark physics etc.

L. W. JONES

INCLUSIVE NEUTRONS

$p + p \rightarrow n + X$

- EARLY FERMILAB EXPTS GENERATED n BEAM FROM EXTERNAL p BEAM ON W TARGET AT 0°

- LATER MADE SYSTEMMATIC STUDY OF n PRODUCTION $d^3\sigma/dp^3$ (or $d\sigma/d\Omega$ vs E_n, θ_n) FROM VARIOUS TARGETS; H — W

E 404 DATA NEVER PUBLISHED

'THO IN COS RAY CONF. PROC.

LOOK AT: $p + p \rightarrow n + X$

400 GeV STATIONARY

- σ (FORWARD n) $\simeq \frac{1}{4} \sigma_I$
- $\langle p_\perp \rangle_n \simeq 300$ MeV/c
- $\langle x \rangle_n \simeq 0.25$ $(= E_n / E_p)$

NEUTRON PRODUCTION

EXPERIMENTAL DATA

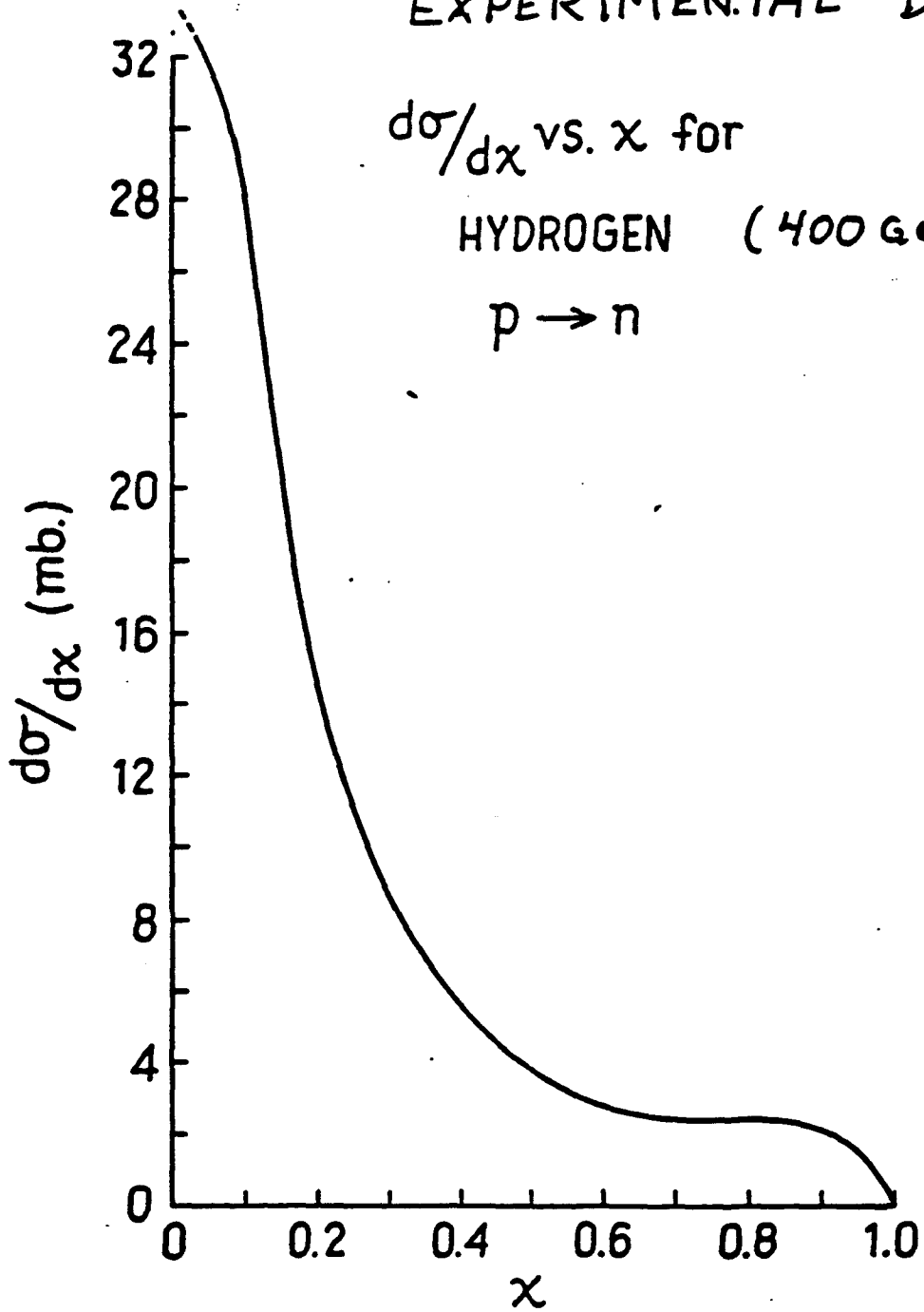

$x = E/E_0$

E_0 : ENERGY OF INCIDENT PROTON

NEUTRON SPECTRUM AT 0°

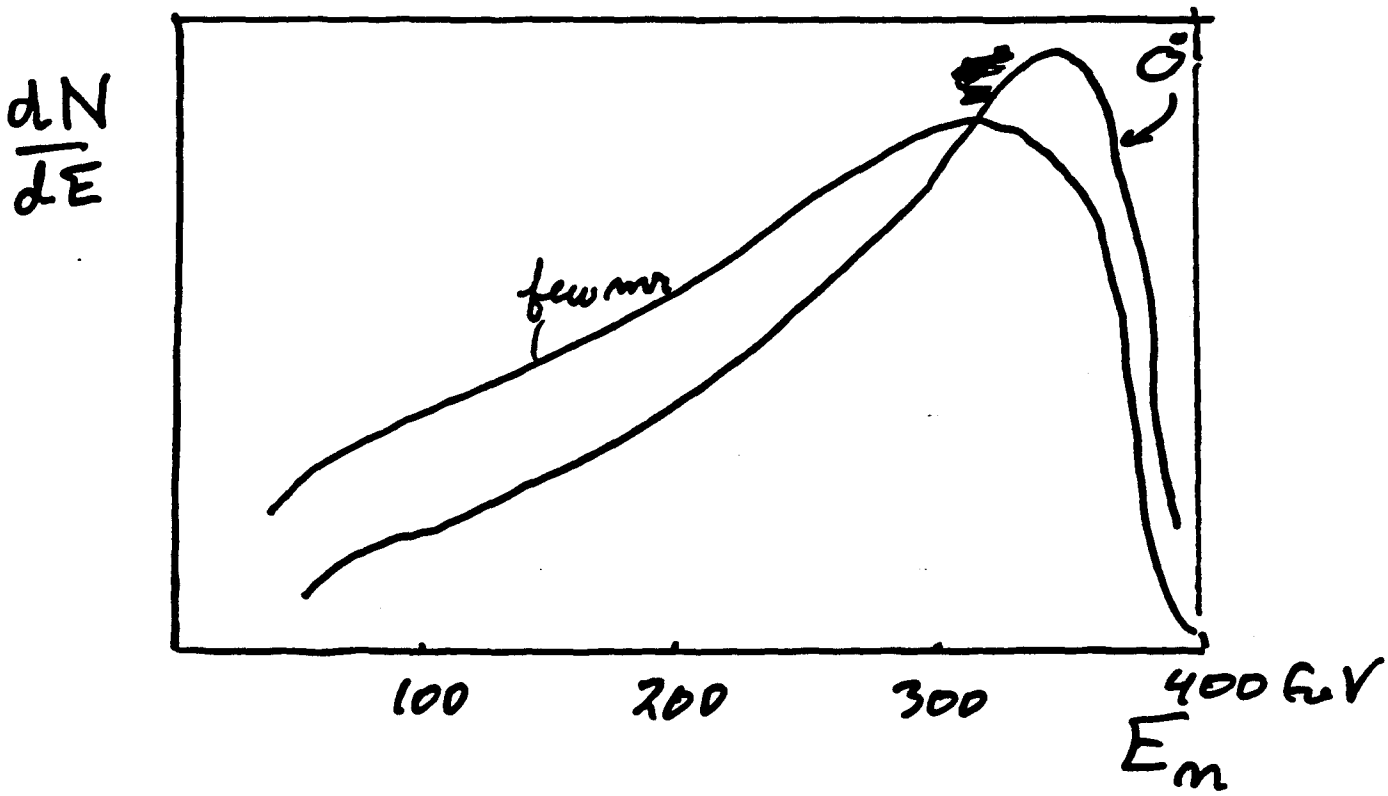

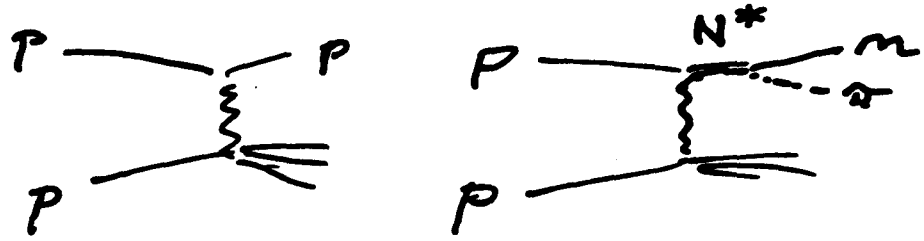

The

VII International Symposium on Very High Energy Cosmic Ray Interactions

Ann Arbor, MI June 21-27, 1992

(A continuation of a biennial series begun in 1982 which has met in Nahodka, LaPaz, Rio de Janeiro, Tokyo, Beijing, Lodz, and Tarbes)

<u>Primary objective:</u>

- to bring together accelerator and cosmic ray people to attack and seek resolution to common problems in particle physics at and above a TeV cm.

100 GeV

$\sqrt{s} = 14$ GeV.

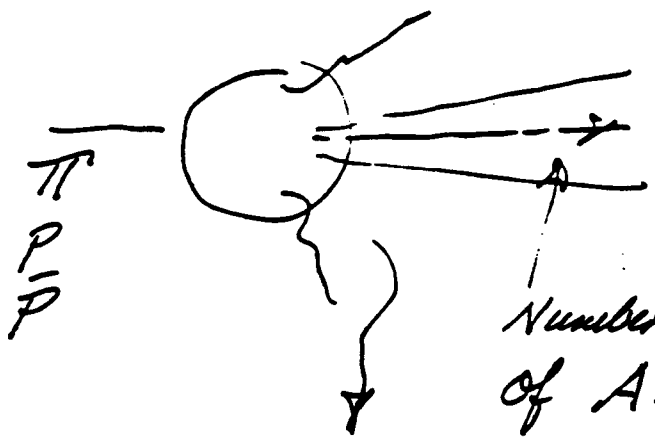

Number nearly independent of A.

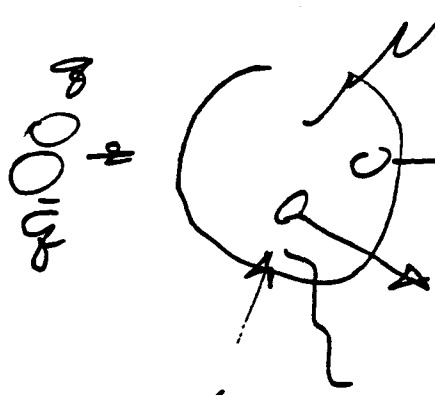

fragments ~ .6 - .7 E_{inc}

lower energy quark.

10 - 12 Fermi

$\sigma_{qN} \sim 3$ mb $\qquad \lambda_q \sim D_{Au}$

$\sigma_{qqN} \sim 3$ mb

~~QGP~~ OPE

$$\frac{d^3\sigma}{dt} = \frac{1}{\pi^3 \cdot s^2} \sigma_1 (s_1)^{3/2} \sigma_1 \frac{1}{(t^2-\mu^2)^2} s_2^{3/2} \sigma_2 \cdot d\sqrt{s_{1,0}}$$

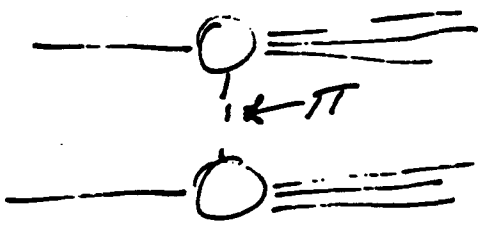

big effect!

Results

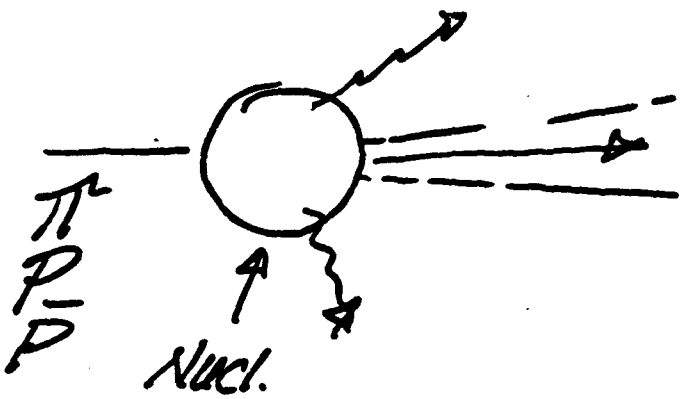

100 GeV
$\sqrt{s} = 14$ GeV

Number <u>nearly</u> independent of A

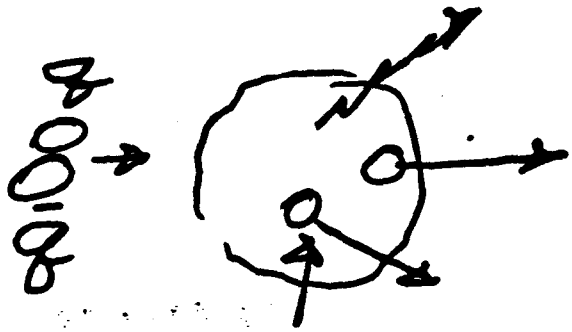

fragments ~ .6 - .7 $E_{inc.}$

lower energy quark

$\sigma_{qN} \sim 3$ mb

$\lambda_q \sim D_{Au}$

One Pion Exchange

$$\frac{d\sigma}{dt} = \frac{1}{\pi^3 s^2} \frac{\sigma_1 s_1^{3/2} ds_1^{1/2} \sigma_2 s_2^{3/2}}{(t^2-\mu^2)^2}$$

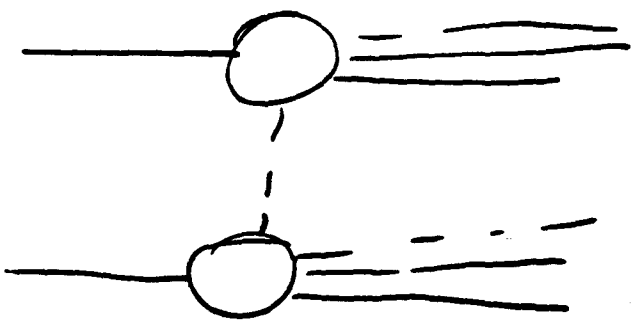

likely a big effect !

$\sigma_{increase}$ —

QGP - B_j

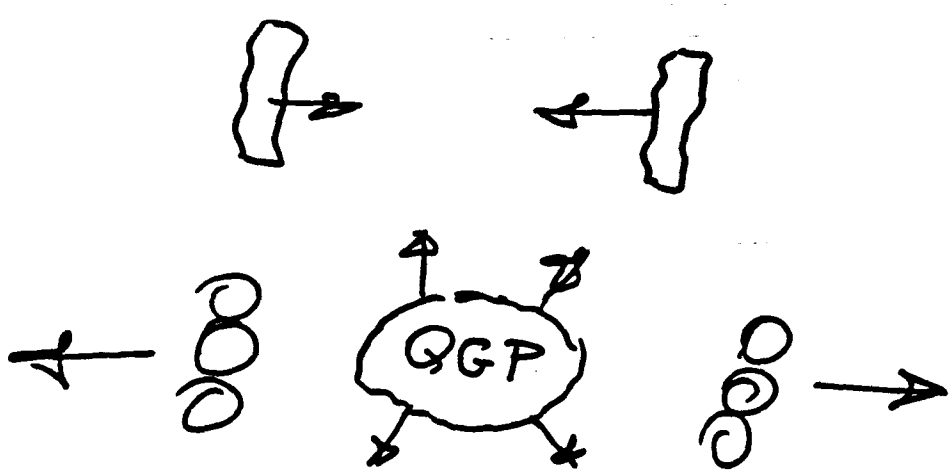

$\rho_E \sim 2\ \mathrm{GeV}/F^3$

SSC - big effect

$n_\pi \sim 500$

characteristic n_K/n_π - large

Are there <u>fragile</u> but very interesting objects produced?

b b b

Might well go down the beam pipe.

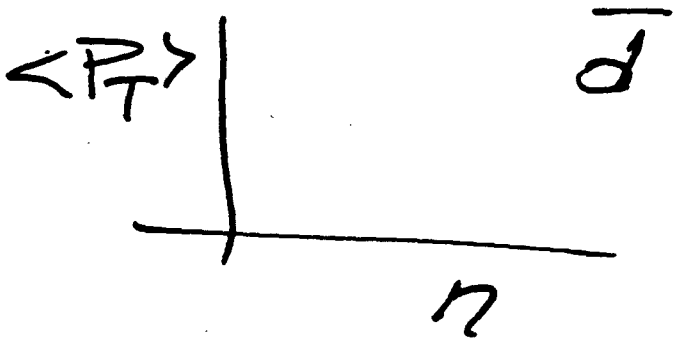

Note for Bill

$m = 15\ \mathrm{GeV}$

$E = 15\ \mathrm{TeV}$

$\gamma = 10^3$

$$\Theta_{crit} = \frac{1}{\gamma} = \frac{10\ \mathrm{cm}}{100\ \mathrm{km}}$$

THE L.P.M. EFFECT AT THE F.A.D.

STEVEN STRAUSZ
UNIVERSITY OF WASHINGTON

⊗ BREMSSTRAHLUNG

ELECTRONS LOSE ENERGY IN COULOMB FIELD OF NUCLEI

$$E = E_0 e^{-x/x_0}$$

$X_0 \equiv$ RADIATION LENGTH

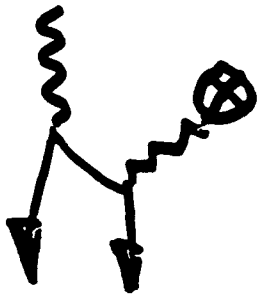

⊗ PAIR PRODUCTION

GAMMA RAYS TRAVEL THE AVERAGE DISTANCE BEFORE PAIR PRODUCTION

$$= \frac{9}{7} X_0$$

Bethe Heitler, Proc. Royal Soc. A 146

Photon Cross Section

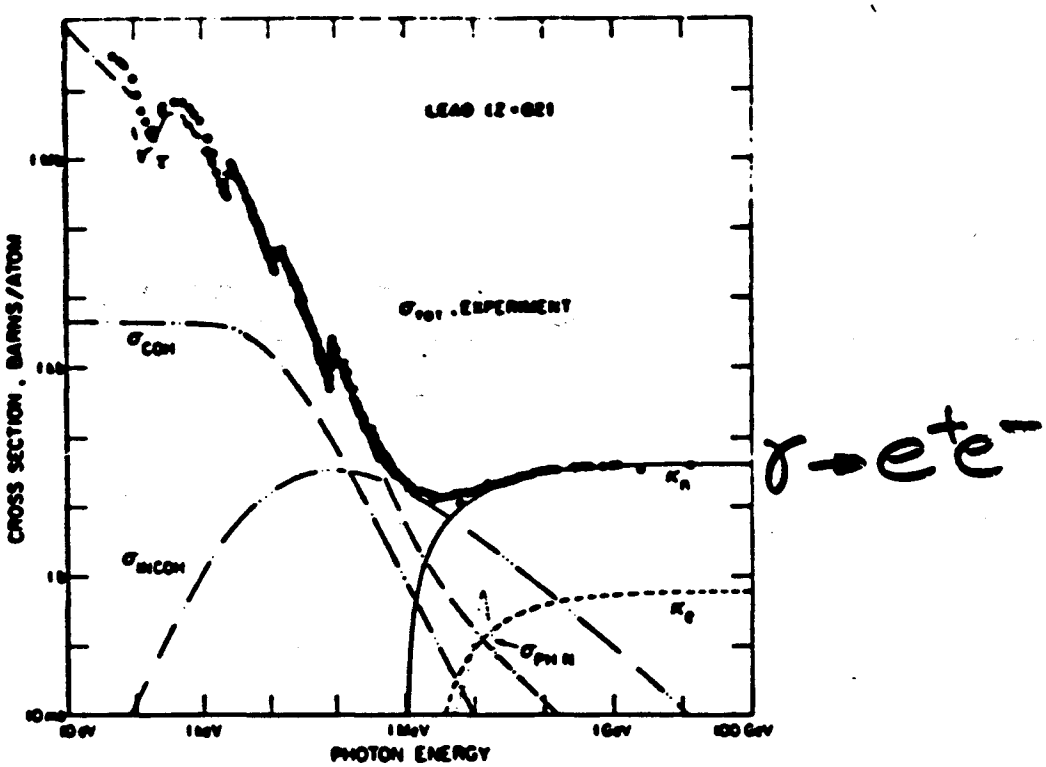

PARTICLE DATA GROUP (1990)

LPM EFFECT

BREMSSTRAHLUNG AND PAIR PRODUCTION ARE SUPPRESSED AT RELATIVISTIC ENERGIE WHEN THE FORMATION LENGTH EXPANDS AND MULTIPLE COULOMB SCATTERING FROM NEIGHBORING NUCLEI CAUSES DECOHERENCE BETWEEN THE PARTICLE STATES.

THE CROSS SECTIONS DECREASE AS

$$\sigma \propto E^{-1/2}$$

AT ENERGIES ABOVE

$$E > 61 \text{ TeV} \left(\frac{X_0}{\text{cm}}\right) \qquad X_0^{Pb} = .56 \text{ cm}$$

THE SECONDARY PRODUCTION SPECTRUM IS MODIFIED.

LANDAU POMERANCHUK ('53) MIGDAL ('56

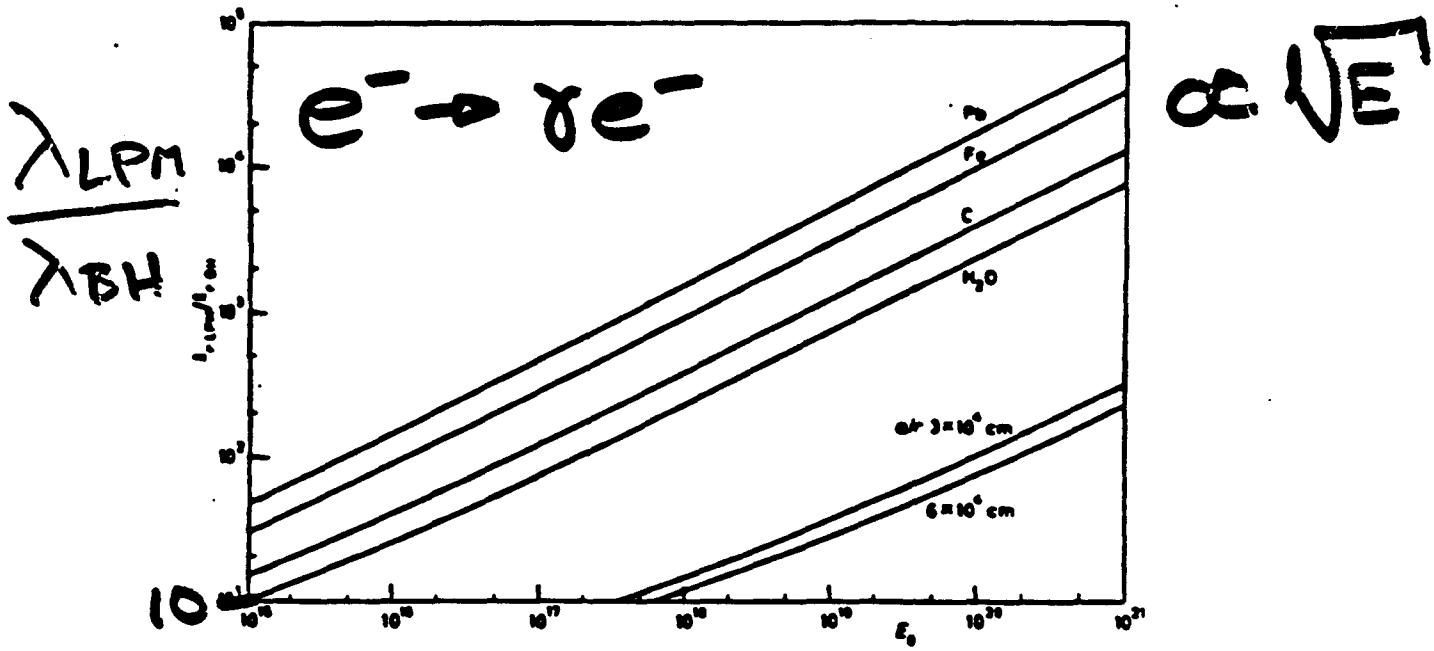

Fig. 5. – Ratios of mean free paths of the electron in air, water, carbon, iron and lead including the LPM effect to those of the Bethe-Heitler theory. The cut-off energy of radiation process is chosen to be 10^6 eV.

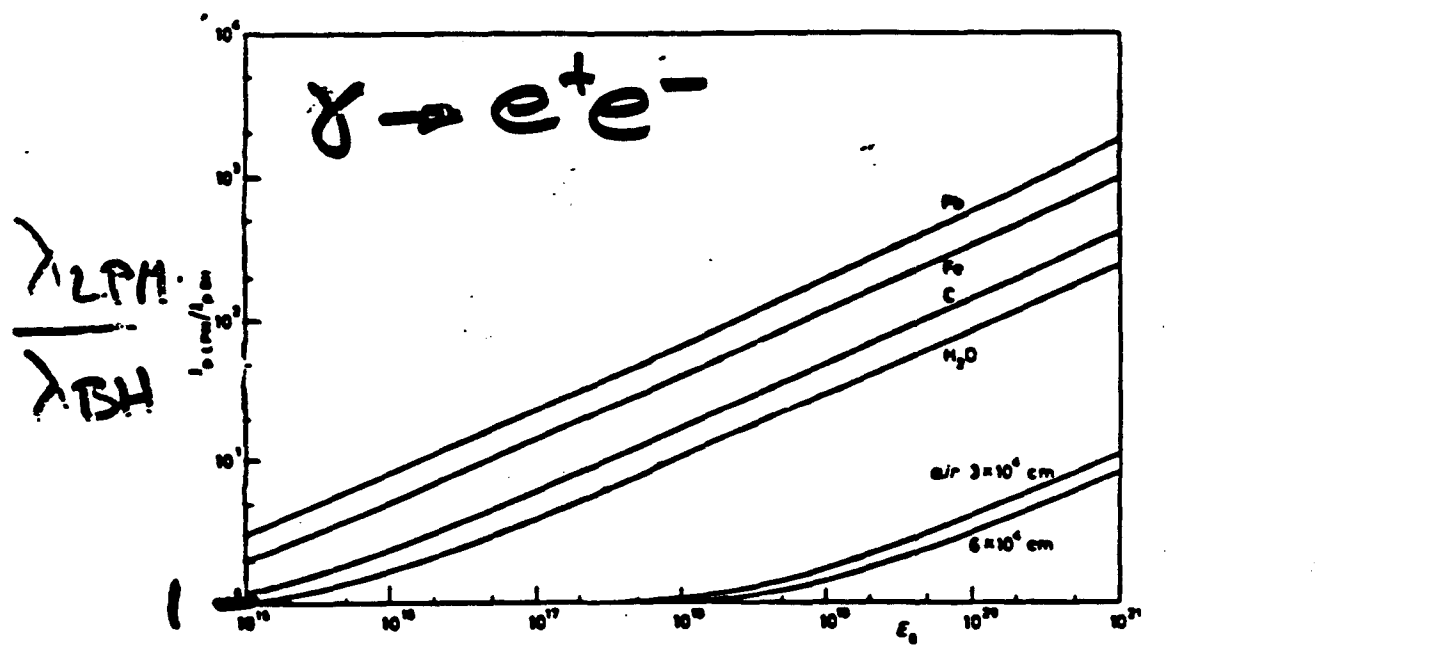

Fig. 6. – Ratios of mean free paths of the photon in the same materials as fig. 5.

KONISHI IL NUOVO CIMENTO 44 509 (78)

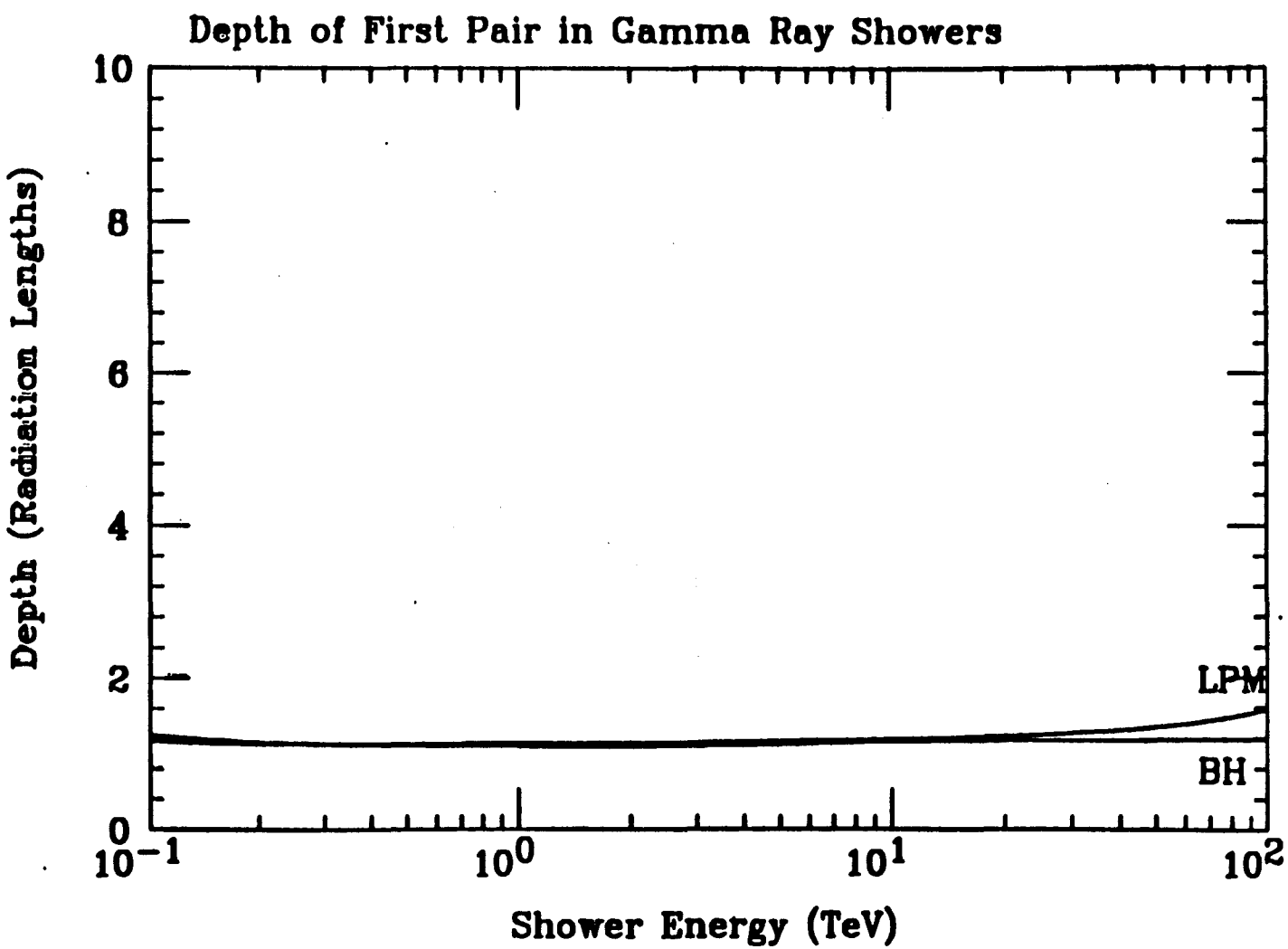
Depth of First Pair in Gamma Ray Showers
Depth (Radiation Lengths)
10
8
6
4
2
0
LPM
BH
10^{-1}
10^{0}
10^{1}
10^{2}
Shower Energy (TeV)

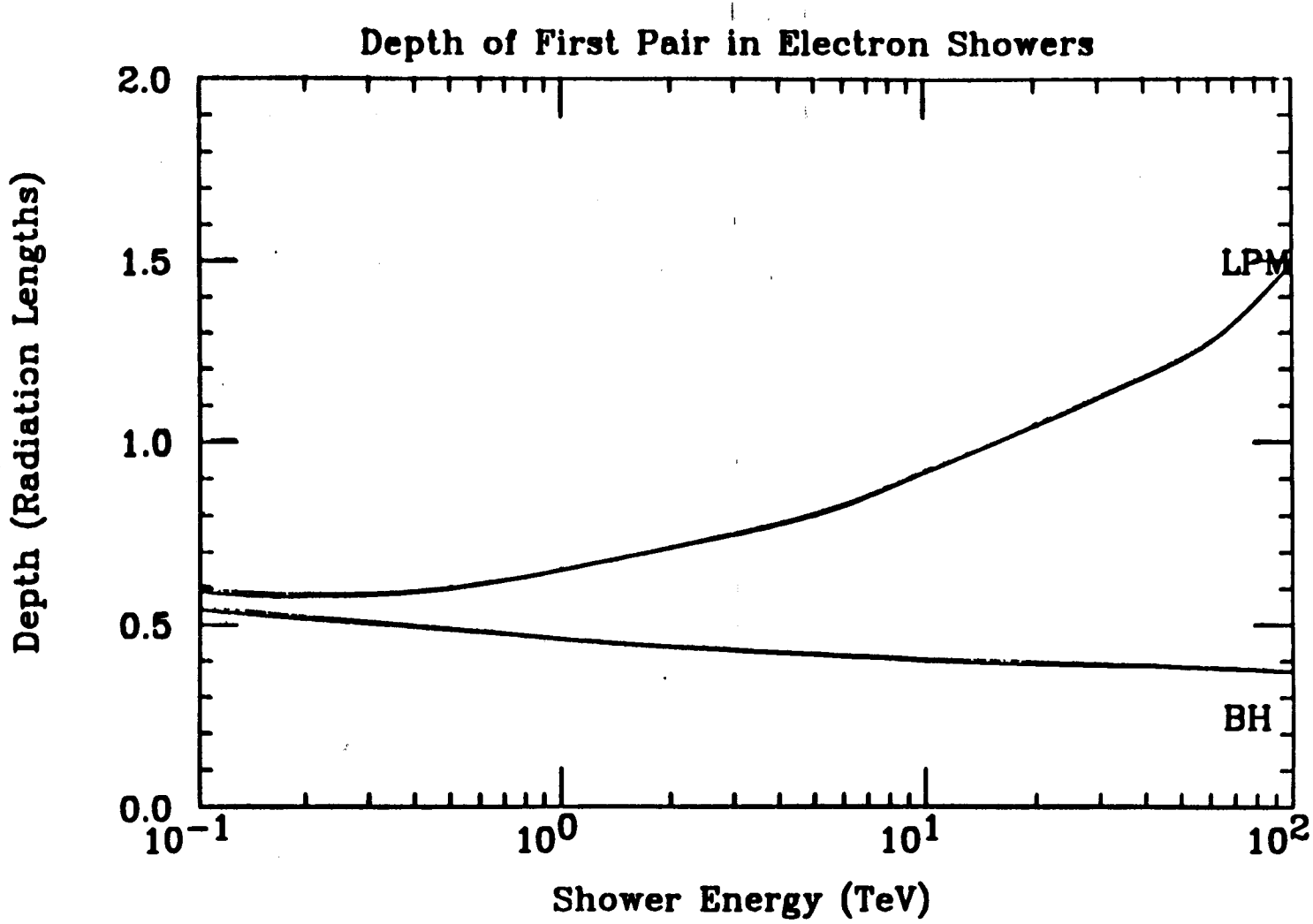
Depth of First Pair in Electron Showers
Depth (Radiation Lengths)
2.0
1.5
1.0
0.5
0.0
LPM
BH
10^{-1}
10^{0}
10^{1}
10^{2}
Shower Energy (TeV)

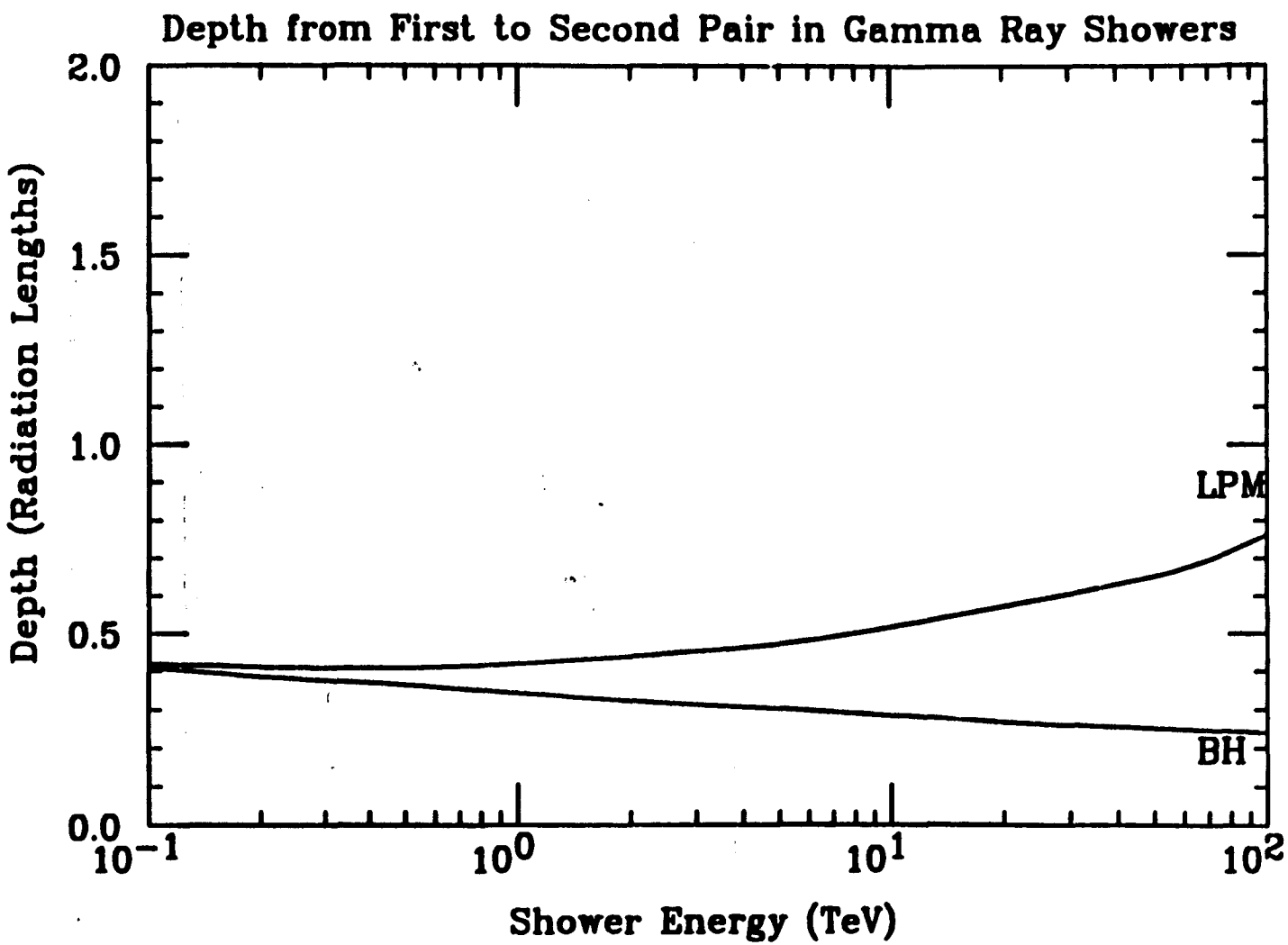
Depth from First to Second Pair in Gamma Ray Showers
Depth (Radiation Lengths)
2.0
1.5
1.0
0.5
0.0
LPM
BH
10^{-1}
10^{0}
10^{1}
10^{2}
Shower Energy (TeV)

GAMMA RAY SHOWER DEVELOPMENT

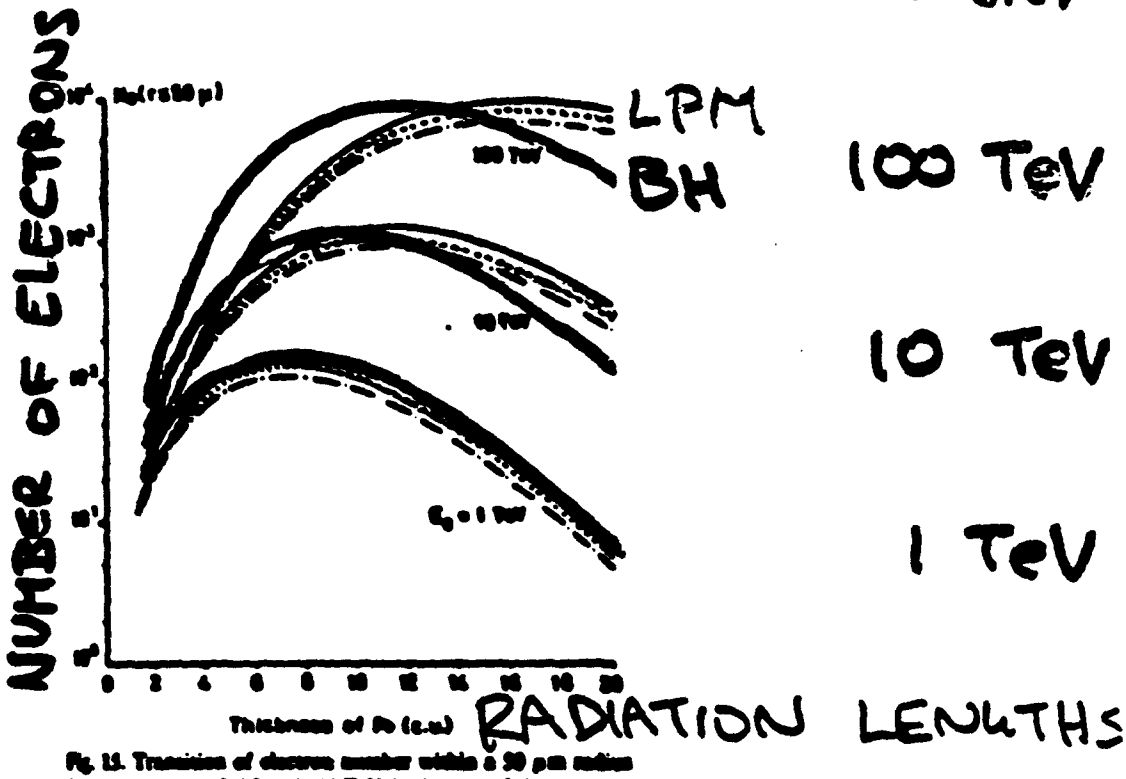

Fig. 11. Transition of electron number within a 50 μm radius for three energies, 1, 10 and 100 TeV, in the case of diamond-pair production. The solid, dotted and broken curves are obtained by the present calculations, each corresponding to counting positions 0, 500 and 1000 μm from the bremsstrahlung of the overlying lead plate. The heavy solid curves were obtained by Nishimura.

OKAMOTO NIM A257 (87)

COSMIC GAMMA RAYS IN EMULSION
105 EVENTS
DISTANCE FROM FIRST TO SECOND PAIR

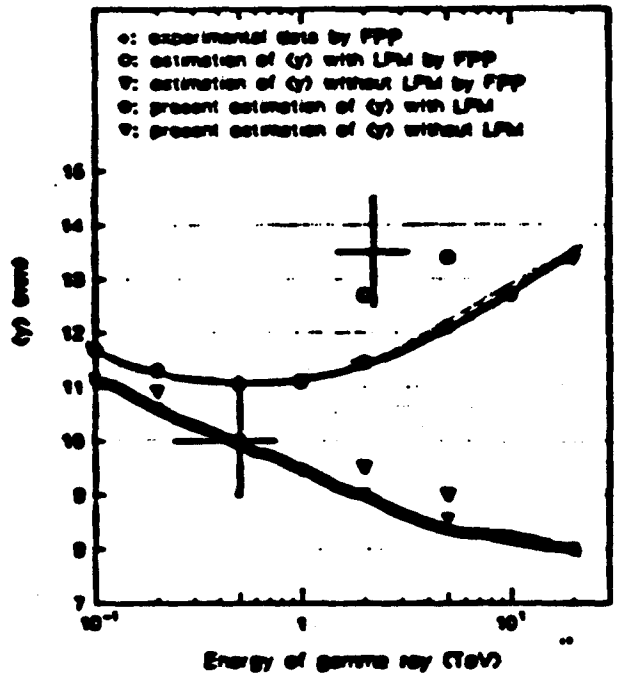

FIG. 11. Average value of the distance y between the first two pair-creation points in γ-ray-initiated cascade showers in nuclear emulsion. Crosses are experimental data by Fowler, Perkins, and Pinkau (Ref. 6) (FPP) for a group with energies greater than 1 TeV and another less than 1 TeV. Since FPP determine the energy very roughly and they do not mention the average value of the energies in each group, the positions of the crosses in the energy scale are not very accurate. Open circles, estimation of $\langle y \rangle$ with LPM effect by FPP; open triangle, same without LPM effect by FPP. Closed circles, same with LPM effect by the present author; closed triangle, same without LPM effect by the present author. Curves are only to guide the eye.

(FOWLER 1959)

VARFOLOMEEV (1960) JETP 11 23

COSMIC RAY PHOTONS (~TeV)

IN EMULSION

COUNTED ELECTRON PAIRS AT

1.5 RADIATION LENGTHS

"A QUALITATIVE PROOF OF THE INFLUENCE OF THE MEDIUM ON BREMSTRAHLUNG HAS BEEN OBTAINED. FOR A QUANTITATIVE TEST OF THE MIGDAL FORMULAS, IT IS NECESSARY TO INCREASE THE STATISTICAL MATERIAL."

VARFOLOMEEV (1975) JETP 42 218

40 GeV ELECTRON BEAM

COUNTED BREMSSTRAHLUNG

PHOTONS FROM C, Al, W, Pb TARGETS

"REDUCTION IN EMISSION FROM

HEAVY SUBSTANCES IN NOT LESS

THAN PREDICTED BY L.P.M."

KASAHARA (1985) PHYS REV. D31 27.7

MOUNTAIN TOP LEAD/X-RAY FILM

10 SHOWERS SHOWED A

INCREASED WIDTH DUE TO

L.P.M. OR WERE HADRON INDUCED

COSMIC RAYS + SSC

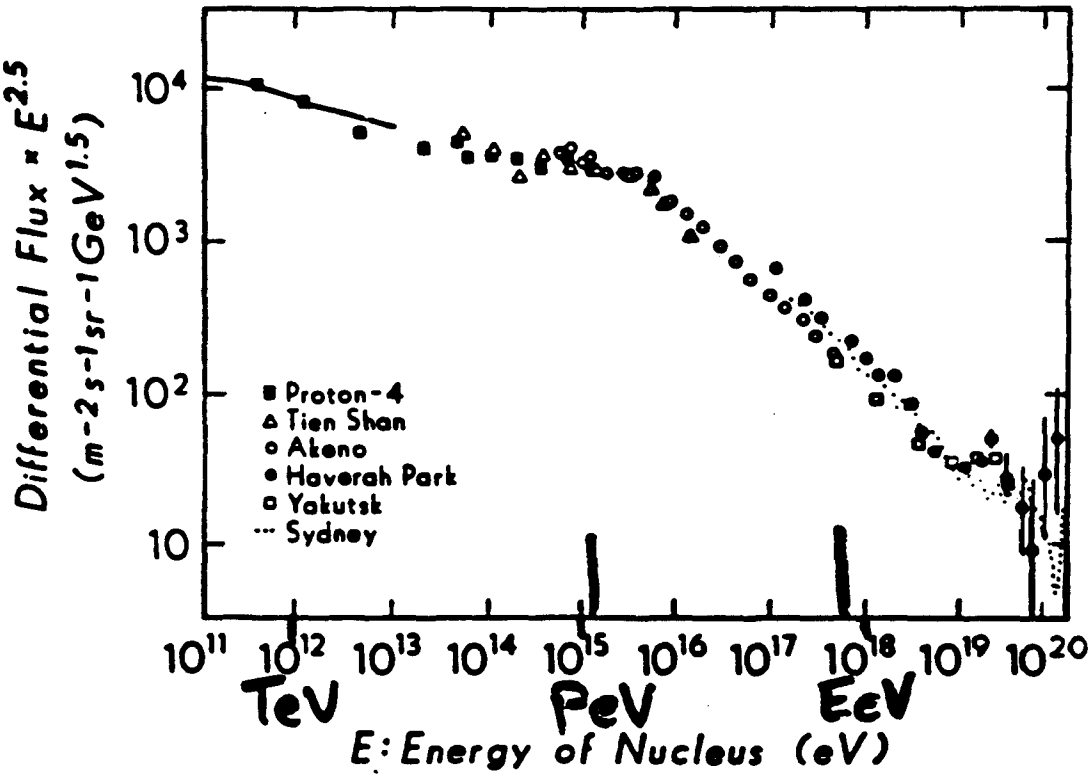

FERMILAB .9+.9 TeV → 1.6 PeV

SSC 20+20 TeV → 800 PeV

WHAT IS σ_{pp}, $\langle n_{prod} \rangle$, $\langle p_t \rangle$?

)KOLSKY - INTRO. ULTRAHIGH ENERGY COSMIC RAY PHYSICS.

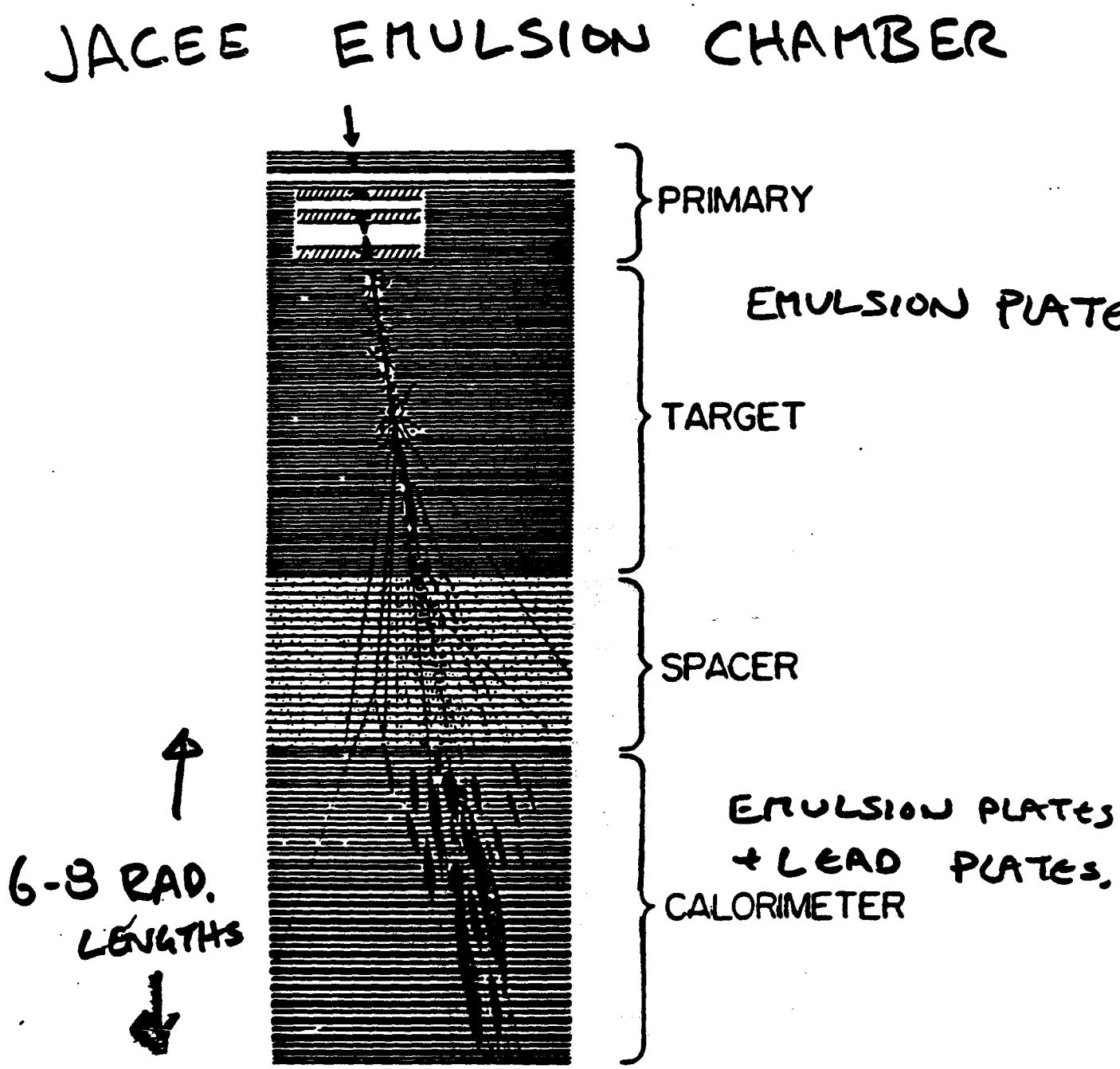
JACEE EMULSION CHAMBER
PRIMARY
EMULSION PLATE
TARGET
SPACER
EMULSION PLATES
+ LEAD PLATES.
CALORIMETER
6-8 RAD.
LENGTHS

Figure 1

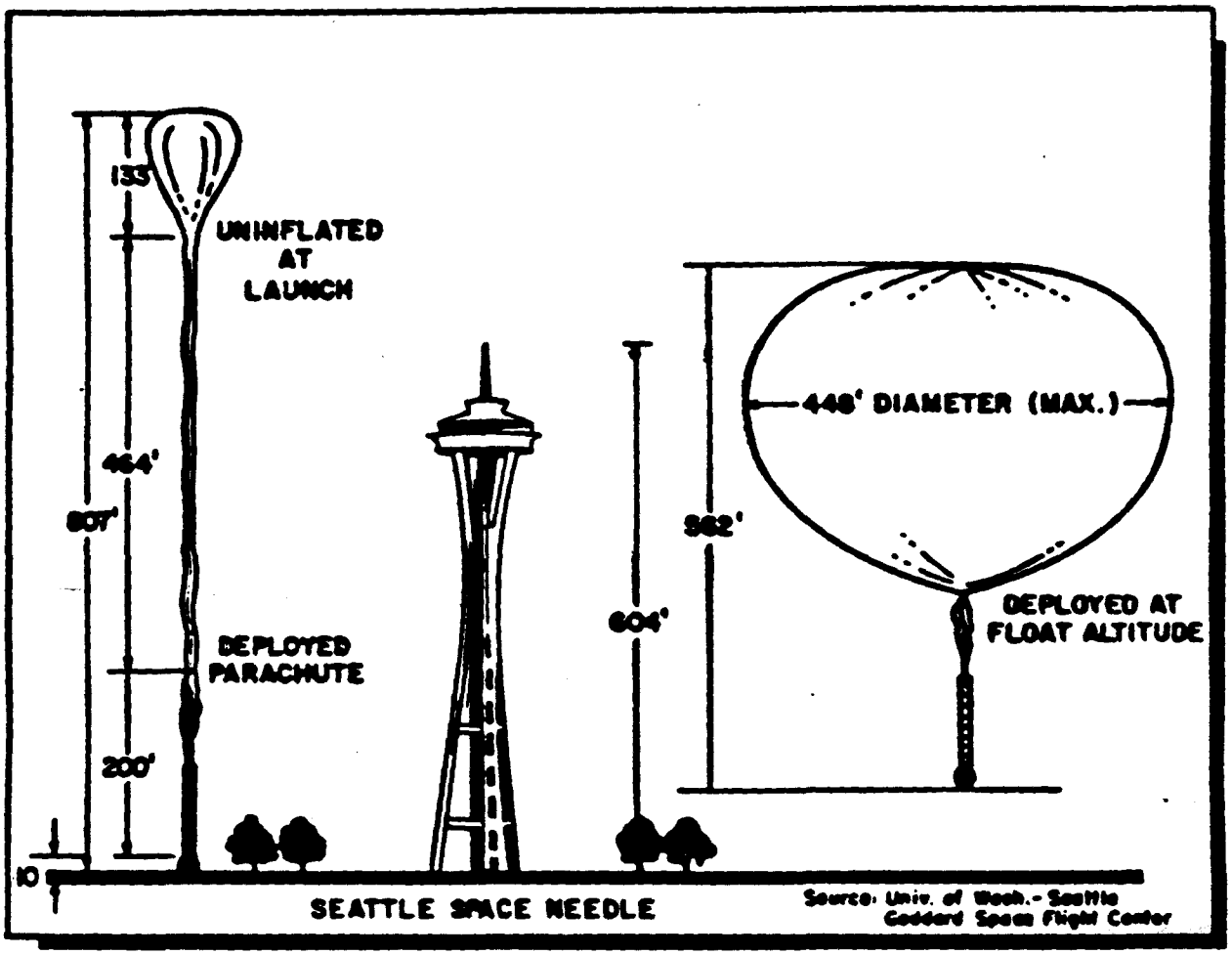
133'
UNINFLATED AT LAUNCH
464'
607'
DEPLOYED PARACHUTE
200'
10
604'
448' DIAMETER (MAX.)
562'
DEPLOYED AT FLOAT ALTITUDE
SEATTLE SPACE NEEDLE
Source: Univ. of Wash.- Seattle
Goddard Space Flight Center

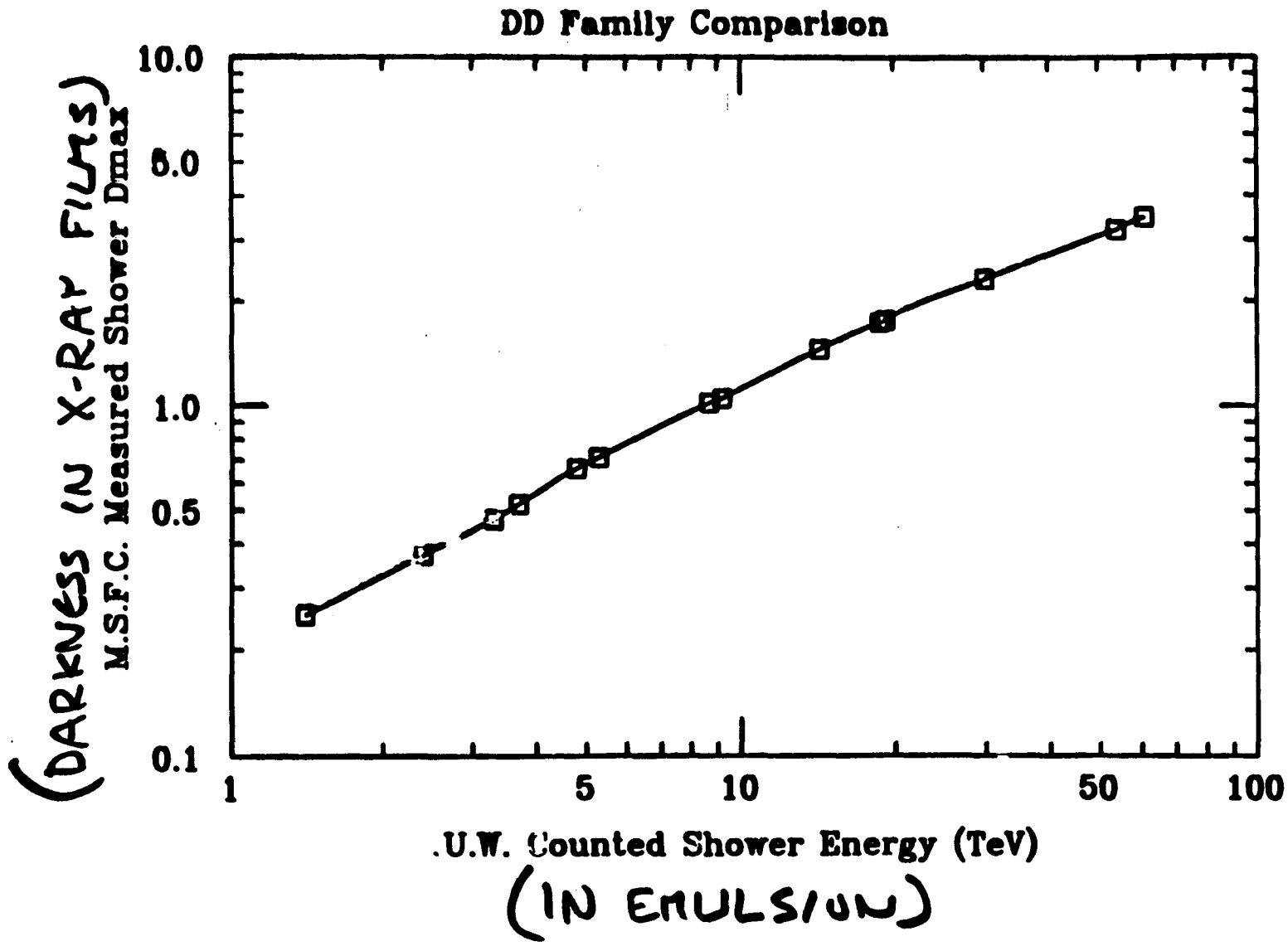
DD Family Comparison
10.0
5.0
1.0
0.5
0.1
1
5
10
50
100
M.S.F.C. Measured Shower Dmax
(DARKNESS IN X-RAY FILMS)
.U.W. Counted Shower Energy (TeV)
(IN EMULSION)

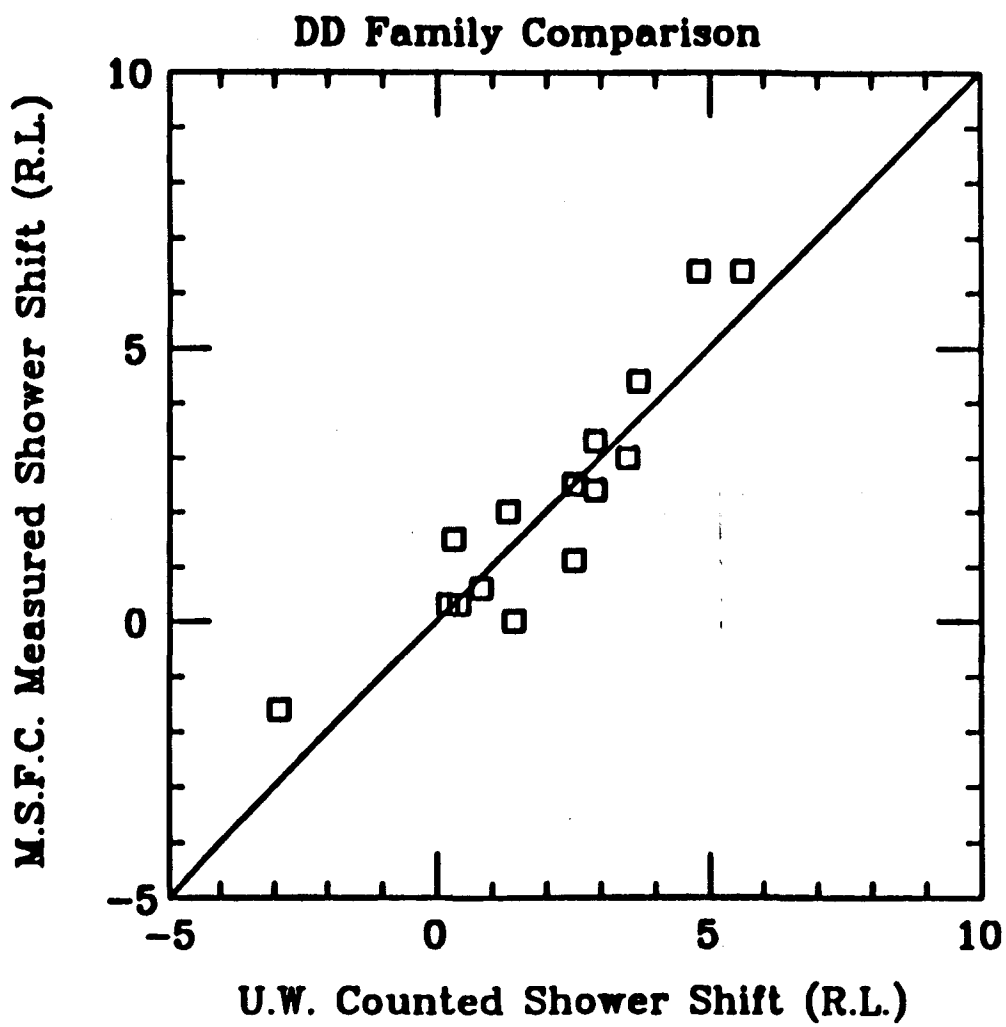
DD Family Comparison
M.S.F.C. Measured Shower Shift (R.L.)
U.W. Counted Shower Shift (R.L.)
10
5
0
−5
−5
0
5
10

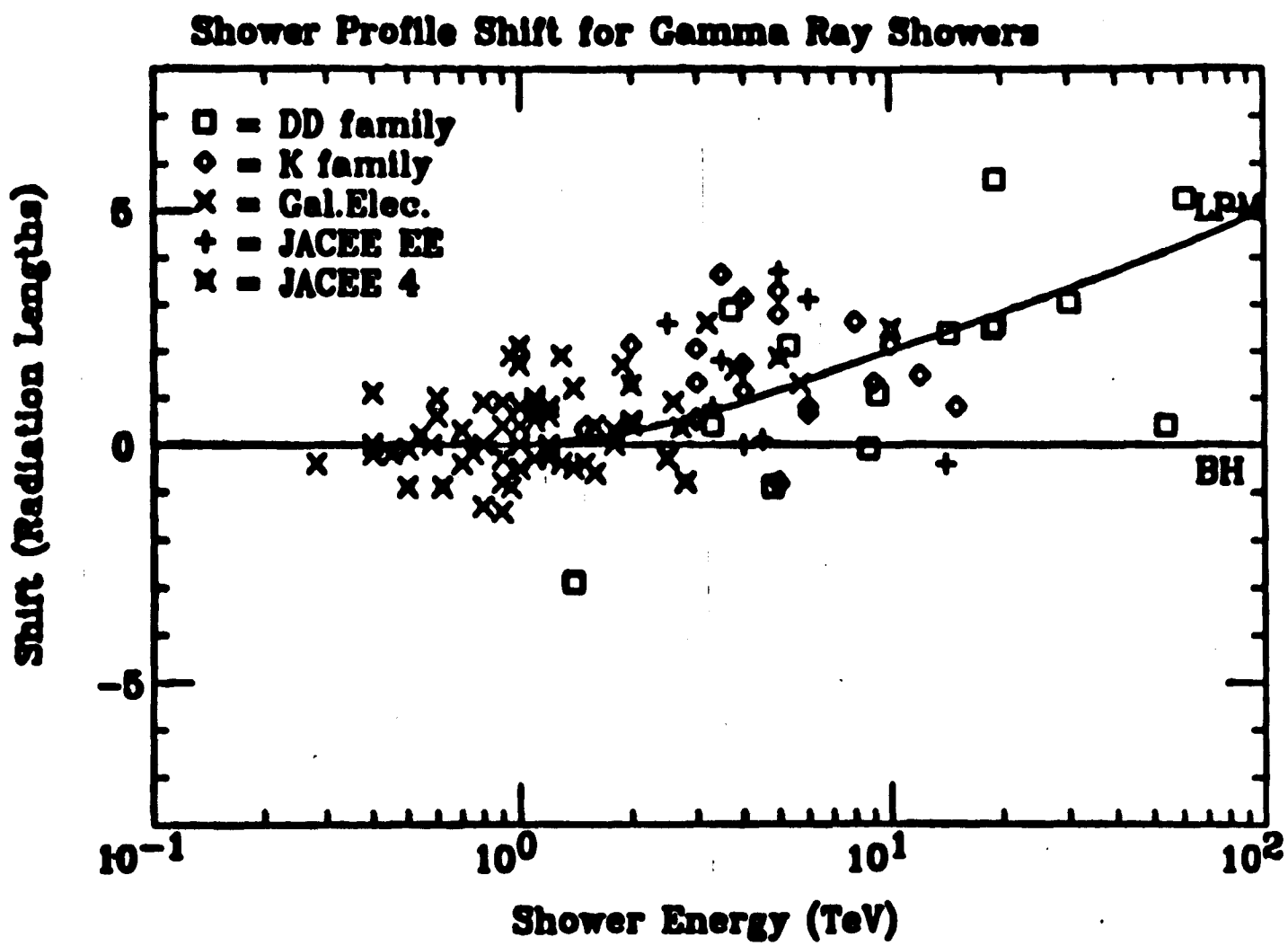
Shower Profile Shift for Gamma Ray Showers
□ = DD family
◇ = K family
× = Gal.Elec.
+ = JACEE EE
✱ = JACEE 4
LPM
BH
5
0
-5
Shift (Radiation Lengths)
10^{-1}
10^{0}
10^{1}
10^{2}
Shower Energy (TeV)

CALORIMETER SUGGESTIONS

MATERIAL

LEAD WITH MINIMAL SAMPLING LAYERS

ENERGY RESOLUTION

$\frac{\Delta E}{E} \sim 30\%$

INITIAL LONGITUDINAL SEGMENTATION

$\Delta L \sim 0.1$ R.L. (1ST - 2ND PAIR)

FINAL LONGITUDINAL SEGMENTATION

$\Delta L \sim 1.$ R.L. = 5 MM

TOTAL LONGITUDINAL LENGTH

$L \sim 20.$ R.L.

INITIAL CHARGE RESOLUTON

$\Delta Q \sim 1.$ UNIT (1 PAIR - 2 PAIR)

TRANSVERSE RESOLUTION

$\Delta Y \sim 10.$ CM $\quad \frac{\Delta Y}{1.\text{KM}} = \frac{(P_t = 100)}{(P_t = 1\ \text{T}}$

COSMIC RAYS - Interesting Observations 4odt

DIRECT: JACEE Nucleus - Nucleus Collisions TeV/an
- Rapidity fluctuations

Accelerator/collider planned → RHIC

INDIRECT

PEV EAS → Scale violation at large x (W^2) → P-dominated composition (↓ 30 year problem)

σ ↑

PEV EAS → "Conventional" models e.g. Gaisser Halzen → Mixed Comp. Fe dominated > 10 PeV ⇓ Models of CR Acc, Prop, Origin

> EeV EAS → ARE THEY DECAYS OF PRIMORDIAL "THINGS" → γ, p

ARE THEY ACCELERATED ISM MATERIAL → Fe ⇓ LOCAL VS Cosmological

- NEED TO FIND ENERGY DEPENDENCE OF $x\,dn/dx$ large x, inelasticity, Nuclear Screening

Anomalies : NOT UNDERSTOOD

① MUON BUNDLES .... MIYAKE' event

② CENTAUROS, CHIRONS ..... CHACALTAYA EM. EXP

③ Long Flying Component (YAKOVLEV – TIENSHAN)

Deep Penetration of shower cores or hadrons in dense materials above 20 TeV .... What carries the energy? How?

④ 'Muonic' Showers from

CYG X-3	1978-84
HER X-1	1986
CRAB	Feb 89

High multiplicity
High Inelasticity

OR

Scale violations in large x regions

MAKE P-showers Look Like Fe showers As far as Shower size is concerned

↑

This determines triggers

GBY-4

COMMENTS ON RELEVANCE TO COSMIC RAYS OF FAD

Gaurang B.Yodh

SIMULATION STUDY

INTERACTION MODEL DEPENDENCE OF SOME SHOWER PARAMETERS

Strong Dependence on Scaling Violation at Large x

- Model F-Y00 Fixed interaction lengths and Scaling in x
- Model M-Y00 Decreasing λ_{int} and scaling in x
- Model M-F00 Decreasing λ_{int} and Violation so scaling in x
- Model M-F01 Decreasing λ_{int} and Violation of scaling in x and Charge exchange added in pion and kaon collisions.
- Model R-F01 More rapidly Decreasing λ_{int} and Violation of scaling in x and Charge exchange added in pion and kaon collisions.

Problem of treating Nucleus-Nucleus Interactions

- Use superposition Model
- Use more sophisticated model. e.g. Gaisser et al.

WADTNIAK & YODH LA JOLLA ICRC 1985 HE volume

Table 1 Comparison of features of two basic models used.

	Model F-Y00	Model M-F00
Mean free paths for inelastic interaction	Energy-independent: nucleons: 75 g/cm² pions: 110 g/cm² kaons: 130 g/cm²	Below 1 TeV nucleons: 84 g/cm² pions,kaons: 117 g/cm² Above 1 TeV $L(E) = L_0/(1+.0383*\mathrm{Ln}\ E)$
Inelasticity	Uniform in (0,1) for nucleons and (1/3,1) for mesons	
Inclusive distributions in x = E/E[interaction] for secondaries	Energy-independent: scaling extrapolation of the ISR data	Below 1 TeV as Y00; above: the functional shape is unchanged, but the scale x-value decreases as $1/E[\mathrm{int}]^{.125}$
Secondaries produced	Charged pions - 60% Neutral pions - 30% Charged kaons - 5% Neutral kaons - 5%	Below 1 TeV as Y00; above: the fractions of kaons and neutral pions increase with energy, reaching at 1EeV 6.8% (each) and 53.7%, respectively
Charge exchange of an interacting meson	None (i.e. the leading particle emerging from the interaction is always identical in kind to the interacting one)	
Transverse moments	See [3]; irrelevant here, as we present only longitudinal EAS properties	

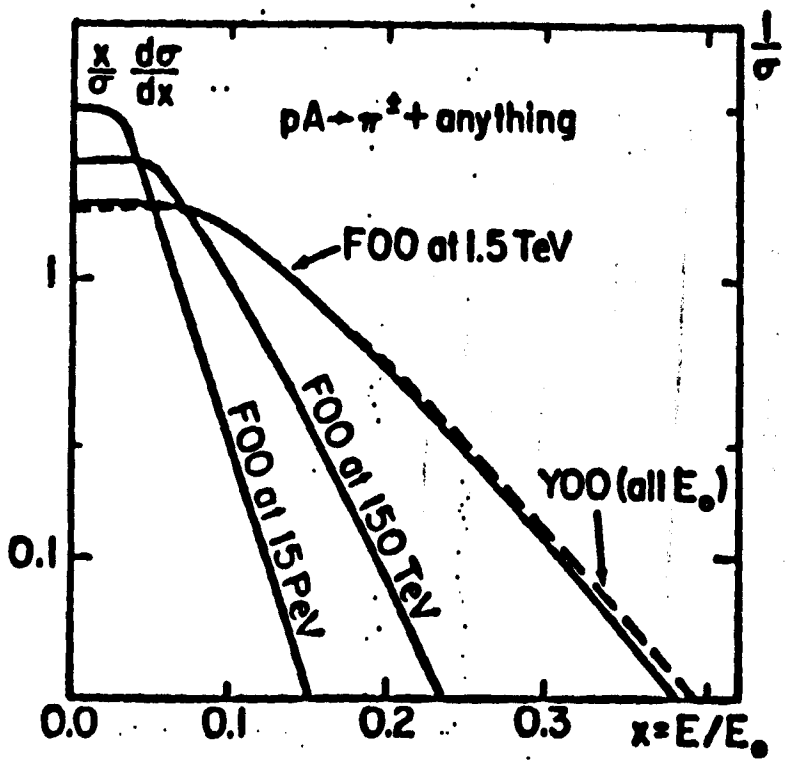

Fig.1. The distributions of x=E/E(int) for models used in our study.

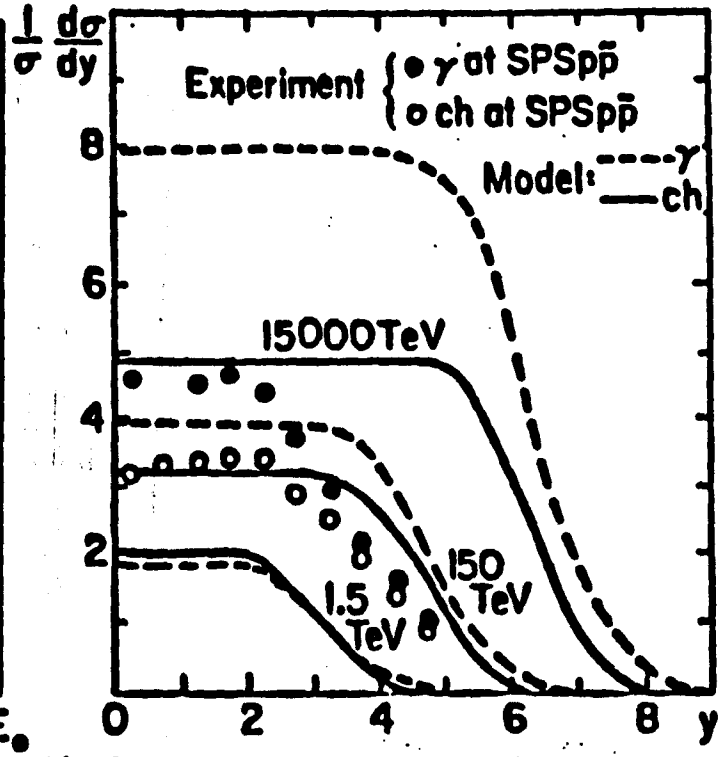

Fig.2. The rapidity distributions compared with pseudorapidity data from SPSpp.

REMARKS ON COMPOSITION OF COSMIC RAYS AND MODELS

- It is important to know the energy dependence of the interaction length or P-P cross section at 40 TeV.
- The energy scale for the highest energy cosmic ray experiments , even if they are of single species, can vary by as much as 1.4 GeV/particle to 1.6 GeV/particle at shower maximum the difference increasing at larger depths.
- Mass sensitivity does depend on the model

GBY-

- Above 10 EeV it is essential to know the nature of the particle initiating the shower. Can one tell the difference between a gamma or proton initiated shower ? Can one tell p and γ from iron initiated shower ? The latter would be expected if cosmic rays are galactic.

- Showers propagation depends on the shape of the x distribution at large x . It of course depends on the inelasticity. End cap calorimeter in FAD could measure the production of neutral particles at very large x. This is shown in figures that follow

GBY-7

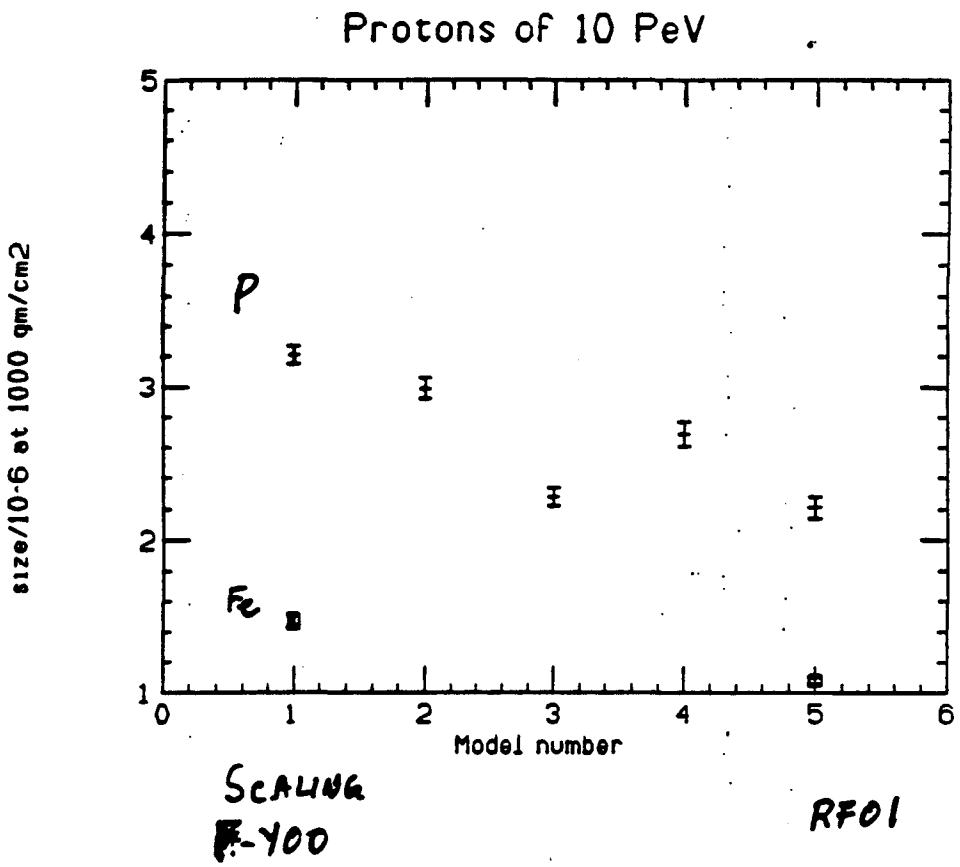
Protons of 10 PeV
size/10-6 at 1000 gm/cm2
Model number
P
Fe
SCALING
F-400
RF01

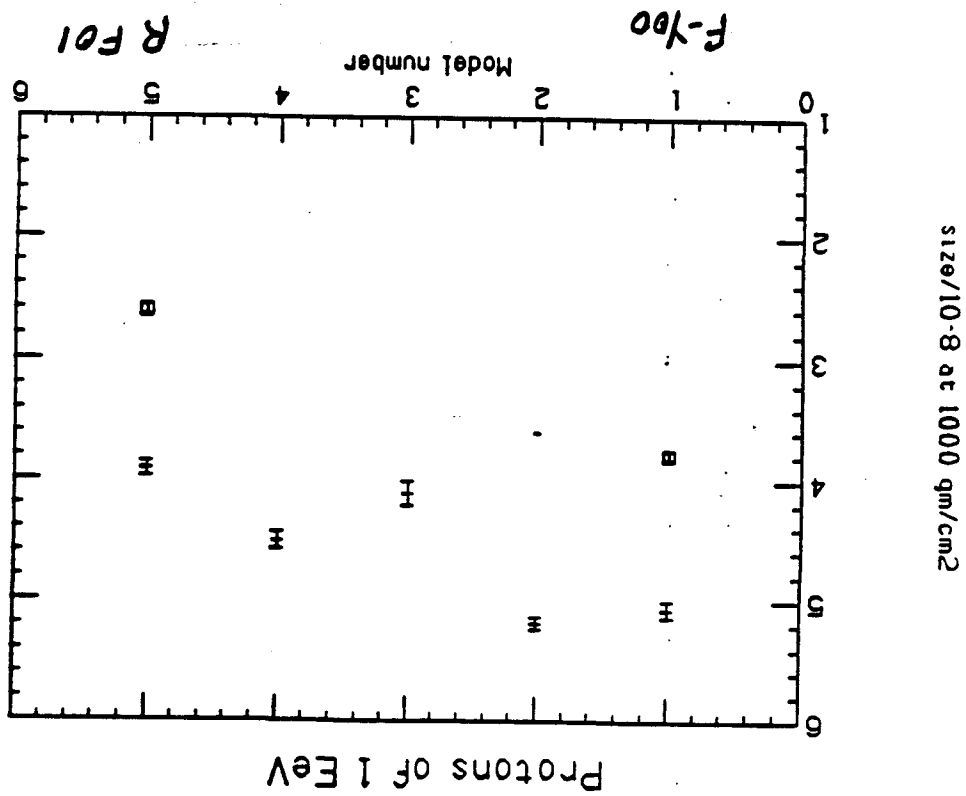
Protons of 1 EeV
size/10-8 at 1000 gm/cm2
Model number
F-400
R F01

G 67-11

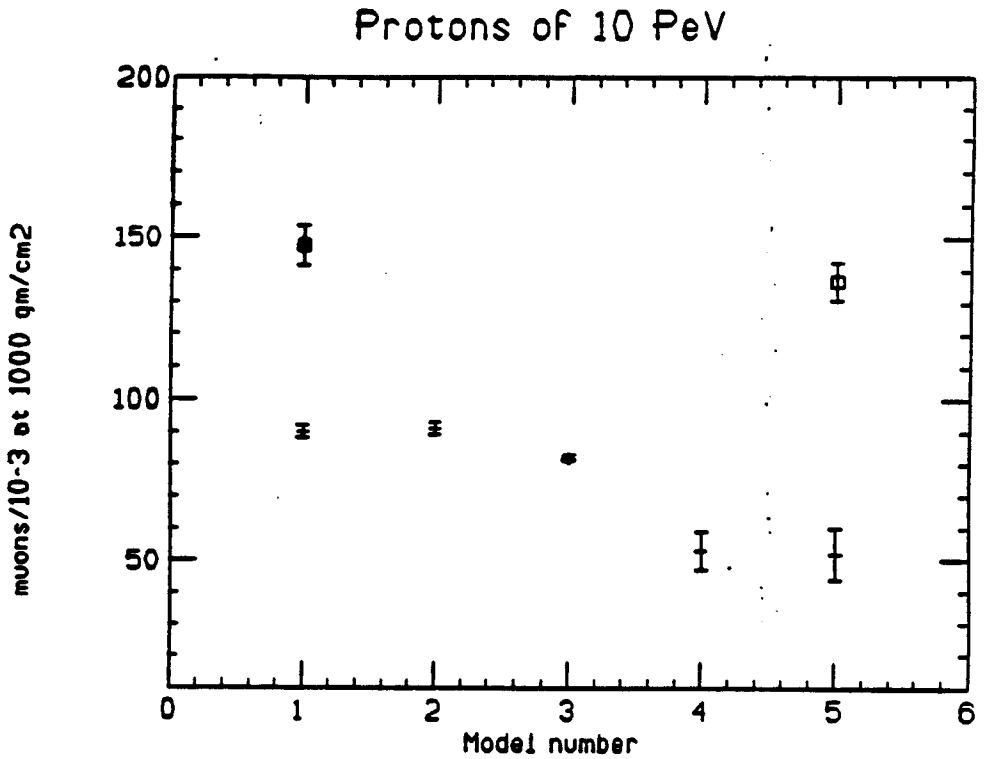
Protons of 10 PeV
muons/10-3 at 1000 gm/cm2
200
150
100
50
0
1
2
3
4
5
6
Model number

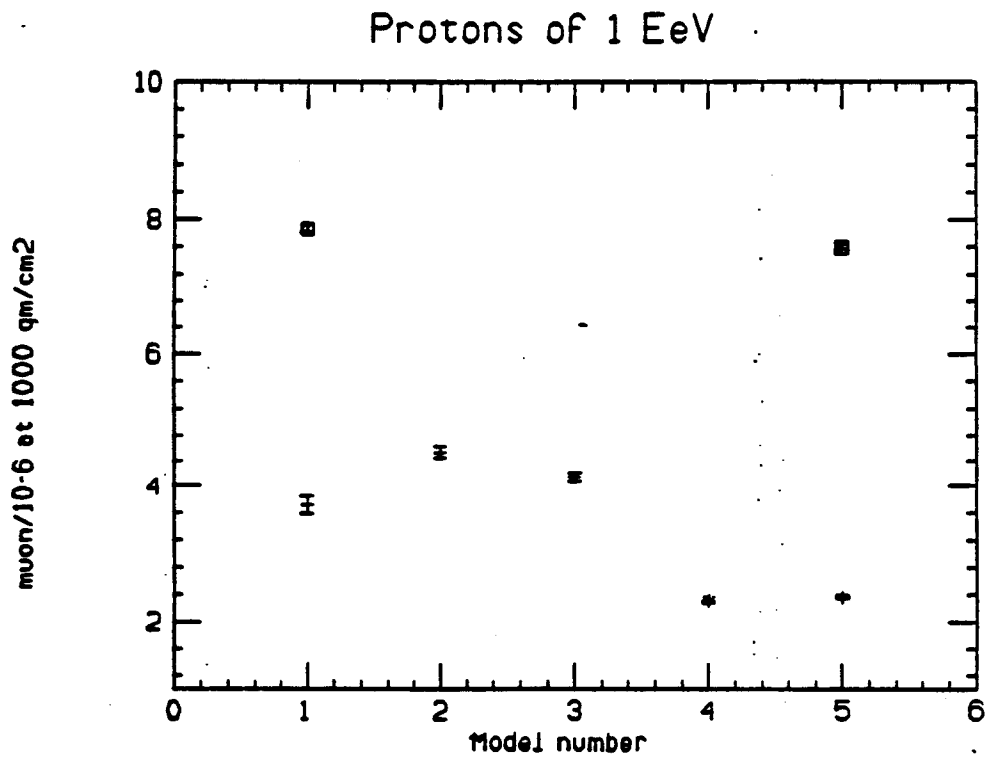
Protons of 1 EeV
muon/10-6 at 1000 gm/cm2
10
8
6
4
2
0
1
2
3
4
5
6
Model number

GBY-12

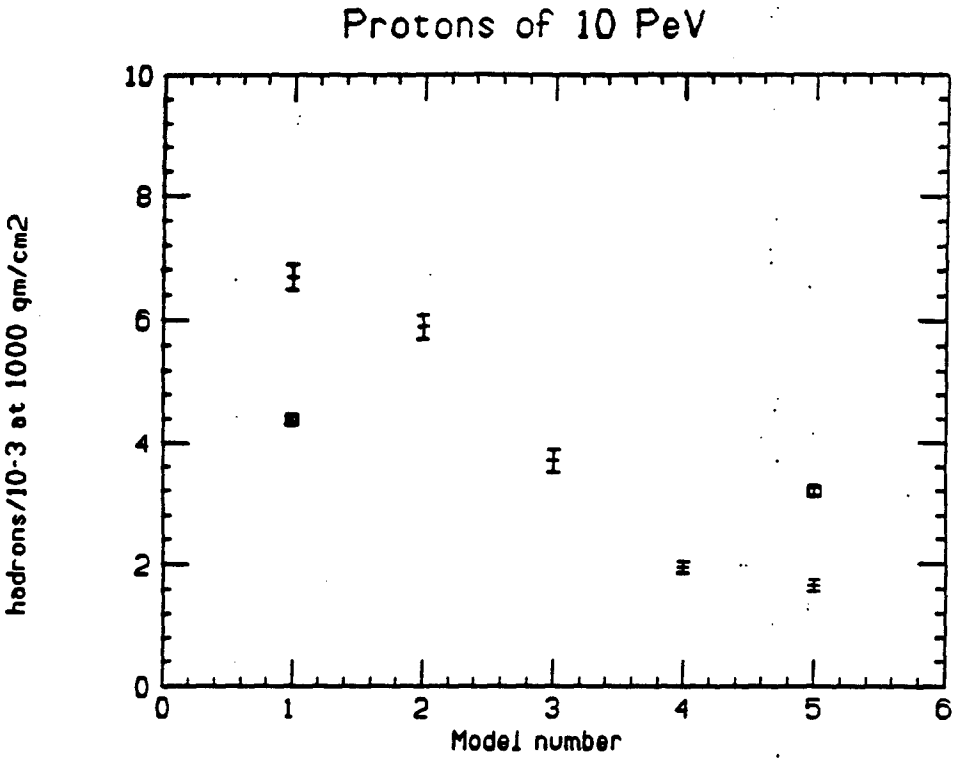
Protons of 10 PeV
hadrons/10-3 at 1000 gm/cm2
Model number
0
2
4
6
8
10
0
1
2
3
4
5
6

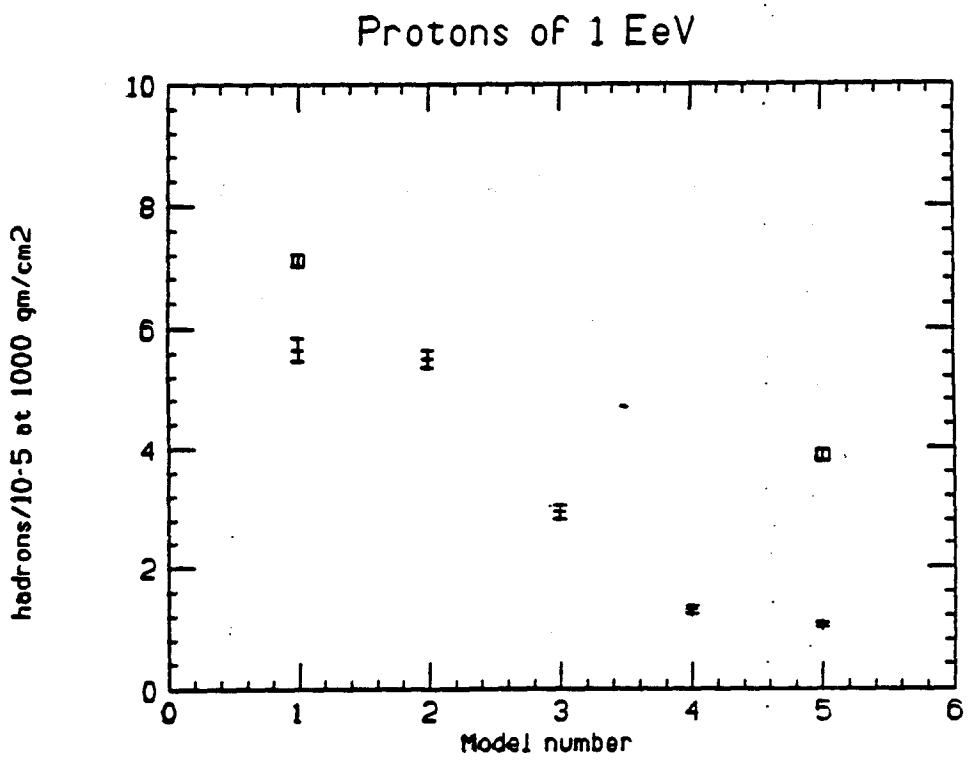
Protons of 1 EeV
hadrons/10-5 at 1000 gm/cm2
Model number
0
2
4
6
8
10
0
1
2
3
4
5
6

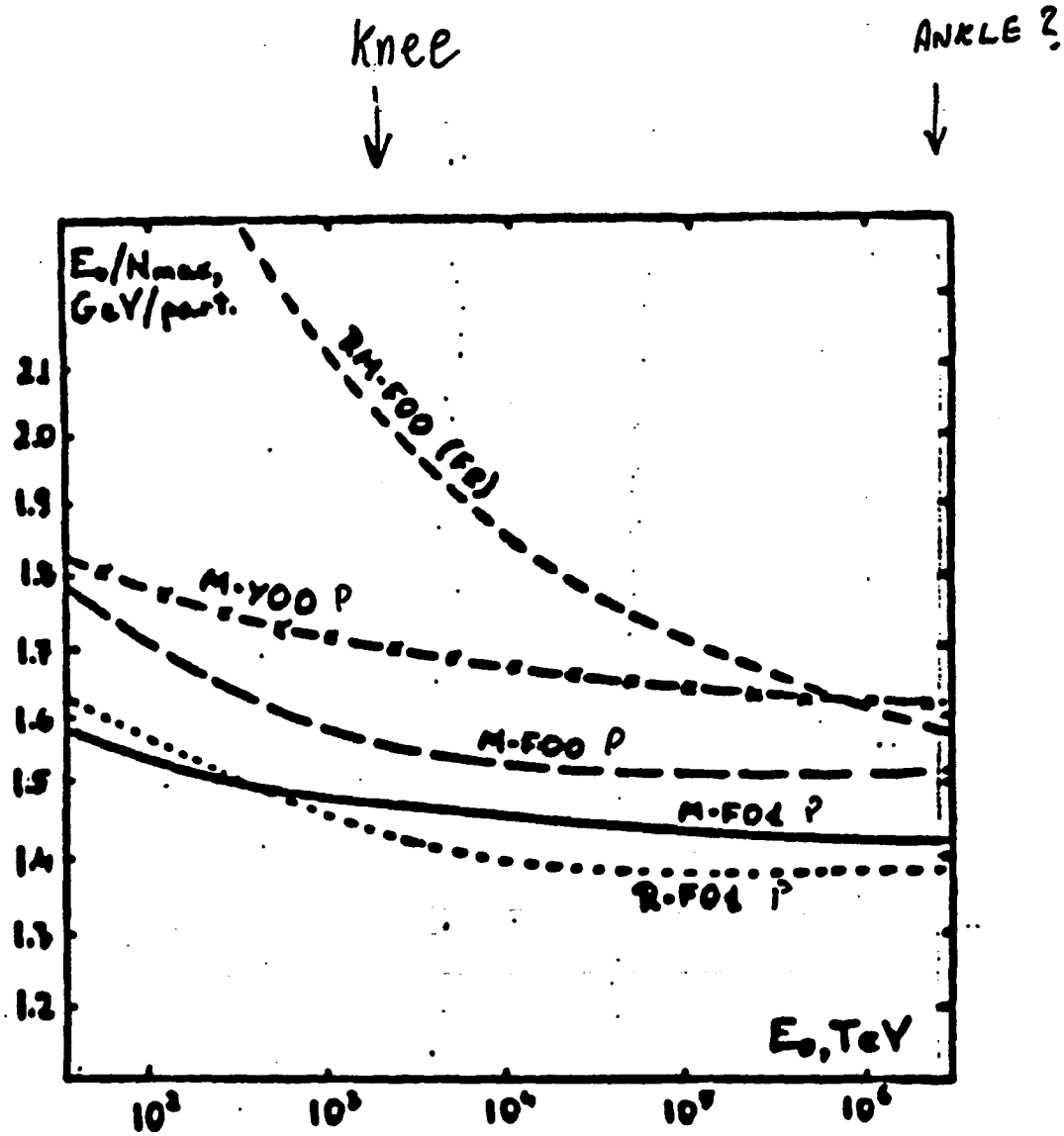

Fig.2. Energy per electron at the shower maximum.

SIMULATION OF MINIMUM BIAS EVENTS

Regions of x_F and p_t accessible to a FAD Wall Calorimeter

by Robert Ellsworth

- Two different configurations for wall Calorimeter used:
  - 45 cm lateral dimension
  - 15 cm lateral dimension
  - For 45 cm Three energies: ISR, Tevatron Collider, SSC
  - For 15 cm Only SSC energy

Remarks on the Results:

- Model was a previously used model for Cosmic Ray simulations called BANG2
- Table 1 compares simulation with experiment:
- Some observations:
  - The average charged multiplicity for $\eta < 3$ at 1.8 TeV compares well with observations, so does the maximum rapidity density for charged particles. KNO scaling is reproduced.
  - Change in invariant pi-zero cross section is seen in going from 63 GeV to 40 TeV.
  - Distributions of x_F for γs with psuedorapidity $\eta > 8.4$ are shown. Also shown are the distributions for gammas hitting a detector at 1 Km of 45 cm and of 15cm transverse size.
  - Detected x values go to rather small x s with low p_ts.
  - For a 45 cm detector: $< p_t >= 173 MeV$ for Triggered γ s whose average number was 2.8 and an energy deposit of 1.7 TeV.

GBY-16

1.8 TeV

40 TeV

Ch Mult

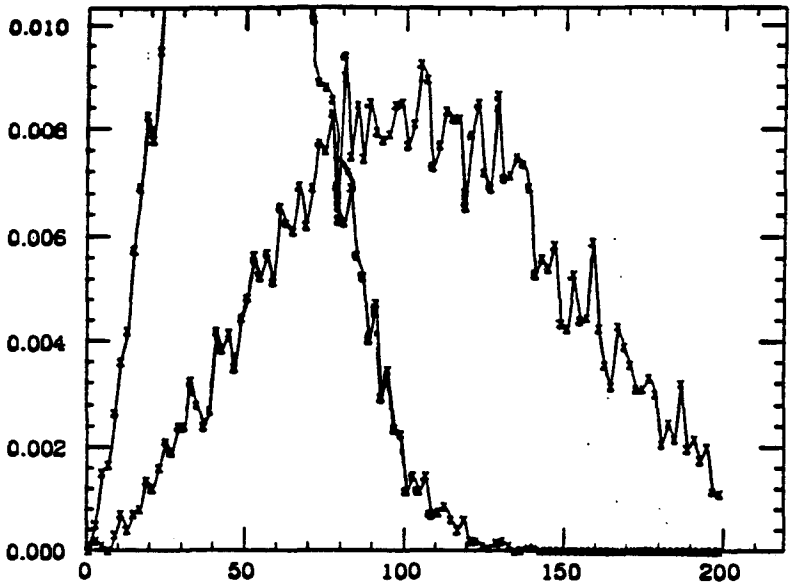

Ch Mult, Eta<Etamin

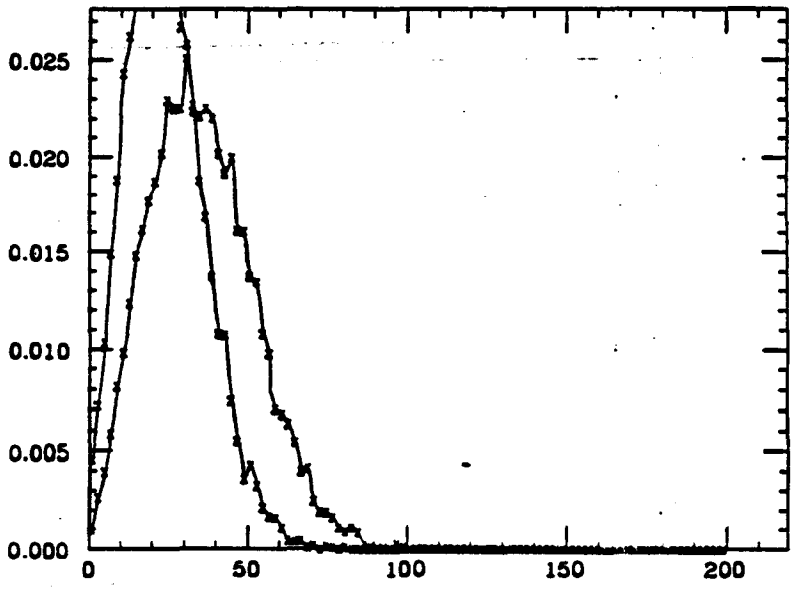

MC distribution Input -1

Pt, ch sec

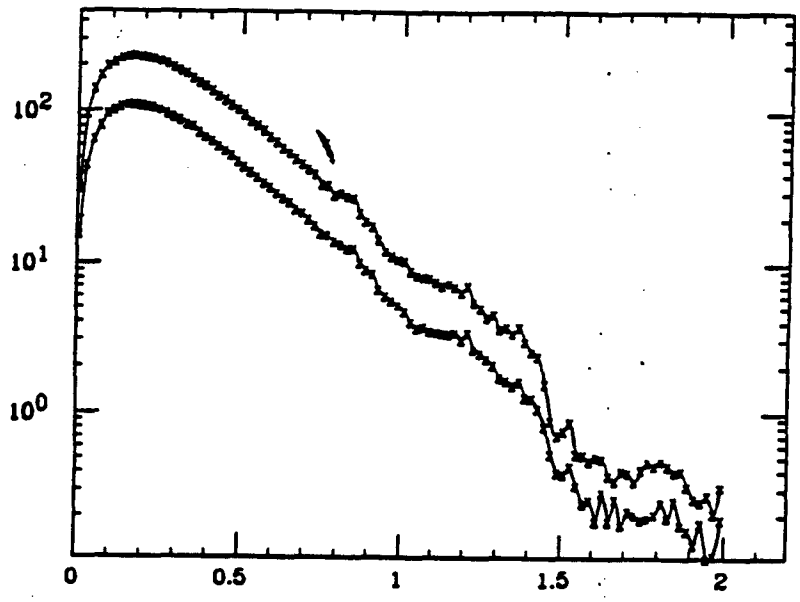

Pt Gammas

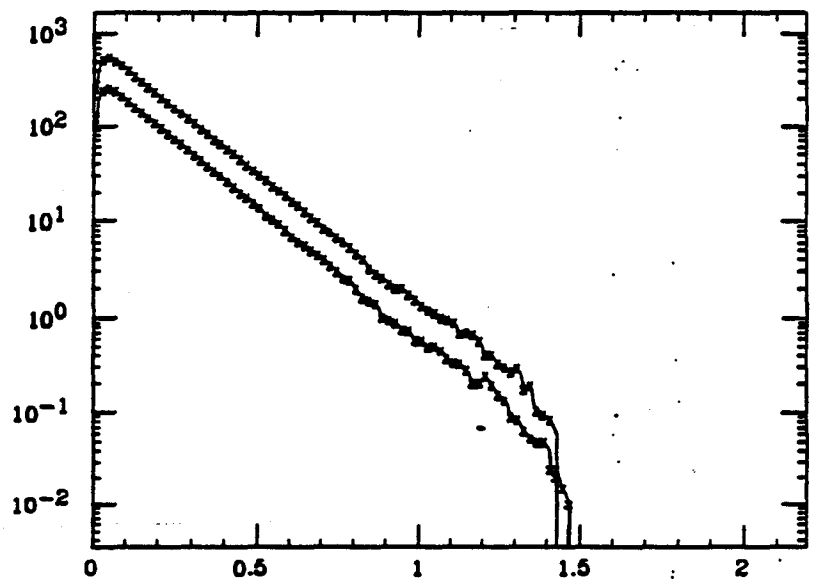

Mc simulation input -2

GBY-18

Eta Gammas

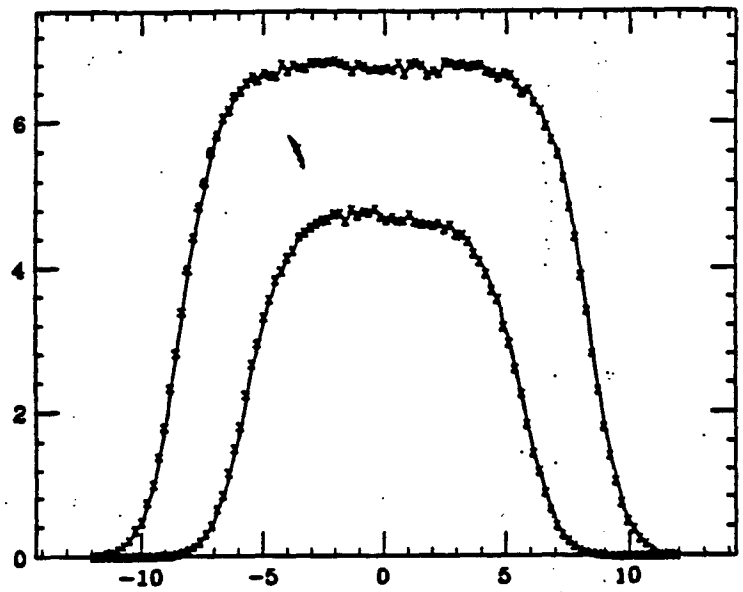

Gamma energy

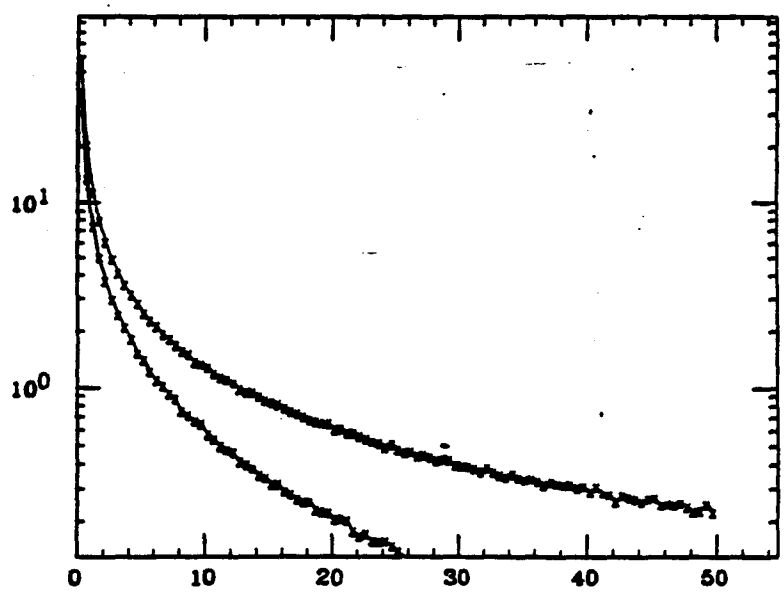

MC Simulation Input-3

GBY-19

True rapidity, ch

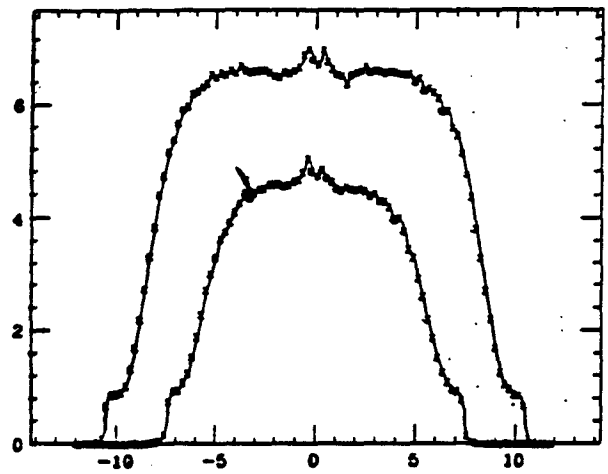

x*dn/dx gammas

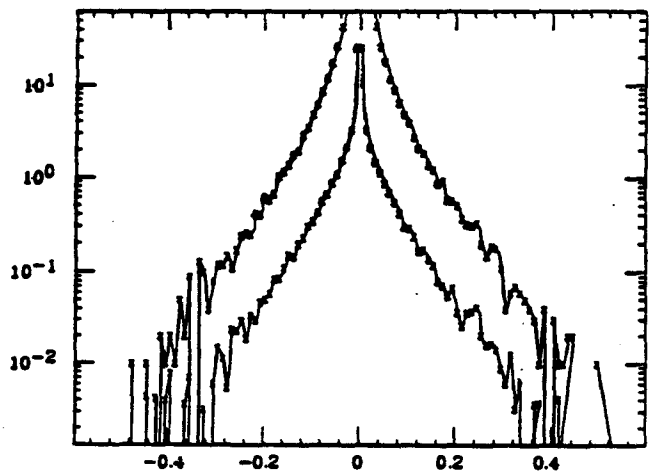

MC-Sim. Input-4

TABLE 1

$\sqrt{s}$	$\langle n_c \rangle^{ob}$	$\langle n_c \rangle^{sim}$	$\left(\frac{dn}{d\eta}\right)^{o}_{max}$	$\left(\frac{dn}{d\eta}\right)^{sim}_{max}$
63	12.7	14.8	2.0	1.8
1800	28.0	24.6	4.7	4.4
40,000		109		7.5

Fig 1 x*dn/dx pizeros

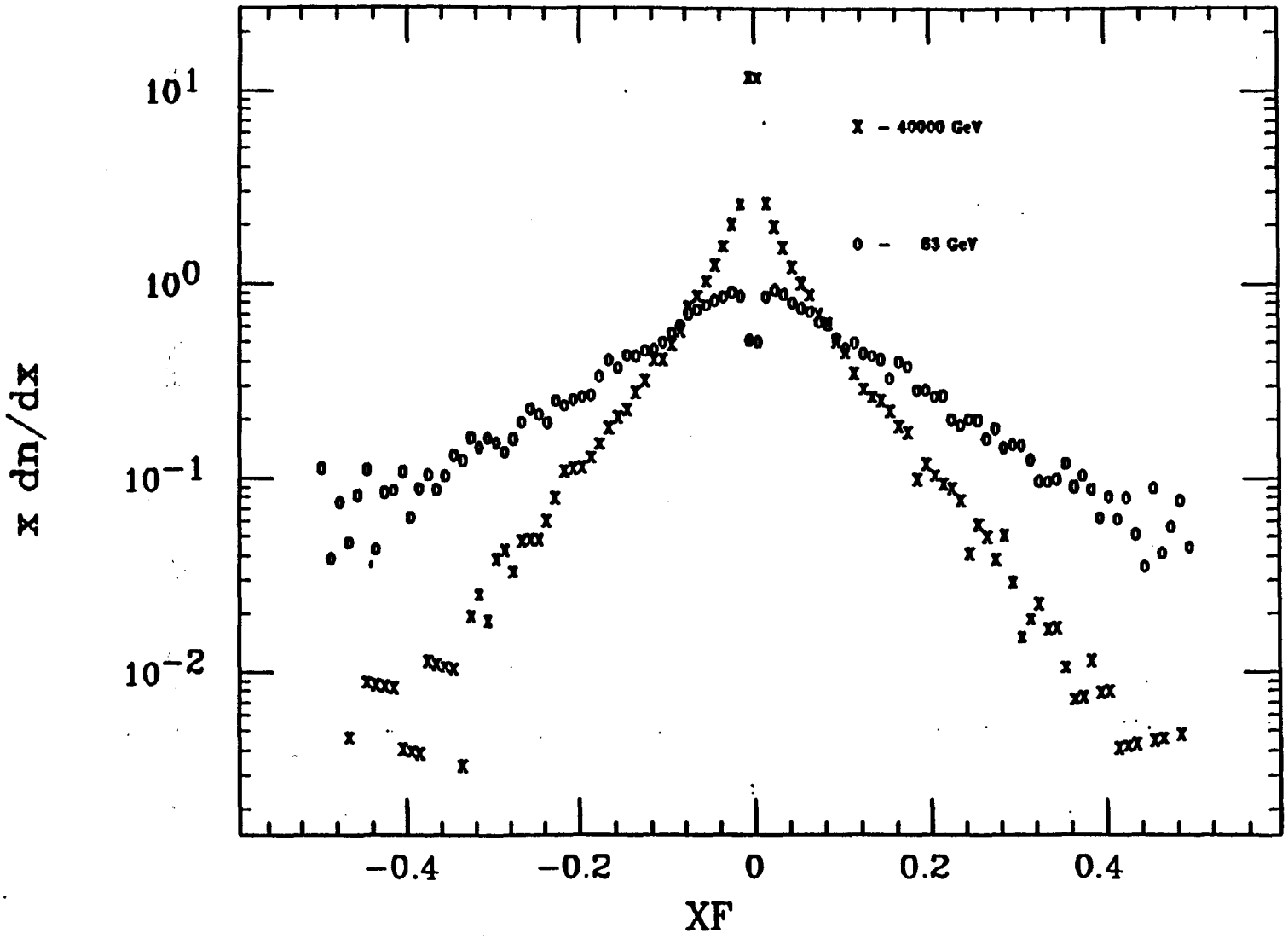

5-MAR-92 11:58:00

6697-21

FIG 2 XF gammas 45cm End WALL

$\eta > 8.4$

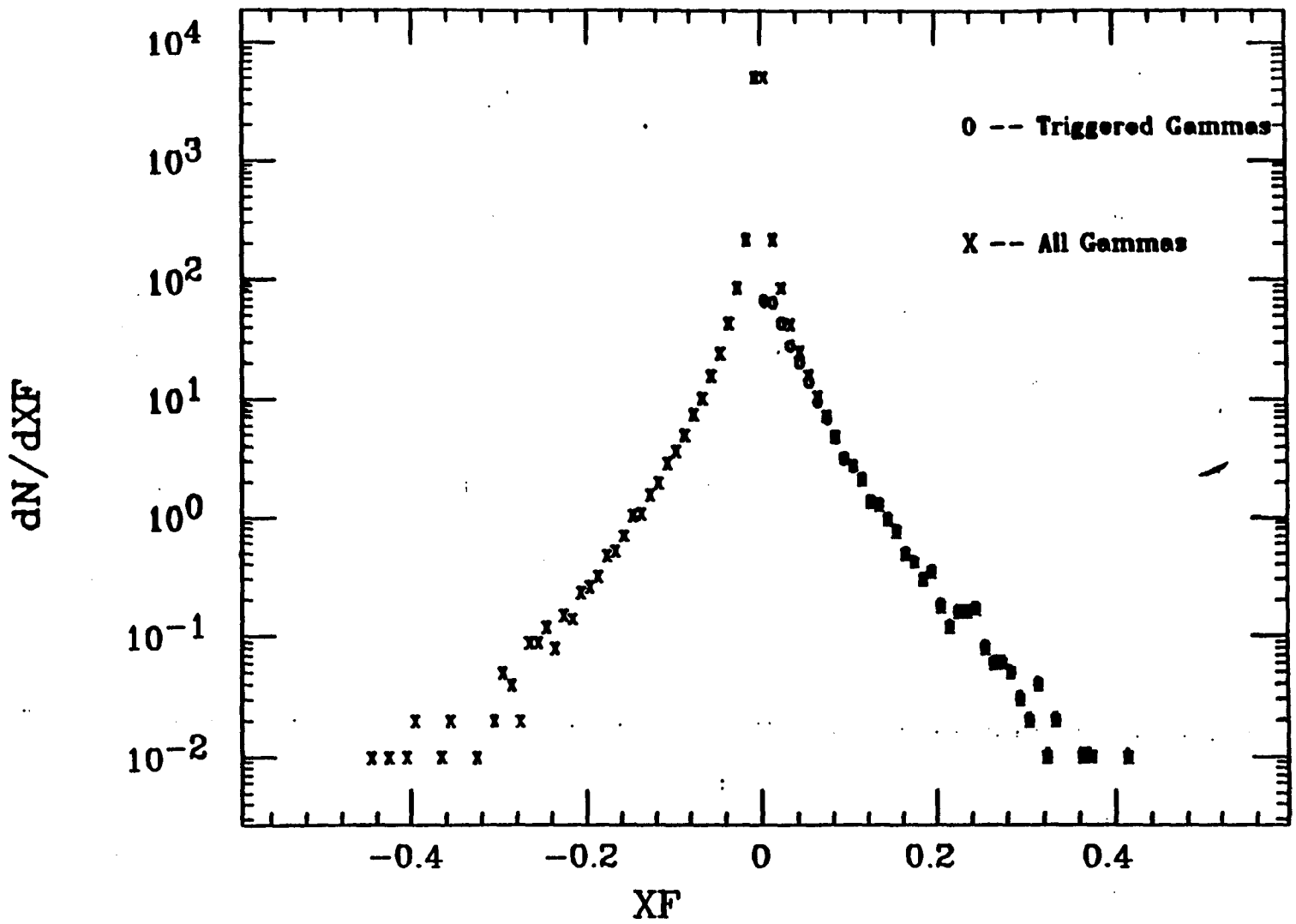

66Y-32

x*dn/dx ALL, TRIG GAMMAS ETA>9.5

15cm

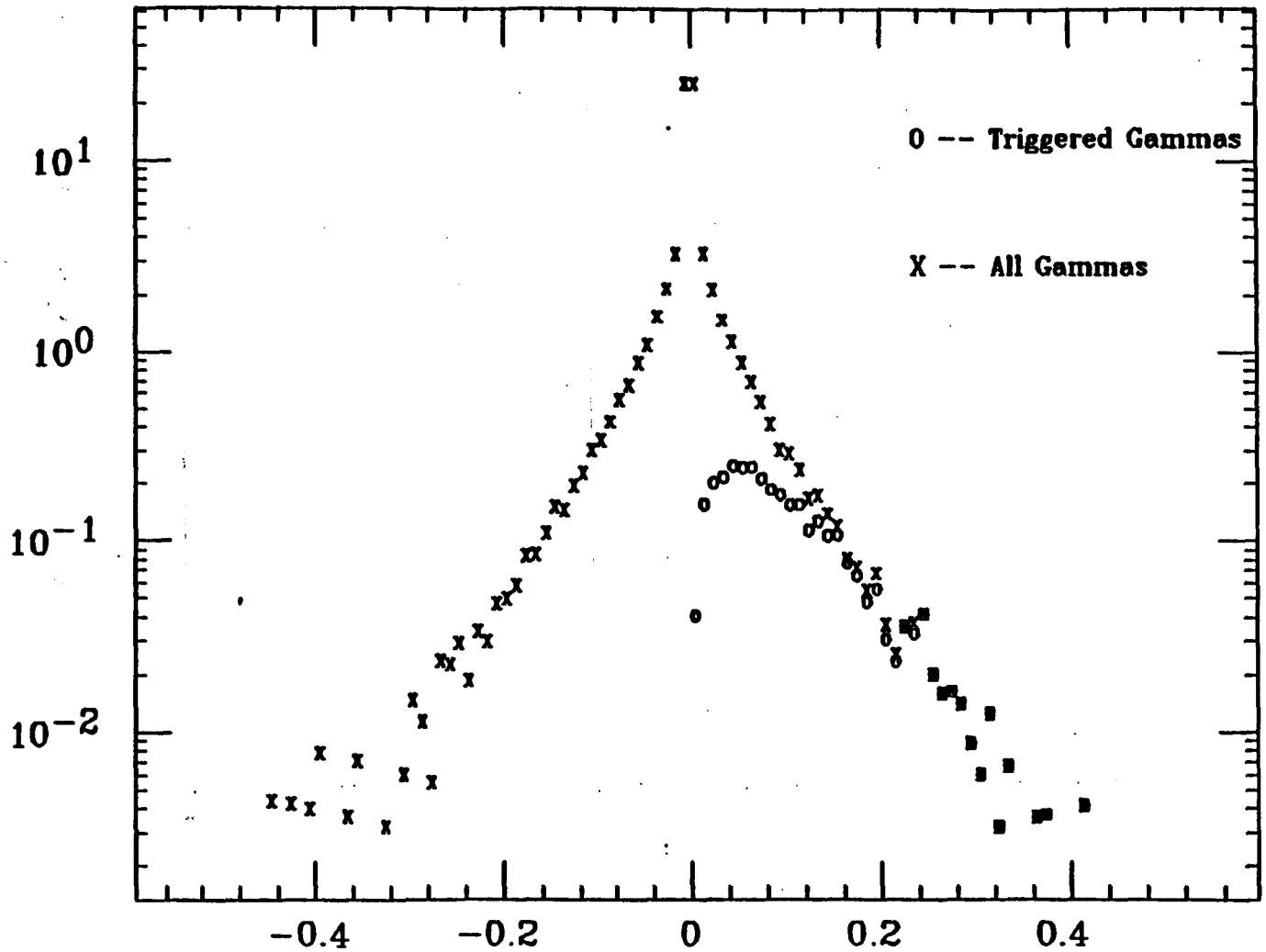

10-MAR-92 17:53 30 40 00

GGY-23

GBY-24

x*dn/dx trig gammas

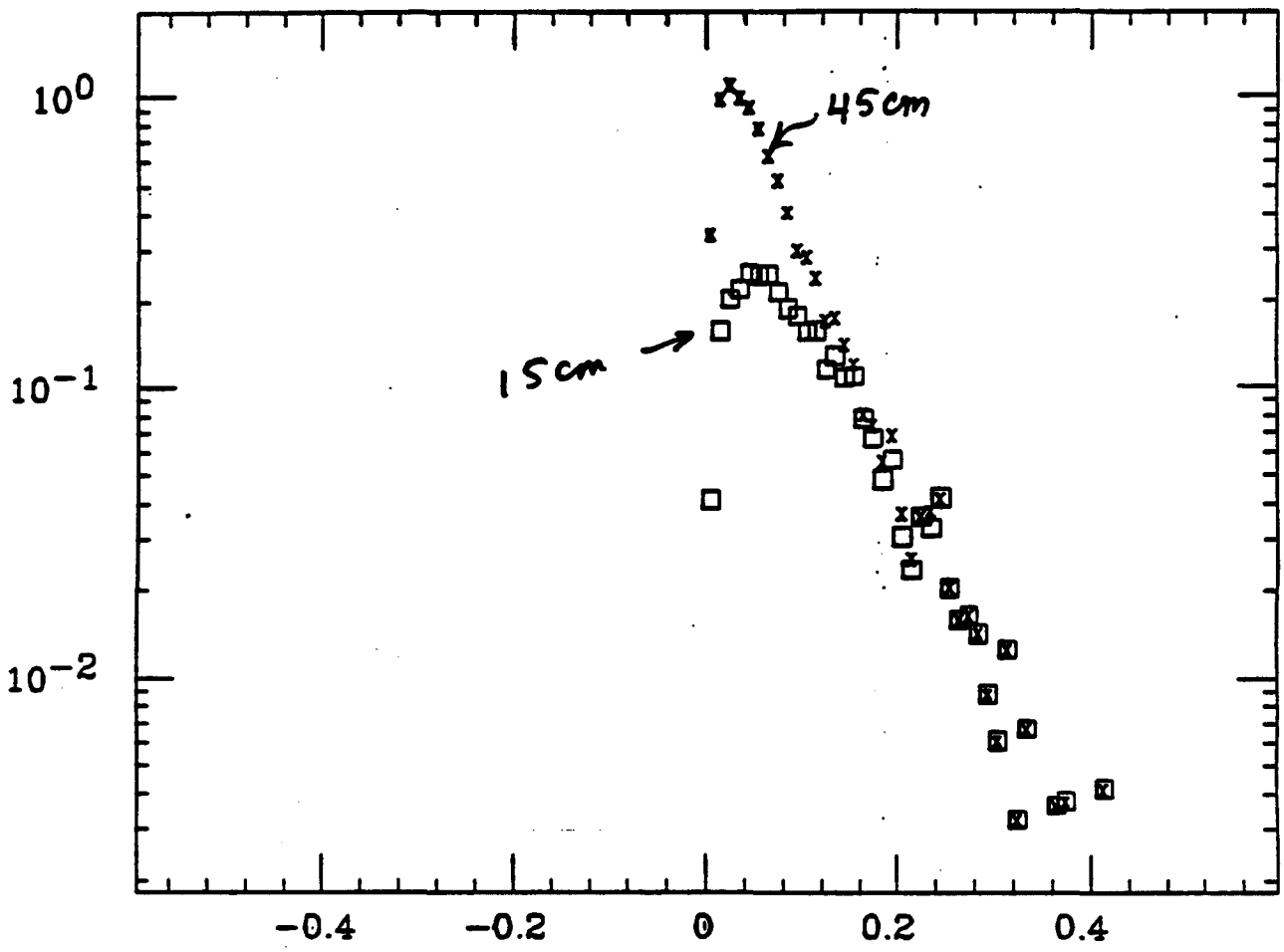

10-MAR-82 15:43:27 40.00

x ... 45 cm

□ ... 15 cm

GB4-25

Inter-gamma dist at Wall

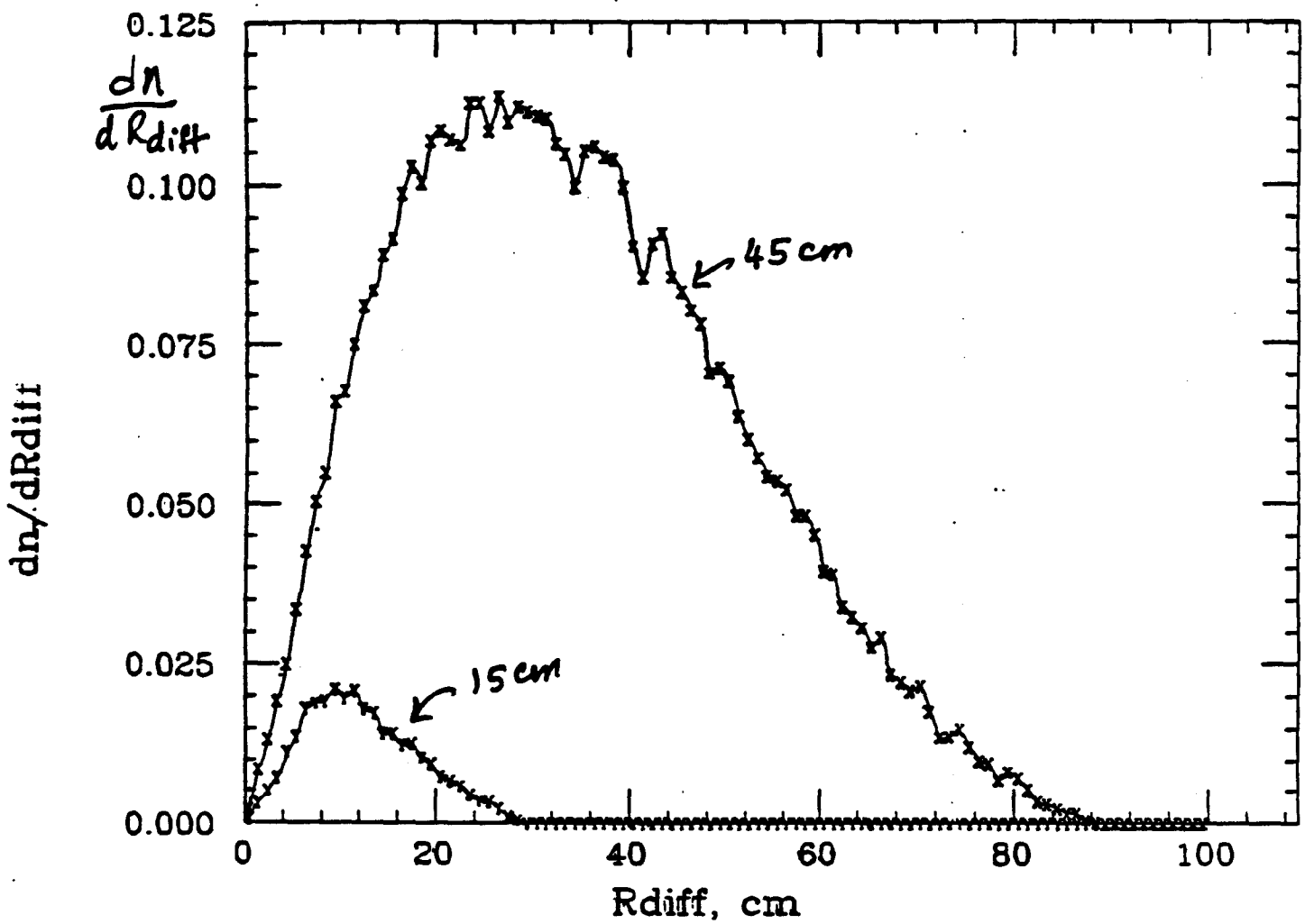

10-MAR-92 15:43:30 40.00

Kalbfleisch

[GRK → B_j WKSHP "SECRETARIAT" 3/14/1992]

3/14/92

$B\bar{B}$ @ SSCL

① $\sigma \rightarrow X4$ BERGER ELLIS

$\Rightarrow$ 2-3% σ_T

② PROBABLY UNCORRELATED

$\Rightarrow \sim (\Delta\eta)^2$ B_1 + TAG

BUT DECAY SPREAD

$\sim \Delta\eta = 1^+$

$$\sim (\Delta\eta - 1^+)^2$$

③ TOTAL $\Delta\eta$

$\approx \pm 5.5$ B's

$$\left(\frac{\Delta\eta - 1^+}{11 - 1}\right)^2 = \text{F.O.M}$$

$\downarrow$

FULL "~~BCD~~" 100%

WANT ?

SINGLE ARM, BARREL

$\Delta\eta \sim 3$

$\Longrightarrow$ $\boxed{\text{few \%}}$

? START IN 3 COM ?

attainable just with the silicon tracking within the beam pipe should be competitive with what is attained for particles of p_t of 1·2 GeV using the full detector. Likewise the low p_t photons, difficult to see at 90 degrees in most detectors, turn into reasonably energetic ones in the forward direction beyond, say, rapidities of four or so. We might mention that the interesting products of the pion clouds of the projectiles have laboratory angles of no more than 50 microradians.

It should be clear that if bulk chiral condensate is in some sense observable in hadron-hadron collisions, it is a matter of quite fundamental importance. Just as the relationship of the quark-gluon plasma phase to the normal phase tells us about the nature of confinement, this phenomenon might tell us something about the nature of the chiral phase. Phenomena involving the chiral phase may in turn be very similar to what happens in the Higgs sector. Additional insights into the poorly-understood hadronic analogue might have quite far-reaching implications.

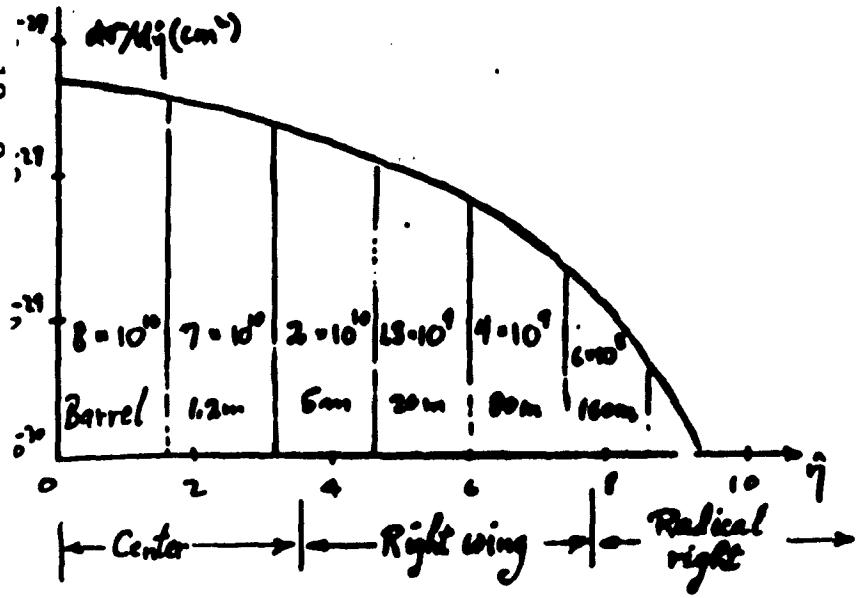

Figure 3.2. Yield of charmed hadrons as function of rapidity, along with the number acquired per SSC year by the various modules of the detector.

EOI- 19

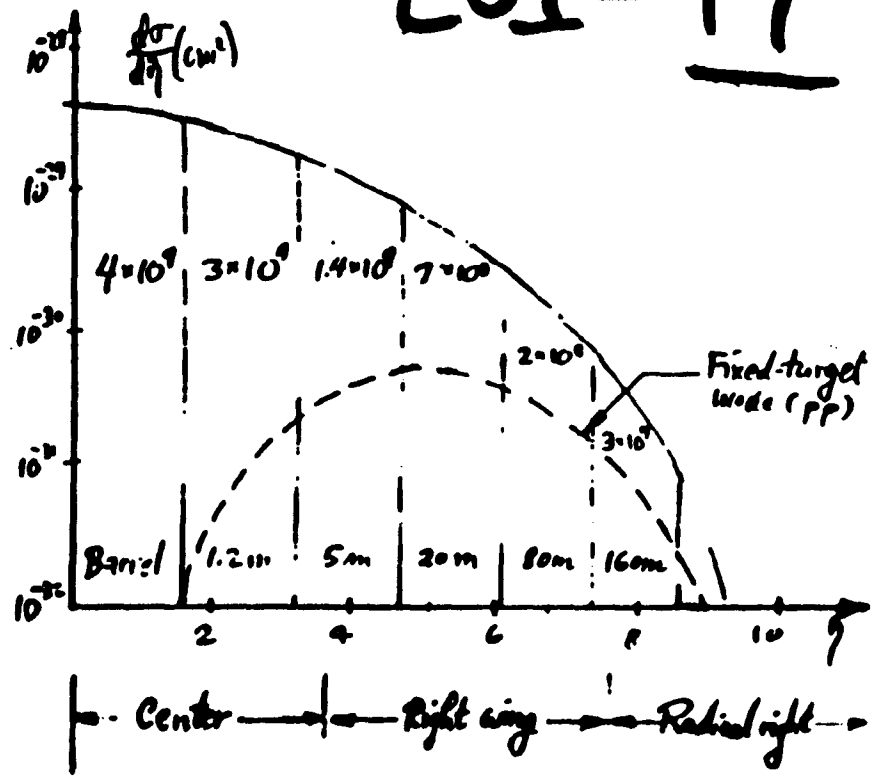

Figure 3.3. Yield of bottom hadrons as function of rapidity along with the annual yield into the modules of the spectrometer. Also shown is the yield in fixed-target mode. A hydrogen gas-jet target is assumed.

8. Charm

The yield of charmed hadrons into this spectrometer is enormous, and is shown in Fig. 3.2. One sees that much of the yield is quite far forward, allowing a lot of choice in where to concentrate one's efforts. By the year 2000, the state of the art should be, according to Fermilab planning, over one million reconstructed charm events per experiment. In addition, large super-clean samples of comparable size should be available from the electron-positron tau-charm factory in Spain. Looking

Central or Forward?

- **Central:** $|\eta| < 1.2 - 1.5$

  Low $P \Rightarrow$ poorer secondary vertex resolution.

  Solenoid or dipole?

  Solenoid is poor match to $\eta > 1.5$.

  Tracking, P_t trigger easier in solenoid.

  20% loss of azimuth in central dipole.

- **Forward:** $1.2 < \eta < 5.5$

  Detectors more accessible, $\Rightarrow$ cheaper.

  Vertex detector can use disks only.

  Interactions in beam pipe are troublesome.

  Good momentum analysis via central dipole.

  Compensating dipoles $\Rightarrow$ no net kick for $|\eta| > 5.5$.

Table 2: The minimum values of $\sin 2\varphi_i$ resolvable to three standard deviations in 10^7 sec of running at luminosity of 10^{32} cm^{-2}sec^{-1}in an SSC experiment covering $1.2 < \eta < 5.5$.

Angle	Mode	Tag	Tagged Events	$1-2p$	b	x_q	D	$\sin 2\varphi_{\min,3\sigma}$
φ_1	$B_d^0 \to J/\psi K_S^0$	$e^\pm$	9,600	0.60	0.1	0.7	0.47	0.11
φ_1	$B_d^0 \to J/\psi K_S^0$	$K^\pm$	73,000	0.40	0.1	0.7	0.47	0.066
φ_2	$B_d^0 \to \pi^+\pi^-$	$e^\pm$	40,000	0.60	1.0	0.7	0.47	0.076
φ_2	$B_d^0 \to \pi^+\pi^-$	$K^\pm$	307,000	0.40	1.0	0.7	0.47	0.041
φ_3	$B_s^0 \to \rho^0 K_S^0$	$e^\pm$	267	0.60	1.0	~ 10	0.64	0.68
φ_3	$B_s^0 \to \rho^0 K_S^0$	$K^\pm$	2,300	0.40	1.0	~ 10	0.64	0.34
φ_3	$B_s^0 \to K^+K^-$	$e^\pm$	1,000	0.60	~ 0.1	~ 10	0.64	0.27
φ_3	$B_s^0 \to K^+K^-$	$K^\pm$	9,200	0.40	~ 0.1	~ 10	0.64	0.12
φ_4	$B_s^0 \to J/\psi\phi$	$K^\pm$	107,000	0.40	~ 0.1	~ 10	0.64	0.039

Table 1: Update of Table 11 of the BCD EOI to include a Kaon tag. The minimum values of $\sin 2\varphi_i$ resolvable to three standard deviations in 10^7 sec of running at luminosity of 10^{32} $cm^{-2}sec^{-1}$. The factor $1-2p$ is the analysing power of the tag which has a probability p for a wrong tag. b is the background to signal for the final-state reconstruction. The dilution factor D due to mixing is given by $x_q \coth(\pi/2x_q)/(1+x_q^2)$.

Angle	Mode	Tag	Tagged Events	$1-2p$	b	x_q	D	$\sin 2\varphi_{min,3\sigma}$
φ_1	$B_d^0 \to J/\psi K_S^0$	$e^\pm$	57,600	0.60	0.1	0.7	0.47	0.047
φ_1	$B_d^0 \to J/\psi K_S^0$	$K^\pm$	440,000	0.40	0.1	0.7	0.47	0.027
φ_2	$B_d^0 \to \pi^+\pi^-$	$e^\pm$	240,000	0.60	1.0	0.7	0.47	0.031
φ_2	$B_d^0 \to \pi^+\pi^-$	$K^\pm$	1,840,000	0.40	1.0	0.7	0.47	0.017
φ_3	$B_s^0 \to \rho^0 K_S^0$	$e^\pm$	1,600	0.60	1.0	~ 10	0.64	0.28
φ_3	$B_s^0 \to \rho^0 K_S^0$	$K^\pm$	14,000	0.40	1.0	~ 10	0.64	0.14
φ_3	$B_s^0 \to K^+K^-$	$e^\pm$	6,240	0.60	~ 0.1	~ 10	0.64	0.11
φ_3	$B_s^0 \to K^+K^-$	$K^\pm$	55,200	0.40	~ 0.1	~ 10	0.64	0.05
φ_4	$B_s^0 \to J/\psi\phi$	$K^\pm$	640,000	0.40	~ 0.1	~ 10	0.64	0.016

Table 3: The sensitivity of an asymmetric e^+e^- collider to $\sin 2\varphi_1$ at 3-σ statistical significance via the decay $B_d^0 \to J/\psi K_S^0$. A 'year' consists of 10^7 sec. The BCD sensitivity is 0.03 (0.07 for Phase I) in one year of running.

$\mathcal{L}$	Running Time (Years)		
$cm^{-2}sec^{-1}$	1	3	10
10^{33}	0.48	0.28	0.15
3×10^{33}	0.28	0.16	0.09
10^{34}	0.15	0.09	0.05

Table 4: The sensitivity of an asymmetric e^+e^- collider to $\sin 2\varphi_2$ at 3-σ statistical significance via the decay $B_d^0 \to \pi^+\pi^-$. The BCD sensitivity is 0.02 (0.04 for Phase I) in one year of running.

$\mathcal{L}$	Running Time (Years)		
$cm^{-2}sec^{-1}$	1	3	10
10^{33}	0.61	0.35	0.19
3×10^{33}	0.35	0.20	0.11
10^{34}	0.19	0.11	0.06

Summary

- Hadron colliders are the best B-factory investment in terms of ultimate potential.
- A dedicated B-physics experiment at FNAL could be comparable to one at an e^+e^- collider.
- The SSC promises statistical power $\gtrsim 10$ times that of FNAL or e^+e^-.
- A Phase I, \$50M-experiment at the SSC still has a factor of 3 statistical advantage over FNAL or e^+e^-.

BCD Program in 1991-1993

- Design lower-cost collider detector ($\sim$ \$50M).

  1. Naive scaling:

     Acceptance for both B's $\sim (\Delta\eta)^2 \sim (\text{cost})^2$.

     $\Rightarrow$ learn how to do better.

  2. $\Delta\eta = 3$ at SSC $\sim \mathcal{L} = 10^{34}$ at e^+e^- collider.

  3. Initial configuration: Central, Intermediate, or Forward?

  4. Preserve option to expand after successful Phase I.

- R&D

  1. Silicon vertex detector.

  2. Straw-tube tracking.

  3. Hadron ID.

  4. Online parallel computer farm (trigger, DAQ)

Silicon Detector Beam Tests

Iowa State U. – U. Oklahoma – Yale U.

- Study position resolution *vs.* angle of incidence.

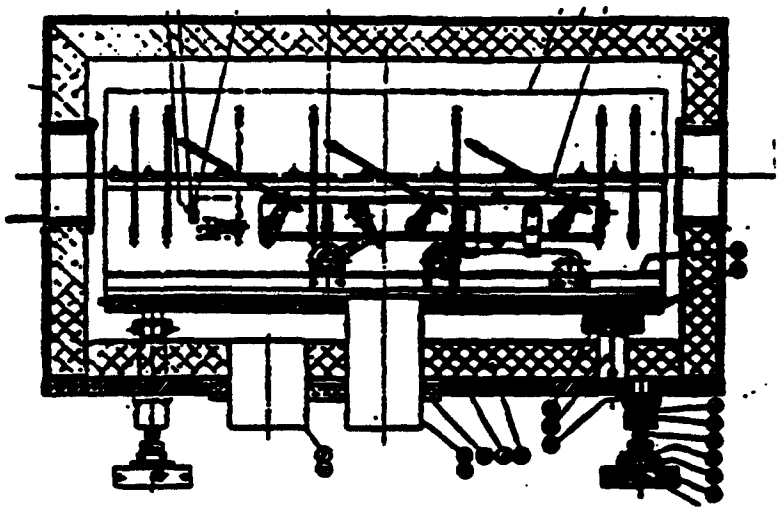

- Results on resolution ⊥ to track:

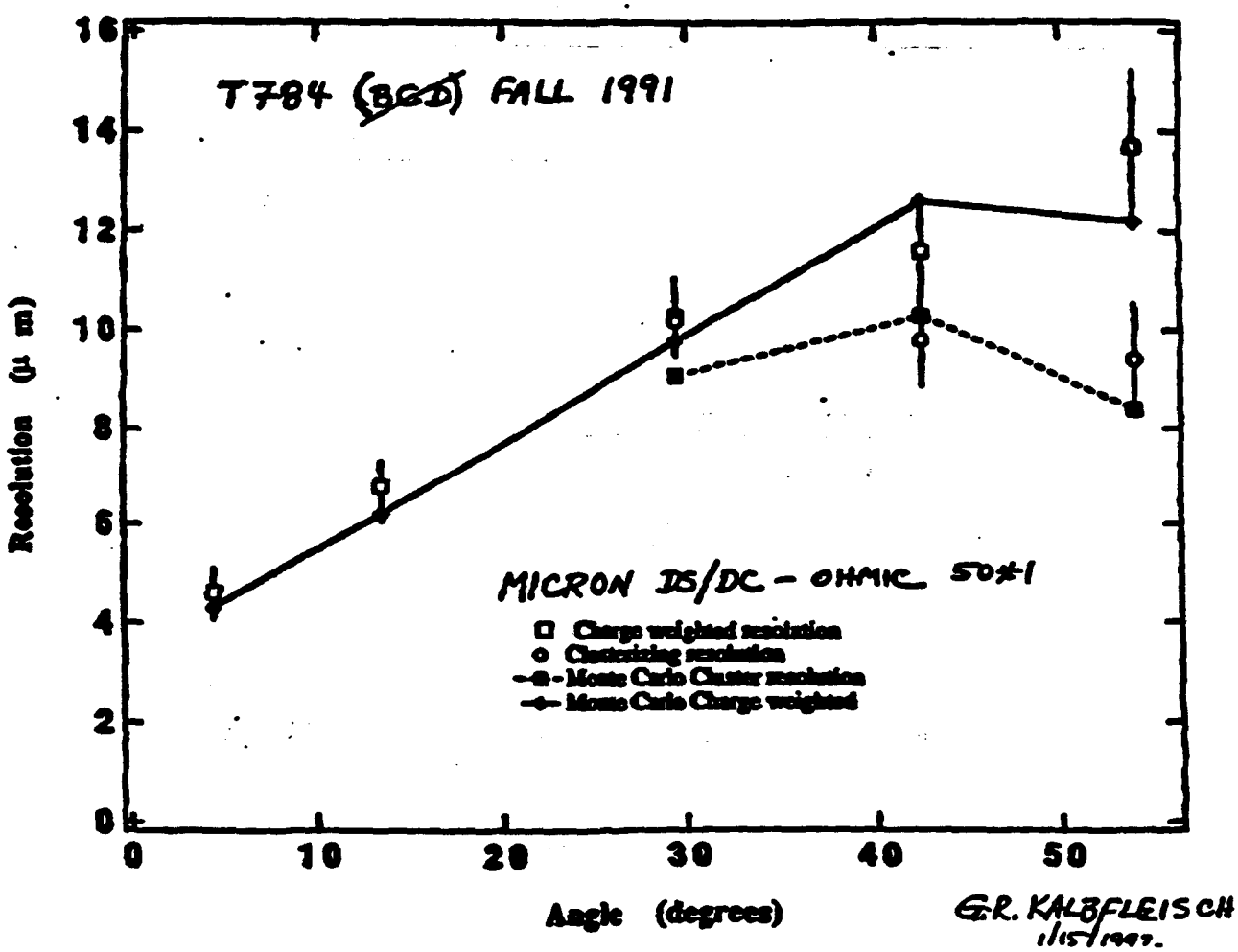

A Silicon Vertex Detector with Interleaved Disks and Barrels

Fermilab–Langston U.–U. Oklahoma–Princeton U.

- Hexagonal **modules** with spiral cooling path.

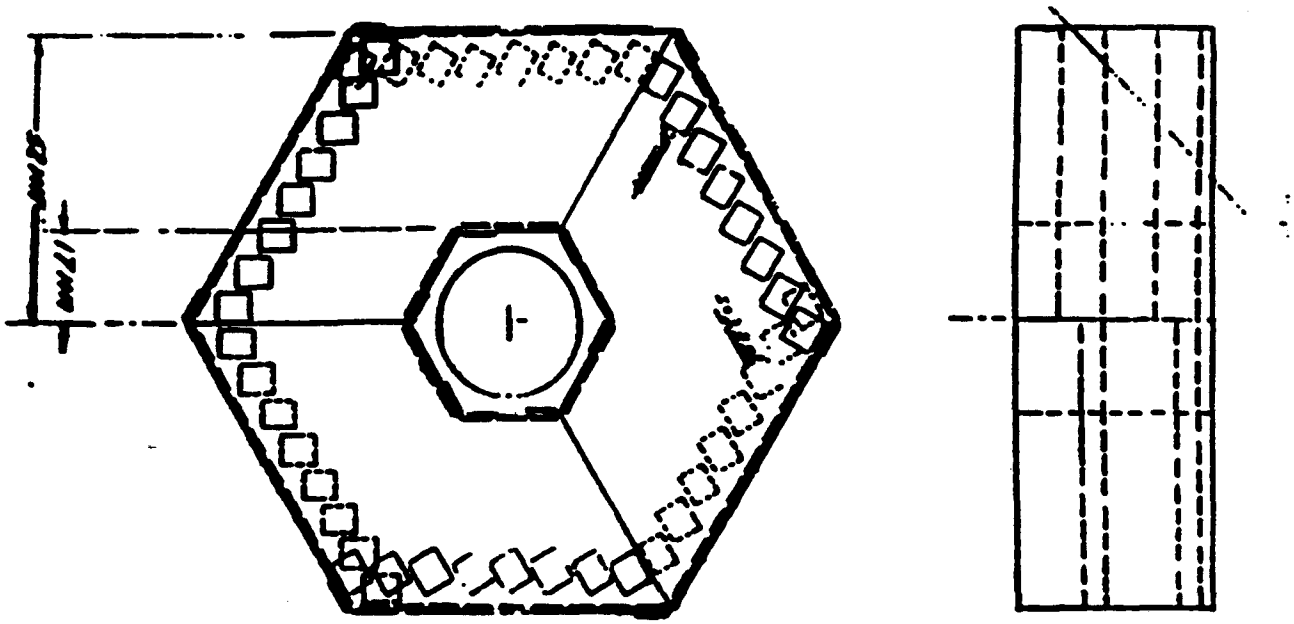

- **Custom** silicon-strip detectors from two 4″ wafers.

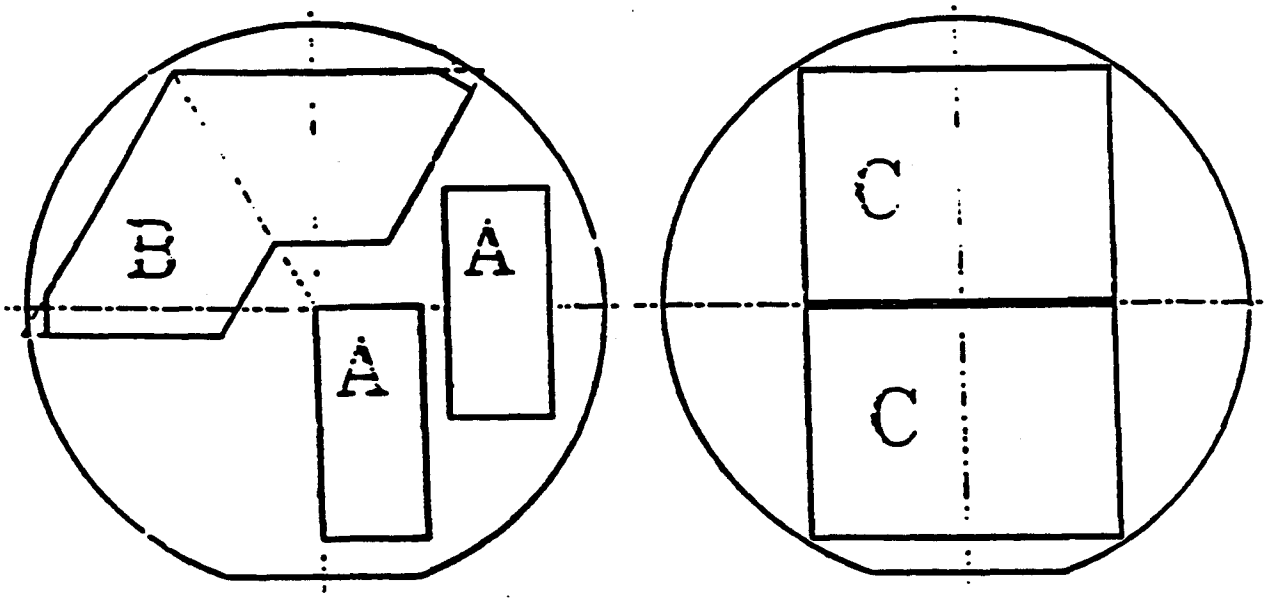

BCD/SSC FORWARD ARM

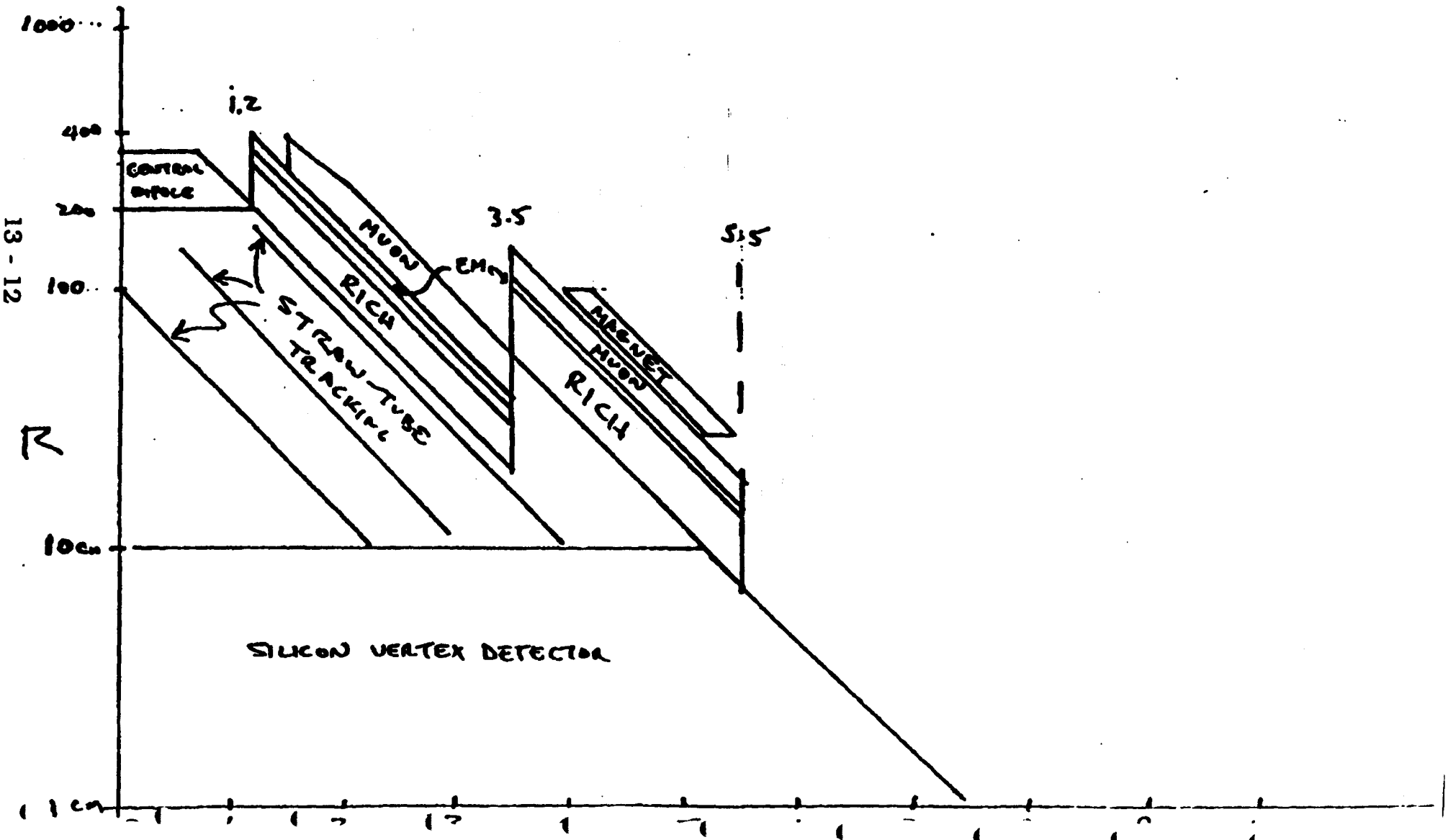

BCD/SSC

THIS SAGITTA IS W.R.T. THE E.M CALORIMETER - NO IS LARGER THAN THAT IN THE TRACKING SYSTEM ONLY.

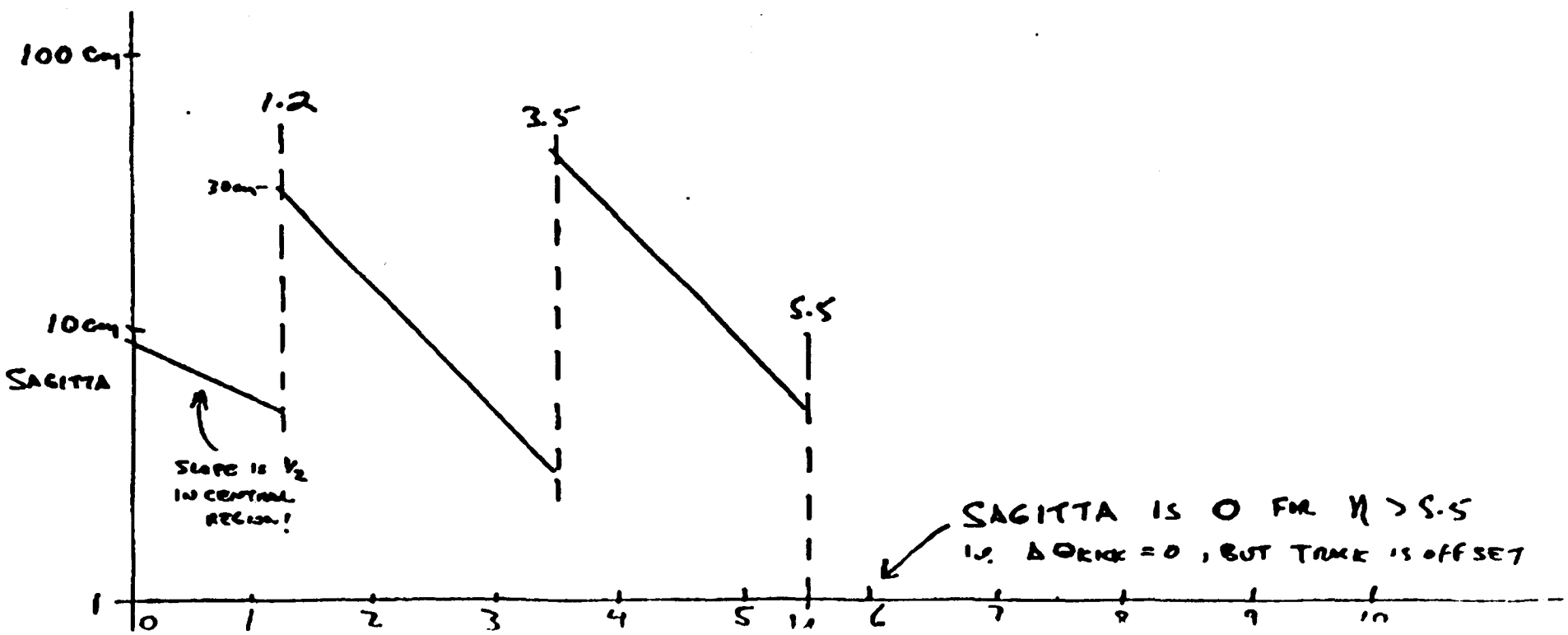

Rosen

SSC $b\bar{b}$ PHYSICS

PRECISION, FINE GRANULARIT
EXPLICIT STATES

CONSTRAINTS:

I COLLIDER COMPATIBILITY
↳ ∴ NO EXTRACTED BEAM VIABILITY

II COST
$\leq$ 50M\$
i.e. $< 5\%$ (GEM + SDC)

WANT FLAVOR TAGGED $B, \bar{B}$'s
IN SELECTED FORWARD η
BAND. $\approx 3-6$ $\theta_{MAX} \approx 60$ mrad
$\theta_{MIN} \approx 2$ "

$\langle \lambda_{DECAY} \rangle \sim 5$ cm
Proper time Resolution
$\sim$ few $\sigma_0 \langle \tau \rangle$

Bjorken E.O.I.

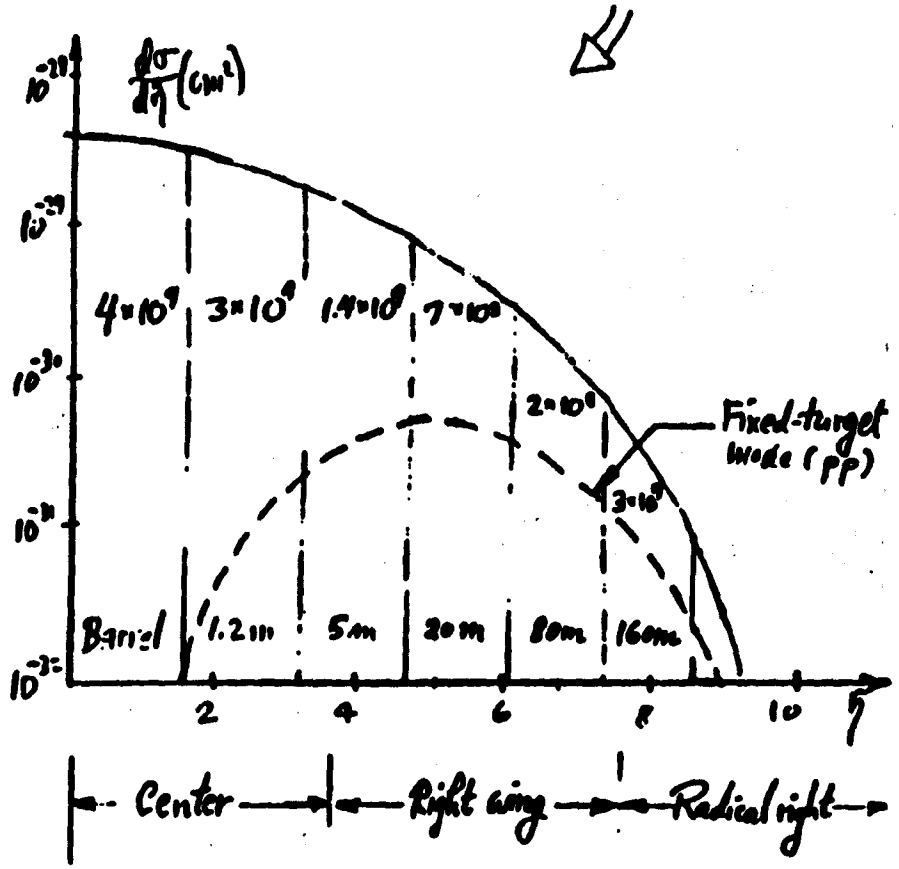

Figure 3.3. Yield of bottom hadrons as function of rapidity along with the annual yield into the modules of the spectrometer. Also shown is the yield in fixed-target mode. A hydrogen gas-jet target is assumed.

WHAT REALLY COUNTS IS YIELD/INTERACTION !

NUCLEAR TARGET IS QUITE ADVANTAGEOUS.

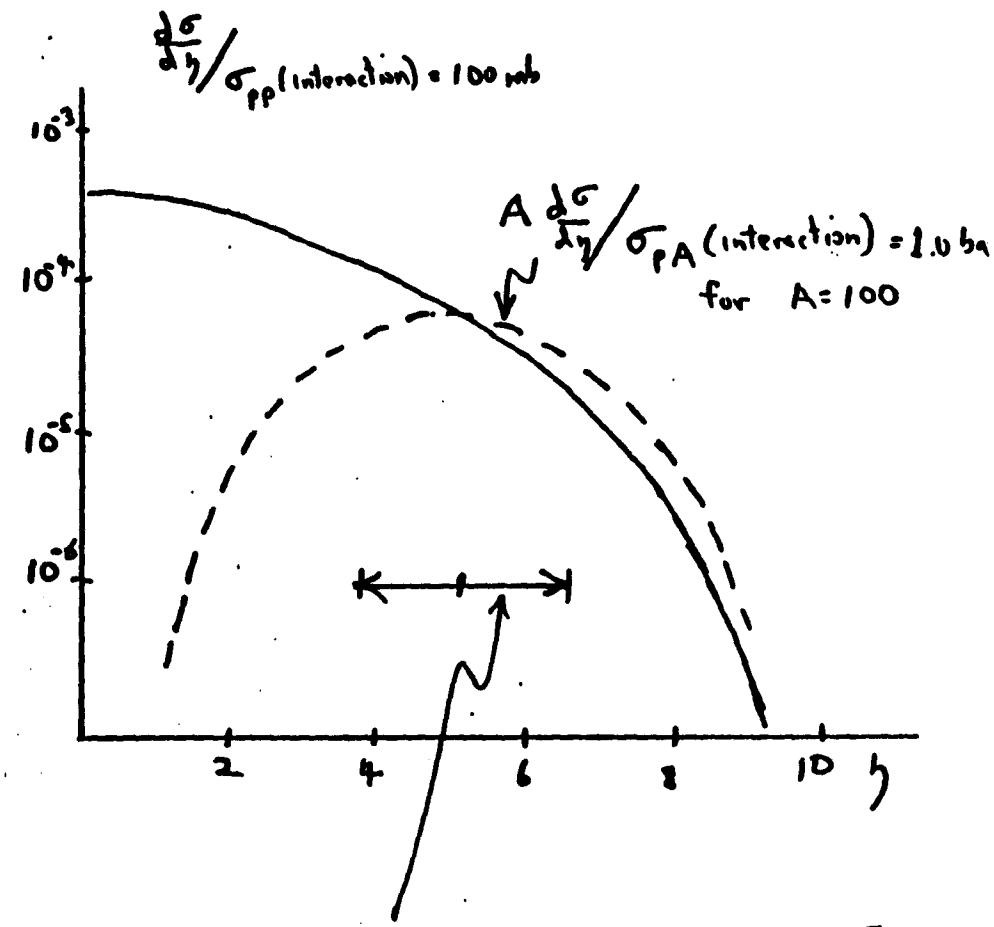

REGION OF GOOD ACCEPTANCE FOR EOI-13,

- LARGER RAPIDITY IS QUITE DIFFICULT
- SMALLER RAPIDITY IS MUCH MORE EXPENS AND THE DECAY LENGTHS ARE SOMEWHAT UNIMPRESSIVE.

DIGRESSIONS

(1) FNAL IS NOW PRIMARILY DIRECTED TOWARD COLLIDER PHYSICS

BUT K AND HYPERON BEAM PHYSICS IS STRONG.

LESSON: LARGE ENERGY IN THE C.M. IS PREEMINANT, BUT LARGE ENERGY OF C.M. CAN BE ADVANTAGEOUS.

(2) MARK III (HITLIN et.al.) PROVED TO BE QUITE INTERESTING.

$c\bar{c}$ $\tau^{\pm}$ → NATURE WAS KIND TO SPEAR, NOT SO KIND TO P.E.P.

IT IS PRUDENT TO ACCOMODATE, BUILD IN SSC FIXED TARGET OPTIONS.

We can retain the option of Fixed Target OR Collider vertex.

Hydrogen Jet is P in the A.

how A, non-cryogenic is safe conv. substitute.

MICROVERTEX PLANE DEPLOYMENT
7/90 ITERATION

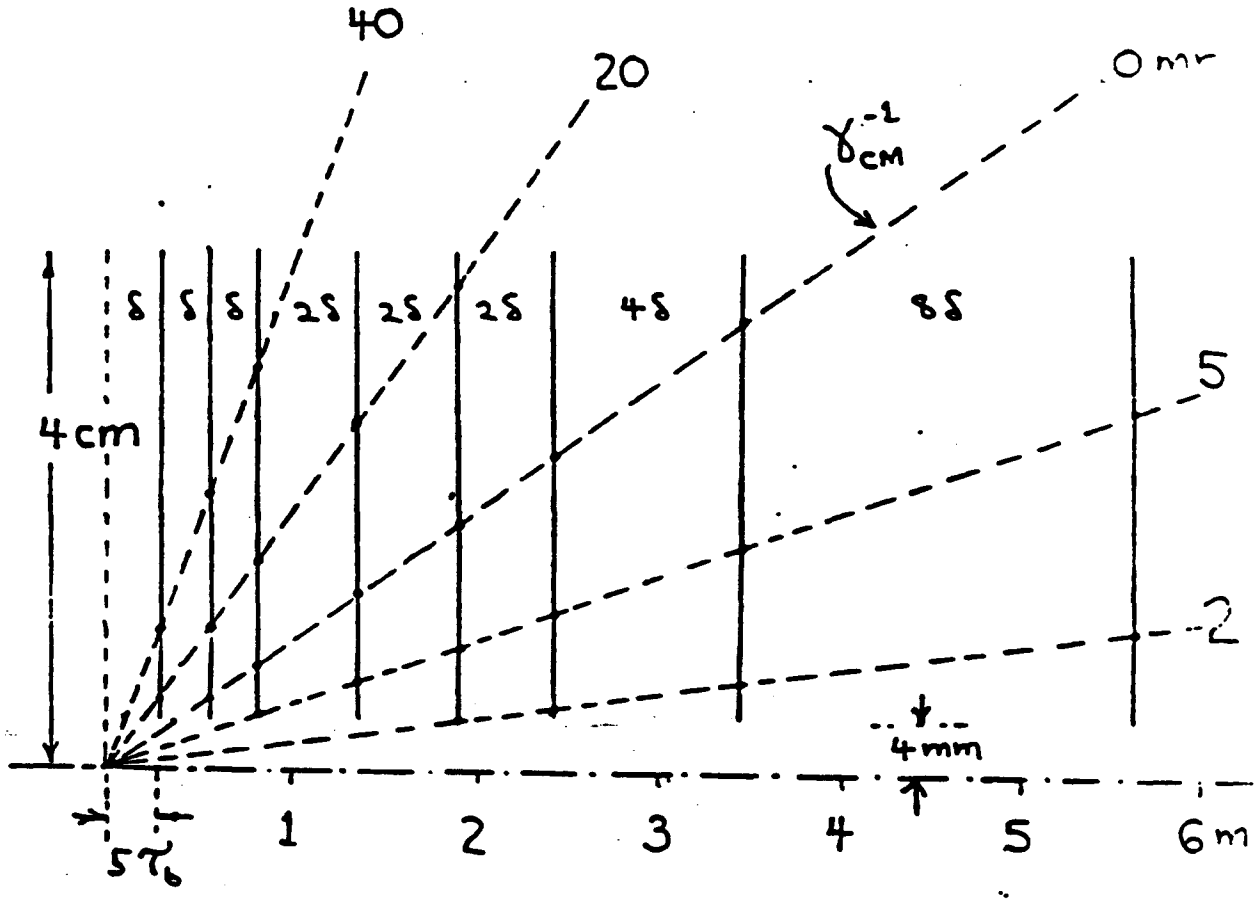

4 mm (radius) ocluded

8 PLANES
50μ CELLS → 800 CELLS/4cm QUADRANT
8x + 8y + 2u + 2 → 64K CELLS TOTAL

(OPTIONAL)

This illustrates the basic idea of the decay track definition.

1. 3 collinear hits pointing to the decay region.
2. Hits deleted if 2 or more of them plus target coordinates are collinear i.e. Suppress primary vertex hits for trigger purposes.

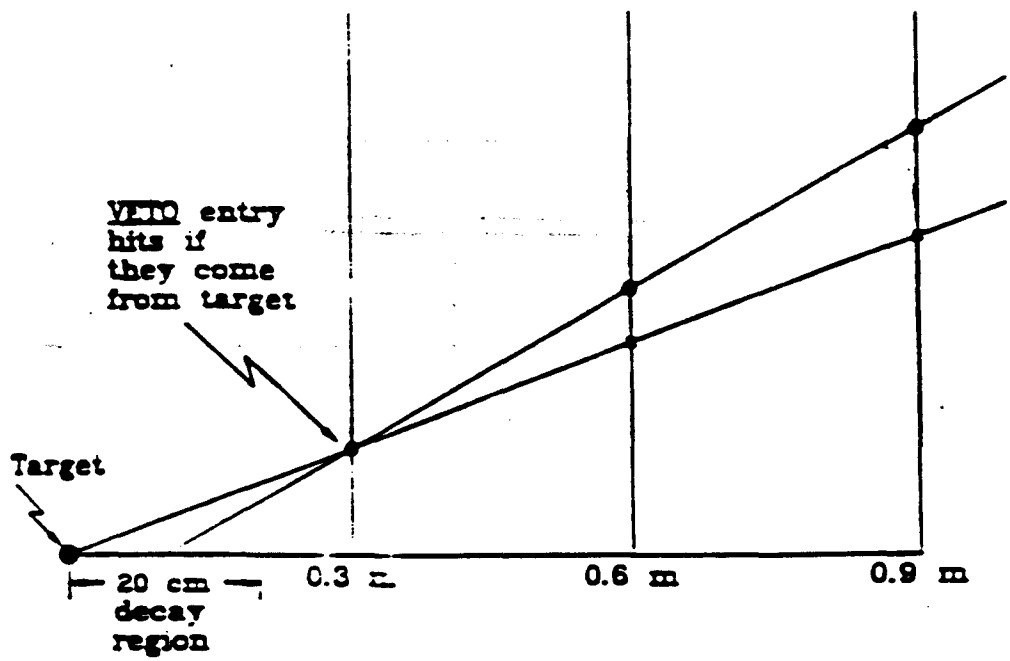

REQUIRE 2 OR MORE DECAY TRACKS IN SEPARATE QUADRANTS.

** FIDUCIARY PROPER TIME EFFICIENCY WILL BE VERY LARGE.

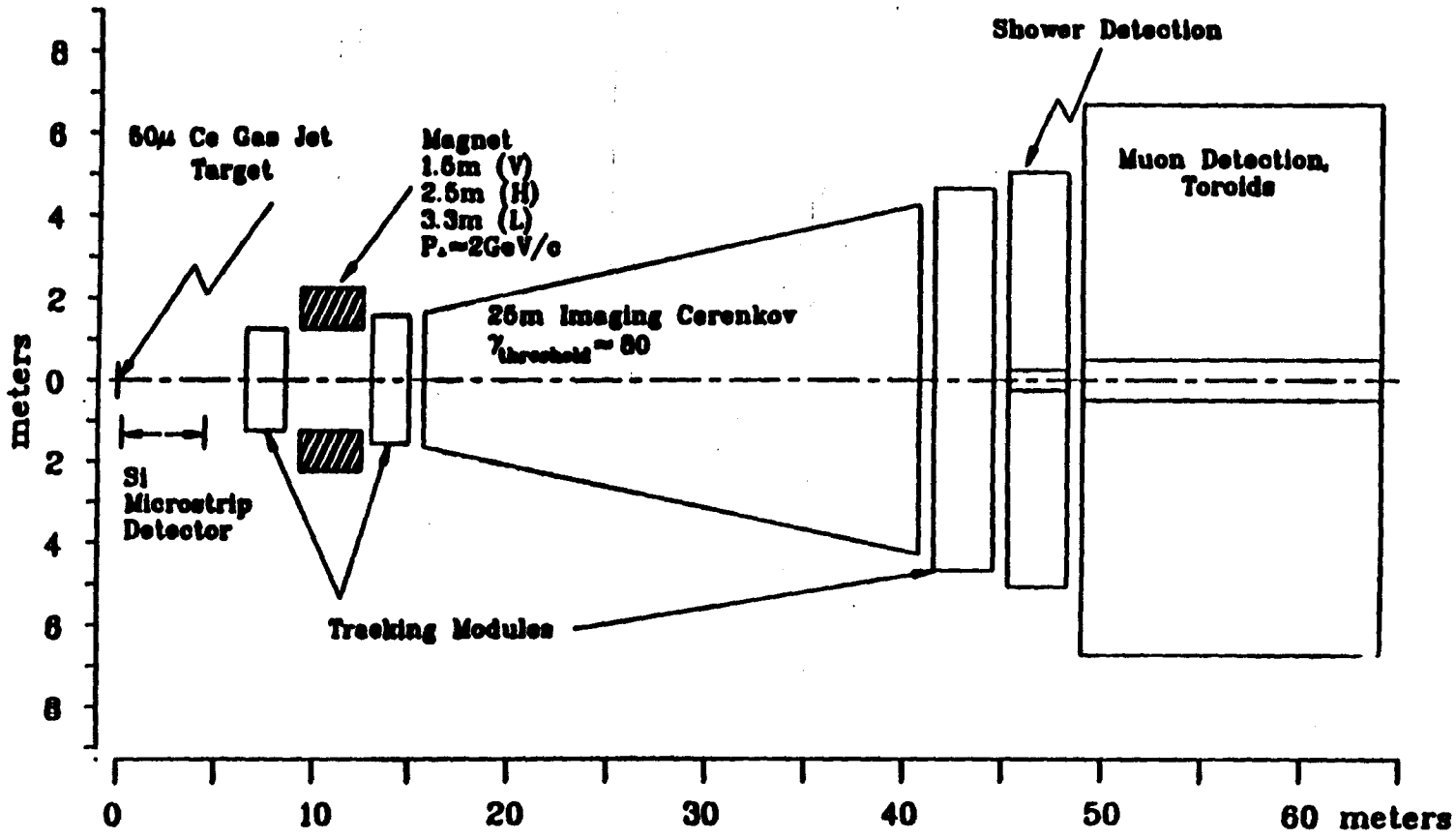
Shower Detection
50μ Ce Gas Jet
Target
Magnet
1.5m (V)
2.5m (H)
3.3m (L)
P⊥≈2GeV/c
Muon Detection,
Toroids
25m Imaging Cerenkov
γthreshold ≈ 80
Si
Microstrip
Detector
Tracking Modules
meters
8
6
4
2
0
2
4
6
8
0
10
20
30
40
50
60 meters

SPECTROMETER $\left(\frac{0.01}{4\pi}\right) 4\pi$!

1) μ VERTEX
QUADRANT STRIPS
$\sim 10^5$ strips
& PIXELS ?

2) CHARGE TRACKING
LARGE APERTURE MAGNET
$p_\perp \sim 2$ GEV/c

3) IMAGING $\check{C}$
10 - 30 m long

4) EM Shower Det.
$\gtrsim$ 5000 Cells

5) HADRON CALOR.
$E_\perp$ 0th LEVEL
TRIGGER

6) MUON TOROIDS, TRACKING

I CAN SUCH A SPECTR. SHARE A COLL. AREA WITH FAD ?

HOW PAINFUL, THE COMPROMISES HERMITICITY AT

Θ_{MAX}, Θ_{MIN}

MIGHT BE IRRITATING

II EVOLUTION

DETECTOR STAGING (PROPOSED)

REQT'S: (0.1 - 1) % INTERACTION SOLID TARGET

SLOW SPILL EXTRACTED BEAM ~ 10^{10} proton/s

a) FNAL 1994-5

0.9 TeV → E_{CM} = 40 GeV

3d COLL AREA BEFORE 1997 UNREALISTIC.

b) SSC 2 TeV extracted beam 1997+

$E_{CM} \approx 60$ GeV

- TRAINING WHEELS FOR ACCEL. OPERATIONS
- SHOW PIECE, MORALE BOOSTER.

CAN PHYSICS BE DONE DURING STAGING?

a) LIMITED b SPECTROSCOPY
$\sim 10^6$ $b\bar{b}$

b) PRECISION CHARM
D, D_s, Λ_c EXCITED STATES
HADRO MOLECULES – DK BOUND?
$D\bar{K}$ BOUND?

c) DIFFRACTIVE PHYSICS REVISITED

$p + A \rightarrow A + p^*$

$\bar{p} + \bar{p}$ FUSION

$\rightarrow \chi_0$? $\left\{ \begin{array}{l} \text{B.R.} \\ \chi_0 \rightarrow \pi^0\pi^0 \\ \underline{0.4\%} \end{array} \right\}$

d) η_c PRODUCTION

e) OTHER

A SUPER FIXED TARGET SPECTR (WITH STATE OF THE ART) HAS NEVER EXISTED AT FNAL.

<u>SOCIOLOGY</u> 2000 AD IS A LONG WAY OFF.

VERY OLD (ME) $\rightarrow$ ENFEEBLEMENT? RETIREMENT?

VERY YOUNG $\rightarrow$ WANT EARLY PHYSICS PUBLICATIONS PROMOTIONS

DISCUSSION TOPICS

* PHYSICS ANALYSIS : WHAT DO WE WANT TO DETECT? γ's, π^0, CHARGED particles?

* STAGE I — Physics Goals

* MAGNETIC PART. ANALYSIS — MAGNETIC FIELD
* DETECTOR ARCHITECTURE

* LATTICE/DETECTOR INTERFACE
* FREE SPACE : IP → 160M?
* DOWNSTREAM : 160M → ∞

* STEERING COMMITTEE

* NEXT MEETING (S) ? WHERE? WHAT? WHO?
* "F.A.P" WORKSHOP in SEPTEMBER (Allan WHITE)
* F.A.D AT MADISON MEETING in APRIL

* TNRLC
* HOW CAN "WE" GET SUPPORT FOR PEOPLE?

* TRIGGER — NOW? — LATER? — WHEN?
* TEST BEAMS $t \lesssim \infty$

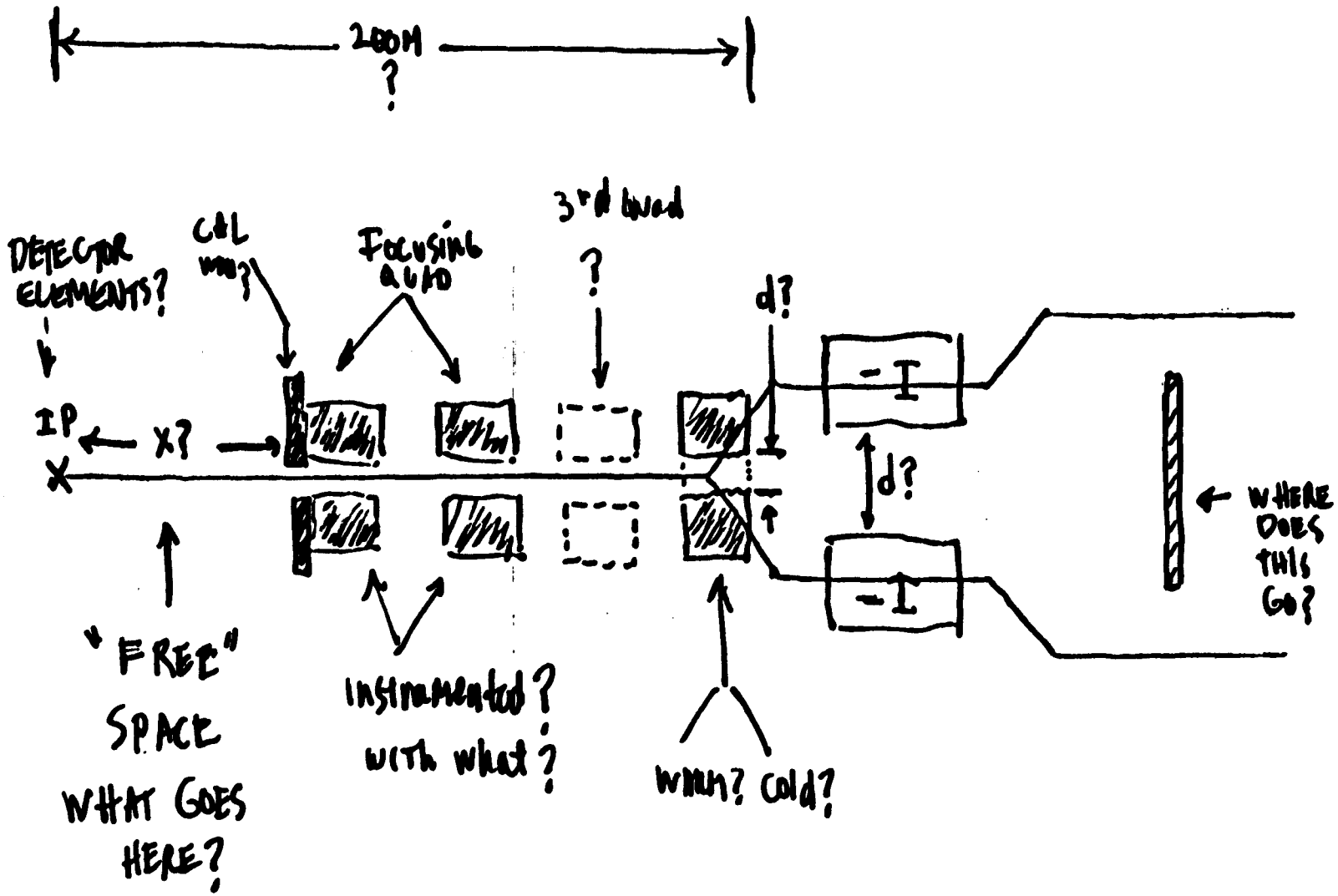
200M
?
DETECTOR ELEMENTS?
C&L
FOCUSING QUAD
3rd quad
?
d?
IP
X?
-I
-I
d?
WHERE DOES THIS GO?
"FREE" SPACE WHAT GOES HERE?
INSTRUMENTED? WITH WHAT?
WARM? COLD?

Sequencing of CAD Work

March — Endwall: 100 – 1000 m

April — Beam pipe / Calorimetric architectures

May — Tracking architectures

June — Magnetic architectures

July — Iterations & beginning of decision sequence.

POSSIBLE WORKSHOP

"F.A.D.-TYPE PHYSICS AT THE TEVATRON $\sqrt{s} = 1.8$ TeV"

—DO NOT WANT TO EXCLUDE SSC—

or "DIFFRACTIVE & SMALL-x PHYSICS"

IF WE DECIDE (YOUR INPUT PLEASE) TO GO AHEAD, & LAB AGREES (PROB OK)

~ 3 DAYS

SEPTEMBER 16 - 18 ?

@ FERMILAB

ANY REASON WHY NOT NO

INITIAL ORGANIZERS

ALAN WHITE — ARW @ ANLHEP

MIKE ALBROW — FNALD::ALBROW

N. Mokhov
03/13/92

F.A.D. - Collider Interaction

1. Beam Halo / Beam Loss

2. Background

3. Radiation

1. Beam Halo / Beam Loss

- beam-gas
- pp → elastic, diffractive → long range beam loss
  pp → secondaries → beam pipe, centr. showers
- injection
- instabilities, RF-noise
- tales from scrapers, beam abort

Torr

Cold 80%

10^{-8} H_2 ✓

10^{-10} CO

10^{-11} CO_2

Warm 20%

10^{-9} N'

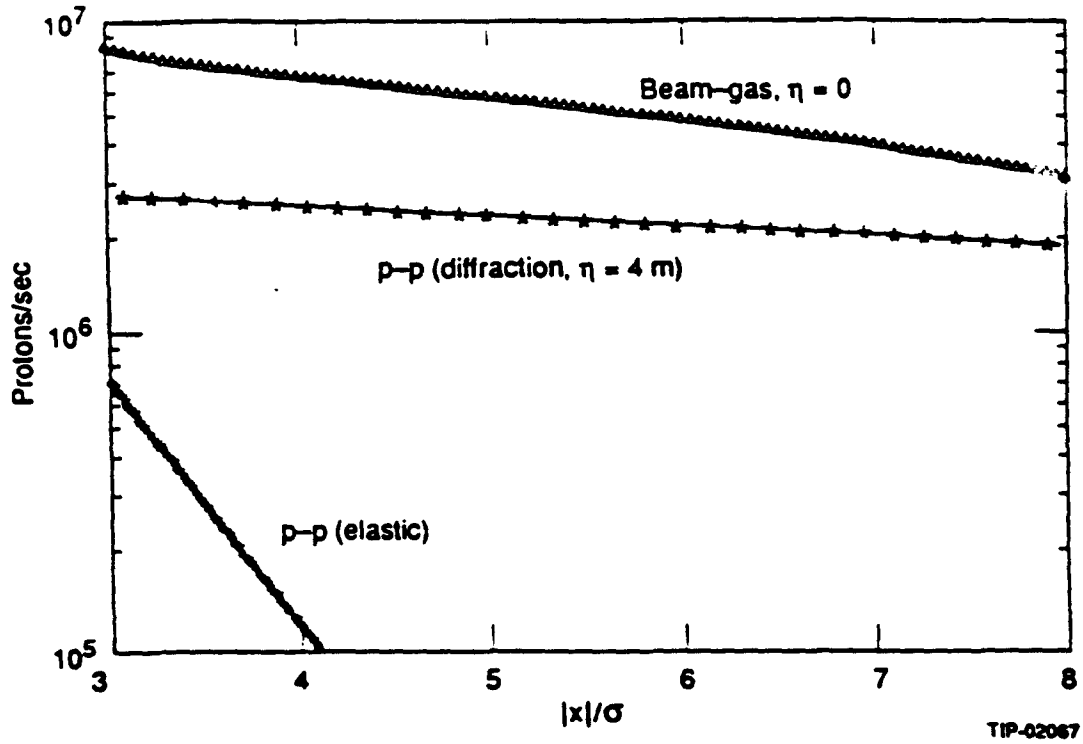

Figure 1. Beam Halo Rate Due to pp-Collisions and Beam-Gas Scattering Versus Distance from the Beam Centerline (from Reference 15).

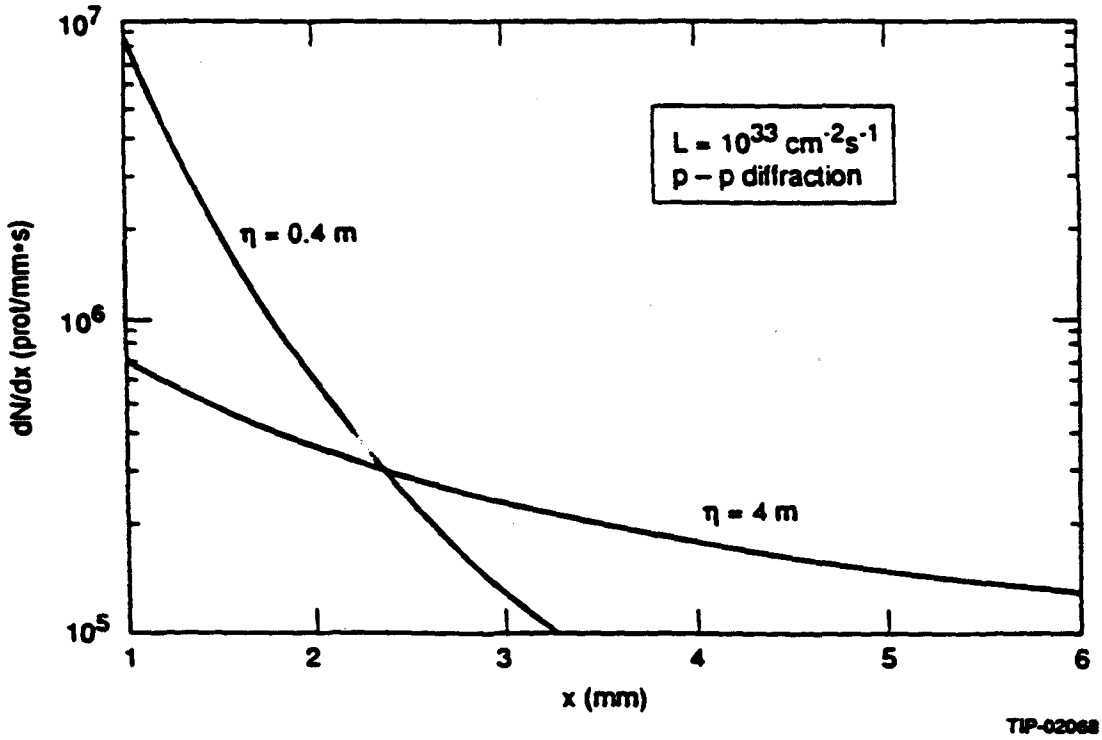

Figure 2. Transverse Distribution of Protons from pp-Diffraction for Two Values of Dispersion.

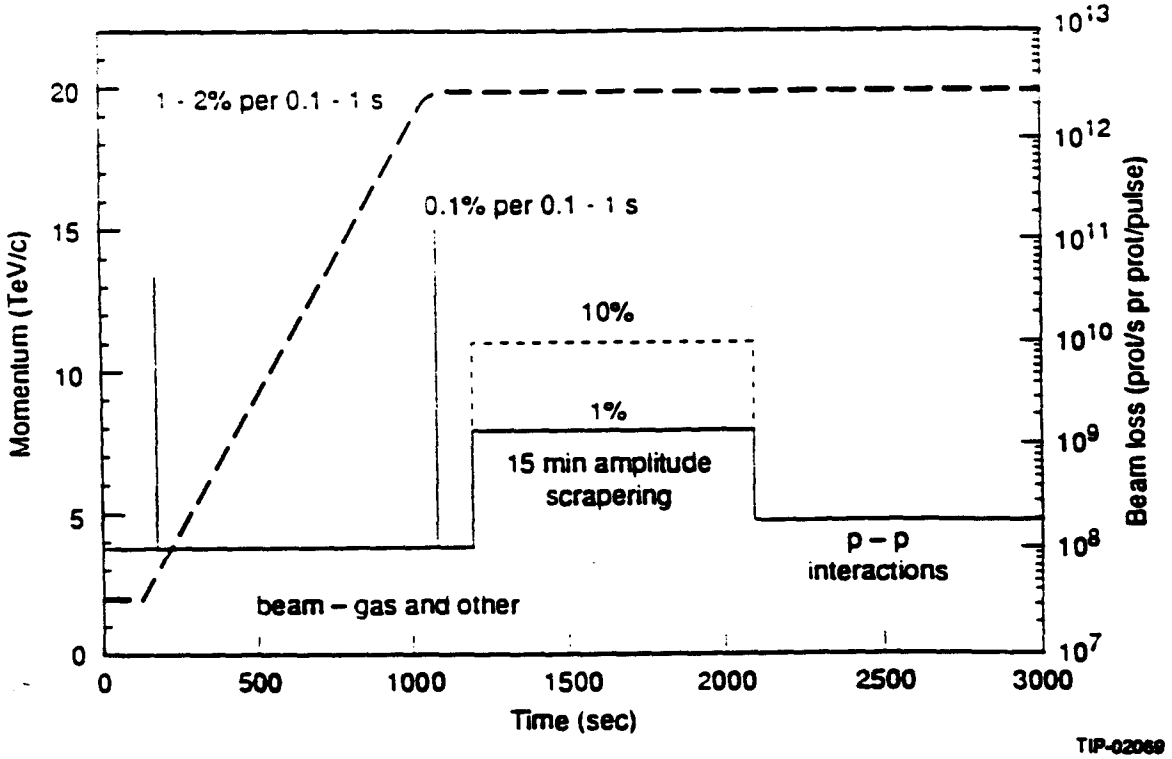

Figure 3. The SSC Beam Loss Scenario.

5.0 SCRAPING AND MATERIAL CHOICE

A beam scraping system must minimize beam loss in the machine throughout the cycle, form the required transverse emittance before the collisions, and save this emittance during the whole collider run. Such a system should be capable of intercepting a high halo rate and absorbing most of its energy with minimal effect to the downstream equipment and IP. Most of the above beam halo particles have to be trapped with a scraper at a distance from the beam axis x_o, which defines the minimum machine aperture (Figure 4). To intercept protons with the large amplitude one needs to put the scraper in the region with the largest β-function. To trap off-momentum protons a non-zero dispersion at that position is required to provide $\Delta = \eta\, \Delta p/p \neq 0$ (Figure 4). The primary x_o is chosen to be 10σ (see Tables 2–5 and Reference 6). To provide favorable experimental conditions, according to Fermilab[5] and CERN[6] experience, this distance should be as small as 6σ or even less (3σ). This can be achieved by moving the beam slowly with some velocity in the 3–10σ range with the simple bump-magnet (see Section 9.0).

The average impact parameter Δ of the halo particles at the scraper face grows linearly with this velocity and with the proton transverse drift speed V. Figure 5 shows this dependence for the average and maximum Δ for $\beta = 400$ m and scraper in final position = 3σ. According to CERN experience[6] $V \sim 1$ σ/s and 6 σ/s at $x_o = 3\sigma$ and 6σ, respectively. It corresponds to $V = 0.14$ and

2. Background

Criteria
Limits ?

- from IP to F.A.D.
- to IP from machine
- μ-vectors

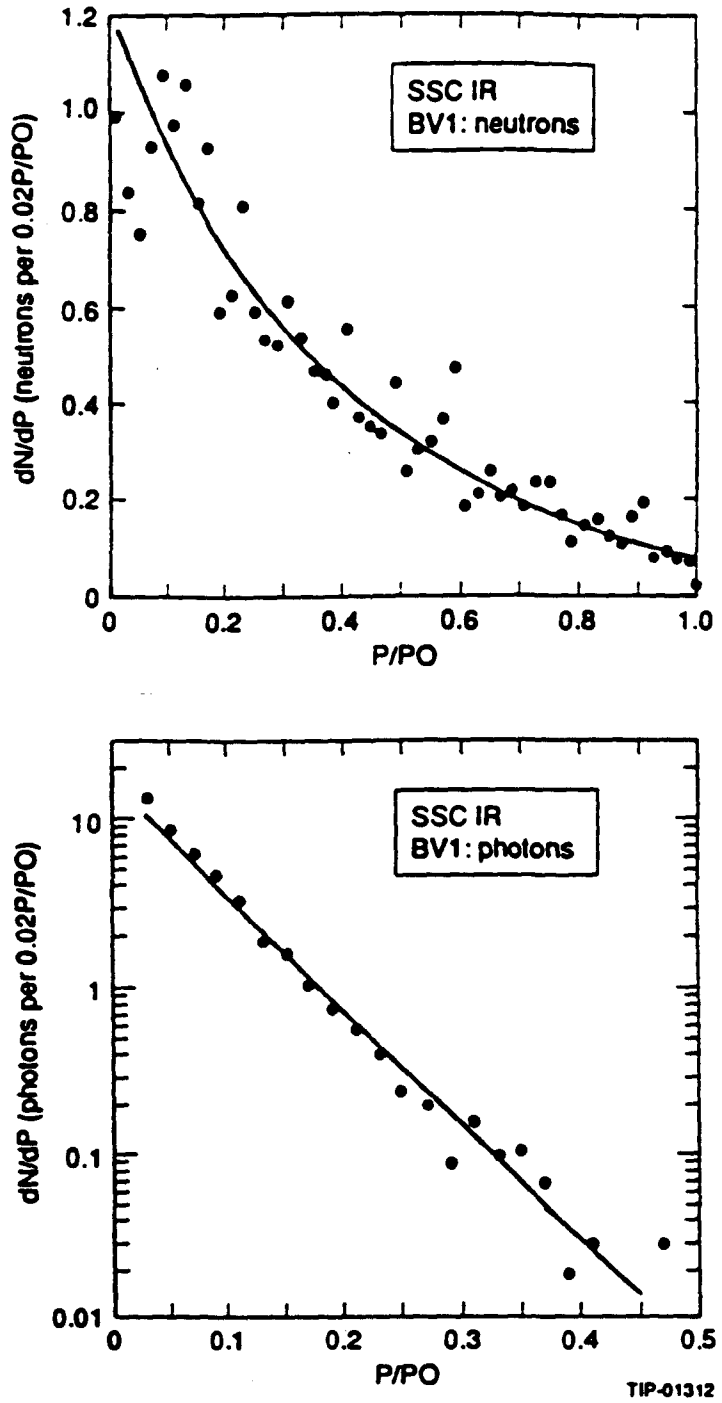

Figure 12. Momentum Distributions of the Neutrals at the Zero - angle Calorimeter Position Downstream of the 20 × 20 TeV Interaction Point.

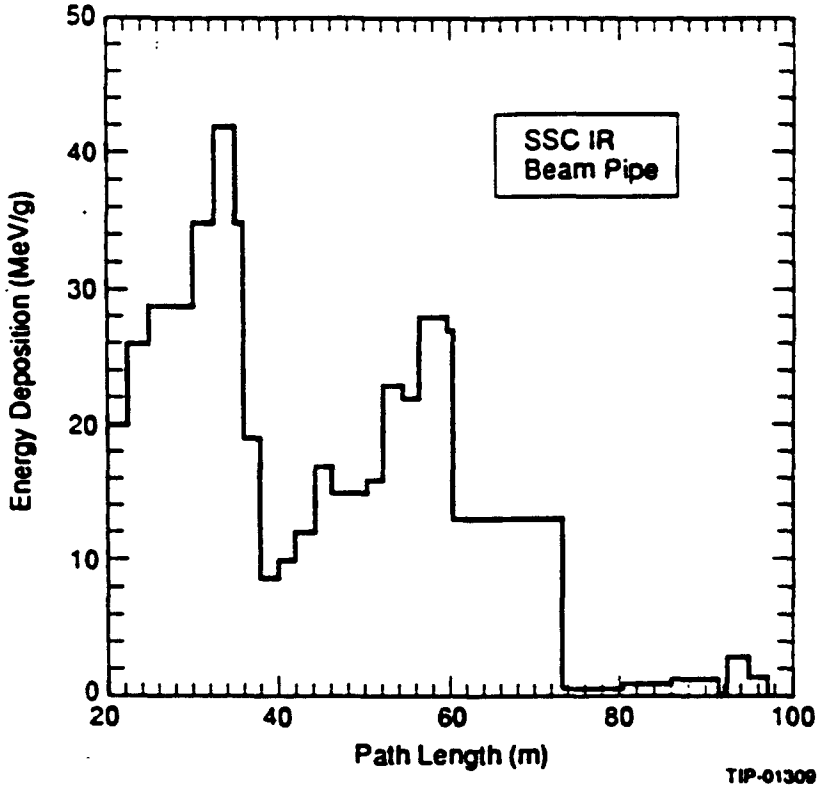

Figure 9. Longitudinal Distribution of the Maximal Energy Deposition in the Beam Pipe in the Low-β Region Downstrea of the SSC IP.

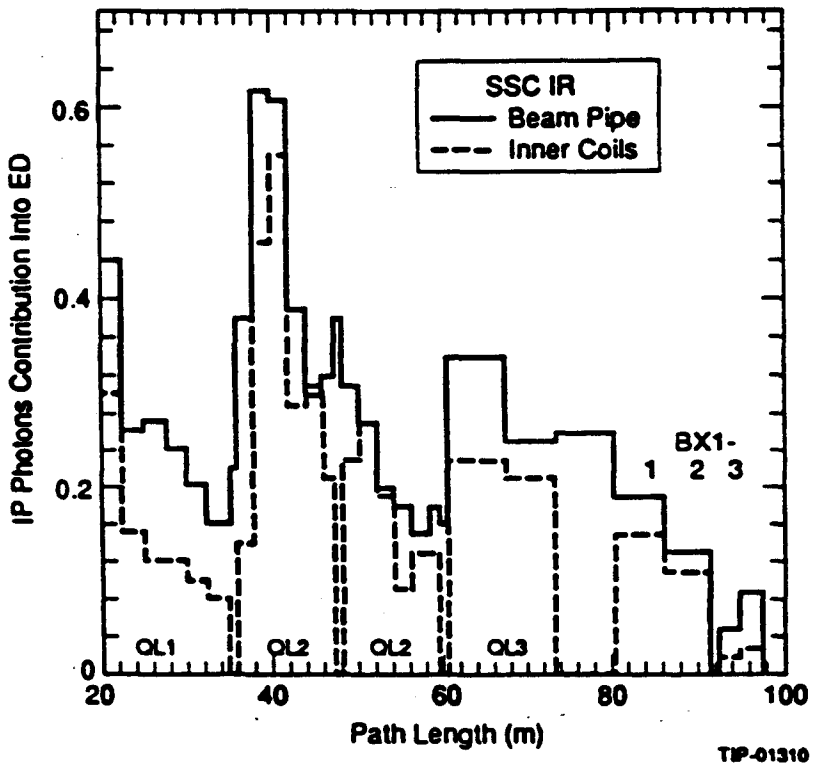

Figure 10. Contribution into the Maximal Energy Deposition of Photons from the 20 × 20 TeV pp Interaction Point.

April 02, 1991
MARS12

SSC SCRAPER SYSTEM

NUMBER OF OUTSCATTERED PROTONS (x 0.01) PER 1 INCIDENCE

E (TeV)	Case	Elastics	Others with delta(p)/p < 0.001	< 0.01	< 0.3
20	1	4.460	0.026	0.053	2.520
	2	0.240	0.020	0.031	0.175
	3	0.005	0	0	0.007
	1(W)	4.160	0.150	0.347	1.730
	1(C)	8.640	0.915	1.710	6.680
2	1	6.920	0.154	0.551	3.140
	2	0.170	0.003	0.007	0.154
Yield angle (mrad) at 20 TeV		< 0.05	< 0.05	< 0.05	< 0.3
at 2 TeV		< 1	< 1	< 1	< 3

Case: 1 - single Cu scraper with L = 2 m
2 - target + scraper (1 mm W at Beta=400 m)
3 - crystal + scraper (5 mm Si at Beta=400 m)

Case: 1(W) - single W scraper with L = 1 m
1(C) - single C scraper with L = 4 m

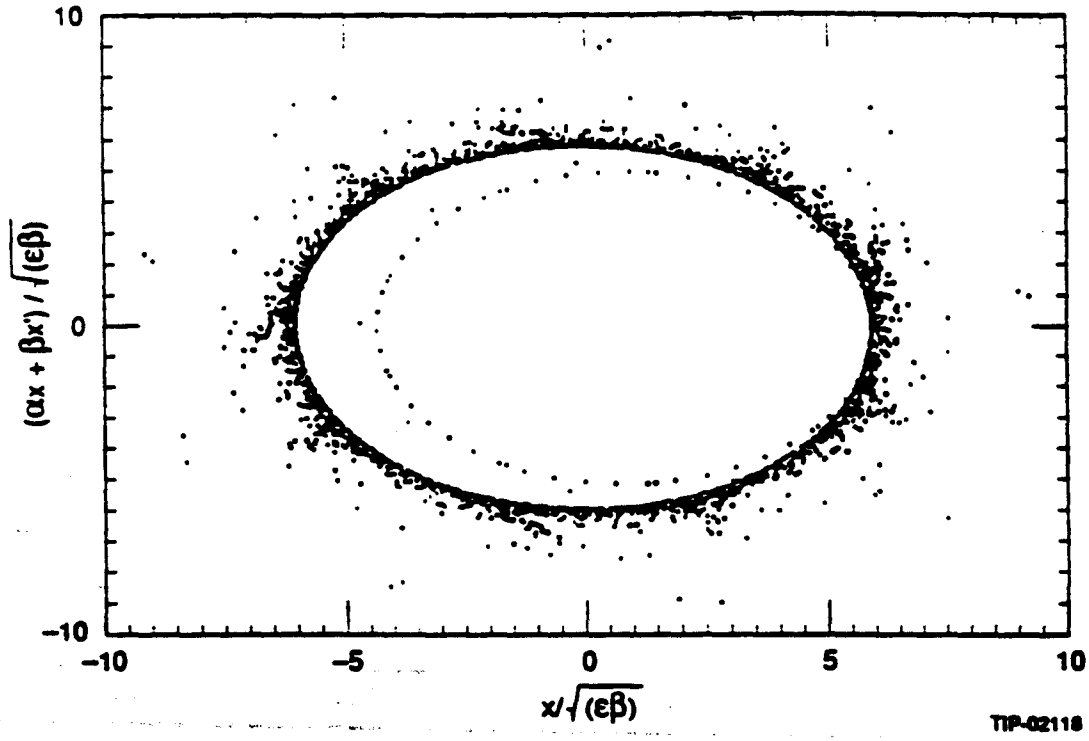

Figure 49. Normalized Phase Space Portrait of Protons Outscattered from the Scraper.

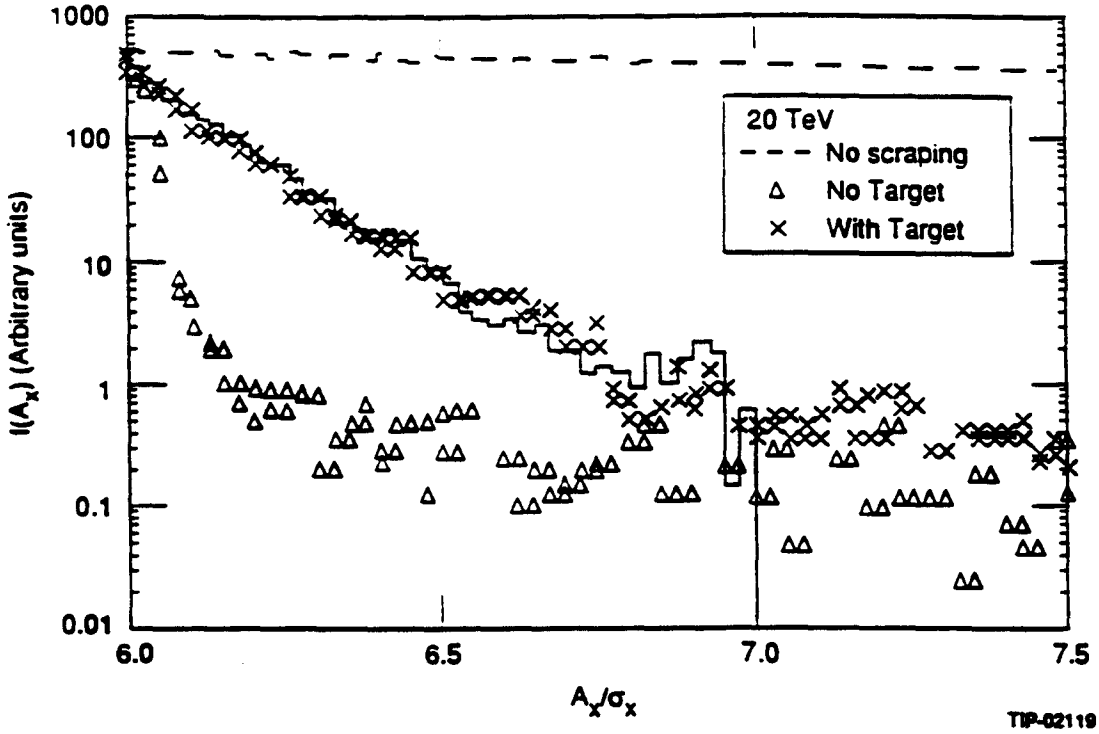

Figure 50. Distribution of Halo Particles With No Scraping, With Single Scraper, With Target/Scraper Couple, and With Collimators C1 and C3 Installed Additionally at 7σ from the Beam Centerline (histogram).

3. Radiation

- quench in SC
- radiation damage (detector components, electronics)
- induced radioactivity
- shielding and shafts
- absorbers

Table 9

Maximal Energy Deposition ε, Absorbed Dose Rate D', and Annual Dose D in the Superconducting Cc of the SSC Low-β IR Beam Elements. The last column is the power P deposited in the eleme Interaction rate at the IP is 10^9 per second at $L = 10^{34} cm^{-2} s^{-1}$. The operational year is 10^7 sec.

Name	Length (m)	Path Length (m)	ε (MeV/g per 1 int.)	D' (mW/g)	D (Mrad per year)	P (W)
		0				
DL0	15.00	15.00				38.4
DL1	5.00	20.00				16.8
FWD CAL	3.00	18.00				140.8
COLLIM	2.00	20.00				24.8
QL1	15.14	35.14	20	3.20	3200	513.1
OR	0.80	35.94				3.7
QL2	11.22	47.16	12	1.92	1920	155.3
D	1.00	48.16				2.0
QL2	11.22	59.38	14	2.22	2220	260.3
OR	0.80	60.18				3.6
QL3	12.96	73.14	6	0.96	960	161.9
D3	7.00	80.14				1.0
BV1-	5.00	85.14	0.4	0.06	64	5.4
D	1.00	86.14				0.7
BV1-	5.00	91.14	0.7	0.11	1112	7.6
D	1.00	92.14				0.3
BV1-	5.00	97.14	1.3	0.21	208	12.7
D	33.00	130.14				1.6
Z-CAL	1.00	131.14				809.8
D	76.00	207.14				3.6
C10	4.00	211.14				78.7
D	78.00	281.94				
BV1+	5.00	286.94				0.1
Total						2242.2

*Maximal numbers ε, D' and D in the superconducting elements correspond to the maxima in the azimuthal distributions at the inner radii of the inner coils.

**Outer radius for all the elements assumed to be equal to 15 cm.

Because loss rates at the collimators vary within two orders of magnitude, one might be tempted t remove "insignificant" collimators C13, C15 and C17. But remembering uncertainty in the pp interactio model and possible lattice changes, it would be strongly recommended to avoid "improvements" of th: kind.

8. BEAM ABORT SYSTEM

8.1 Lambertson as a Source of Radiation

In the beam abort system, the extraction Lamertson septum magnet followed by horizontal an vertical scrapers (SHV) [1] should be the narrowest places in the both collider rings during the infectior acceleration and collision stages in the SSC. This way the beam halo growths, for various reasons, woul

FAD 11 March

Comments on the Far-Forward Spectrometer

The region for the far-forward spectrometer is the endcap wall at $\sim$ 100m and the system which is downstream of the hole in that wall. Figures 1 and 2 respectively show layouts corresponding to EoI–19 (Fig. 1) and to the intermediate-β IR laid out by SSC Lab in the design book (SSCL–SR–1056, p. 57) (Fig. 2). Some comments:

1. The transverse dimension is *full-scale.*
2. The longitudinal scale is "Lorentz-contracted" by a factor 2000. Since the resolution of any transverse tracking elements (wires, pads, shower-counter elements) is boost-invariant, we may view these spectrometer layouts as if they are *full-scale* in *all* dimensions provided we Lorentz-boost the collider beams by a factor 2000; i.e. 10 GeV (to the right) $\times$ 40 PeV (to the left).
3. The number and distribution of right-moving beam fragments (from a 10 GeV primary) should be easy to visualize—only a few in the forward cone. Location of vees and kinks from K_S and Y decays are within a few cm from the beam axis. The decay length of a 10 TeV Λ is $\sim$ 300m.
4. The magnetic fields are compressed by the boost into submillimeter longitudinal thickness, but the p_t kick they impart is unchanged. Thus sagittas of order 1 cm are reasonable for upstream tracks which traverse a dipole magnet (or magnets) at $\sim$ 80m and miss the hole, provided the p_t kick is $>$ 1 GeV.
5. In both layouts a fundamental constraint for the downstream system is the aperture of the splitting-dipole for the circulating beams (location 300-400m downstream; p_t kick $\sim$ 40 GeV).
6. The double dogleg present in the SSC designs puts a long string of magnets in the 300-500m range. These are put there in order to remove vertical dispersion. From an accelerator-physics standpoint, it is an unpleasant thing to modify them although—we are told—thinkable.

With all this in mind, a path-of-least-resistance is to stick with the SSC

intermediate-β lattice and see whether it is viable. My very tentative opinion is that maybe it is OK. In Fig. 3 is the downstream layout to half-scale, relative to Figs. 1-2. More useful perhaps is Fig. 4, where any additional "boost" has been made, so that we now view things in terms of 2.5 GeV $\times$ 160 PeV.

More comments:

7. Tracking the neutrals looks good, assuming precision tracking elements (20 μ resolution) and lots of preradiator for converting the γ's.

8. Tracking as close to the beam just upstream of the 100m endcap wall (via Roman pots) is important, in order to locate as many charged tracks as possible before they disappear into the hole.

9. After they disappear into the hole, most will get blown into the quad or dipole magnet yokes (or, more likely, coils) by the extremely strong fields. This includes the (important!) secondary protons of energy, say, 5-15 TeV. When they hit something, some shower products should get into the downstream tracking region. Provided the magnet gaps are tapered as shown, the reconstruction of this shower vertex (good to $\sim 20\mu$ in the transverse coordinate??) should serve as a good momentum measurement ($\delta p/p \sim 20\,\mu/4mm \sim 0.5\%$??).

10. My rule for placing tracking elements is to keep them at a relatively small angle from collision axes of the obvious hot sources, since particle density increases exponentially with increasing production angle. This is what defined the tracking regions shown in Fig. 4.

11. There seems to be not much lost by spreading out the shower counters longitudinally (length $\sim$ 50-100m?; $\sim 30\ X_0$ layers spaced 2-3m apart?)—it is still pretty short as seen in Fig. 4. This turns the hot point source of neutrons and damaging ionization into a line source and reduces the radiation damage problem. The fraction of shower particles sampled goes way down, but there are so many that sampling errors would remain small. Addition of a modest transverse B-field might supply more useful information.

The bottom line is that once background simulations are up and running, some good tracking studies through the intermediate-β SSC system will be an important next step.

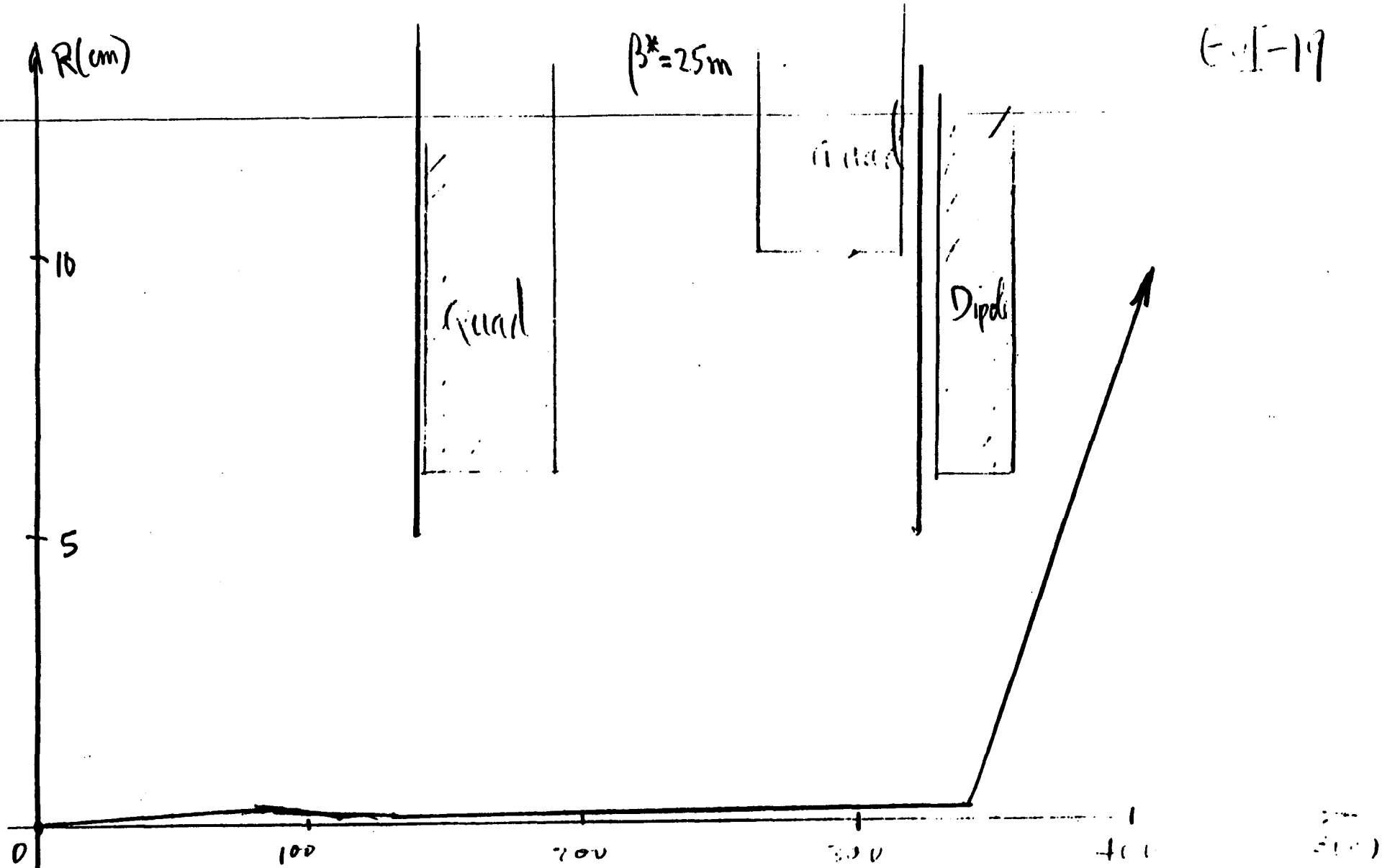

Note: This is full scale in boosted frame: 10GeV x 40PeV

Fig 1

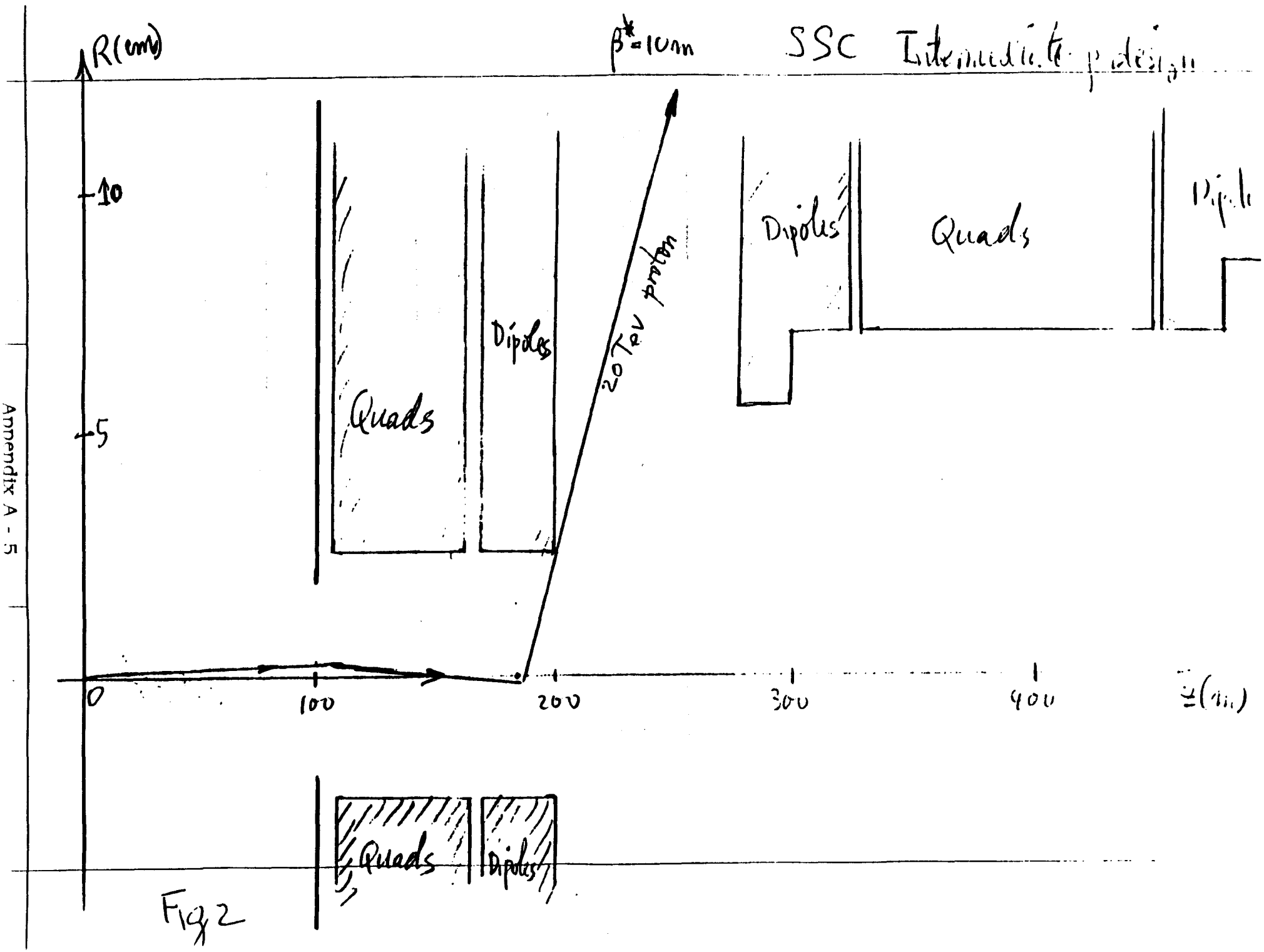
R(cm)
β*=10m
SSC Intermediate p design
10
5
Quads
Dipoles
20 TeV proton
Dipoles
Quads
0
100
200
300
400
Quads
Dipoles

Fig 2

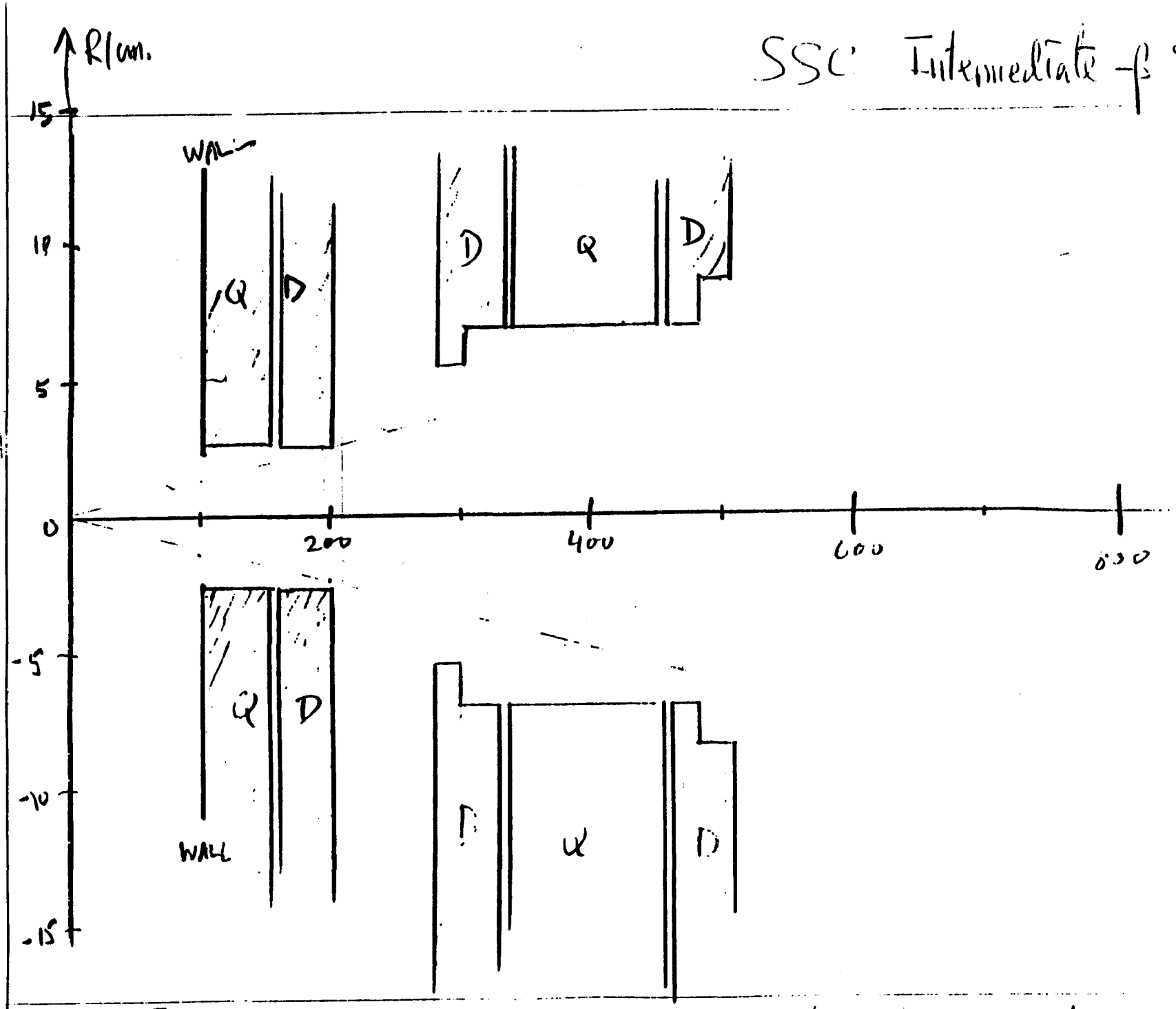

SSC Intermediate-β Design

Fig 3

Half-scale in Boosted Frame

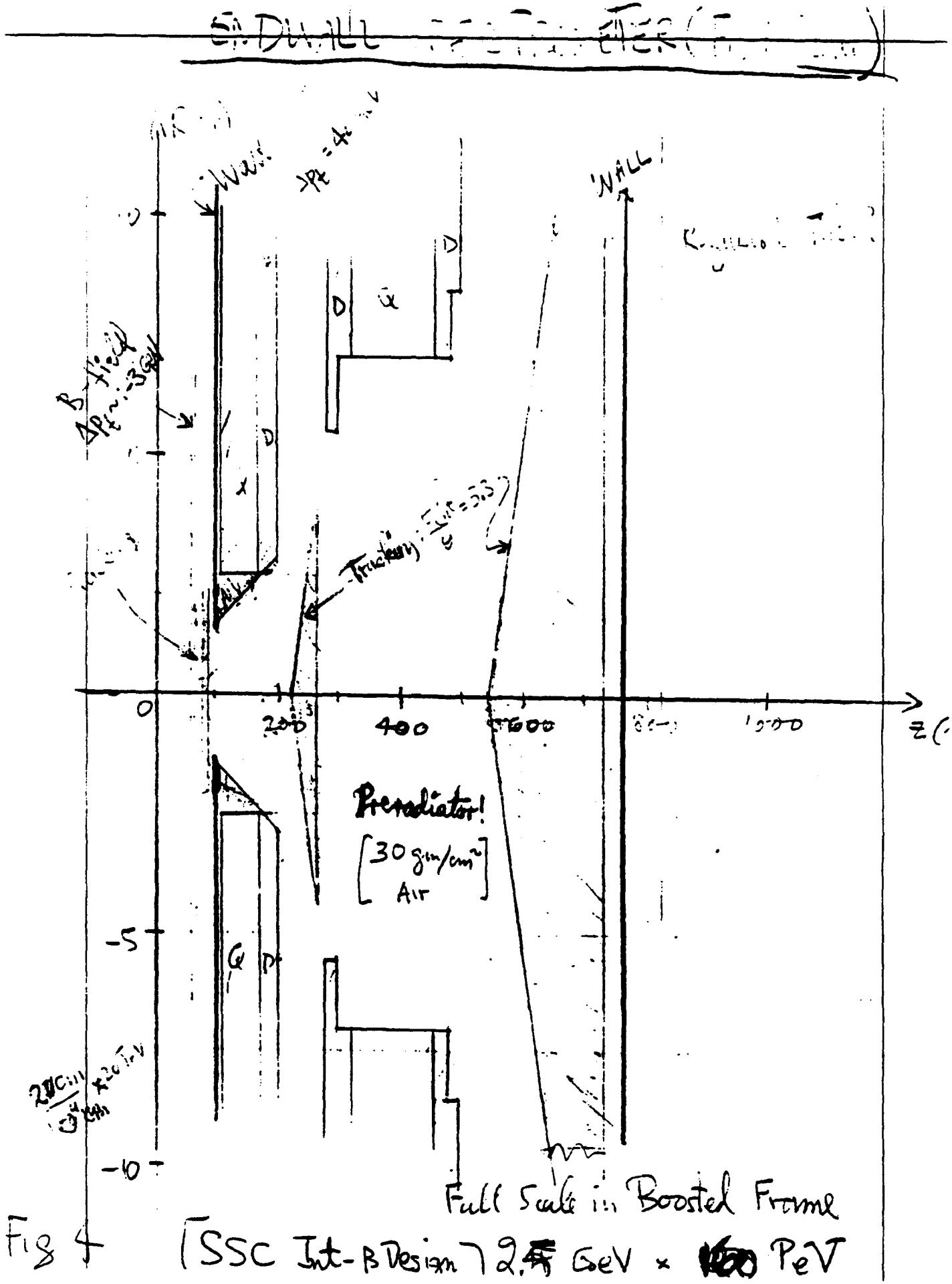

Full Scale in Boosted Frame

Fig 4 [SSC Int-B Design] 2.4 GeV × 100 PeV

J. Bjorken
5 March 199

High-energy Jet Phenomenology for FAD

A high energy jet will be defined as something between, say 2 and 20 TeV, initiated by a valence-parton, probably quark. Consider the nominal case of a 6 TeV jet. It might have p_t anywhere from 6 GeV to, say, 60 GeV. A six TeV jet with p_t of 6 GeV lands 10 cm off-axis at a 100m wall, and the 60 GeV jet 1m out (it is mainly intercepted upstream in the EoI-19 version of FAD). The $\sim$ 80 GeV tagging jets of $qq \to qqH$ are still further out, so here we are mainly talking of Mueller-Navelet jets (5-20 GeV p_t).

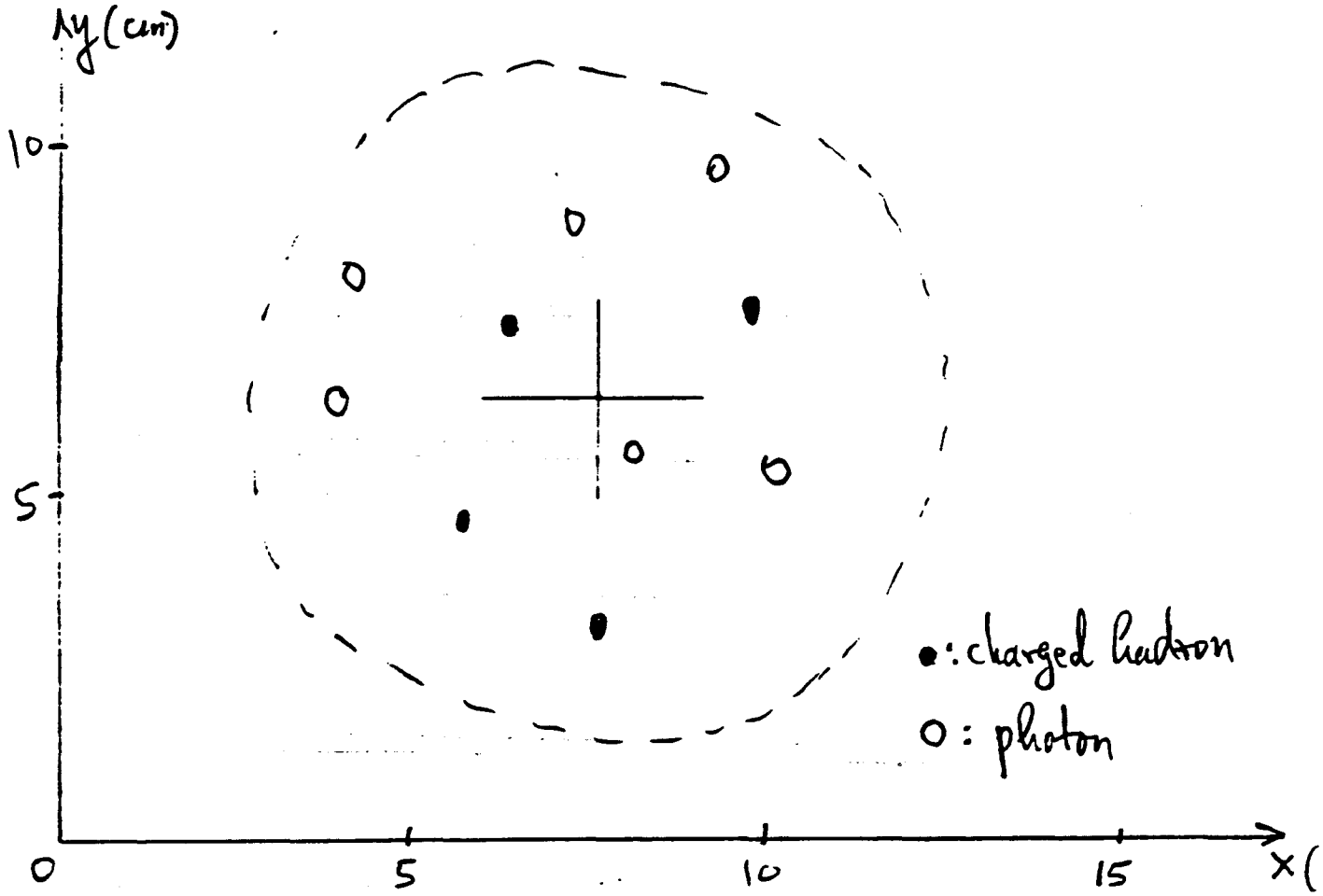

A full scale picture of the 6 TeV jet, with $p_t = 6\ GeV$, is shown in Fig. 1. The circle-of-radius 0.7 is shown, within which there are only a few hits. For $p_t \sim 6\ GeV$, the jet multiplicity is $\overline{n}_{\rm jet} \lesssim \frac{1}{2}\overline{n}_{e^+e^-\to q\overline{q}}(\sqrt{s} = 12\,GeV) \sim 6$ (charged

+ neutral). So the spacing is set by the two leading particles in the jet. Let them be 4 TeV and 1.5 TeV, with relative $p_t = 300\ MeV$. Then the angle between them is $\Delta\theta \cong 0.3\ GeV/1.5\ TeV \approx 0.2$ mrad $= 2\ cm/100m$.

Now if the jet has $p = 6\ TeV$ (fixed) and a larger p_t, then when it hits a 100m endwall, hereafter called endcap, it is further off-axis, but its internal structure is the *same*, provided that there is Feynman scaling of the fragmentation products. Thus on this endcap the pixel size is best taken as *uniform* in rectangular coordinates and *not* uniform in lego coordinates. For example a 1 cm pixel at 100m turns into $\Delta\eta \sim \Delta\phi \sim 1\,cm/50\,cm \sim 0.02$ at the nominal outer edge of the calorimeter at, say, $R = 50\ cm$. At $R = 50\ cm$, $z = 100m$, $\theta = 5$mrad ($\eta = 6$), and for $p = 20\ TeV$, we have $p_t = 100\ GeV$.

Some Inferences

1) An idealized calorimeter for jets (and chirons; it doesn't matter) is a barrel with endcap:

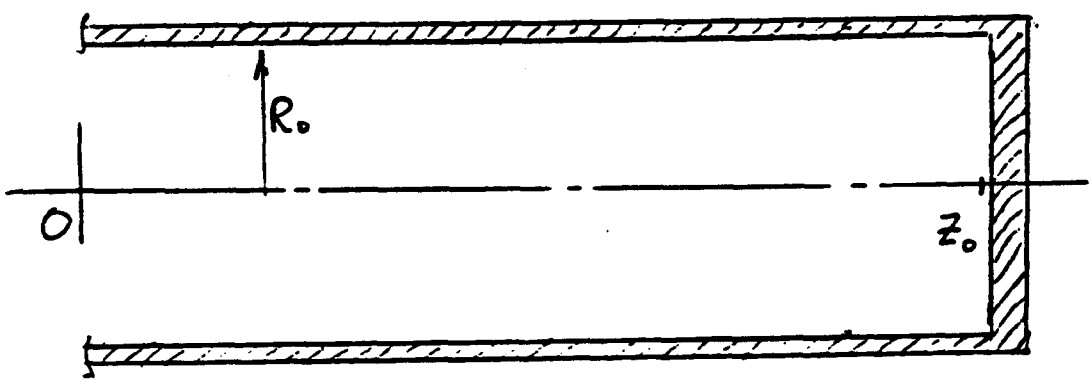

Of course most of that barrel gets replaced with annular walls. Choose R_0, z_0, and pixel size as follows:

2) Near $\eta = 0$ the pixel size in the barrel$(\Delta x) \times (\Delta y) = R_0^2(\Delta\eta \times \Delta\phi)$ should be good enough to resolve well jet components up to some design goal $p_t \leq p_{t_0}$. For

a given technology this criterion sets R_0 and the pixel sizes $\Delta x_0 = \Delta y_0$; therefore the lego pixels $\Delta\eta_0 = \Delta\phi_0$ are also fixed..

3) In the downstream barrel region (which transmogrifies into annular walls), subdivide into pixels whose sizes are $\Delta\eta_0$, $\Delta\phi_0$, even when the barrel sections are replaced by annular walls.

4) Choose z_0 so that

$$\frac{R_0}{z_0} \sim \frac{(p_{t0})}{20\ TeV}$$

$$\left(\frac{z_0}{100m}\right) \sim \left(\frac{R_0}{50\ cm}\right) \cdot \left(\frac{100\ GeV}{p_{t0}}\right)$$

5) Then the endcap pixel size should be *uniform* and of size $\Delta x_0 = \Delta y_0$, the same as in the barrel near $\eta = 0$.

What is the total number of pixels as functions of p_{t0}?? For half the detector,

$$\begin{aligned} N &\sim \frac{2\pi}{\Delta\eta\Delta\phi}\left(\log\frac{2x_0}{R_0}\right) + \frac{\pi R_0^2}{\Delta x\Delta y} \\ &= \frac{\pi R_0^2}{\Delta x\Delta y}\left\{2\ell n\,\frac{40\ TeV}{p_t^0} + 1\right\} \\ &= \frac{\pi R_0^2}{\Delta x\Delta y}\left\{2\left(6 + \ell n\,\frac{100\ GeV}{p_t^0}\right) + 1\right\} = \frac{\pi R_0^2}{\Delta x\Delta y}\left\{13 - 2\ell n\,\frac{p_t^0}{100\ GeV}\right\}. \end{aligned}$$

The barrel plus annuli dominate the cost.

J Bjorken
5 March

Chiron/Centauro Phenomenology for FAD

1. Introduction

Define the Centauro phenomenon as a production of spherical volume of disoriented condensate enveloped within a shell of ordinary hadrons expanding at the speed of light. Use a "fireball approximation", with fireball properties:

M^* : mass

E^* : momentum

$p_\perp^*$: transverse momentum

ϵ : fraction of mass in condensate

R^* : radius at decoupling

This means an approximately gaussian distribution with FWHM of two units, as sketched in Fig. 1. (This is a piece of cosmic-ray lore.):

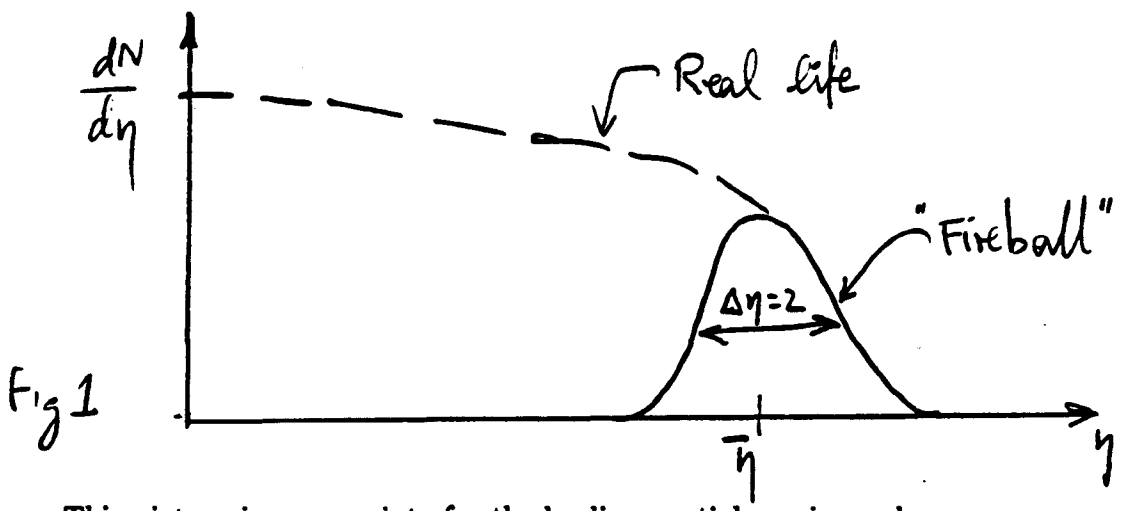

Fig 1

This picture is appropriate for the leading-particle region only.

We now use extremism to estimate the maximum condensate energies, condensate masses (soft pion multiplicities) and maximum condensate p_i^* in order to put the fireball products into as small a circle in the lego plot as possible. The

reason for this extremism is to examine the demands on detector resolution and properties—especially for the photons.

2. Photon Resolution

Assume the π^0's are very nonrelativistic in the rest frame of the fireball. Then all the γ's have E^* of $m_\pi/2 = 70\ MeV$!! In the lego plot they make a fireball because the emission is isotropic.

What is $\overline{\eta}$ versus M^*?? Assume $p_t \ll M^*$. Then the energy of pion system in the lab frame is ϵE^*, and the energy of a single π is

$$E_\pi = \epsilon \frac{E^*}{n_\pi} .$$

The lab angle of emission of a decay γ from a π^0, which was emitted at 90° in the fireball rest frame is now $\overline{\theta}_\gamma = M^*/E^*$.

$$\overline{\eta} = \log \frac{2}{\overline{\theta}_\gamma} = \log \frac{2E^*}{M^*} .$$

But

$$n_\pi m_\pi \cong \epsilon M^*$$

and, if a fraction x of 20 TeV goes into the system, we have

$$E^* = x\, E_0 \equiv x\,(20\ TeV) .$$

Therefore

$$\overline{\eta} = \log \frac{2x\, E_0 \epsilon}{n_\pi m_\pi} = \log \frac{2E_0}{m_\pi} - \log\ n_\pi - \log x - \log \epsilon$$

$$= 12.5 - \log n_\pi - \log x - \log \epsilon$$

It is marginally thinkable that $x \sim 1$ and $\epsilon \gtrsim 0.3$, say, which puts $\overline{\eta} \sim 11.5 - \log n_\pi$. If we demand $n_\pi \gtrsim 10$ in order to create excitement, this already puts $\overline{\eta} \lesssim 9.2$.

The size of the spot at 100 meters downstream is

$$\overline{\theta} \approx 2e^{-\overline{\eta}} \approx 2e^{-9.2} \approx 2 \times 10^{-4} = 0.2\,\text{mrad}$$

or in physical dimensions $\overline{R} \sim 2$ cm. For an "anti-Centauro" final state (20 γ's; no charged π's), the pattern on a 100m endcap (full scale) is shown in Fig. 2.

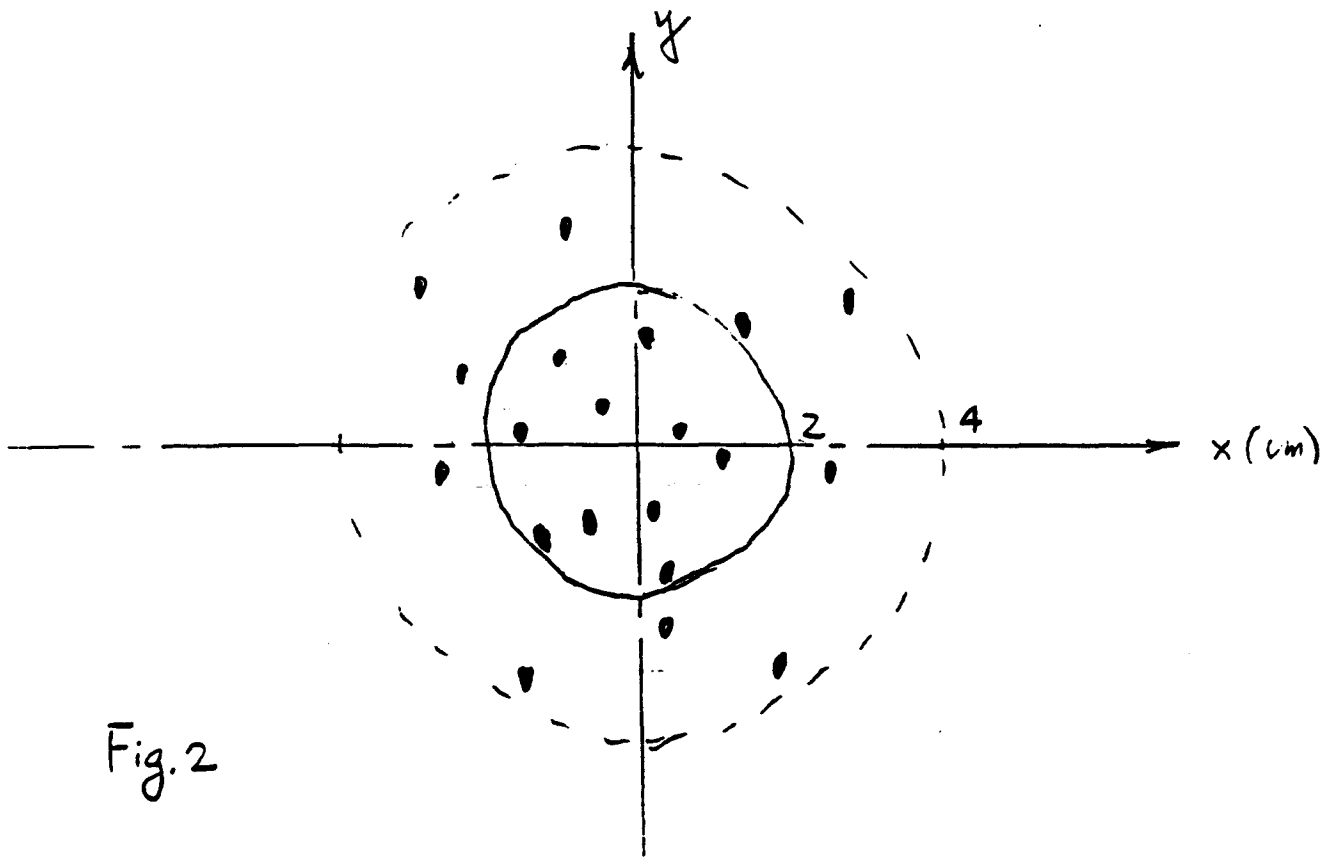

Fig. 2

The central photon density is roughly

$$\frac{dN\gamma}{dA} \approx \frac{10}{\pi(2^2)} \approx 0.75/\text{cm}^2 \quad \text{at} \quad z = 100m\ .$$

This scenario corresponds to a "fireball" with momentum 20 TeV and mass $M^* = 1.5\,GeV/\epsilon$.

If this system is given a transverse momentum $p_t = M^*$, then the pattern moves only slightly outward (Fig. 3)

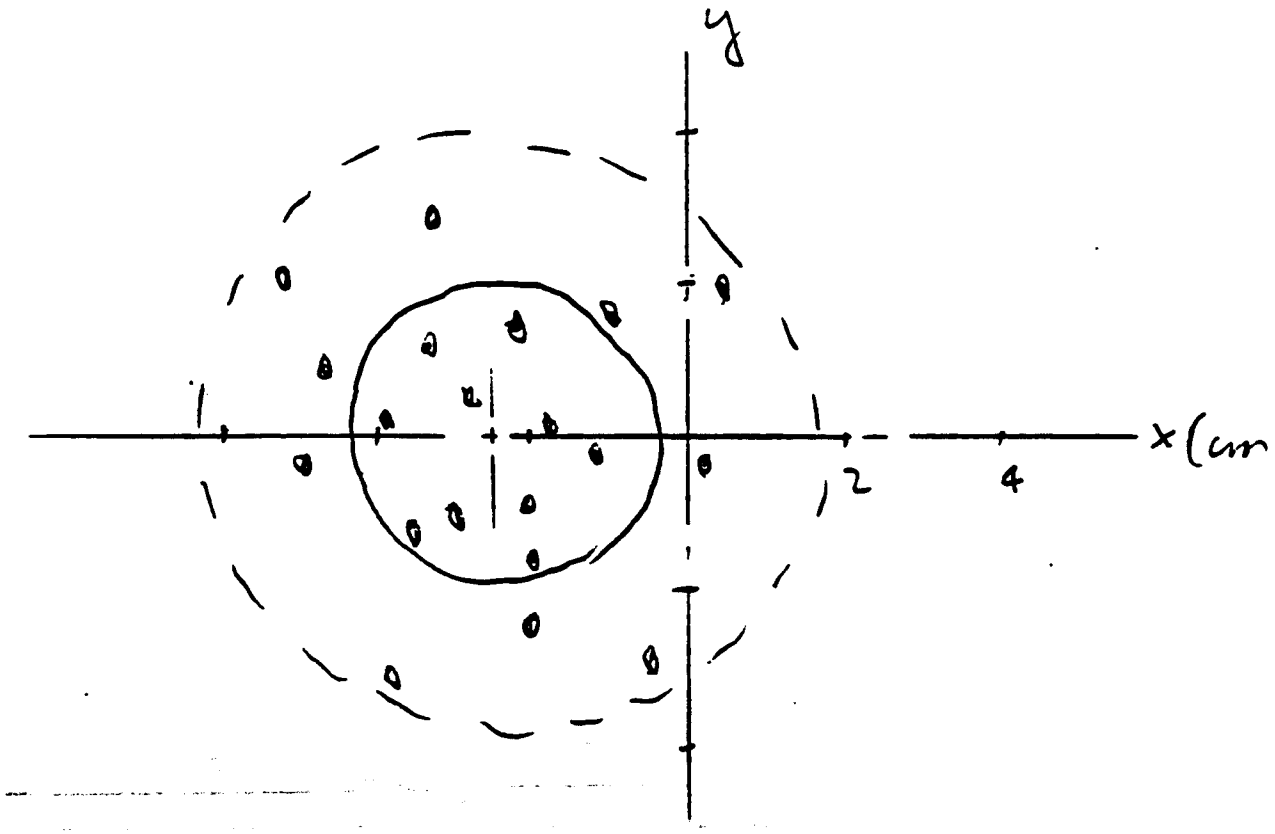

Consider now bigger masses (at any p_t). Then if M^* doubles, $\overline{\eta}$ decreases by 0.7 and the opening angle of the cone of γ's doubles. Also (for the same ϵ) the number of low-p_t, coherent pions doubles. So the net effect on the pion density is to cut it in half. We have (at $\epsilon = 0.3,\ x = 1$) for a pure anti-Centauro:

$$\text{Fireball-radius at 100m} = (2\text{cm}) \times \frac{M^*}{5\ GeV} = (4cm) \cdot \left(\frac{M^*}{10\ GeV}\right)$$

$$\text{Total number of gammas} = 40 \cdot \left(\frac{M^*}{10\ GeV}\right)$$

$$\text{Central density of } \gamma\text{'s at } 100m \approx 0.4\ \left(\frac{10\ GeV}{M^*}\right)\ cm^{-2}$$

Charged tracks may have a smaller p_t at very large R. If so they can, in the absence of magnetic fields, be concentrated in a smaller core, with the γ's from π^0 decays forming a "halo":

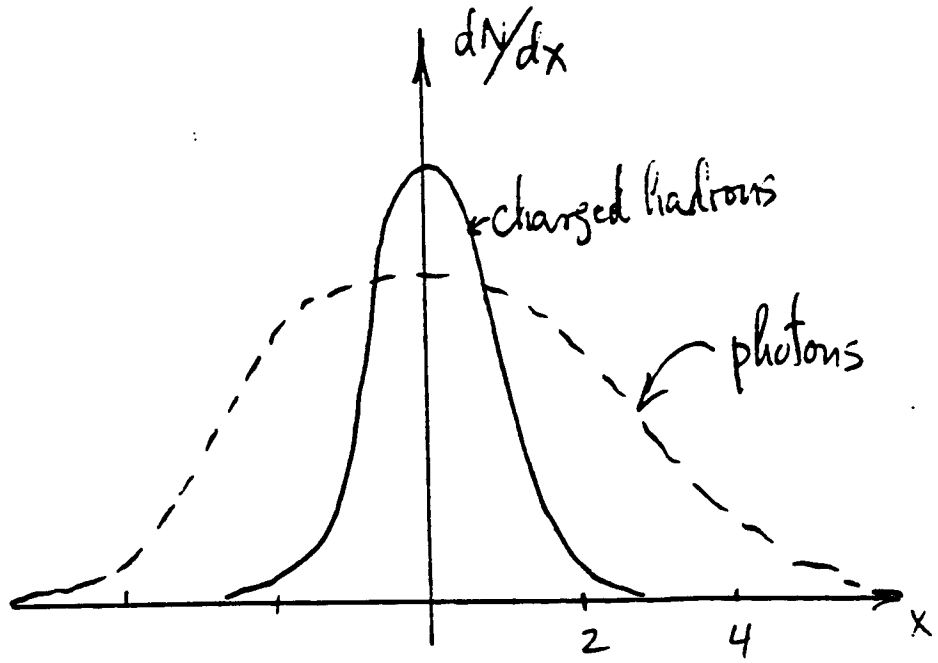

<u>Summary:</u>

A photon density of order $1/cm^2$ at 100m is the most that can be expected from Chiron/Centauro phenomena, and it could be less. And there is , of course, the possibility that it does not exist at all!

Simulation of Minimum-Bias Events
on FAD Forward Wall Calorimeter
R.W. Ellsworth 9 March 92

1 Introduction

A central problem in the intepretation of cosmic ray air shower data is the extrapolation of measured fluxes to the top of the atmosphere. The shower development is determined by the multiparticle production processes in primary-Nitrogen/Oxygen collisions, together with electromagnetic cascade processes. The latter are well-understood in comparison with the former. The features of multiparticle production to which the showers are most sensitive are (a) the secondary momentum spectra and (b) the average "inelasticity" i.e. the fraction of the incident proton (lab) energy which is used to produce secondary particles.

A Monte Carlo simulation of minimum bias events was used to study the regions of x_F and $p_\perp$ accessible to a FAD wall calorimeter.

2 Description of Event Generator

The event simulator, "BANG92A"[1] approximates an independent particle emission model by choosing secondary CM momenta from assumed distributions. Two "leading" particles,

[1]Thr algorithm "BANG" dates from the mid- 1970's; the basic idea was suggested by Tom Gaisser (Bartol); the first implementation was written by Allen Stottlemyer (Univ of Maryland); it is described in more detail in Phys Rev D26, 1043 (1982).

one each in the forward and backward hemispheres, are chosen from a flat distribution. The remaining secondaries are chosen from approximations to x_F and $p_\perp$ observed at ISR and FNAL. Momentum is approximately balanced, as the event is generated, by pointing a secondary CM momentum into the octant opposite to that of the vector sum of previously chosen particle. The process ends when all the CM energy is used up. Then small corrections are made to each momentum to enforce conservation of momentum and energy. The current algorithm chooses 10% of the secondaries to be kaons and the remainder are charged and neutral pions.

The adjustable parameters in the algorithm are those which specify the shapes of the x and $p_\perp$ distributions. The particle multiplicity is most sensitive, of course, to the x distributions. The pseudo-rapidity (η) density at small η would be constant if the x_F distributions did not change with CM energy. The observed increase is included by increasing, logarithmically, the slopes of the x_F distributions. The x_F distribution parameters have been adjusted to give, approximately, the experimentally observed charged particle multiplicity, and η density at ISR and Tevatron energies. These results are tabulated below:

$\sqrt{s}$ (GeV)	n^-_{ch} obs	Simulation	$maxdn/d\eta$obs	Simimulation
63	12.7	14.8	2.0	1.8
1800	28.0	24.6	4.7	4.4
40000		109		7.5

The mean charged-particle multiplicity at 1800 GeV is for $\eta < 3.0$. The ratio of average/dispersion for the charged multiplicity distribution remains constant, at 2.4, over the entire

energy range. The simulation thus produces KNO scaling. The distribution $x_F * dn/dx_F$ for gamma rays from π^0 decay is shown in Figure 1 for $\sqrt{s}$ of 63 and 40,000 GeV. This distribution is proportional to the invariant cross section $E\frac{d^3\sigma}{dp^3}$ for large x. The change in the distribution is evident.

3 Results

The distributions x_F for produced gammas and for those with $\eta > 8.4$ are shown in Figure 2. The latter corresponds to those gammas hitting a detector of radius .45 m at a distance of 1 km, a possible FAD component. Note that the detected x_F's go down to very low values. Because of the steep energy distribution, the detector picks out low x_F events, with low $p_\perp$. The average $p_\perp$ for all gammas was 173 MeV/c, for the "triggered" gammas, i.e. those with $\eta < 8.4$, the average was 129 MeV/c. For this simulation, the average number of gammas in the detector, per pp interaction is 2.8; the average deposited energy is 1.7 TeV. None of these numbers should be taken too seriously since the simulation only roughly agrees with lower energy data, and it is assuming a particular model for the multiplicity increase. Nonetheless, the qualitative features are instructive.

4 Next

The next steps will be to simulate the response from a smaller detector, and to change the algorithm to fit the ISR and FNAL multiplicities by changing the mean inelasticity rather than the

X_F distributions.

I have graphs of many other distributions; let me know of any you would like to have sent to you (in TopDrawer form.) Also, anybody who wants to run the code is welcome to.

Fig 1 x*dn/dx pizeros

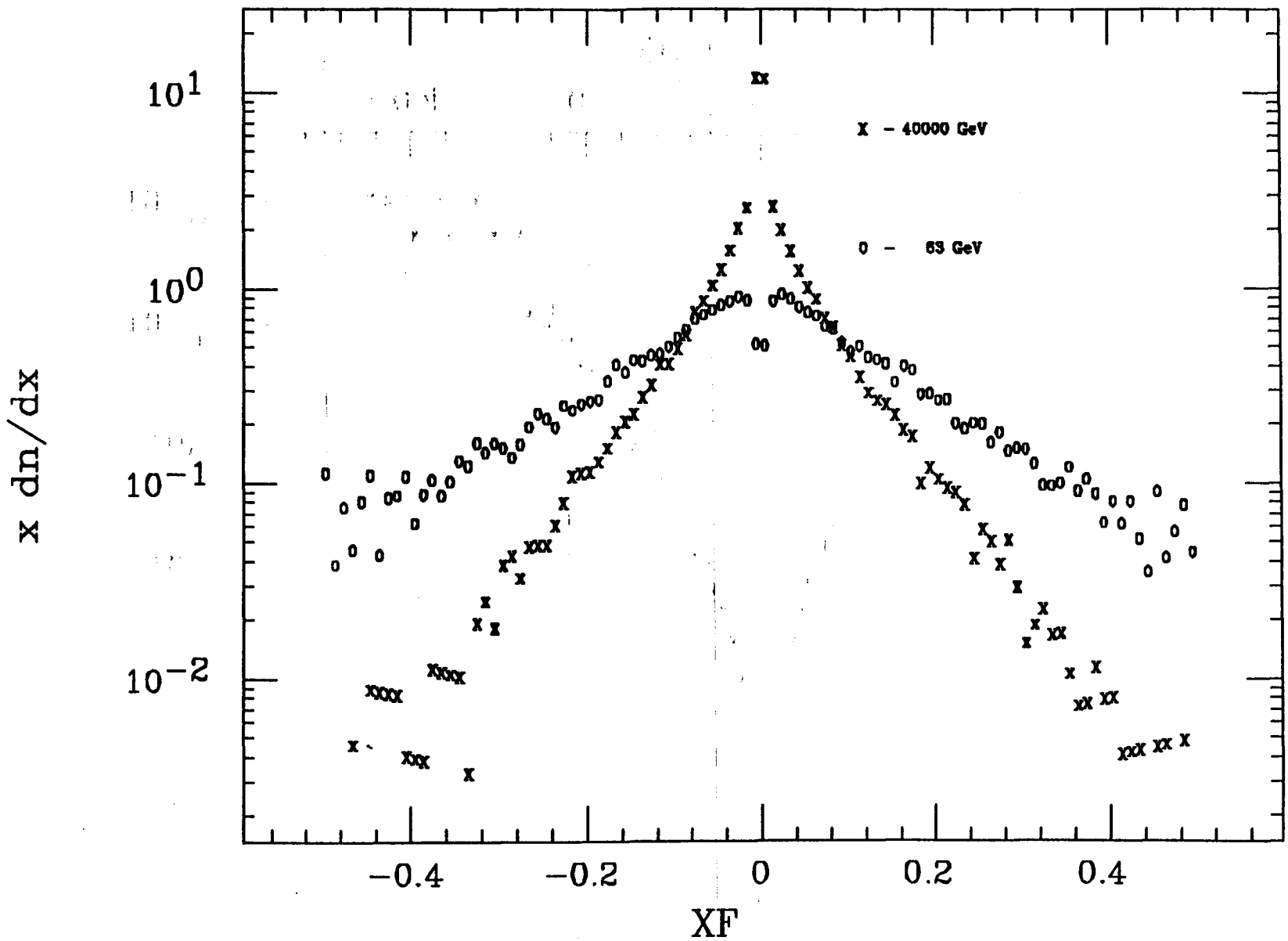

5-MAR-92 11:58:00

FIG 2 XF gammas

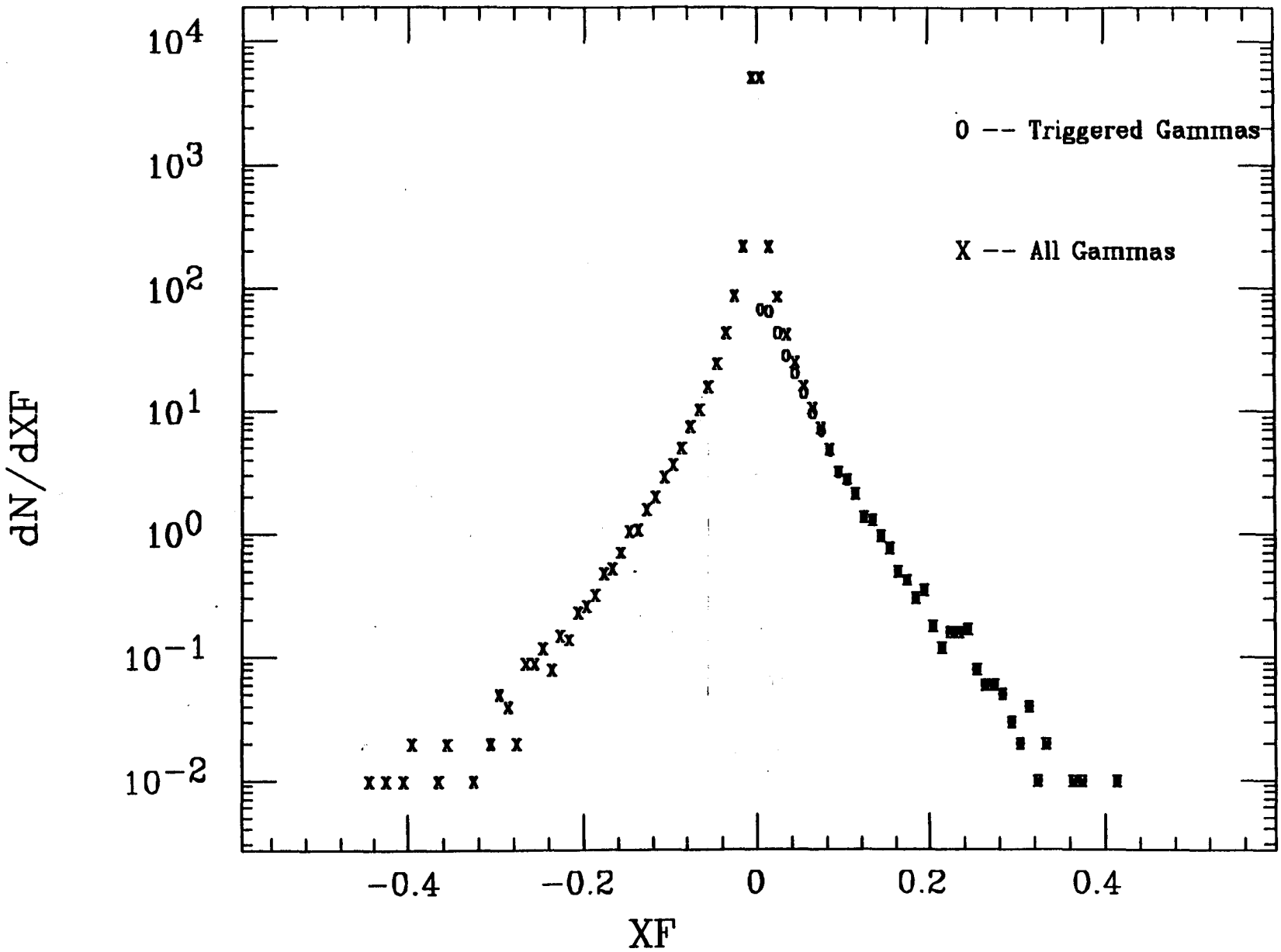

From: Bob Ellsworth
Subject: More results from FAD Wall simulation
Date: 10 March 92

I send along two results; the first is a set of sample events which "triggered" the wall. It is a list of momenta of gammas with eta > 8.4. The other result is a TopDrawer file of the distribution of distances between hits on the wall. (The wall is a circle of radius 45 cm at a distance of 1 km from the interaction.) The mean of the distribution is 34.1 cm. The shape of the distribution, however, seems to be imposed by the 45 cm circle. The average number of gamma hits per event is 2.76; the average energy of hitting gammas is 1.73 TeV. The simulation code was BANG92A, as described in the previous communication. Fig.3

Sqrt(s)=40000 GeV Gammas with eta > 8.4
First 20 events

EVENT #	SEC #	PX GeV/c	PY GeV/c	PZ GeV/c
1	1	2.9689671E-02	3.4718256E-02	245.9641
1	2	-0.1166909	2.1000454E-02	356.3142
1	3	1.6898266E-03	6.1443809E-04	36.07052
1	4	5.1690701E-02	0.1265490	1265.694
1	5	-8.6840466E-02	0.1951499	1815.224
1	6	2.3806043E-02	-1.4928185E-03	59.33966
1	7	-5.4751174E-03	2.9446350E-02	67.50470
1	8	0.2687488	8.6902708E-02	1237.312
1	9	0.3612732	0.1598630	2550.574
3	1	-0.2622850	2.0868570E-02	833.6702
3	2	-1.5189118E-02	9.4802883E-03	65.47964
3	3	-4.6249703E-02	-1.1948576E-02	133.9389
3	4	9.4125144E-02	1.4302487E-02	297.6960
3	5	0.1624769	-0.1260011	897.3123
3	6	2.9476374E-02	6.6703089E-02	190.9802
3	7	0.2211211	7.8538032E-03	564.9908
3	8	-1.2421725E-02	-2.3560081E-02	142.7130
4	1	1.8577434E-03	-0.1033811	287.4823
4	2	6.2144160E-02	-3.0330742E-02	199.6907
4	3	-4.6329726E-02	-2.0994201E-02	132.7866
4	4	-1.4398007E-02	5.5458706E-02	149.8990
4	5	0.2989669	0.7938312	2019.495
4	6	-2.8035449E-02	9.4875857E-02	270.4640
4	7	0.2302038	-0.1900037	701.3021
5	1	6.1378996E-03	6.3058279E-02	144.5664
5	2	-0.3228108	-0.2034906	1083.366
5	3	-2.1630455E-02	-5.9357964E-02	299.4059
5	4	-0.2047391	-2.9138764E-02	553.4344
6	1	2.5439961E-03	1.2121261E-02	138.3187
6	2	1.1083321E-02	1.1940958E-02	41.57285
7	1	-0.2105768	-7.9945125E-02	641.5310
7	2	-2.5844729E-02	4.2223342E-02	133.8434
7	3	2.8615400E-02	6.0796458E-03	71.24830
7	4	-8.4184103E-02	-3.9341208E-02	257.8253
9	1	0.1204655	2.9926752E-03	450.1539
9	2	-2.0526126E-02	5.2332614E-02	199.4560
9	3	-3.6675502E-02	-8.0962181E-02	408.7011

11	1	2.6478572E-02	0.1381019	723.5850
11	2	1.4371552E-02	1.4420604E-02	101.0563
11	3	3.7244603E-02	1.3243607E-02	125.4639
11	4	0.1550654	-5.0300863E-03	550.8884
11	5	0.2718425	-0.1738105	860.3596
12	1	-5.2331746E-02	-5.9031211E-02	710.6857
12	2	-0.1008600	-1.0305267E-02	264.1205
12	3	-5.5532024E-04	8.6605875E-03	36.92649
13	1	1.6604014E-02	-3.3624120E-02	210.1806
13	2	1.3867008E-02	1.9035423E-02	179.7696
13	3	0.3814026	6.5479964E-02	950.0274
13	4	-5.1102255E-02	-0.1905561	558.3316
13	5	-1.3540071E-02	4.5567315E-02	516.4551
15	1	0.2502478	-0.1953333	949.2625
15	2	0.2618055	-5.9022773E-02	931.3611
16	1	-1.3822101E-02	5.0248064E-02	277.3197
16	2	-0.1807003	-2.8553186E-02	678.5159
18	1	3.6853924E-02	0.2034071	491.4392
18	2	1.7963242E-02	0.1217430	1370.730
18	3	-0.1268044	0.1265610	1755.143
18	4	-1.0325605E-02	7.3243335E-02	200.4377
18	5	-0.1073120	-7.1168482E-02	816.2670
18	6	-0.1082987	-1.1946285E-02	255.2998
18	7	-0.2078252	-7.7991113E-02	1146.387
18	8	9.8414179E-03	-9.0968879E-03	85.41016
18	9	-3.5689771E-02	0.3170011	879.9230
19	1	4.1573025E-02	-0.2531112	2327.679
19	2	3.7279725E-02	-4.7461898E-03	175.3970
20	1	0.1303246	0.2466045	759.7153
20	2	1.0154916E-02	-3.5047187E-03	181.9695
20	3	4.9439102E-02	1.1337606E-02	124.7855
20	4	-2.3866283E-02	1.5617706E-02	69.47807

Inter-gamma dist at Wall

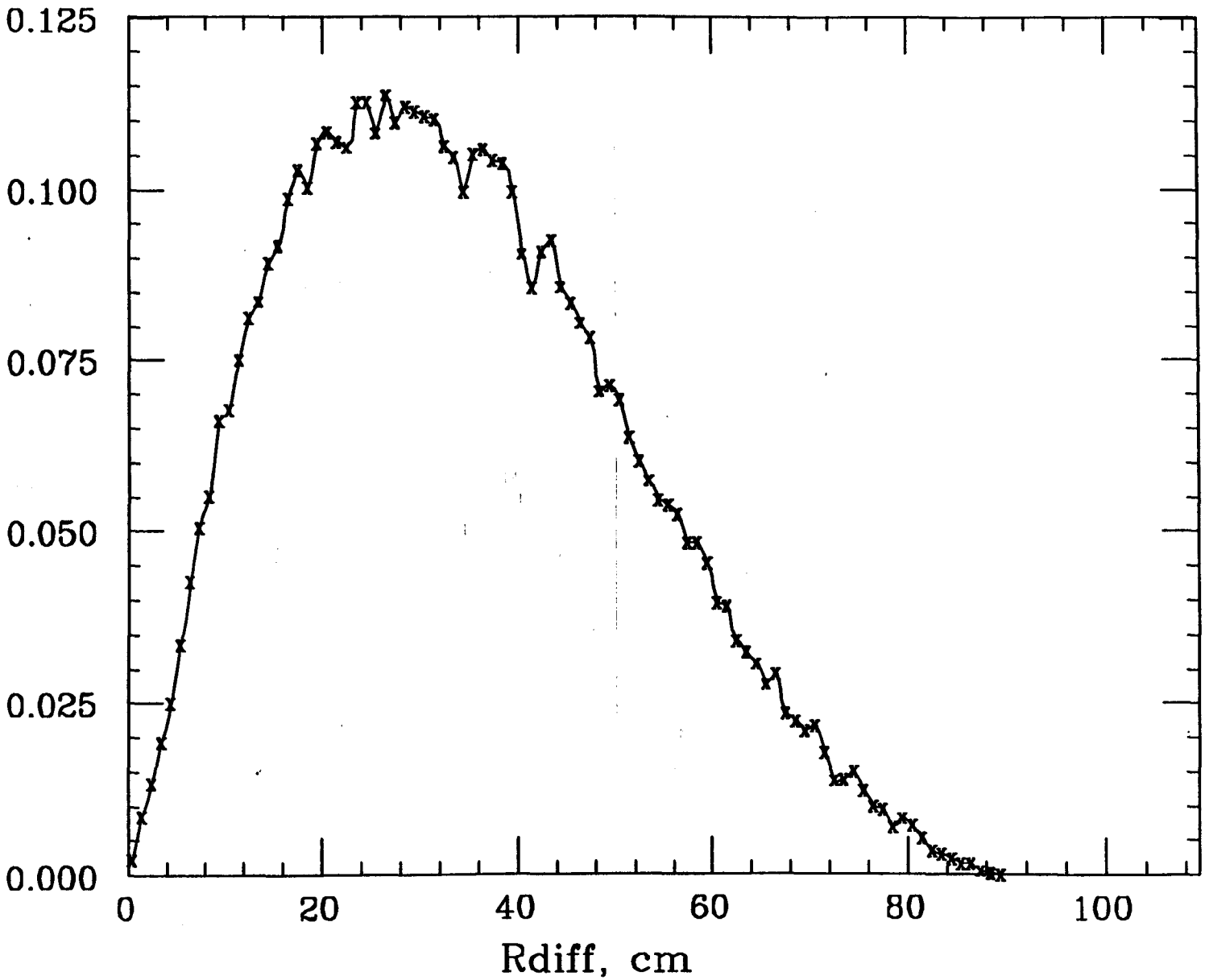

10-MAR-92 15:43:44 40.00

Fig 3

x*dn/dx ALL, TRIG GAMMAS ETA>9.5

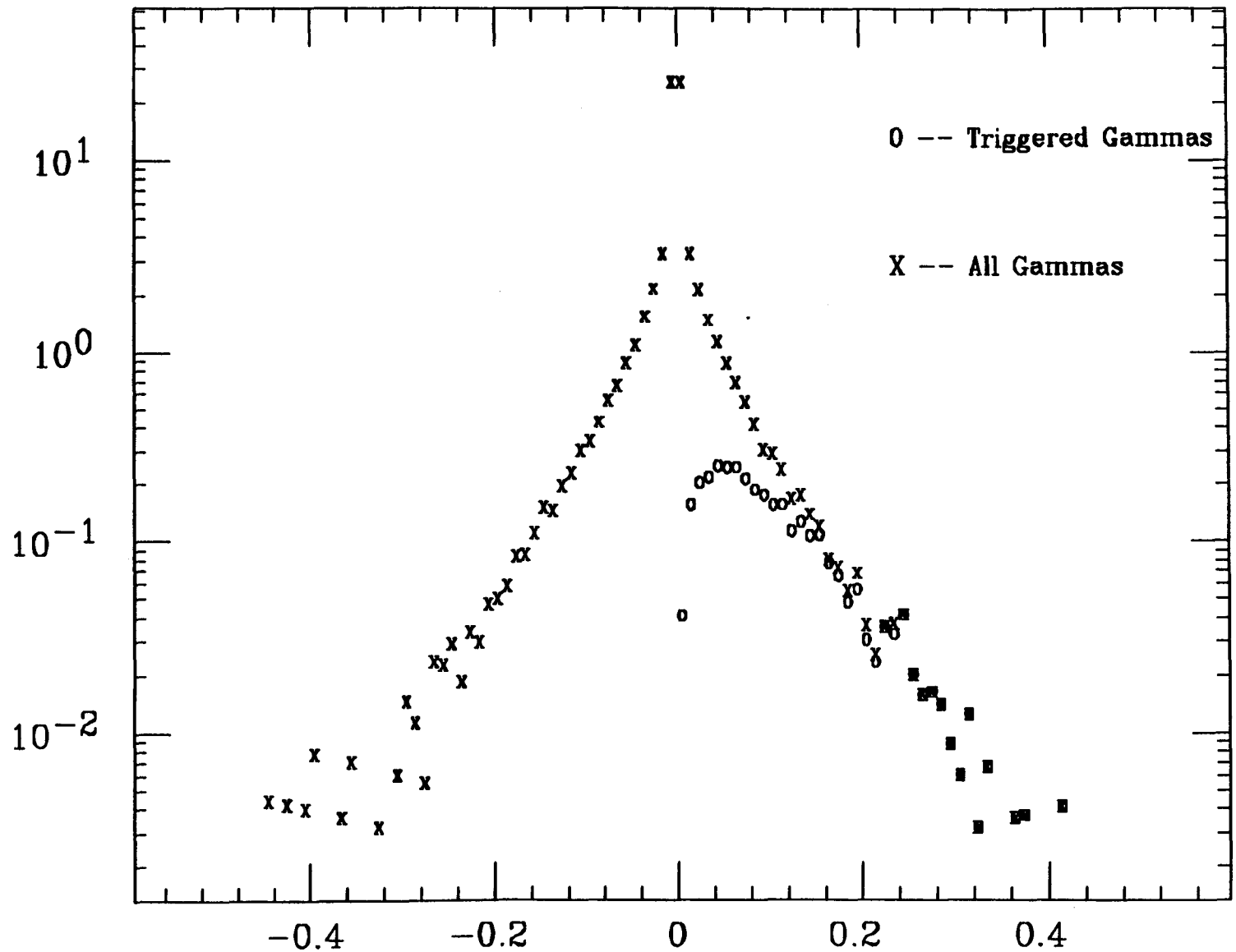

TopDrawer File / Fig. 4 Only;
Produced and detected gammas for 15 cm detector, eta>9.5
Avg number trig gammas = .62 per int

10-MAR-92 17:53:30 40.00